

**Investigating LysM effector function and the biotrophic growth phase
of *Magnaporthe oryzae***

Submitted by Thomas Andrew Mentlak

to the University of Exeter as a thesis for the degree of

Doctor of Philosophy in Biological Sciences

In June 2012

This thesis is available for Library use on the understanding that it is copyright material and that no quotation from the thesis may be published without proper acknowledgement.

I certify that all material in this thesis which is not my own work has been identified and that no material has previously been submitted and approved for the award of a degree by this or any other University.

Signature:

Abstract

During intracellular biotrophic growth, the rice blast fungus *Magnaporthe oryzae* secretes a large battery of effector proteins, which are thought to suppress host cell defence responses. Although a number of these effector proteins have been identified, their precise biological functions and contribution towards plant infection remains unclear. In this thesis, I report that during biotrophic growth, the secretion of a LysM effector protein, Slp1, is required for rice blast disease. I show that Slp1 binds chitin and is able to suppress the chitin-induced oxidative burst and defence gene-expression in rice cells. Slp1 competes with the membrane-localised chitin receptor CEBiP in rice, and this competitive interaction results in a reduction in virulence associated with $\Delta slp1$ null mutants. Slp1 is secreted by intracellular hyphae specifically during biotrophic growth, and accumulates around hyphal tips at the plant-fungal interface. Using transgenic rice lines which express fluorescent marker proteins targeted to the plasma membrane and endoplasmic reticulum, I investigate the biotrophic growth phase of *M. oryzae*. I show that the rice host plasma membrane becomes tightly apposed to invasive biotrophic intracellular hyphae. I also show that the rice host plasma membrane and endoplasmic reticulum accumulate around the Biotrophic Interfacial Complex (BIC), a bulbous structure attached to the sub-apical region of intracellular fungal hyphae, which accumulates fluorescently-labelled avirulence effector proteins. Using a fungal plasma membrane marker, I show that the BIC resides outside the fungal plasma membrane and cell wall is made exclusively of plant cellular material.

Table of contents

	Page
List of Figures	9
List of Tables	11
Acknowledgements	12
Abbreviations	13
1. Introduction	14
1.1 The global significance of plant disease	14
1.2 Rice blast disease	15
1.3 The life cycle of <i>M. oryzae</i>	16
1.4 Appressorium-mediated development in <i>M. oryzae</i>	19
1.4.1 Cyclic AMP signalling	19
1.4.2 MAPK signalling	20
1.5 Biotrophic growth and host cell colonisation in <i>M. oryzae</i>	21
1.6 The role of effector proteins in <i>M. oryzae</i>	23
1.7 Localisation of rice blast effector proteins during biotrophic growth	24
1.8 Translocation and delivery of <i>M. oryzae</i> effector proteins during biotrophic growth	26
1.9 Molecular secretion apparatus in filamentous fungi	27
1.9.1 The molecular components required for secretion and exocytosis in <i>M. oryzae</i>	27
1.9.2 The role of the Spitzenkörper in polarised exocytosis in filamentous fungi	29
1.9.3 Establishing polarity and the role of the polarisome complex in fungal secretion	30
1.9.4 The role of the exocyst complex in polarised exocytosis in fungi	32
1.10 Introduction to the current study	34
2. Materials and methods	36
2.1 Growth and maintenance of fungal stocks	36
2.1 Pathogenicity and infection related development assays	36
2.2.1 Plant infection assays	37

2.2.2	Assays for measuring germination and appressorium formation rate	37
2.2.3	Assays for examining intracellular infection-related development on rice leaves	37
2.3	Nucleic acid analysis	38
2.3.1	Extraction of fungal DNA	38
2.3.1.1	Preparing fungal material for genomic DNA extraction	38
2.3.1.2	Preparation of putative fungal transformants for genomic DNA extraction	38
2.3.1.3	Fungal DNA extraction	38
2.3.2	Extraction of fungal and plant RNA	39
2.3.2.1	Preparation for RNA extraction	39
2.3.2.2	Extraction of total <i>M. oryzae</i> and plant RNA	40
2.3.4	DNA manipulation	41
2.3.4.1	Digestion of genomic or plasmid DNA with restriction enzymes	41
2.3.4.2	DNA gel electrophoresis	41
2.3.4.3	The polymerase chain reaction (PCR)	41
2.3.4.4	Gel purification of DNA fragments	42
2.3.4.5	Southern blotting	42
2.3.4.6	Radio-labelled DNA probe synthesis	43
2.3.4.7	Hybridisation conditions	43
2.3.5	DNA cloning procedures	44
2.3.5.1	Bacterial DNA mini preparations (Alkaline Lysis preparations)	44
2.3.5.2	High quality plasmid DNA preparations	45
2.3.5.3	DNA ligation and selection of recombinant clones	46
2.3.5.4	Preparation of competent cells	47
2.3.5.5	Transformation of bacterial hosts	47
2.3.6	RNA manipulations	48
2.3.6.1	RNA gel electrophoresis	48
2.3.6.2	Reverse-transcription-PCR	48
2. 4	DNA-mediated transformation of <i>M. oryzae</i>	49
3.	Investigating effector-mediated suppression of chitin-triggered immunity by a rice blast LysM effector protein	51
3.1	Introduction	52
3.2	Methods	56
3.2.1	Affinity precipitation of recombinant Slp1 protein with polysaccharides	56

3.2.2	Cell protection assays using crude extract of chitinase from tomato leaves	56
3.2.3	Medium alkalisation of tomato cells	56
3.2.4	Production of recombinant Slp1 protein	57
3.2.5	Affinity labeling of Rice Membranes with Biotinylated (GlcNAc) ₈	58
3.2.6	Measurement of ROS Generation and Gene Expression Analysis	58
3.2.7.1	Yeast-two hybrid screen	59
3.2.7.2	Small scale yeast transformation	59
3.2.7.3	Plating and screening of yeast transformants	60
3.3	Results	61
3.3.1	Chitin in the fungal cell wall is exposed to the plant during intracellular growth	61
3.3.2.	Identification of <i>M. oryzae</i> secreted LysM effector proteins	63
3.3.3	Multiple amino acid sequence alignment of Slp1 and Slp2 demonstrates shared homology with other fungal LysM proteins	66
3.3.4	Phylogenetic tree of fungal LysM effector proteins	66
3.3.5	Generation of the <i>SLP1</i> targeted gene replacement vector	70
3.3.6	Analysis of putative $\Delta slp1$ transformants	72
3.3.7	Generation of the <i>SLP2</i> targeted gene replacement vector	74
3.3.8	Analysis of putative $\Delta slp2$ transformants	76
3.3.9	$\Delta slp1$ vegetative growth and colony morphology	79
3.3.10	$\Delta slp2$ vegetative growth and colony morphology	79
3.3.11	The $\Delta slp1$ mutant is reduced in virulence	82
3.3.12	The $\Delta slp2$ mutant is fully pathogenic	84
3.3.13	The $\Delta slp1$ mutant exhibits normal patterns of appressorium-mediated development	86
3.3.14	The $\Delta slp1$ mutant is less able to colonise epidermal host cells	86
3.3.15	Slp1 co-precipitates specifically with chitin but not other cell-wall polysaccharides	89
3.3.16	Slp1 does not protect fungal hyphae from hydrolysis by plant-derived chitinases	91
3.3.16.1	<i>M. oryzae</i> is insensitive to crude-extract of plant-derived chitinase enzymes	91
3.3.16.2	Using <i>Trichoderma viride</i> as a model species demonstrates that Slp1 does not shield fungal hyphae from hydrolysis by chitinases	93
3.3.17	Slp1 inhibits medium alkalisation of tomato cell suspensions	95
3.3.18	Slp1 inhibits the chitin-induced oxidative burst by rice cells	97
3.3.19	Slp1 inhibits chitin-induced expression of defence genes in rice cells	99

3.3.20	Slp1 competes with the rice PRR CEBiP	99
3.3.21	Targeted gene silencing of CEBiP in rice restores the ability of <i>Δslp1</i> mutants of <i>M. oryzae</i> to cause rice blast disease	102
3.3.22	Employing a yeast two-hybrid screen for detection of Slp1-Slp1 interactions	104
3.2.23	Construction of DNA-BD and AD gene fusions	104
3.3.24	Slp1 interacts with itself in a yeast two-hybrid screen but does not independently activate reporter genes	105
3.4	Discussion	109
4.	Slp1 is a putative apoplastic effector secreted by the rice blast fungus <i>M. oryzae</i> specifically during biotrophic growth	112
4.1	Introduction	113
4.2	Methods	116
4.2.1	Construction of the C-terminal GFP fusion vector <i>SLP1::GFP</i>	116
4.2.2	Construction of the <i>SLP1</i> ²⁷⁻¹⁶² :: <i>GFP</i> fusion vector	117
4.2.3	Generating the <i>SLP1</i> ¹⁻²⁷ :: <i>GFP</i> fusion vector	118
4.2.4	Generating the <i>AVR-Pia</i> ¹⁻¹⁹ :: <i>SLP1</i> ²⁷⁻¹⁶² :: <i>GFP</i> fusion vector	119
4.3	Results	121
4.3.1	Slp1 is secreted into the apoplastic space	121
4.3.1.1	Generating and construction of a C-terminal <i>SLP1::GFP</i> fusion vector	121
4.3.1.2	Expression and localisation of <i>SLP1::GFP</i> during infection-related development of <i>M. oryzae</i>	124
4.3.1.3	Expression and localisation of <i>SLP1::GFP</i> cannot be detected during <i>in vitro</i> vegetative growth	126
4.3.1.4	<i>SLP1::GFP</i> accumulates at the plant-fungal interface during intracellular biotrophic growth	128
4.3.1.5	<i>SLP1</i> is only expressed during <i>in planta</i> growth	130
4.3.2	Slp1:GFP does not accumulate at the Biotrophic Interfacial Complex	132
4.3.3	Slp1:GFP co-localises with the putative apoplastic effector protein Bas4:mRFP	134
4.3.4	The N-terminal Slp1 signal peptide is required for secretion at the plant-fungal interface	136
4.3.4.1	Construction of the <i>SLP1</i> ²⁷⁻¹⁶² :: <i>GFP</i> vector	136
4.3.4.2	Expression and localisation of the <i>SLP1</i> ²⁷⁻¹⁶² :: <i>GFP</i> construct	137
4.3.5	Using GFP gene fusion vectors to complement the <i>Δslp1</i> mutant	

4.3.5.1	Complementation of the $\Delta slp1$ mutant with the <i>SLP1::GFP</i> vector	139
4.3.5.2	The N-terminal Slp1 secretion peptide signal is required for complementation of the $\Delta slp1$ mutant	141
4.3.6	The mature Slp1 protein is not required for secretion and delivery into the apoplastic space	143
4.3.6.1	Construction of the <i>SLP1¹⁻²⁷::GFP</i> vector	143
4.3.6.2	Localisation of Slp1 ¹⁻²⁷ ::GFP in invasive hyphae	144
4.3.7	Replacement of the Slp1 signal peptide with the BIC-localised Avr-Pia signal peptide fails to re-direct Slp1 to the BIC	146
4.3.7.1	Construction of the <i>AVR-Pia¹⁻¹⁹::SLP1²⁷⁻¹⁶²::GFP</i> vector	146
4.3.7.2	Avr-Pia ¹⁻¹⁹ ::Slp1 ²⁷⁻¹⁶² ::GFP localises to the plant-fungal interface and not to the BIC	149
4.4	Discussion	151
5.	Investigating biotrophic growth of <i>M. oryzae</i> and dissecting the structure of the Biotrophic Interfacial Complex (BIC)	155
5.1	Introduction	156
5.2	Methods	160
5.2.1	Construction of the <i>toxA::RFP</i> vector	160
5.2.2	Construction of the C-terminal <i>PIP2a::GFP</i> gene fusion in the plant binary expression vector pCAMBIA 1302	161
5.2.3	<i>Agrobacterium</i> - mediated transformation of rice	162
5.2.4	Total protein extraction and Western blotting of rice transformants	163
5.2.4	Construction of the <i>PMA1::GFP</i> fusion vector	164
5.3	Results	166
5.3.1.1	The <i>toxA::RFP</i> vector as a suitable marker for visualising fungal cytoplasm	166
5.3.1.2	Construction and introduction of the <i>toxA::RFP</i> vector	166
5.3.2	Expression of LTi6B::GFP in transgenic plants localises GFP to the plant plasma membrane	171
5.3.3.1	Construction of the PIP2a::GFP plant expression vector	173
5.3.3.2	Stable transgenic plants expressing the PIP2a::GFP construct localise GFP to the plant plasma membrane	176
5.3.4	Stable transgenic plants expressing GFP:HDEL localise GFP to an intricate and dynamic endoplasmic reticulum structure	178
5.3.5	During intracellular growth of <i>M. oryzae</i> , the host plant plasma membrane becomes invaginated	180

5.3.6	Host plasma membrane accumulates at the Biotrophic Interfacial Complex (BIC)	182
5.3.7	Visualisation of transgenic GFP:HDEL plants reveals that host Endoplasmic Reticulum accumulates at the BIC	185
5.3.8	Fungal cytoplasm is unable to diffuse into the BIC	187
5.3.9.1	Generating a fungal plasma membrane marker <i>PMA1:GFP</i>	189
5.3.9.2	Construction and introduction of the <i>PMA1:GFP</i> gene fusion vector	193
5.3.9.3	Visualising the fungal plasma membrane using the <i>PMA1:GFP</i> vector enables the structure of the fungal plasma membrane around the BIC to be determined	196
5.3.10.1	Using transgenic <i>Oryza sativa</i> cv. <i>sasanishiki</i> plants to study compatible and incompatible interactions	198
5.3.10.2	Inoculation of <i>M. oryzae</i> isolate TH68-140 on transgenic <i>GFP:HDEL</i> plants reveals that the host nucleus is recruited to the site of appressorium formation	200
5.4	Discussion	202
6.	General Discussion	206
7.	Bibliography	215

Appendix 1 Mentlak, T. A., Kombrink, A., Shinya, T., Ryder, L. S., Otomo, I., Saitoh, H., Terauchi, R., Nishizawa, Y., Shibuya, N., Thomma, B. P. H. J. and Talbot, N. J. (2012) Effector mediated suppression of chitin-triggered immunity by *Magnaporthe oryzae* is necessary for rice blast disease. *The Plant Cell*, **24**: 322-335

Appendix 2 Mentlak, T. A., Talbot, N. J. and Kroj, T. (2012) Effector translocation and delivery by the rice blast fungus *Magnaporthe oryzae*. In “Effectors in Plant-Microbe Interactions”, Edited by Francis Martin and Sophien Kamoun. Wiley-Blackwell Press.

List of Figures	Page
Figure 1.1	The life-cycle of the rice blast fungus <i>Magnaporthe oryzae</i> 18
Figure 3.1	Chitin within the fungal cell wall is exposed to the plant during biotrophic growth 62
Figure 3.2	Nucleotide sequence and putative amino acid sequence of the <i>M. oryzae</i> <i>SLP1</i> gene 64
Figure 3.3	Nucleotide sequence and putative amino acid sequence of the <i>M. oryzae</i> <i>SLP2</i> gene 65
Figure 3.4	Multiple amino acid sequence alignment of fungal LysM proteins 68
Figure 3.5	Phylogenetic analysis of LysM amino acid sequences from a range of fungal organisms 69
Figure 3.6	Schematic representation of the targeted deletion of <i>SLP1</i> using a PCR-based split-marker deletion method 71
Figure 3.7	Targeted gene replacement of <i>SLP1</i> and confirmation by Southern Blotting analysis 73
Figure 3.8	Schematic representation of the targeted deletion of <i>SLP2</i> using a PCR-based split-marker deletion method 75
Figure 3.9	Southern blotting analysis of putative $\Delta slp2$ transformants 77
Figure 3.10	Confirmation of putative $\Delta slp2$ transformants by PCR 78
Figure 3.11	Vegetative growth and colony morphology of $\Delta slp1$ mutants 80
Figure 3.12	Vegetative growth and colony morphology of $\Delta slp2$ mutants 81
Figure 3.13	The $\Delta slp1$ mutant is reduced in virulence 83
Figure 3.14	<i>SLP2</i> is dispensible for plant infection 85
Figure 3.15	Appressorium-mediated morphogenesis is unaltered in the $\Delta slp1$ mutant 87
Figure 3.16	The $\Delta slp1$ mutant is reduced in its ability to colonise host cells 88
Figure 3.17	Slp1 co-precipitates with chitin but not other insoluble cell wall polysaccharides 90
Figure 3.18	<i>M. oryzae</i> spores exhibit normal appressorium-mediated changes in morphology in the presence of basic intracellular chitinases 92
Figure 3.19	Slp1 is unable to protect fungal hyphae from crude extract of plant-derived chitinases 94
Figure 3.20	Medium alkalinisation of tomato cell suspensions is suppressed in the presence of Slp1 96
Figure 3.21	Slp1 inhibits the chitin-induced oxidative burst in rice suspension cells 98
Figure 3.23	Expression of rice defense genes PAL1 and β -glucanase induced by (GlcNAc) ₈ is suppressed in the presence of Slp1 100
Figure 3.24	Slp1 competes with the plant membrane PRR CEBiP for chitin-binding 101
Figure 3.25	The ability of a $\Delta slp1$ mutant to cause rice blast disease is restored when inoculated onto a rice cultivar in which CEBiP has been silenced by RNAi 103
Figure 3.26	Schematic representation of the cloning strategy to perform yeast two-hybrid analysis 107
Figure 3.27	A yeast two-hybrid screen reveals an Slp1-Slp1 interaction 108
Figure 4.1	Schematic representation of the construction of the C-terminal <i>SLP1::GFP</i> fusion vector 122

Figure 4.2	Southern blot analysis of putative <i>SLP1:GFP</i> transformants	123
Figure 4.3	<i>SLP1</i> is not expressed during appressorium-mediated morphogenesis	125
Figure 4.4	<i>SLP1:GFP</i> is not expressed <i>in vitro</i>	127
Figure 4.5	Slp1:GFP accumulates at the plant fungal interface	129
Figure 4.6	<i>SLP1</i> is only expressed during <i>in planta</i> growth	131
Figure 4.7	Slp1:GFP does not co-localise with BIC-localised avirulence effectors	133
Figure 4.8	Slp1:GFP and Bas4:mRFP partially co-localise	135
Figure 4.9	The N-terminal 27 amino acids of Slp1 is required for secretion at the plant-fungal interface	138
Figure 4.10	Complementation analysis of $\Delta slp1$ mutants using the <i>SLP1:GFP</i> vector	140
Figure 4.11	Introduction of the <i>SLP1</i> ²⁷⁻¹⁶² : <i>GFP</i> fails to restore the virulence phenotype of $\Delta slp1$	142
Figure 4.12	The initial 27 amino acids of Slp1 is sufficient to guide secretion	145
Figure 4.13	Schematic representation of the <i>AVR-Pia</i> ¹⁻¹⁹ <i>SLP1</i> ²⁷⁻¹⁶² : <i>GFP</i> vector	148
Figure 4.14	Replacing the Slp1 signal peptide with the N-terminal Avr-Pia signal peptide fails to re-direct the protein to the Biotrophic Interfacial Complex (BIC)	150
Figure 5.1	<i>Magnaporthe oryzae</i> avirulence effectors localise to the Biotrophic Interfacial Complex (BIC)	159
Figure 5.2	Schematic representation of the strategy used to generate the <i>toxA</i> :RFP vector	168
Figure 5.3	Construction and confirmation of the <i>toxA</i> :RFP vector	169
Figure 5.4	Southern blot analysis of putative <i>toxA</i> :RFP transformants	170
Figure 5.5	Plants expressing the LTi6B:GFP vector localise GFP to the plant plasma membrane	172
Figure 5.6	Schematic representation of the cloning strategy for generating the PIP2a:GFP fusion vector in the pCAMBIA 1302 plant expression vector	174
Figure 5.7	Confirmation of the PIP2a:GFP fusion construct in the plant expression vector pCAMBIA 1302 by diagnostic digests	175
Figure 5.8	Plants expressing the PIP2a:GFP vector localise GFP to the plant plasma membrane	177
Figure 5.9	Epidermal plant cells expressing the GFP:HDEL construct enables the visualisation of a highly dynamic and intricate network of plant endoplasmic reticulum	179
Figure 5.10	The host membrane becomes invaginated during rice blast disease	181
Figure 5.11	The BIC co-localises with the host plant plasma membrane (PM)	183
Figure 5.12	The BIC partially co-localises with plant endoplasmic reticulum (ER)	185
Figure 5.13	Fungal cytoplasm is incapable of diffusing into the BIC	188
Figure 5.14	The <i>M. oryzae</i> Plasma Membrane ATPase (<i>PMA1</i>) gene encodes an H ⁺ ATPase membrane pump	190
Figure 5.15.	Schematic representation of the cloning strategy used to generate the <i>PMA1:GFP</i> vector	194
Figure 5.16	Visualisation and localisation of the Pma1:GFP marker during <i>in vitro</i> vegetative growth	195
Figure 5.17	The BIC resides outside the fungal plasma membrane	197
Figure 5.18	Using the <i>Oryza sativa</i> cv. <i>sasanishiki</i> cultivar for studying compatible and incompatible interactions	199

Figure 5.19	During an Incompatible HR, the host nucleus as demonstrated by perinuclear ER is recruited to the site of appressorium formation	201
Figure 6.1	Model describing the relationship between Slp1 and CEBiP	214

List of Tables

Table 3.1	Oligonucleotide primers used in the targeted gene deletion of <i>SLP1</i>	70
Table 3.2	Oligonucleotides primers used in the targeted gene deletion of <i>SLP2</i>	74
Table 3.3	Oligonucleotide primers used in the amplification of <i>SLP1</i> cDNA	105
Table 5.1	Plant expression vectors used for transformation in this study	164

Acknowledgements

I would first of all like to thank the Gatsby Charitable Foundation for their generous funding and support which enabled me to carry out this research. I would like to thank Nick Talbot for all his supervision, advice and patience during this research. Special thanks go to the rest of lab 301 for the feedback and advice on this project, particularly Lauren Ryder for all her feedback on this thesis. I would like to acknowledge Bart Thomma and Anja Kombrink at the University of Wageningen for being excellent hosts during my stay in the Netherlands and for their significant contribution to the project. I would like to thank Hiromasa Saitoh, Ryohei Terauchi and all the technicians at the Iwate Biotechnology Research Center in Japan for generating the transgenic rice lines presented in Chapter 5. Many thanks go to all our other collaborators on this project, including Ippei Otomo, Tomonori Shinya, Yoko Nishizawa and Naoto Shibuya for their significant contributions. I would finally like to thank all my friends and family, particularly my parents and brother Dave for their continual love and support throughout my life. Most notably, however, I would like to thank my fiancée Bekki Morson for all her love, and especially for her patience for all the times she listened to me complaining about failed experiments and PCRs, of which there were many.

Abbreviations

bp	base pair
cAMP	cyclic 3', 5' adenosine monophosphate
cDNA	complementary DNA
CM	complete medium
°C	degrees Celcius
ddH ₂ O	double distilled water
DNA	deoxyribonucleic acid
g	grams
gL ⁻¹	grams per litre
H ₂ O ₂	hydrogen peroxide
kb	kilobase
L	litre
µg	microgram
µl	microlitre
µm	micrometre
MAPK	mitogen-activated protein kinase
mg	milligram
mL	millilitre
mm	millimetre
mM	millimolar
mRNA	messenger RNA
NADPH	nicotinamide adenine dinucleotide phosphate
ng	nanogram
ORF	open reading frame
PCR	polymerase chain reaction
%	percentage
% w/v	percentage weight by volume
% v/v	percentage volume by volume
RNA	ribonucleic acid
RNase	ribonuclease
ROS	reactive oxygen species
rpm	revolutions per minute

Chapter 1. General introduction

1.1 Global significance of plant disease

By 2050, the global human population is predicted to reach more than 9 billion, which represents a 6-fold increase since the year 1900 (Food and Agricultural Organization, 2009). Global food production will have to increase approximately three-fold over the next fifty years to meet this demand (Godfray *et al.*, 2010). During the mid-20th century, semi-dwarf rice indica lines were cross-bred into high-yielding rice cultivars, resulting in yield increases of approximately ten times that of traditional rice, in what is now referred to as the “green revolution” (De Datta *et al.*, 1968). Research has focussed to attempt to create the “next green revolution”, which includes research into modifying leaf architecture by genetic engineering enabling more efficient photosynthesis in important crop species (Hibberd *et al.*, 2008; Langdale, 2011). Improvements in techniques used to generate genetically engineered plant species, such as *Agrobacterium*-mediated transformation, may contribute to future efforts to generate more efficient genetically modified crops (Heie and Komari, 2008). Future applications for crop improvement using GM technology include the introduction of nitrogen-fixing genes into cereal crops, improving salinity and drought tolerance, and improving resistance against fungal, viral and bacterial pathogens (Royal Society of London, 2009; Godfray *et al.*, 2010).

It is estimated that plant disease is responsible for average global yield losses of approximately 10 % among significant crop species (Strange and Scott, 2005; Busa *et al.*, 2010). Global rice production recently reached approximately half a billion tonnes each year, the staple food crop of more than 3 billion people who are dependent on rice as their main source of calorific intake (Goff, 1999). As global human populations increase, rice yields will have to double by 2050 in order to meet global demand (Godfray *et al.*, 2010).

1.2 Rice blast disease

Rice blast disease is caused by the filamentous heterothallic ascomycete fungus *Magnaporthe oryzae* (Hebert) Barr [anamorph: *Pyricularia oryzae* Sacc.] (Barr, 1977). *M. oryzae* is capable of infecting and causing disease on more than 50 species of grass including a number of economically important crop species such as rice (*Oryza sativa*), barley (*Hordeum vulgare*), wheat (*Triticum aestivum*) and finger millet (*Eleusine coracana*) (Talbot, 2003). It has also been reported that *M. oryzae* is capable of infecting other agriculturally significant crop species including wheat (Silva *et al.*, 2009). Wheat blast disease first appeared in Brazil in the state of Paraná in 1985, where it is now one of the most significant diseases of wheat owing to a lack of suitable fungicides (Urashima and Kato, 1994; Urashima *et al.*, 2004). It is estimated that between 10 - 30% of the rice harvest is lost annually due to rice blast disease, making rice blast one of the most significant threats to global food security (Zeigler *et al.*, 1994; Skamnioti and Gurr, 2009). In Bhutan in 1995 for example, *M. oryzae* alone was responsible for a loss of over 1000 tonnes of the rice harvest over an area of 45,000 hectares (Thinlay *et al.*, 2000). *M. oryzae* is capable of infecting all aerial parts of a plant including the stem, nodes, neck and panicle (Wilson and Talbot, 2009). It has also been reported that *M. oryzae* is able to infect the root system and spread systemically in rice plants (Sesma and Osbourn, 2004; Marcel *et al.*, 2010). In addition to rice, *M. oryzae* is able to cause disease more than fifty other grass species, including finger millet (*Eleusine coracana*), a major food security crop in parts of sub-saharan Africa (Lenne *et al.*, 2007), as well as Triticale (*X. tritico-secale*) and barley (*Hordeum vulgare*) (Urashima *et al.*, 2004). A number of low impact control measures to reduce the impact of *M. oryzae*, including the avoidance of excess nitrogen-based fertilizers and planting disease-free seeds is rarely efficient (Skamnioti and Gurr, 2009).

The ability to culture *M. oryzae* away from its host plant *in vitro*, combined with its high genetic tractability, has made the rice blast fungus an important model organism for studying plant pathogen interactions (for reviews see Talbot, 1995; Talbot, 2003; Wilson and Talbot, 2009). The complete genome sequences of both *M. oryzae* and its rice host is now available (Dean *et al.*, 2005; International Rice Genome Sequencing Project, 2005), adding to the molecular toolkit

for studying rice blast disease and facilitating gene identification and genome-wide expression profiling (Oh *et al.*, 2008; Wilson and Talbot, 2009). The low frequency of DNA-mediated transformation in filamentous fungi has largely precluded the use of forward genetics, although the use of *Agrobacterium*-mediated transformation to generate large-scale mutant libraries recently enabled the generation of more than 20,000 mutants in *M. oryzae*, helping to identify a number of novel pathogenicity determinants in *M. oryzae* (Jeon *et al.*, 2007). Further to this, targeted gene replacement of the *KU70* and *KU80* genes in *M. oryzae*, which lack the non-homologous DNA end-joining pathway, has improved the speed at which gene replacement mutants can be generated creating a high-throughput molecular method for studying gene function (Kershaw and Talbot, 2009).

1.3 The life cycle of *M. oryzae*

The life cycle of *M. oryzae* commences when a three-celled asexual spore known as a conidium lands on the leaf surface. A diagram depicting the life cycle of *M. oryzae* is shown in Figure 1.1. Conidia are transferred to the leaf surface of new host plants by splash and/or wind dispersal of a spore inoculum (Talbot, 1995; Wilson and Talbot, 2009). An adhesive known as spore tip mucilage is released from the apical tip of the pyriform conidium which enables attachment and anchorage to the waxy hydrophobic leaf surface (Hamer *et al.*, 1988). In the presence of water, a single polarised germ tube emerges from the apical tip of the conidium approximately 2-3 hours after landing on the leaf surface. The germ tube subsequently undergoes a process known as “hooking” (Bourett and Howard, 1990), in which the germ tube becomes flattened against the leaf surface and swells slightly at the tip. It is thought that this stage is required for recognition of the plant surface prior to formation of the appressorium, a dome-shaped cell required for penetration of the plant cuticle (Bourett and Howard, 1990). In *M. oryzae*, an absence of exogenous nutrients and a hard, hydrophobic surface is required for successful formation of an appressorium (Dean, 1997). Under laboratory conditions, however, the formation of an appressorium can be induced on non-inductive surfaces when incubated in the presence of soluble cutin or lipid monomers, such as *cis*-9,10-epoxy-18-hydroxyoctadecanoic acid or 1,16-hexadecanediol respectively (Gilbert *et al.*, 1996; Talbot, 2003; Ebbole, 2007). These

biochemical and physiological cues on the leaf surface are responsible for the initiation of cell signalling cascades which ultimately lead to the formation of the appressorium. Initiation and development of the appressorium is regulated by a DNA replication dependent checkpoint and entry into S-phase of mitosis and maturation is dependent on a G2-M phase (Saunders *et al.*, 2010).

Once formed, the appressorium is a dome-shaped cell with a highly differentiated cell wall rich in chitin and containing a distinct melanised layer between the cell membrane and cell wall (Bourett and Howard, 1990). The melanin layer acts as a critical barrier to the efflux of compatible solute which accumulates inside the appressorium allowing a high internal turgor pressure to develop (Chumley and Valent, 1990; Howard *et al.*, 1991; de Jong *et al.*, 1997). Melanin deficient mutants in *M. oryzae*, including *albino*, *buff* and *rosy*, lack a melanin synthesis pathway and are consequently non-pathogenic due to an inability to develop sufficiently high concentrations of solute (Chumley and Valent, 1990). The accumulation of up to 3.2 M glycerol within the appressorium causes an influx of water into the appressorium resulting in a high internal hydrostatic pressure. This internal pressure has been estimated to be as high as 8.0 MPa, equivalent to fifty times the pressure within a car tyre, and enables a narrow penetration peg which forms at the base of the appressorium to mechanically break through the tough host cuticle (Howard *et al.*, 1991; de Jong *et al.*, 1997).

The penetration peg which emerges at the base of the appressorium grows initially within the first epidermal host cell before differentiating into a narrow primary filamentous hypha (Kankanala *et al.*, 2007). These primary hyphae subsequently differentiate into more bulbous secondary hyphae which proliferate into adjacent tissues (Bourett and Howard, 1990). After 72 hours post-inoculation, it has been estimated that fungal biomass accounts for up to 10 % of the total leaf biomass (Talbot *et al.*, 1993). At this stage, typical disease symptoms become apparent, with the formation of ellipsoidal necrotic lesions apparent on the leaf surface (Talbot, 1995; Talbot, 2003; Wilson and Talbot, 2009). Sporulation of conidia from these lesions completes the life cycle as new conidia are transferred to new host plants.

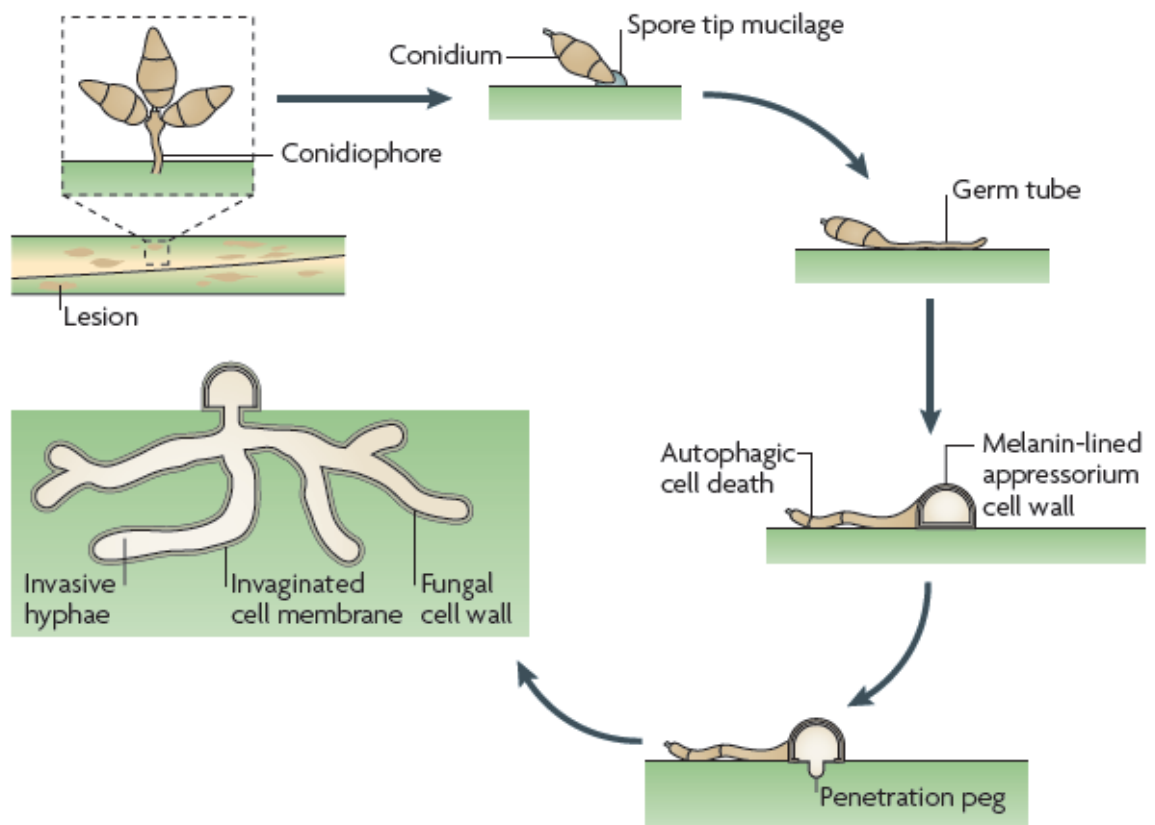


Figure 1.1 The life-cycle of the rice blast fungus *Magnaporthe oryzae*. The life cycle commences when a three-celled asexual spore known as a conidium lands and attaches to the hydrophobic leaf surface. In the presence of biochemical and physiological cues, the conidium germinates producing a narrow polarised germ tube which grows briefly before the apex of the germ tube differentiates into a melanised dome-shaped structure known as the appressorium. The generation of a high concentration of glycerol inside the appressorium causes an influx of water into the appressorium enabling high hydrostatic pressure to develop within the appressorium. A narrow penetration peg which develops at the base of the appressorium enables penetration of the tough leaf cuticle by mechanical force. This penetration peg differentiates into a primary filamentous hyphae which grow and differentiate into bulbous pseudohyphae which proliferate and ramify within the epidermal host tissue. After 96 hours, typical necrotic disease lesions form. The life cycle is completed as the fungus sporulates from lesions, resulting in the transfer of conidia to new host plants. Figure taken with permission from Wilson and Talbot, 2009.

1.4 Appressorium-mediated development in *M. oryzae*

1.4.1 Cyclic AMP signalling

To generate an appressorium, *M. oryzae* must detect and respond to physiological and biochemical cues to co-ordinate and ensure that the appressorium develops on an appropriate host cell surface (Gilbert *et al.*, 1996). During these early stages of infection-related development, a number of signal transduction cascades are activated, and a number of studies have confirmed the role of a cyclic AMP (cAMP) pathway in surface recognition and regulation of appressorium formation (Mitchell and Dean, 1995; Choi and Dean, 1997). A gene encoding a putative adenylate cyclase known as *MAC1* is thought to be involved in the initiation of the cAMP pathway. Targeted gene replacement of *MAC1* results in null mutants that are unable to form a functional appressorium, and are consequently unable to cause disease (Choi and Dean, 1997). Significantly, appressorium formation and pathogenicity can be restored in $\Delta mac1$ mutants by addition of exogenous cAMP, confirming the significance and role of Mac1 in the generation of cAMP (Adachi and Hamer, 1998; Choi and Dean, 1997). The addition of cAMP can also induce appressorium formation on non-inductive surfaces (Gilbert *et al.*, 1996). Another gene which is thought to be involved in host surface recognition in *M. oryzae* is the secreted class I hydrophobin *MPG1*, which is highly expressed during germ tube extension (Talbot *et al.*, 1993; Kershaw and Talbot, 1998). Targeted gene replacement of *MPG1* results in mutants that are unable to cause disease, although restoration of pathogenicity can be achieved by the addition of exogenous cAMP, suggesting that attachment of the germ tube is required for initiating signalling cascades during appressorium formation (Talbot *et al.*, 1993). It is thought that cAMP generated by Mac1 can interact with the regulatory subunit of cAMP dependent protein kinase, encoded by the *M. oryzae* *PKA* gene (Choi and Dean, 1997). Inactivation of the Pka regulatory subunit results in cAMP-independent activation of CpkA, the catalytic subunit of PKA encoded by the *CPKA* gene, resulting in restoration of the $\Delta mac1$ appressorium phenotype as a result of over-riding of the cAMP signalling pathway (Adachi and Hamer, 1998).

Other genes involved in surface recognition leading to appressorium formation have been identified, including *PTH11*, which encodes a membrane-localised receptor protein thought to be involved in detecting surface hardness and hydrophobicity (De Zwaan *et al.*, 1999). Pth11 is an integral G-protein coupled receptor protein containing seven transmembrane domains and an extracellular cysteine-rich EGF-like domain (Kulkarni *et al.*, 2005). Such G-protein coupled receptors are heterotrimeric proteins comprised of α , β and γ subunits which, upon detection of surface signals, relay information and initiate the cAMP response and other signalling pathways (Bölker, 1998). cAMP generated by the adenylate cyclase Mac1 activates cAMP-dependent protein kinase A (PKA), a tetrameric holoenzyme which phosphorylates downstream targets (Kronstrad, 1997). Results obtained to date suggest that activation of PKA is required for successful appressorium-mediated development (Wilson and Talbot, 2009).

1.4.2 MAPK signalling

In addition to the role of cAMP signalling, mitogen-activated protein kinases (MAPKs) also play a crucial role in signalling pathways of pathogenic fungi (Xu, 2000). MAPK signalling cascades are important in eukaryotes to relay extracellular signals received at the cell membrane to the nucleus where they phosphorylate and thereby activate transcription factors (Xu, 2000). MAPKs are regulated by phosphorylation of a MAPK kinase (MAPKK), which are in turn regulated by phosphorylation of a MAPKK kinase (MAPKKK). Three MAPK signal transduction pathways have been identified in the *M. oryzae* genome, and all of which have been identified as key determinants for regulating infection-related development (Rispaill *et al.*, 2009). In *M. oryzae*, the *PMK1* gene encodes homologues of the *Saccharomyces cerevisiae* mitogen activated protein kinases Fus3 and Kss1. Targeted replacement of the *PMK1* gene in *M. oryzae* results in null mutants that are unable to form appressoria, and are non-pathogenic, even when a spore inoculum is used to infect wounded leaf tissue (Xu and Hamer, 1996). Activation of the Pmk1 MAPK pathway is thought to occur through Mst7 and Mst12, proteins which are homologues of the *S. cerevisiae* proteins Ste7, a MAPKK, and Ste11, a MAPKKK (Zhou *et al.*, 2005). Targeted gene replacement of both *MST7* and *MST12*-encoding genes results in mutants that are non-pathogenic and are unable to form appressoria, even on normally

inductive hydrophobic surfaces (Zhou *et al.*, 2005). Although a direct interaction between Mst7 and Pmk1, and Mst12 and Pmk1 could not be determined, Mst7 and Mst11 were shown to have a weak interaction in a yeast two-hybrid screen (Zhou *et al.*, 2005). Interestingly, a homologue of the *S. cerevisiae* Ste50 protein, known as Mst50, was found to interact directly with both Mst7 and Mst12, and may act as an adaptor protein upstream in the Pmk1-Mst7-Mst12 signalling cascade (Zhou *et al.*, 2005; Park *et al.*, 2006). No Mst50-Pmk1 interaction could be determined, however (Park *et al.*, 2006). Both Mst12 and Ste50 contain an N-terminal sterile α -motif (SAM), and proteins containing a SAM domains have previously been shown to interact directly with each other (Park *et al.*, 2006). A direct interaction using bimolecular fluorescence complementation has been reported between Mst7 and Pmk1 during appressorium formation (Zhao and Xu, 2007).

1.5 Biotrophic growth and host-cell colonisation of *M. oryzae*

After rupturing the host cuticle, a penetration peg differentiates into a narrow filamentous primary hypha. *M. oryzae* is a hemibiotrophic fungus, meaning that the fungus initially undergoes a period of biotrophic growth in which the fungus proliferates and obtains nutrients from living plant tissue without causing disease symptoms, before later switching to a necrotrophic lifestyle in which the fungus derives nutrients by killing plant cells. Genetic determinants of this switch in lifestyles have yet to be determined (Talbot, 2003). After rupturing the plant cuticle, the host plasma membrane is not breached, but instead becomes invaginated to accommodate fungal invasive hypha, establishing an intimate host-pathogen interface known as the Extra Invasive Hyphal Membrane (EIHM) (Kankanala *et al.*, 2007). This host-derived EIHM becomes tightly sealed around the invasively growing hyphae which continue to grow and proliferate within the initial epidermal host cell. The inability of the amphiphilic sterol dye FM4-64 to label the EIHM suggests that this membrane is sealed around invasive fungal hyphae and is a separate compartment to the bulk apoplast (Kankanala *et al.*, 2007). Apoplastically-applied FM4-64 initially labels the plant plasma membrane and eventually moves into internal cellular membranes by a time-dependent endocytotic process before finally labelling the vacuoles (Kankanala *et al.*, 2007). Further to this, plasmolysis assays

in which infected host tissue was treated with hyperosmotic sucrose solutions demonstrate that the EIHM remains intact during biotrophic growth. This is consistent with the hypothesis that rice cells remain viable during early *M. oryzae* infection when biotrophy is occurring (Kankanala *et al.*, 2007). The EIHM was recently visualised directly using transgenic rice plants which target GFP to the plant plasma membrane, demonstrating experimentally that the rice plasma membrane is tightly opposed against intracellular fungal hyphae (Mentlak *et al.*, 2012a). Secondary bulbous hyphae continue to grow within the initial epidermal host cell until the host cell becomes completely occupied by fungal hyphae. Live-cell imaging at this time point revealed that hyphae undergo extreme constriction when moving into adjacent host cells. Transient expression in infected host cells of fluorescently-labelled tobacco mosaic virus MP:GFP and FM4-64-treated fungal cells suggests that *M. oryzae* might exploit plasmodesmata at pit field sites in order to colonise neighbouring host cells (Kankanala *et al.*, 2007). Consistent with this idea, is the observation that *M. oryzae* is unable to colonise stomatal guard cells which lack plasmodesmata (Kankanala *et al.*, 2007). Immediately after crossing the plant cell wall into a neighbouring host cell, fungal hyphae grow initially as narrow filamentous hyphae before differentiating into bulbous pseudohyphae (Kankanala *et al.*, 2007).

Several independent lines of evidence suggest that the rice host plasma membrane becomes invaginated during intracellular growth (Kankanala *et al.*, 2007; Marcel *et al.*, 2010; Mentlak *et al.*, 2012a). It is not currently known, however, whether the nature of the invaginated EIHM protein structure differs to that of the bulk rice plasma membrane. Biotrophic oomycete pathogens such as *Phytophthora infestans* and *Hyaloperonospora arabidopsidis* develop specialised pathogenic hyphae known as haustoria which are required for the acquisition of nutrients during biotrophic growth (O'Connell and Panstruga, 2006). Haustoria are surrounded by a membrane known as the Extra-Haustorial Membrane (EHM), and several studies have demonstrated that the EHM differs in structure to that of non-infected plant plasma membrane, with particular enrichment of pathogenesis-related membrane proteins (Micali *et al.*, 2011; Lu *et al.*, 2012). During *M. oryzae* infection, it is not currently known how the EIHM differs in structure to that of non-infected rice plasma membrane.

1.6 The role of effector proteins in *M. oryzae*

During biotrophy, effector proteins are secreted by *M. oryzae* which are thought to act to suppress host defence responses (Mosquera *et al.*, 2009; Khang *et al.*, 2010; Valent and Khang, 2010). The number of secreted proteins by *M. oryzae* based on the presence of an N-terminal secretion peptide and SignalP 3.0 analysis has been estimated to be as high as 1546, which represents approximately 12 % of the total number of predicted proteins encoded by the *M. oryzae* genome (Dean *et al.*, 2005; Soanes *et al.*, 2008). Although several lines of evidence have been presented to suggest that rice blast effectors are delivered into the host cytoplasm (Jia *et al.*, 2000; Khang *et al.*, 2010), it is not currently known, however, how these effectors proteins are transported from the fungal cytoplasm through the fungal cell wall and across the EIHM (Mentlak *et al.*, 2012b). Moreover, the precise function of these effector molecules and their role in causing disease has yet to be determined. One of the best characterised *M. oryzae* effector proteins is Avr-Pita which confers avirulence activity and induces resistance responses on rice cultivars expressing the corresponding resistance gene (R) product Pita. In a yeast-two hybrid screen, Avr-Pita and Pita have been shown to interact directly, suggesting that Avr-Pita is delivered by *M. oryzae* across the EIHM and into the host cytoplasm (Jia *et al.*, 2000). Transient expression of Avr-Pita in rice cells induces an HR in plants expressing Pita, providing further support to *in vitro* observations that Avr-Pita and Pita do indeed interact in the host cytoplasm (Jia *et al.*, 2000). Avr-Pita encodes a small peptide of 233 amino acids which is similar in structure to class 35 deuterolysin neutral zinc proteases (Orbach *et al.*, 2000). Although Avr-Pita is predicted to encode a putative metalloprotease (Jia *et al.*, 2000; Orbach *et al.*, 2000), its precise function has yet to be established.

A number of other *M. oryzae* effector proteins have been shown to AVR activity. The *PWL* gene family (Pathogenicity towards Weeping Lovegrass) were identified based on their ability to trigger non-host resistance responses in weeping lovegrass (*Eragrostis curvula*) (Sweigard *et al.*, 1995; Kang *et al.*, 1995). Pwl proteins are small glycine-rich proteins which are highly expressed and secreted specifically during biotrophic growth and which appear to be translocated into host cytoplasm (Schneider *et al.*, 2010; Khang *et al.*, 2010).

Map-based cloning has been an important molecular tool for the identification and cloning of a number of *M. oryzae* effector proteins, including *AVR-Piz-t*, which in addition to conferring avirulence activity on cultivars carrying the resistance gene *Piz*, also inhibits Bax-triggered cell death in transient assays in *Nicotiana benthamiana* (Li *et al.*, 2009). An array of genetic techniques have been implemented for the identification of *M. oryzae* effector proteins. Association genetics, for example, was recently used in the identification of *AVR-Pia* and *AVR-Pii* (Yoshida *et al.*, 2009). Both *AVR-Pia* and *AVR-Pii* are small secreted proteins (85aa and 70aa respectively), and confer avirulence on rice cultivars expressing the R genes *Pia* and *Pii* respectively (Yoshida *et al.*, 2009). Although a number of effector molecules with Avr activity have been described, more than 80 rice blast resistance genes have been identified, suggesting that many more *M. oryzae* Avr effectors remain to be identified (Ballini *et al.*, 2008).

Although effector molecules with Avr activity have been discussed, some *M. oryzae* effectors have been described which do not have avirulence activity and the functional role of many of these effectors has yet to be determined (Mosquera *et al.*, 2009). Using a sensitive laser-microdissection technique for extracting RNA from infected rice tissue, a number of putative effector candidates were identified based on their differential expression pattern during biotrophic growth compared with growth in axenic culture (Mosquera *et al.*, 2009). These genes, which are referred to as Biotrophy Associated Proteins 1-4 (BAS1-4), were shown to be more than 50-fold up-regulated during biotrophic growth compared to growth *in vitro* (Mosquera *et al.*, 2009). Although their pattern of localisation has been investigated, the function of all Bas proteins remains to be determined (Mosquera *et al.*, 2009).

1.7 Localisation of rice blast effector proteins during biotrophic growth

To investigate the localisation of *M. oryzae* effector proteins during intracellular biotrophic growth, genetically engineered strains of *M. oryzae* have been developed which express translational fusions of the effector protein to fluorescent marker proteins. The use of such fluorescent marker proteins, such as Green Fluorescent Protein (GFP) and its allelic variants, has greatly advanced our understanding of protein localisation and tracking *in vivo* (Reiser *et*

al., 1999; Bruno *et al.*, 2004; Mosquera *et al.*, 2009; Khang *et al.*, 2010). Indeed, GFP has been used widely in the study of protein localisation in a number of fungal pathogens such as the corn smut fungus *Ustilago maydis* (Spellig *et al.*, 1996), and has also been a useful marker for studying protein localisation in *M. oryzae* (Kershaw *et al.*, 1998; Egan *et al.*, 2007; Mosquera *et al.*, 2009; Saunders *et al.*, 2010; Khang *et al.*, 2010). These genetically engineered marker strains have demonstrated that effector proteins with Avr activity, including Avr-Pita, Pwl2 and Avr-Pia all accumulate at a bulbous membrane-rich structure at the plant-fungal interface, referred to as the Biotrophic Interfacial Complex (BIC) (Mosquera *et al.*, 2009; Yoshida *et al.*, 2009; Khang *et al.*, 2010). Bas1 has also been shown to accumulate at the BIC, although a functional role for Bas1 has yet to be determined (Mosquera *et al.*, 2009). In contrast, Bas4, a putative apoplastic effector protein has been shown to accumulate uniformly around the periphery of invasive fungal hyphae and demonstrates only weak BIC localisation (Mosquera *et al.*, 2009). Plasmolysis assays have demonstrated that Bas4 is most likely an apoplastic effector protein which accumulates between the invaginated EIHM and the fungal cell wall (Khang *et al.*, 2010). Another putative effector, Bas3, was shown to accumulate at cell-wall crossing points and underneath the appressorium (Mosquera *et al.*, 2009).

As stated, the BIC is a bulbous membrane-rich structure tightly apposed to the side of invasively growing fungal hyphae. The BIC initially develops at the tip of a primary filamentous hypha, suggesting that the secretion of effector proteins at this time involves the Spitzenkörper, polarisome and exocyst components for polarised secretion and exocytosis (Virag and Harris, 2006; Steinburg, 2007; Shoji *et al.*, 2008). However, as the fungus differentiates to form secondary pseudohyphae, the BIC remains seemingly attached to the fungal hyphae, which is now at a sub-apical position, but continues to accumulate fluorescently-labelled effector proteins (Mosquera *et al.*, 2009). Surprisingly, Fluorescence Recovery After Photobleaching (FRAP) experiments have demonstrated that effector proteins continue to accumulate into a sub-apical BIC (Khang *et al.*, 2010). This suggests that the original apical secretory apparatus might continue to direct effector proteins to the BIC using conventional ER-related secretory components after cellular differentiation of the fungus from a filamentous to a

pseudohyphal morphology (Valent and Khang, 2010). Interestingly, only the N-terminal secretion peptide and the upstream promoter region of effectors have been shown to contribute to BIC-localisation (Mosquera *et al.*, 2009). By contrast, the mature protein does not contribute to preferential BIC localisation (Mosquera *et al.*, 2009).

1.8 Translocation and delivery of *M. oryzae* effector proteins during biotrophic growth

To date, the best characterised *M. oryzae* effector protein is the putative metalloprotease Avr-Pita (Jia *et al.*, 2000). Initial *in vitro* assays using a yeast two-hybrid screen demonstrated that Avr-Pita is able to interact directly with the rice resistance gene Pita, providing the first evidence that *M. oryzae* effector proteins have targets within the rice host cytoplasm (Jia *et al.*, 2000; Orbach *et al.*, 2000). Live-cell imaging of *M. oryzae* strains expressing fluorescently labelled *PWL2:mRFP* revealed that effector proteins can be observed directly in the host cytoplasm by epifluorescence imaging (Khang *et al.*, 2010). Plasmolysis assays, in which infected epidermal tissue was treated with a hyperosmotic sucrose solution, resulted in accumulation and concentration of Pwl2:mRFP in the shrinking rice protoplast and could be readily detected by confocal fluorescent imaging (Khang *et al.*, 2010). Attachment of a host nuclear-localisation signal (NLS) to the C-terminus of *PWL2:mRFP* resulted in accumulation of a fluorescent signal in the host nucleus, providing further support that *M. oryzae* effector proteins are delivered into rice cells (Khang *et al.*, 2010). Pwl2:mRFP could also be detected in neighbouring host cells distal to the current infected host cell, suggesting that translocated effector proteins are capable of cell-to-cell movement, potentially via plasmodesmata (Khang *et al.*, 2010; Valent and Khang, 2010). The extent of systemic movement of delivered *M. oryzae* effector proteins is dependent on the molecular weight of the protein, and might be a means of priming adjacent cells for future cell colonisation (Khang *et al.*, 2010). Fluorescently labelled *PWL2:tdTomato* for example, with a molecular weight of 68 kD, was rarely observed in adjoining non-invaded neighbouring rice cells. In contrast, *PWL2:mRFP*, with a smaller molecular weight of 39 kD, could frequently be observed non-invaded neighbouring host cells, suggesting that systemic movement of *M. oryzae* effector proteins is dependent on molecular weight (Khang *et al.*, 2010). Current evidence also suggests that the extent of movement of

translocated effector proteins is dependent on host cell type, with a greater degree of systemic movement from “vein-associated” infection sites compared to “regular” epidermal leaf cells (Khang *et al.*, 2010). The reasons for differential systemic movement is not clear at this stage, but it is hypothesised that this can be explained by differences in plasmodesmal aperture (Valent and Khang, 2010; Mentlak *et al.*, 2012b). Interestingly, transient expression of *AVR-Pia* and *AVR-Pii* in rice protoplasts induces an HR (Hypersensitive Response), providing additional biochemical evidence that effector proteins with avirulence activity are delivered into the rice cytoplasm (Yoshida *et al.*, 2009).

Interestingly, attachment of an NLS-coding sequence to BAS4:GFP did not result in accumulation of a fluorescent signal at the host nucleus and fluorescence continued to localise at the tips of biotrophic hyphae (Mosquera *et al.*, 2009; Khang *et al.*, 2010). Further to this, plasmolysis assays demonstrated that Bas4:GFP could be observed accumulating in the space between the plant cell wall and the membrane of the shrinking rice protoplast (Khang *et al.*, 2010). These two lines of evidence support a role for Bas4 in the apoplastic space between the EIHM and the fungal cell wall (Khang *et al.*, 2010; Valent and Khang, 2010).

1.9 Molecular secretion apparatus in filamentous fungi

1.9.1 The molecular components required for secretion and exocytosis in *M. oryzae*

In plant pathogenic bacteria, the type III secretion system is a well characterised pilus structure required for the delivery of virulence-promoting effector proteins from bacteria residing in the apoplastic space to the plant cytoplasm (Alfano and Collmer, 2004; Lindeburg *et al.*, 2005). The tomato pathogen *Pseudomonas syringae* pv. tomato DC3000, for example, is known to deliver approximately 30 type III effector proteins by this means, which are thought to be responsible for disrupting host immune responses (for reviews see Alfano and Collmer, 2004; Martin, 2012). Although a great deal is understood about the molecular mechanisms of delivery of bacterial effector proteins using the type III secretion mechanism, an analogous structure for delivery of fungal effector proteins has yet to be identified (Caracuel-Rios and Talbot, 2008). Despite this, research on oomycete pathogens, such as the late blight pathogen *Phytophthora*

infestans, is starting to reveal how fungal pathogens such as *M. oryzae* might deliver effector proteins into their host cells (Kamoun, 2006). The RXLR motif (Arg, any amino acid, Leu, Arg), for example, is a conserved molecular motif found in a number of oomycete species which is essential for translocation of effector proteins across the oomycete membrane and into host cells (Whisson *et al.*, 2007; Win *et al.*, 2007; Birch *et al.*, 2009). The RXLR motif may enable binding to phosphatidylinositol-3-phosphate (PI3P), a phospholipid which is abundant on the outer surface of plant and animal plasma membranes to mediate entry of the effector protein into the host cell (Kale *et al.*, 2010). Inhibition of PI3P prevented uptake of the *Phytophthora sojae* RXLR-dEER AVR1b effector protein into both animal and plant cells, suggested that PI3P-mediated binding is required for endocytosis into host cells (Kale *et al.*, 2010). More recent evidence has, however, challenged the hypothesis of the RXLR-PIP interaction (Ellis and Dodds, 2011). In filter-binding assays, mutations in the RXLR motif of the *P. sojae* effector AVR1b and the *P. infestans* effector protein AVR3a did not disrupt interactions with PIPs and conclude that the RXLR motif does not bind PIPs (Yaeno *et al.*, 2011). In contrast, Yaeno *et al.*, (2011) report that mutations of positively charged amino acids within the alpha-helices of AVR1b and AVR3a significantly diminish or abolish binding to PIPs. Screening of the *M. oryzae* genome failed to find an analogous RXLR motif in secreted effector proteins (Soanes *et al.*, 2008), although there is partial evidence of two motifs; an [LI]xAR[SE][DSE] motif in the novel effector Avr-Piz-t and an [RK]CxxCx₁₂H motif in Avr-Pia (Yoshida *et al.*, 2009; Oliva *et al.*, 2010). A role for either of these motifs for the delivery of *M. oryzae* effector proteins has yet to be determined.

Although relatively little is known about how *M. oryzae* secretes effector proteins into host cells, protein secretion in filamentous fungi involves endoplasmic reticulum (ER)-dependent and Golgi secretory apparatus (Steinberg, 2007; Shoji *et al.*, 2008). During polarised exocytosis of filamentous fungi, proteins are packaged into secretory vesicles having been directed through the secretory pathway involving the ER and Golgi apparatus. Protein secretion commences when translated proteins containing an N-terminal secretion peptide are directed into the ER lumen for post-translational modification including protein folding and glycosylation. Within

the ER lumen, peptides are packaged into vesicles and directed to the Golgi apparatus for further modification, before being trafficked via cytoskeletal components to the plasma membrane for exocytosis.

In *M. oryzae*, putative type IV aminophospholipid translocases belonging to the P-type ATPase family may have a role in effector delivery (Gilbert *et al.*, 2006; Wilson and Talbot, 2009). *MgAPT2* encodes an aminophospholipid translocase which is involved for maintaining the symmetrical distribution of aminophospholipids along cellular membranes. Interestingly, $\Delta apt2$ mutants are able to form functional appressoria, but are unable to cause disease symptoms or secrete extracellular enzymes. Significantly, $\Delta apt2$ mutants are also unable to induce an Avr-Pita/Pita incompatible response on the rice cultivar IR-68, suggesting that Apt2 has a potential role in effector delivery into rice cells (Gilbert *et al.*, 2006). Like other filamentous fungi, secretion of *M. oryzae* effectors is likely to involve endoplasmic reticulum-dependent secretory apparatus. The *M. oryzae* genome contains homologues of the heat shock protein (Hsp70) family, which have been shown to act as ER chaperones in yeast and direct unfolded proteins into the ER lumen (for reviews see Jensen and Johnson, 1999; Kampinga and Braig, 2010). Targeted gene replacement of *LHS1* in *M. oryzae*, a gene involved in directing proteins to the ER lumen for translational modification, results in mutants that are unable to secrete extracellular enzymes and are also unable to localise fluorescently labelled effector proteins at the BIC (Li *et al.*, 2009). Significantly, $\Delta lhs1$ mutants are also unable to induce an Avr-Pita/Pita hypersensitive (HR) response, suggesting that ER chaperone proteins are critical for appropriate protein folding and delivery into host cytoplasm.

1.9.2 The role of the Spitzenkörper in polarised exocytosis in fungi

In filamentous fungi, post-Golgi secretory vesicles are transported via kinesin motor proteins to a “vesicle organisation centre” known as the Spitzenkörper, a phase-dark refractile body found slightly adjacent to the cell apex of polarized hyphae. As well as proteins destined for the cell surface, vesicles directed to the Spitzenkörper also contain cell wall components required for hyphal cell growth and extension. The Spitzenkörper is only present in filamentous fungi of the

Pezizomycotina (such as *Aspergillus nidulans*, *Neurospora crassa* and *M. oryzae*), and is not present in yeasts (such as *Saccharomyces cerevisiae* and *Schizosaccharomyces pombe*), which either do not form true hyphae or undergo some form of pseudohyphal growth during their life cycle. The Spitzenkörper is essential for polarised growth and maintaining unidirectional movement of vesicles to the hyphal tip apex. A great deal of variation in the size and shape of vesicles which accumulate at the Spitzenkörper can be observed, and whether the contents of such “micro” and “macro” vesicles differ in nature is the subject of debate (Harris *et al.*, 2005; Virag and Harris, 2006). A number of other cell components accumulate at the Spitzenkörper, including ribosomes, microtubules and microfilaments. The Spitzenkörper can only be observed in actively growing regions of highly polarized hyphal tips, providing indirect evidence that this structure is likely to be involved in polarised growth. The temporal and dynamic nature of the Spitzenkörper within a single hypha has led some to speculate that the Spitzenkörper is merely a visual manifestation of the accumulation of vesicle and cellular movements at the hyphal tip, rather than a discrete cellular component or organelle (Virag and Harris, 2006). The Spitzenkörper is not observed when growth ceases, lending further support to this hypothesis. Little is known about the components of the Spitzenkörper, its role in infection-related development and pathogenesis in fungal pathogens, and how the Spitzenkörper is regulated and assembled (Harris *et al.*, 2005). Although genetic determinants affecting the size and shape of the Spitzenkörper have been described in filamentous fungi (Browning *et al.*, 2003; Konzack *et al.*, 2005), how the Spitzenkörper is regulated remains to be elucidated. Indeed the role of the Spitzenkörper for the delivery of *M. oryzae* effector proteins remains to be determined (Valent and Khang, 2010).

1.9.3 Establishing polarity and the role of the polarisome complex in fungal secretion

Like other filamentous fungi, *M. oryzae* localises apical growth to a distinct region of a growing cell, a process referred to as polarised growth (Steinberg, 2007). As well as being a fundamental feature of the growth of filamentous fungi (Steinberg, 2007), this asymmetrical distribution of proteins and cellular functions can be observed in all eukaryotes, ranging from the polarised growth of pollen tubules and root hairs in plants to the release of neurotransmitters at nerve

synapses in mammals (Nelson, 2003; Virag and Harris, 2006). Polarised growth is essential in many fungal pathogens for the successful invasion of host tissues and for the formation of mature mating structures (Brand and Gow, 2009). In *M. oryzae*, polarized growth can be observed during the pre-penetration stages of infection, when an axis of polarity is set up in the small germ tube that emerges from the apex of the fungal spore.

In yeast, the polarisome is a cap-shaped multi-protein complex which is located beneath the apical plasma membrane in polarised cells. The polarisome is thought to organise cytoskeletal and cellular components and direct them towards the tip apex to enable functional polarised cell extension and hyphal growth (Virag and Harris, 2006). The yeast polarisome is made up of four proteins; Bni1, Spa2, Bud6 and Pea2. One of the most significant proteins in this complex is the actin-binding formin, Bni1, which mediates directed filament assembly at the hyphal tip. Other components of the polarisome are thought to regulate the activity of Bni1 by ensuring the appropriate timing and location of its activity. Together, this protein complex is responsible for interactions with Rho-GTPases, such as the signalling protein Cdc42, to mediate the formation of unbranched linear F-actin filaments. These F-actin cables are subsequently used for the transport of exocytic vesicles from the Spitzenkörper to the hyphal membrane for exocytosis.

The release of publically available genome data of filamentous fungi has enabled the identification of homologues of the yeast polarisome complex in filamentous fungi. Although several polarisome protein homologues have been identified, it is not known whether these fungal homologues function in the same way as yeast (Virag and Harris, 2006). Although filamentous fungi possess homologues of Bni1, Spa2 and Bud6, no homologues of Pea2 have been identified (Harris and Momany, 2004). A homologue of Bni1 in *Aspergillus nidulans*, known as SepA was characterised and shown to localise to an area slightly retracted from the hyphal tip, suggesting localisation to the Spitzenkörper rather than the polarisome. Further to this, SpaA and BudA, homologues of the yeast scaffold protein Spa2 and Bud6, have been identified and characterised in the filamentous fungus *A. nidulans* (Virag and Harris, 2006). SpaA was shown to localise to the hyphal tip apex as predicted if involved in the polarisome complex, whereas BudA was found to function mainly in the formation of septa, providing

speculation that the polarisome components function differently between filamentous and non-filamentous fungi (Virag and Harris, 2006). The ability to establish multiple axes of polarity is unique to filamentous fungi, and cannot be explained by an oversimplified extrapolation of what is known in yeast (Harris and Momany, 2004). Further characterisation of polarisome components including gene functional and localisation studies are needed to further understand how the polarisome functions in filamentous fungi. Research on how the polarisome complex alters actin filaments to deliver secretory vesicles and its role in maintaining polarity is still required.

The function of the *M. oryzae* polarisome and its role in polarised growth and effector delivery is not currently understood. During the biotrophic invasion of rice cells, bulbous pseudohyphal cells of *M. oryzae* proliferate within host cells and are thought to secrete effector proteins at this stage (Kankanala *et al.*, 2007; Mosquera *et al.*, 2009). The polarisome of the opportunistic human pathogen, *Candida albicans*, for instance, is not present in pseudohyphal cells, suggesting that the polarisome components are spatially and temporally dynamic at different developmental stages and in morphologically distinct cells (for review see Berman, 2006). Whether the polarisome components are present in intracellular pseudohyphae of *M. oryzae*, and the role of the polarisome in effector delivery is not currently known. A greater understanding of the polarisome and its interacting partners is needed to understand the contribution of this complex to effector delivery. Visualisation of the polarisome components during biotrophic growth will enable a greater understanding of the role of the polarisome in *M. oryzae* for effector delivery.

1.9.4 The role of the exocyst complex in polarised exocytosis in fungi

Following delivery to the Spitzenkörper on microtubules, secretory vesicles are transported to the exocyst complex on actin cables, an octomeric protein complex required for mediating the tethering of vesicles to the plasma membrane of polarised fungal hyphae. In yeast, these eight proteins are Sec3, Sec5, Sec6, Sec8, Sec10, Sec15, Exo70 and Exo84. Components of the exocyst are highly structurally conserved between organisms, invariably characterised as a

series of helical bundles containing linked α -helices, suggestive of a common evolutionary origin of the exocyst (He and Guo, 2009). Soluble N-ethylmaleimide-sensitive factor attachment protein receptors (SNAREs), such as Snc1 and Snc2, in addition to Rho, Rab and Ral GTPases including Cdc42, Rho1 and Rho3, assist exocyst components with the fusion of exocytic vesicles to the plasma membrane (for reviews see Wu *et al.*, 2008; He and Guo, 2009). Initial tethering of a secretory vesicle is mediated by a Rab GTPase known as Sec4, which has previously been described as the “master regulator of post-Golgi trafficking” (France *et al.*, 2006). In a GTP-bound state, Sec4 binds directly to Sec15 and together they mediate the assembly and regulation of the exocyst complex (Guo *et al.*, 1999). Sec3 and Exo70 are involved in anchoring the exocyst complex to the plasma membrane, which have been shown to bind directly to phosphatidylinositol 4,5-bisphosphate (PI(4,5)P₂). Positively charged residues on Sec3 and Exo70 are required for binding to the negatively charged PI(4,5)P₂ residing in the phospholipid bilayer of the plasma membrane. Sec3 interacts with Rho1 and Cdc42, and is thought to self-assemble at polarized sites of exocytosis independently of F-actin cables. Exo70, in contrast to Sec3, interacts with Rho3 at the plasma membrane and its delivery to polarised sites of tip growth appears to be dependent on actin cables (Boyd *et al.*, 2004). Similarly, delivery of the other exocyst components to the plasma membrane is also thought to depend on actin-mediated trafficking.

The significance of the exocyst in *M. oryzae* and its role in effector delivery is currently unknown. The *M. oryzae* homolog of Rho3, a Rab GTPase which interacts with Exo70, is however a key determinant of appressorium development and $\Delta mgrho3$ mutants form abnormal appressoria and are unable to cause disease (Zheng *et al.*, 2007). Significantly, $\Delta mgrho3$ mutants are also unable to cause disease on abraded leaf tissue, suggesting that Rho3 in *M. oryzae* might have a role in the delivery of effector proteins. Cdc42 homologues have also been identified and described in *M. oryzae* and are pathogenicity determinants of disease. Null mutants of the *M. oryzae* Cdc42 form abnormal appressoria, but the precise function of Cdc42 in delivering effectors and its interaction with the exocyst is not currently known (Zheng *et al.*,

2009). The importance of other rice blast exocyst components and the role of this protein complex for delivering effector proteins is unknown.

1.10 Introduction to the current study

Research on rice blast disease has focussed almost exclusively on the genetic determinants of appressorium formation, and relatively little is known about the biotrophic growth phase and how *M. oryzae* secretes effector proteins to perturb host cell defence responses. In this study, I have attempted to investigate the mechanisms deployed by *M. oryzae* to overcome the chitin-induced defence response. To do this I characterised the function and secretion of a LysM-encoding effector gene, which I named *SLP1*, for Secreted LysM Protein 1.

In Chapter 3, recombinant Slp1 is generated and its biological function is investigated. I show that Slp1 is capable of specifically binding chitin oligosaccharides and is able to suppress the chitin-induced immune responses in rice cells, including the release of reactive oxygen species during this oxidative burst. In collaboration with others, I show that Slp1 competes with the rice pattern recognition receptor (PRR) chitin-elicitor binding protein (CEBiP) for chitin binding. Targeted gene replacement of *SLP1* was carried out, and I show that $\Delta slp1$ mutants are less able to colonise host cells, suggesting that *SLP1* is required for successful colonisation of host tissues during the biotrophic growth phase of rice blast disease.

In Chapter 4, I investigate the molecular mechanisms for secretion of Slp1. I show that Slp1 is secreted specifically during biotrophic growth and accumulates at the plant-fungal interface. Unlike symplastically-delivered *M. oryzae* effector proteins, I show that Slp1 is secreted into the apoplastic space. I demonstrate that a peptide region within the initial 27 amino acids of Slp1 is required for secretion at the hyphal tips, and the mature protein of Slp1 does not contribute to its cellular localisation.

Finally in Chapter 5, in collaboration with others, I generated a number of transgenic rice lines which target the fluorescent marker protein GFP to the rice plasma membrane and endoplasmic reticulum. Using a genetically engineered fungal strain of *M. oryzae*, I investigate the cellular nature of the Biotrophic Interfacial Complex (BIC), a structure attached to the sub-apical region

of intracellular fungal hyphae which accumulates symplastically delivered effectors during biotrophic growth. The results presented in Chapter 5 provide the first evidence that the BIC is a structure made exclusively of plant cellular material.

Partial results gained from this study have contributed to a recent publication in the January 2012 edition in the *Plant Cell*. A copy of this manuscript can be found in Appendix 1. Extracts from this chapter also contributed to the publication of a book chapter in “Effectors in Plant-Microbe Interactions”. A copy of this manuscript can be found in Appendix 2.

Chapter 2. Materials and Methods

2.1 Growth and maintenance of fungal stocks

Isolates of *Magnaporthe oryzae* used and generated in this study are stored in the laboratory of N. J. Talbot (University of Exeter). For long-term storage of fungal strains, *M. oryzae* was grown on filter paper disks (2 mm, Whatman International), which were desiccated and stored at -20 °C. Fungal strains were routinely incubated in a room with a controlled temperature and environment at 26 °C with a 12 h light and dark cycle. Fungal strains were grown on complete medium (CM) (Talbot *et al.*, 2003). CM is 10 g L⁻¹ glucose, 2 g L⁻¹ peptone, 1 g L⁻¹ yeast extract (BD Biosciences), 1 g L⁻¹ casamino acids, 0.1 % (v/v) trace elements (22 mg L⁻¹ zinc sulphate heptahydrate, 11 mg L⁻¹ boric acid, 5 mg L⁻¹ manganese (II) chloride tetrahydrate, 5 mg L⁻¹ iron (II) sulphate heptahydrate, 1.7 mg L⁻¹ cobalt (II) chloride hexahydrate, 1.6 mg L⁻¹ copper (II) sulphate pentahydrate, 1.5 mg L⁻¹ sodium molybdate dehydrate, 50 mg L⁻¹ ethylenediaminetetraacetic acid), 0.1 % (v/v) vitamin supplement (0.001 g L⁻¹ biotin, 0.001 g L⁻¹ pyridoxine, 0.001 g L⁻¹ thiamine, 0.001 g L⁻¹ riboflavin, 0.001 g L⁻¹, 0.001 g L⁻¹ nicotinic acid), 6 g L⁻¹ NaNO₃, 0.5 g L⁻¹ KCl, 0.5 g L⁻¹ MgSO₄, 1.5 g L⁻¹ KH₂PO₄, [pH to 6.5 with NaOH], 15 g L⁻¹ agar. When making liquid stocks, agar is omitted. All chemicals were obtained from Sigma unless otherwise stated.

2.1 Pathogenicity and infection related development assays

2.2.1 Plant infection assays

Unless otherwise stated, rice infections were performed using a dwarf Indica rice (*Oryza sativa*) cultivar, CO-39, which is susceptible to rice blast (Valent *et al.*, 1991). Conidia of *M. oryzae* were harvested from ten-day-old cultures grown on CM agar and suspended in 5 mL of sterile de-ionized water. The resulting conidial suspension was filtered through sterile Miracloth (Calbiochem) before being centrifuged at 5,000 x g (Beckman, JA-17) for 10 min at room temperature. The pellet was resuspended in 0.2 % gelatine (BDH) to a final concentration of 5 x 10⁴ conidia mL⁻¹. This suspension was then used in plant infections by spray inoculation using

an artist's airbrush (Badger Airbrush, Franklin Park, Illinois, USA). Rice plants were grown in 9 cm diameter pots (8 plants per pot) and three pots were inoculated when 14 days old (2-3 leaf stage). After spray-inoculation, plants were watered well and incubated in polythene bags for 48 h and grown for a further 5 d in a controlled environment chamber (REFTECH, Holland) at 24 °C with a 12 h light / dark cycle and 90 % relative humidity, as described by Valent *et al.* (1991). The formation of lesions was monitored for 3 d post inoculation and lesion density recorded 5 d post inoculation.

2.2.2 Assays for measuring germination and appressorium formation rate

Germination of conidia and subsequent appressorium formation was performed and monitored over time using a method adapted from Hamer *et al.* (1988). A conidial suspension of 5×10^4 conidia mL⁻¹ was generated in double-distilled water and inoculated onto the surface of borosilicate glass coverslips (Fisher Scientific UK Ltd.) before being incubated in a moist chamber at 24 °C. The percentage of conidia undergoing germination and appressorium formation was monitored over a period of 24 h and examined by microscopy.

2.2.3 Assays for examining intracellular infection-related development on rice leaves

To examine the intracellular growth phase of *M. oryzae*, the leaf sheath assay was performed on 3-4 week old (3-4 leaf stage) rice leaves, based on a method adapted from Kankanala *et al.* (2007). A conidial suspension at a concentration of 5×10^4 conidia mL⁻¹ was prepared in 0.2 % gelatine (BDH) and inoculated into the leaf vein using a syringe and incubated in a moist chamber at 24 °C. After a period of at least 20 h, an epidermal layer of leaf tissue was dissected using a blade before being mounted onto a slide for microscopic analysis.

2.3 Nucleic acid analysis

2.3.1 Extraction of fungal DNA

2.3.1.1 Preparing fungal material for genomic DNA extraction

Liquid cultures of *M. oryzae* were generated routinely by blending a 2 cm² plug of mycelium into 200 mL of liquid CM in a commercial blender (Waring, Christison Scientific). Cultures were incubated at 24 °C for 48 h on an orbital incubator (New Brunswick Scientific) at 150 rpm. Mycelium was harvested by filtration through two-layers of sterile Miracloth (Calbiochem) and lightly dried by blotting with paper towels (Kimberley Clark Corporation) in a sterile environment. Harvested mycelia was placed in a pre-chilled mortar and ground to a fine powder using liquid nitrogen. Powder was decanted into 1.5 mL microcentrifuge tubes before being stored at -80 °C.

2.3.1.2 Preparation of putative fungal transformants for genomic DNA extraction

When preparing small-scale DNA extraction, required for example when routinely screening putative fungal transformants following homologous recombination, an alternative protocol was employed. Agar cultures of *M. oryzae* were generated by placing a small plug of fungal mycelium onto CM agar overlaid with a cellophane disc (Lakeland). Cultures were incubated for approximately 6-8 days at 24 °C until a mat of fungal mycelium had grown over the surface of the cellophane disc. This cellophane disc carrying the mat of fungal material was then peeled back from the agar plate and placed into mortar and ground to a fine powder using liquid nitrogen. Powder was then decanted into 1.5 mL microcentrifuge tubes before being stored at -80 °C.

2.3.1.3 Fungal DNA extraction

Mycelial powder generated either by liquid culture or using cellophane discs was used for fungal DNA extraction. An aliquot of 500 µL of CTAB buffer, pre-heated to 65 °C, was added to 1.5 ml microcentrifuge tubes containing the mycelia powder and incubated at 65 °C for 30

min with regular shaking at ten minute intervals. CTAB buffer is 2 % (w/v) Hexadecyltrimethylammonium Bromide (CTAB), 100 mM Tris base, 10 mM Ethylenediaminetetraacetic acid (EDTA) and 0.7 M NaCl. An equal volume of chloroform:pentanol (24:1) was added and the tubes shaken vigorously for 30 min at room temperature. Following centrifugation of the samples at 17,000 x g for 10 min using a microfuge (IEC, Micromax), the supernatant was transferred to a fresh sterile 1.5 mL microcentrifuge tube. The chloroform:pentanol extraction was repeated twice by adding an equal volume of chloroform:pentanol (24:1) to the solution and mixing by vigorous shaking. The aqueous upper phase was removed and transferred to a fresh tube before adding an equal volume of isopropanol to precipitate the nucleic acids. Samples were incubated at -20 °C for 10 min before being centrifuged in a microcentrifuge at 17,000 x g for 10 min (IEC, Micromax). The isopropanol was removed gently and the resulting nucleic acid pellet was dried and re-suspended in 500 µL of TE and then re-precipitated using 0.1 volume of 3 M sodium acetate (pH 5.2) and two volumes of 100 % (v/v) ethanol. Purified nucleic acid was recovered by centrifugation at 17,000 x g (IEC, Micromax) for 10 min and washed with 500 µL of 70 % (v/v) ethanol. The nucleic acid pellet was then air-dried for 10 min in a vacuum rotary desiccator and resuspended in 30 µL of water (Sigma) containing 4 µL of DNase-free pancreatic RNase (20 µg mL⁻¹; Promega). Purified samples of genomic DNA were stored at -20 °C.

2.3.2 Extraction of fungal and plant RNA

2.3.2.1 Preparation for RNA extraction

To prevent RNA degradation due to contaminating RNase enzymes, equipment was routinely autoclaved at 121°C for 15 min, and solutions made with double-distilled water treated with Diethyl pyrocarbonate (DEPC, Sigma) prior to use. DEPC-treated water was prepared by adding 0.1 % (v/v) DEPC to double distilled water and incubating overnight at 37 °C. Residual DEPC was removed by autoclaving the solution prior to use.

2.3.2.2 Extraction of total *M. oryzae* and plant RNA

For axenic fungal RNA extraction, RNA was prepared from either liquid cultures, or from infected plant tissue using the method described in Section 2.2.1. For plant RNA extraction, RNA was extracted from fourteen-day-old plants (2-3 leaf stage). In the case of RNA extraction from axenic fungal culture, liquid cultures were generated by blending a 2 cm² plug of mycelium from an agar plate in 200 mL of liquid CM. Cultures were grown for 48 h with 150 rpm aeration at 24 °C on an orbital aerator. Fungal mycelium was harvested by filtering the culture through two layers of sterile Miracloth before being blotted dry with paper towels. Mycelium was then ground to a fine powder using a mortar and liquid nitrogen. In the case of RNA extraction from infected or non-infected plant tissue, 2-3 leaves were routinely used and were ground to a fine powder using liquid nitrogen and a mortar. After grinding with liquid nitrogen, the powder was transferred to a fresh 50 mL Oakridge tube (Lakeland) containing 5 mL of RNA extraction buffer (0.1 M LiCl, 0.1 M Tris [pH 8], 10 mM EDTA, 1 % SDS) and 5 mL of phenol. The tubes were then mixed by inverting for 60 s. 5 mL of chloroform was added before mixing the tubes again by inverting for 30 s before finally being centrifuged at 15,700 x g (Beckman J2-MC, JS13.1) for 30 min at 4 °C. The upper aqueous phase was transferred to a fresh Oakridge tube before adding 1 volume of 4 M LiCl before incubating the sample overnight at 4 °C. The sample was centrifuged for 20 min (15,700 x g, 4 °C, Beckman J2-MC, JS13.1) and the pellet washed with 5 mL of 70 % (v/v) ethanol before being resuspended in 500 µL of DEPC-treated water. The sample was then transferred to a fresh 1.5 mL Microfuge tube (Microfuge tube UK Ltd.) containing 500 µL phenol:chloroform:isoanol alcohol and mixed by inverting for 30 s before centrifugation at 17,000 x g at 4 °C for 10 min (Z 323K, Hermle). The upper aqueous phase was transferred to a fresh microfuge tube and the RNA precipitated by addition of 0.1 volume of 3 M sodium acetate (pH 5.2) and two volumes of 100 % (v/v) ethanol. Samples were stored at -20 °C overnight. RNA was recovered by centrifugation at 17,000 x g (4 °C) for 20 min. The resulting RNA pellet was then washed with 70 % (v/v) ethanol, air-dried and re-suspended in 100 µL of DEPC-treated water before storage at -80 °C.

2.3.4 DNA manipulation

2.3.4.1 Digestion of genomic or plasmid DNA with restriction enzymes

Restriction endonucleases were obtained from either Promega UK Ltd. (Southampton, UK) or from New England Biolabs (Hitchin, UK). To prevent degradation by contaminating DNase enzymes, all material was initially autoclaved. DNA digestion was carried out using buffer solutions provided by the manufacturer and was routinely performed in a final volume of 30-50 μL using 0.2-1 μg of DNA and 5-10 units of enzyme.

2.3.4.2 DNA gel electrophoresis

Digested DNA was fractionated by gel electrophoresis in 0.7 % (w/v) - 1.5 % (w/v) agarose gel matrices using a 1 x Tris-borate EDTA buffer (TBE) (0.09 M Tris-borate, 2 mM EDTA). Visualisation of digested DNA was possible by the addition of ethidium bromide (to a final concentration of 0.5 $\mu\text{g mL}^{-1}$). DNA size markers were included during the gel electrophoresis process and was routinely achieved using the 1 kb plus size marker (Invitrogen) in order to determine the size of the digested DNA products. DNA was visualised on a UV transilluminator using a gel documentation system (Image Master VDS with a Fujifilm Thermal Imaging system FTI-500, Pharmacia Biotech) was employed to record and document fluorescent images.

2.3.4.3 The polymerase chain reaction (PCR)

DNA fragments were amplified using the Polymerase Chain Reaction (PCR) and was carried out using an Applied Biosystems GeneAmp® PCR System 2400 cyclor using either GoTaq® Flexi DNA Polymerase (Promega), *Pfu* DNA Polymerase (Promega) or *Herculase*® Enhanced DNA Polymerase (Stratagene) according to manufacturer's instructions. Routinely using the GoTaq® Flexi Polymerase reaction, 50 - 100 ng of template DNA was used for amplification, along with the GoTaq Flexi DNA Polymerase buffer (5x), 10 nM MgCl_2 , 100 nM each dNTP, 0.25 pM of each primer, 2 units of GoTaq® Flexi DNA Polymerase, made up to a final volume of 50 μL using sterile water (Sigma). Typically, 25 - 35 rounds of the PCR were performed unless otherwise stated.

2.3.4.4 Gel purification of DNA fragments

DNA fragments produced from either digested DNA or PCR were purified from agarose gels using a commercial kit (Wizard Plus SV Gel and PCR Clean-up System, Southampton, UK) according to the manufacturer's instructions. Fragments were excised from the gel using a blade and placed in a pre-weighed microfuge tube. The mass of agarose was determined and an equal volume of membrane binding solution (4.5 M guanidine isothiocyanate, 0.5 M potassium acetate, pH 5.0) was added. Tubes were incubated at 65 °C until the gel slice had dissolved and the gel was no longer visible. The solution was placed in a Wizard® SV Minicolumn connected to a 2 mL collection tube. After centrifugation for 1 min (17,000 x g, IEC Micromax), the DNA became bound to the column. The flow-through was discarded and the column placed back on top of the collection tube. To wash the column, 0.75 mL of membrane wash solution (10mM potassium acetate [pH 5.0], 80 % ethanol, 16.7 µM EDTA, pH 8.0) was added and centrifugation repeated (17,000 x g, 1 min). The flow through was discarded and 0.5 mL of Membrane Wash Solution was added and centrifugation repeated for 5 min (17,000 x g). The flow through was discarded and the column processed by centrifuging for an additional minute (17,000 x g). The Wizard®SV Minicolumn was dried and placed in a clean fresh 1.5 mL microfuge tube and 30 µL of sterile water added (Sigma). After an additional centrifugation step of 1 min (17,000 x g), the DNA could be stored at -20 °C.

2.3.4.5 Southern blotting

Blotting of agarose DNA gels was performed according to Southern (1975). Each gel was submerged in 0.25 M HCl for 15 min in order to de-purinate the fractionated DNA and then denatured by immersing in 0.4 M NaOH, 0.6 M NaCl for 30 min with gentle rocking. The gel was then transferred to Neutralisation buffer (1.5 M NaCl, 0.5 M Tris-HCl, [pH 7.5]) for 30 min with gentle rocking before capillary blocking onto Hybond-N (Amersham Biosciences). Gel blots were performed by placing the inverted gel onto a sheet of filter paper wick, which was supported on a perspex sheet with each end of the wick submerged in 20 x SSPE solution (3.6 M NaCl, 200 mM Na₂HPO₄, 22 mM EDTA). Hybond-N membrane was then placed onto the

gel and overlaid with five layers of wet Whatmann 3 mm paper and five layers of dry Whatman 3 mm paper onto which a 10 cm high pile of towels was placed (Kimberley Clark Corporation). Finally, a 500 g weight was applied by placing on top of the stack and the blot was left to stand at room temperature overnight. The transferred DNA was cross-linked to the membrane using a BLX crosslinker (Bio-link®).

2.3.4.6 Radio-labelled DNA probe synthesis

DNA hybridisation probes were labelled by the random primer method (Feinberg and Vogelstein, 1983) using a Ready-To-Go kit (Amersham Biosciences) according to the manufacturer's instructions. A 25 – 50 ng aliquot was made to a final volume of 47 µL in water. The sample was heated at 100 °C for 5 min to denature the DNA and rapidly chilled on ice for 2 min. The tube was briefly subjected to centrifugation and its contents added to a Ready-To-Go reaction bead mix containing buffer, dATP, dGTP, dTTP, FPLCpure Klenow polymerase (7-12 units) and random oligonucleotides, primarily 9-mers. Reagents were mixed by gentle pipetting and 2 µL of [α -³²P]dCTP (3,000 Ci/mmol) was added. The labelling reaction was incubated at 37 °C for 10 min before being stopped by addition of 100 µL of labelling stop dye (0.1 % SDS, 60 mM EDTA, 0.5 % bromophenol blue, 1.5 % blue dextran). Un-incorporated isotopes were removed by passing the reaction through a Biogel P60 (Bio-Rad) column, and collecting the dextran blue-labelled fraction. The probe was denatured by boiling at 100 °C for 5 min and quenched on ice for 5 min before being added to the hybridisation mixture.

2.3.4.7 Hybridisation conditions

DNA gel blot hybridisations were performed using standard procedures (Sambrook *et al.*, 1989). Blots were incubated in hybridisation bottles (Hybaid Ltd.) in a hybridisation oven (Hybaid) for at least 4 h at 65 °C in 15 – 20 mL of pre-hybridisation solution (6 x SSPE [diluted from a 20 x stock prepared by dissolving 175.3 g of NaCl, 27.6 g of NaH₂PO₄ and 7.4 g of EDTA in 800 mL of ddH₂O, adjusting the pH to 7.5 with NaOH and making up to 1 L with ddH₂O], 5 x Denhardt's solution [diluted from a 50 x stock prepared with 5 g Ficoll (type 400, Pharmacia), 5 g polyvinylpyrrolidone in 500 mL ddH₂O), 0.5 % SDS], with 100 µL denatured

herring sperm DNA (1 % [w/v] in 0.1 M NaCl). A denatured radio-labelled probe was then added and the mixture incubated overnight at 65 °C.

Following hybridisation, the blot was washed at high stringency. The pre-hybridisation solution was removed along with any unbound probe and 25 - 30 mL of 2 x SSPE wash (0.1 % SDS, 0.1 % Sodium pyrophosphate [PPi], 2 x SSPE [diluted from the 20 x SSPE stock][pH 7.4]) added. The mixture was incubated for 30 min at 65 °C. The wash solution was removed and replaced with 25 - 30 mL of 0.2 x SSPE wash (0.1 % SDS, 0.1 % Sodium pyrophosphate [PPi], 0.2 x SSPE, [pH 7.4]) and the blot again incubated for 30 min at 65 °C. The membrane was then dried for 10 min on paper towels. The membrane was wrapped in cellophane and autoradiography was carried out by exposure of membranes to X-ray film (Fuji Medical X-ray film, Fuji Photo Film UK Ltd.) at -80 °C in the presence of an intensifying screen (Amersham). X-ray films were developed using Kodak chemicals.

2.3.5 DNA cloning procedures

2.3.5.1 Bacterial DNA mini preparations (Alkaline Lysis preparations)

Small-scale preparations of plasmid DNA from bacterial colonies were made by modifying a larger scale method based on Sambrook *et al.* (1989). Single colonies were picked and used to inoculate 5 mL of Luria-Bertani broth (LB)(10 g L⁻¹ Tryptone, 5 g L⁻¹ yeast extract, 86 mM NaCl, [pH 7.5]) containing the appropriate antibiotic in a universal bottle. Cultures were grown overnight at 37 °C with vigorous aeration (200 rpm) in an Innova 4000 rotary incubator (New Brunswick Scientific). For long term storage of bacterial cells, a fraction of the initial 5 mL culture was retained to make a glycerol stock. For this, an 800 µL aliquot of bacterial solution was added to 1.5 mL microfuge tubes containing 200 µL sterile 50 % (v/v) glycerol. The suspension was vortexed rapidly and stored at -80 °C. A 1.5 mL aliquot of the culture was transferred to another 1.5 mL microfuge tube and pelleted by centrifugation at 17,000 x g (IEC, Micromax) for 5 min. The supernatant was removed and the bacterial pellet re-suspended in 200 µL of ice-cold re-suspension solution (50 mM Glucose, 25 mM Tris-HCl [pH 8.0], 10 mM EDTA [pH 8.0]) by vigorous vortexing. A 400 µL aliquot of freshly prepared lysis solution (0.2

mM NaOH [freshly diluted from a 10 M stock], 1 % SDS) was added to the cell suspension. The contents of the tube were mixed by inversion, ensuring that the entire surface of the tube came into contact with the solution. The tube was placed on ice for 5 min and then 300 μ L of ice-cold neutralisation solution (3 M potassium acetate, 11.5 % (v/v) glacial acetic acid) was added and the contents mixed by inverting rapidly three times. The tube was then stored on ice for 3 – 5 min, and processed by centrifugation at 12,000 $\times g$ for 5 min in a microfuge (IEC, Micromax). The supernatant was transferred to a fresh tube and precipitated using an equal volume of isopropanol. After incubating this solution at room temperature for 5 min, centrifugation was performed at 17,000 $\times g$ for 10 min (IEC, Micromax) with the resulting supernatant being removed and discarded. The pelleted nucleic acid was washed with 1 mL of 100 % (v/v) ethanol and centrifugation carried out at 17,000 $\times g$ for 10 min in a microfuge. The supernatant was discarded and the pellet dried for 10 min in a vacuum rotary dessicator. The pellet was re-suspended in 50 μ L of TE (10 mM Tris-HCl [pH 7.5]), 1 mM EDTA [pH 8.0] containing DNase-free pancreatic RNase (20 g mL⁻¹), vortexed briefly and incubated at 37 °C for 20 min. Preparations were stored at -80 °C.

2.3.5.2 High quality plasmid DNA preparations

High quality plasmid DNA for sequencing and for fungal transformation was prepared using a commercially available kit (Promega® Wizard Plus SV Midi-Prep DNA purification system) according to manufacturer's instructions. Single colonies were grown in 5 mL of LB media overnight at 37 °C with vigorous aeration (200 rpm) in an Innova 4000 rotary incubator (New Brunswick Scientific). Bacterial cells were recovered by centrifugation at 10,000 $\times g$, re-suspended in 250 μ L of cell re-suspension solution (50 mM Tris [pH 7.5], 10 mM EDTA, 100 μ g mL⁻¹ RNase) and transferred to a microfuge tube. A 250 μ L aliquot of cell lysis solution (0.2 M NaOH, 1 % SDS) was then added and the contents mixed by gentle inversion. A 10 μ L aliquot of alkaline protease solution was added and the tube inverted gently. After a 5 min incubation at room temperature, a 350 μ L aliquot of neutralisation solution (4.09 M guanidine hydrochloride, 0.759 M potassium acetate, 2.12 M glacial acetic acid [final pH 4.2]) was added and the tube

contents mixed by inversion. The samples were processed by centrifugation at 14,000 x g in a microfuge for 10 min. A spin column was then inserted into a collection tube and the cleared cell lysate poured into the top of the column. This was processed by centrifugation at 14,000 x g in a microfuge for 1 min. The flow-through was then discarded and the spin-column re-inserted into the collection tube and 750 L wash solution (60 mM potassium acetate, 8.3 mM Tris-HCl [pH 7.5], 0.04 mM EDTA, 60 % ethanol) then pipetted into the spin column. The spin-column and collection tube were then centrifuged at 14,000 x g for 1 min at room temperature. This centrifugation step was repeated and the column washed again with 250 L of wash solution for 5 min. The flow through was discarded and the column processed by centrifugation for an additional minute (14,000 x g). The spin column was transferred to a fresh steril microfuge tube and 50 L of nuclease free water (Sigma) added to the column. One final centrifugation at 14,000 x g for 1 min was required to elute the DNA from the spin column into the microfuge tube. Plasmid DNA samples were routinely stored at -20C.

2.3.5.3 DNA ligation and selection of recombinant clones

For routine cloning into standard vectors (such as the pGEM® series [Promega], recombinant clones were selected using α -complementation of *lacZ* (Sambrook et al., 1989). When cloning with a single restriction enzyme, treatment with intestinal calf alkaline phosphatase (CIP) (New England Biolabs) was performed to prevent re-circularisation of the linearized plasmid by phosphorylating digested ends. Linearised vectors were separated using gel electrophoresis, gel purified and 5 L of NEBuffer 3 (100 mM NaCl, 50 mM Tris-HCl, 10 mM MgCl₂, 1 mM dithiothreitol [pH 7.9], 0.5 L of CIP enzyme and 14.5 L of nuclease-free H₂O were then added to the precipitated DNA to a final volume of 50 L. This reaction was incubated at 37C for 30 min followed by an additional incubation at 70C for 1 h to denature the CIP enzyme. Digested DNA was gel-purified and ligation reactions prepared. Routinely, vector and insert DNA were added to the ligation mixture at a 1:3 molar ratio and the reactions performed in a final volume of 10 L. Typically, ligation reactions would be performed using manufacturer's ligase buffer and 3 units of T4 ligase (Promega) according to the manufacturer's instructions and would be

incubated overnight at 4°C. Directional cloning would be performed similarly, but negating the treatment with alkaline phosphatase. DNA fragments that had been amplified by PCR were routinely cloned into the vector pGEM-T (Promega) which allows permits one-step TA cloning of PCR fragments generated by thermostable polymerases such as *Taq* polymerase (Mead et al., 1991).

2.3.5.4 Preparation of competent cells

Stocks of laboratory-prepared transformation-competent cells were generated using a protocol adapted from Sambrook *et al.*, (1989). Single bacterial colonies were obtained by streaking bacterial cells across a plate of LB containing the appropriate antibiotic and incubating at 37 °C for 16 h. A single colony was used to generate an overnight culture in 10 mL LB broth (37 °C, 200rpm). A 2.5 mL aliquot of this culture was inoculated into 250 mL of SOC (20 g L⁻¹ tryptone, 5 g L⁻¹ yeast extract, 8.6 mM NaCl, 10 mM MgSO₄, 10 mM MgCl₂) and this was allowed to grow until an OD₆₀₀ = 0.6 had been reached (Sambrook *et al.*, 1989). The culture was transferred to a 50 mL Oakridge tube and incubated on ice for 10 min. Cells were recovered by centrifugation at 2, 510 x g (Beckman J2-MC, JS13.1 rotor) for 10 min at 4 °C. To each tube, 15 mL filter-sterilised FSB (10 mM potassium acetate [pH 7.5], 45 mM MnCl₂·4H₂O, 10mM CaCl₂·2H₂O, 100 mM KCl, 3mM hexamine-cobalt chloride, 10 % glycerol [pH 6.4]) was added and the cells resuspended by gentle pipetting. Samples were incubated on ice for 10 min and the centrifugation step repeated once more. The cells were then resuspended in 4 mL FSB and DMSO (dimethyl sulfoxide, Sigma) was added to a final concentration of 3.4 % (v/v). The mixture was incubated on ice for 15 min. A further volume of DMSO was added such that the final concentration was 6.5 % DMSO (v/v). The cells were then aliquoted into 100 µl and dispensed into pre-chilled microfuge tubes. Samples were immediately frozen by immersion in liquid nitrogen and stored at -80 °C.

2.3.5.5 Transformation of bacterial hosts

Transformation was routinely carried out using *Escherichia coli* strain XL1 Blue (Stratagene). XL1 – Blue has a genotype *supE44 hsdR17 recA1 endA1 gyrA46 thirelA1 lac⁻ [F' pro AB⁺*

lacI^q lacZΔM15 Tn10 (tet^r)]. A 100 µl aliquot of competent cells was decanted into pre-chilled 15 mL tubes (Falcon 2059, BD Biosciences). The tubes were then incubated on ice for 10 min before 0.1 – 50ng DNA was added and the mixture incubated on ice for a further 30 min. Cells were heat-shocked at 42 °C for 45 s and then transferred to ice for 2 min. At this point, 500 µl of SOC media (20 g L⁻¹ tryptone, 5 g L⁻¹ yeast extract, 0.5 g L⁻¹ NaCl, 20 mM glucose, 10 mM magnesium sulphate, 10 mM magnesium chloride), pre-heated to 42 °C, was added to the tube and the recovering cells were incubated at 37 °C for 1 h with gentle shaking (150 rpm). Aliquots were plated on LB agar with the appropriate antibiotic. Where α -complementation selection was available (Sambrook *et al.*, 1989), the agar contained isopropyl-thiogalactosidase (0.8 mg ml⁻¹ IPTG per plate) (Calbiochem, VWR International Ltd.) and 5-bromo-4-chloro-3-indolyl- β -D-galactopyranoside (0.8 mg ml⁻¹ X-Gal per plate)(Calbiochem, VWR International Ltd.). Plates were inverted and incubated at 37 °C overnight.

2.3.6 RNA manipulations

2.3.6.1 RNA gel electrophoresis

Total and Poly (A)⁺ RNA samples were fractionated by denaturing gel electrophoresis. Samples were first denatured in formamide, 50 % (v/v), 2.2 M formaldehyde, 1 x MOPS/EDTA buffer (20 mM 3-[N-morpholino]-propanesulfonic acid, 5 mM sodium acetate, 1 mM ethylenediametetraacetic acid, pH 7.0) at 65 °C for 15 minutes. Gel electrophoresis was performed in 1.2 % (w/v) agarose gel matrices containing 2.2 M formaldehyde using a 1 x MOPS/EDTA buffer (Sambrook *et al.*, 1989). A commercial RNA size marker was used during electrophoresis to enable the determination of molecular mass transcripts (Invitrogen).

2.3.6.2 Reverse-transcription-PCR

Double stranded cDNA was obtained from RNA isolations using the Titanium™One-Step RT-PCR kit (BD Biosciences). A master mix was prepared using the following reagents to give a total volume of 43.5 µl; 5 µl 10 x One-step buffer (400 mM tricine, 200 mM KCl, 30 mM MgCl₂, 37.5 µg ml⁻¹ BSA), 1 µl 50x dNTP Mix (10 mM each dNTP), 0.5 µl Recombinant

RNase inhibitor (40 units μl^{-1}), 25 μl Thermostabilising reagent, 10 μl GC-Melt™, 1 μl Oligo(dT) primer (20 μM ; dT[18]), 1 μl 50x RT-Titanium Taq enzyme mix (includes MMLV-RT mutant, TITANIUM *Taq* DNA polymerase and TaqStart antibody). To this master mix, between 1-5.5 μl of RNA sample was added (1 ng-1 μg), along with 1 μl of each experimental primer (45 μM each) and the volume made up with RNase-free water to give a total volume of 50 μl . The reaction mix was placed in a Thermal Cycler and heated to 50 °C for 1 h. Normal PCR amplification conditions followed on immediately afterwards; 94 °C for 5 min, 94 °C for 30 s, 50 °C (adjust depending on annealing temperature of primers) for 30 s, 70 °C for 3 min (adjust for length of desired product) for 35 cycles, and a final 70 °C extension for 10 min. PCR products were analysed by electrophoresis, as described (Section 2.3.4.2).

2. 4 DNA-mediated transformation of *M. oryzae*

A 2.5 cm^2 section of *M. oryzae* mycelium was removed from a CM plate culture, blended in 150 ml of liquid CM medium and incubated at 24 °C with shaking at 125 rpm in an orbital incubator for 48 h. Mycelium was harvested by filtration through sterile Miracloth (Calbiochem) and washed in sterile distilled water. The mycelium was transferred to a sterile Falcon tube (Becton Dickinson) containing 40 ml of OM buffer (1.2 M magnesium sulphate, 10 mM [pH 5.8] sodium phosphate, 5 % Glucanex (Novo Industries, Copenhagen)) and shaken gently at 75 rpm for 2-3 hours at 30 °C in an orbital incubator. Protoplasts were retrieved by transferring the solution to sterile polycarbonate Oakridge tubes (Nalgene) and overlaid with an equal volume of cold ST buffer (0.6 M sucrose, 0.1 M Tris-HCl [pH 7.0]). Protoplasts were recovered by centrifugation at 5000 x *g* for 15 min at 4 °C in a swinging bucket rotor (Beckman JS-13.1) in a Beckman J2.MC centrifuge. Protoplasts were recovered at the OM/ST interface and transferred to a sterile Oakridge tube, which was filled with cold STC buffer (1.2 M sucrose, 10 mM Tris-HCl (pH 7.5), 10 mM calcium chloride). Protoplasts were pelleted at 3000 x *g* for 10 minutes at 4 °C (Beckman JS-13.1 rotor), and washed twice with 10 ml of cold STC, with complete re-suspension after each wash. Protoplasts were re-suspended in 1 ml of cold STC and a haemocytometer was used to determine the final concentration of protoplasts.

DNA-mediated transformation was undertaken in 1.5 ml microfuge tubes by combining an aliquot of purified protoplasts (10^7 ml^{-1}) with DNA (5-10 μg) in a total volume of 150 μl STC buffer. The mixture was incubated at room temperature for 25 minutes and 1 ml of PTC buffer (60% PEG 4000, 10 mM Tris-HCl (pH 7.5), 10 mM calcium chloride) was added in two aliquots and mixed by gentle inversion. The mixture was incubated at room temperature for 15-20 min and then added to 3 ml TB3 buffer (20 % sucrose, 0.3 % yeast extract) with gentle shaking at 75 rpm at 24 °C in an orbital rotator. After 16 hours, the mixture was transferred to molten (46 °C) 1.5% agar/OCM (CM osmotically stabilised with 0.8 M sucrose), mixed gently and poured into sterile Petri dishes (25 ml plate⁻¹).

For selection of transformants on hygromycin B (Calbiochem), plates cultures were incubated in the dark for at least 16 hours at 24 °C and then overlaid with approximately 15 ml OCM/1 % agar containing hygromycin B, 200 $\mu\text{g ml}^{-1}$.

For selection of sulfonyleurea resistant transformants, OCM was replaced with BDCM (0.8 M sucrose, 1.7 g l⁻¹ yeast nitrogen base without amino acids and ammonium sulphate (Difco), 2 g l⁻¹ ammonium nitrate, 1 g l⁻¹ asparagine, 10 g l⁻¹ glucose, pH 6.0). In the overlay, CM was replaced with BDCM omitting the sucrose, and hygromycin B was replaced with chlorimuron ethyl (50 $\mu\text{g ml}^{-1}$), freshly diluted from a stock solution of 100 mg ml⁻¹.

Chapter 3. Investigating effector-mediated suppression of chitin-triggered immunity by a rice blast LysM effector protein

Abstract

Chitin is a highly conserved and major cell wall component of pathogenic fungi. Although indispensable for fungal growth, chitin oligosaccharides can be released by hyphal tips during host-pathogen interactions. When this happens, chitin oligosaccharides can act as pathogen-associated molecular patterns (PAMPs), eliciting host recognition upon binding and recognition to host membrane pattern recognition receptors (PRRs). To cause disease, fungal pathogens may have evolved a way of perturbing host recognition of PAMPs, such as chitin. We set out to understand the extent to which rice blast effector proteins are employed to overcome chitin-induced host recognition. Two putative *M. oryzae* LysM effector proteins, referred to as Secreted LysM Protein 1 and 2 (*SLP1* and *SLP2*) were characterised. We show that the *M. oryzae* Slp1 protein has chitin-binding properties and plays a significant role in the suppression of chitin-induced immune responses in rice cells, including the suppression of the chitin-induced oxidative burst and defence gene expression. We show that Slp1 competitively inhibits the binding of chitin oligosaccharides to the rice PRR CEBiP (Chitin Elicitor Binding Protein), a membrane bound PRR which induces plant immune responses upon binding chitin. We show by targeted gene replacement that *SLP1* is required for full fungal virulence and we conclude that *SLP1* plays a critical role in the ability of *M. oryzae* to colonise host tissues. The results gained from this Chapter and Chapter 4 resulted in a recent publication in the January 2012 issue of The Plant Cell, a copy of which can be found in Appendix 1.

3.1 Introduction

Chitin is a highly abundant and structurally integral component of the cell walls of pathogenic fungi (Benard and Latgé, 2001; Munro and Gow, 2001; Vega and Kalkum, 2012). Consisting of β -1,4-linked monomers of N-acetyl- β -D-glucosamine [(GlcNAc)_n], these chitin oligosaccharides can be released from fungal hyphal tips during growth on or within host species, leading to detection and elicitation of localised host immune responses, such as the release of reactive oxygen species (ROS). For this to happen, chitin oligosaccharides act as pathogen associated molecular patterns (PAMPs) which activate immune signalling cascades upon binding to host membrane-bound pattern recognition receptors (PRRs). One such PRR in rice (*Oryza sativa*) is CEBiP (for Chitin Elicitor Binding Protein), which resides on the plant plasma membrane and is able to bind chitin oligosaccharides (Shibuya *et al.*, 1995; Kaku *et al.*, 2006; Tanaka *et al.*, 2010; Kishimoto *et al.*, 2011). CEBiP is a glycoprotein of 328 amino acids in length containing a C-terminal membrane spanning domain and two LysM motifs in the extracellular domain (Kaku *et al.*, 2006). Upon elicitor-binding of chitin oligosaccharides to CEBiP, an immune response is activated resulting in a localised oxidative burst and the upregulation and expression of defence related genes including cinnamate 4-hydroxylase, peroxidases and the rice Phenylalanine ammonia lyase gene (*PAL1*) (Kaku *et al.*, 2006). Recent evidence has suggested that CEBiP interacts co-operatively with another rice LysM receptor-like kinase membrane protein, OsCERK1 (Chitin Elicitor Receptor Kinase, also known as LysM-RLK1), to regulate and induce expression of plant defence genes (Shimizu *et al.*, 2010). Similarly within the model plant *Arabidopsis thaliana*, AtCERK1 acts to regulate and induce expression of plant defence genes (Liu *et al.*, 2012). Knockdown of the CEBiP receptor on rice by RNAi significantly increases the susceptibility of rice tissue to infection from *M. oryzae*, suggesting that rice is less able to detect fungal invasion and initiate a plant defence response without a functional CEBiP protein (Kishimoto *et al.*, 2010). Interestingly, *HvCEBiP*, a barley (*Hordeum vulgare*) gene homologous to rice chitin CEBiP, has recently been shown to contribute to basal resistance to *M. oryzae* infection (Tanaka *et al.*, 2010). Homologues of CEBiP have also been found in the model plant species *Arabidopsis thaliana* (Miya *et al.*, 2007), suggesting that

recognition of chitin oligosaccharides may have evolved as an early strategy by plants to recognise conserved chitin oligosaccharides during fungal infection. When exposed to chitin, mice (*Mus musculus*) have been shown to elicit the accumulation of innate immune cells, such as eosinophils and basophils in tissues (Reese *et al.*, 2007), highlighting that the presence of a shared chitin-induced defence system is common across higher eukaryotes.

In addition to the rice membrane receptor proteins CEBiP and OsCERK1, a plethora of proteins containing LysM domains have been characterised, including secreted proteins, outer membrane proteins, lipoproteins and cell wall proteins (Buist *et al.*, 2008). Proteins containing LysM domains are widely thought to serve peptidoglycan-binding functions, such as the binding of chitin (Buist *et al.*, 2008). The first protein with a LysM domain to be characterised was that of the lysozyme enzyme from *Bacillus* phage λ (Garvey *et al.*, 1986). LysM domains have also been implicated in perception of bacteria by leguminous plant Nod Factors, which are required for host perception of lipo-chitooligosaccharides which are released by nitrogen-fixing rhizobia (Nakagawa *et al.*, 2011; Bensmihen *et al.*, 2011). Since then, proteins with LysM domains have been identified across a range of taxonomic groups (Bateman and Bycroft, 2000). Proteins containing LysM domains have subsequently been identified in a range of fungal species (Bolton *et al.*, 2008; de Jonge and Thomma, 2009; de Jonge *et al.*, 2010; Marshall *et al.*, 2011). Recently, the tomato leaf mold fungus *Cladosporium fulvum*, was shown to secrete an apoplastic effector protein Ecp6 (for Extracellular Protein 6) containing three LysM domains. Interestingly, Ecp6 was shown to be secreted exclusively during colonisation of its tomato host, and was shown to have an important role in the virulence of *C. fulvum* (Bolton *et al.*, 2008). Further characterisation revealed that Ecp6 is capable of scavenging chitin oligosaccharides and is able to suppress PAMP-triggered immune responses, perhaps by competition with the plant chitin receptor CEBiP (de Jonge *et al.*, 2010). In contrast to other *C. fulvum* effectors which are perceived by *Cf* receptors (van Esse *et al.*, 2007; Stergiopoulus and de Wit, 2009; de Wit *et al.*, 2009), a cognate receptor in tomato to which Ecp6 binds has yet to be identified (Wang *et al.*, 2010). Interestingly, a number of putative orthologues of Ecp6 have been identified in a wide range of fungal plant pathogens, including *M. oryzae* (de Jonge and Thomma, 2009).

Characterisation of a putative Ecp6 orthologue in *Mycosphaerella graminicola*, the causative agent of *Septoria tritici* leaf blotch disease of wheat (*Triticum aestivum*), Mg3LysM, revealed a similar capacity to suppress chitin-induced plant defence responses (Marshall *et al.*, 2011).

In contrast to *C. fulvum* which exclusively secretes apoplastic effector proteins, *M. oryzae* secretes effector proteins during intracellular growth which have both apoplastic and host cytoplasmic targets (Jia *et al.*, 2000; Mosquera *et al.*, 2009; Khang *et al.*, 2010; Mentlak *et al.*, 2012). Although more than 80 resistance (R) genes to rice blast have been identified in rice (Ballini *et al.*, 2008), only a handful of *M. oryzae* Avr proteins have been described, suggesting that many more rice blast effectors remain to be determined (Khang *et al.*, 2010). Indeed, there is currently a paucity of data regarding the precise biological function and role of these proteins in causing rice blast disease (Khang *et al.*, 2010; Mentlak *et al.*, 2012). To date, the best characterised rice blast effector is Avr-Pita, a putative metalloprotease that was initially identified because it conferred resistance on rice cultivars expressing the R gene Pita (Jia *et al.*, 2000). Although Avr-Pita has been shown to bind directly to Pita in a yeast two-hybrid screen, very little is understood about the nature of secretion and downstream signalling effects of its delivery into host cytoplasm (Jia *et al.*, 2000). During biotrophic growth, fluorescently labelled avirulence effector proteins accumulate at a bulbous membrane-rich structure at the plant-fungal interface known as the Biotrophic Interfacial Complex (BIC) (Mosquera *et al.*, 2009). The correlation between the detection of fluorescently labelled effectors at the BIC and their observation inside host cytoplasm, has raised the hypothesis that the BIC is the portal for delivery of rice blast effector proteins into host cytoplasm (Khang *et al.*, 2010; Valent and Khang, 2010).

In this chapter, I aimed to investigate and characterise the mechanisms employed by the rice blast fungus *M. oryzae* to overcome chitin-induced recognition by its native rice host. Specifically, we wanted to see if the deployment of secreted effector proteins by *M. oryzae* can quash chitin-induced immune responses. Two putatively secreted effector proteins were identified which contain predicted LysM domains, and are referred to as Secreted LysM Protein 1 and 2 (Slp1 and Slp2). I report that the LysM effector protein Slp1 described here is capable

of binding and sequestering chitin oligosaccharides that would otherwise trigger a chitin-induced oxidative burst in rice cells and induce the expression of defence genes. These suppression effects extend outside the native host range and we confirm that Slp1 is also able to suppress chitin-triggered immune responses in tomato cell suspensions. Results provided here suggest that the secretion of LysM effector proteins may have been an early strategy which evolved in fungal pathogenic species to mediate the effects of host chitin recognition and host immune responses.

3.2 Methods

3.2.1 Affinity precipitation of recombinant Slp1 protein with polysaccharides

The affinity of Slp1 for various polysaccharides was investigated by incubating 50 mg ml⁻¹ of Slp1 with 5 mg of chitin beads (New England Biolabs), crab shell chitin, chitosan, xylan or cellulose (Sigma-Aldrich), as described previously (de Jonge *et al.*, 2010; Marshall *et al.*, 2011). Protein and the insoluble polysaccharide were incubated at 24°C on a rocking platform in a final volume of 1 ml of water. After 16 hours, the insoluble pellet fraction was centrifuged at 13,000 x g for 5 minutes and the supernatant collected. The insoluble pellet fraction was pelleted and rinsed a further three times in distilled sterile water to remove unbound protein. Both the supernatant and pellet fractions were boiled in 200 µl of 1% SDS solution before being examined by SDS-PAGE and Coomassie Brilliant Blue staining.

3.2.2 Cell protection assays using crude extract of chitinase from tomato leaves

Intracellular basic chitinases were extracted, as described previously (Joosten *et al.*, 1990; 1995). A 50 ml aliquot of *Trichoderma viride* spores was incubated overnight at room temperature at a concentration of 100 conidia ml⁻¹. Recombinant Slp1 or Avr4 was then added to a final concentration of 10 or 100 µM, as described previously (Joosten *et al.*, 1995; de Jonge *et al.*, 2010). After 2 hours of incubation, 5 ml of crude extract of chitinase was added (Joosten *et al.*, 1990; 1995) and spores were visualised microscopically after 2-4 hours. Similarly, for cell protection assays of *M. oryzae*, spores of the *M. oryzae* Guy11 strain were harvested and inoculated onto borosilicate glass coverslips at a concentration of 5 x 10⁴ spores ml⁻¹. A 20 µl aliquot of crude extract of chitinase was added and spores were visualised microscopically for germination between 2 to 4 hours.

3.2.3 Medium alkalinisation of tomato cells

Medium alkalinisation experiments were performed as described previously (de Jonge *et al.*, 2010; Marshall *et al.*, 2011). Suspension cultured tomato (*Solanum lycopersicum*) cell line Msk8 was maintained as described (Felix *et al.*, 1991), and used 3-4 days following

subculturing for alkalisation experiments (Felix *et al.*, 1993). To measure medium alkalisation, 2.5 ml aliquots of the suspension were placed in 12-well micro titre culture plates on a rotary shaker at 200 rpm and allowed to settle for at least 2 hours. The pH of the medium was continuously monitored using a combined-glass electrode (Mettler Toledo, Switzerland). Prior to measurement and addition of the experimental to the cell medium, mixtures of recombinant protein (either Ecp6, Avr4 or Slp1) and chitin oligosaccharides (either 1 nM or 10 nM GlcNAc₈) were incubated at room temperature for at least one hour with rigorous shaking to allow the mixtures to equilibrate.

3.2.4 Production of recombinant Slp1 protein

RNA was extracted from infected leaf tissue after 144 hours post inoculation, as described in Chapter 2. cDNA synthesis was performed on 500 ng of DNAase I (Invitrogen) treated RNA using the Affinityscript qPCR synthesis kit (Stratagene) according to the manufacturer's instructions and as described in Chapter 2. cDNA of SLP1 was cloned using the primers 5'ATG-SLP1 and 3'TAG-SLP1 and cloned into the vector pGEM-T (Promega) according to the manufacturer's guidelines. Affinity-tagged Slp1 was generated in the yeast *Pichia pastoris* by amplifying the SLP1 cDNA using primers 5'Slp1-pic9 and 3'Slp1-pic9 to include an in-frame HIS₆-FLAG-tag and subsequently cloned into the vector pPIC9 (Invitrogen). Preparation of recombinant Slp1 was performed as described previously (Joosten *et al.*, 1995; de Jonge *et al.*, 2010; Kombrink, 2012). HIS₆-FLAG-tagged Slp1 was purified using a Ni₂₊-NTA Superflow column (Qiagen) according to the manufacturer's instructions. The primers used in the amplification of the Slp1 cDNA and subsequent cloning into the pPIC9 vector in *Pichia pastoris* were as follows:

5'ATG-Slp1
5' ATGCAGTTCGCTACCATCACCA 3'

3'TAG-Slp1
5' CTAGTTCTTGACAGATGGGGATG 3'

5'Slp1-pic9
5'GGTATGAATTCCATCATCATCATCATCCCCGACTACAAGGACGACGATGACAA
GGCCATGCCTCAGGCAAC 3'

3'Slp1-pic9

5' CGTCTAGCGGCCGCCTAGTTCTTGCAGATGGGGATG 3'

3.2.5 Affinity Labeling of Rice Membranes with Biotinylated (GlcNAc)₈

Affinity labeling with biotinylated (GlcNAc)₈ was performed as described previously (Shinya *et al.*, 2010). Suspension-cultured rice cells of *Oryza sativa* cv *nipponbare* were maintained in a modified N-6 medium as described previously (Tsukada *et al.*, 2002). A microsomal membrane preparation from suspension-cultured rice cells was mixed with biotinylated (GlcNAc)₈ in the presence or absence of Slp1 and adjusted to 30 ml with binding buffer. After incubation for 1 hour on ice, 3 ml of 3 % ethylene glycol bis[succinimidylsuccinate] solution (Pierce) was added to the mixture and kept for 30 minutes. The reaction was stopped by the addition of 1 M Tris-HCl, mixed with SDS-PAGE sample buffer, boiled for 5 minutes, and used for SDS-PAGE. Immunoblotting was performed on an Immuno-Blot polyvinylidene fluoride (PVDF) membrane (Bio-Rad Laboratories). Detection of biotinylated proteins was performed using a rabbit antibody against biotin (Bethyl Laboratories) as a primary antibody and horseradish peroxidase–conjugated goat anti-rabbit IgG (Chemicon International) as a secondary antibody. Biotinylated proteins were detected by the chemiluminescence with Immobilon Western Detection reagents (Millipore).

3.2.6 Measurement of ROS Generation and Gene Expression Analysis

ROS generation induced by elicitor treatment was analyzed by chemiluminescence due to the ferricyanide-catalyzed oxidation of luminol (5-amino-2,3-dihydro-1,4-phthalazinedione) (Desaki *et al.*, 2006). Briefly, 40 mg of cultured cells was transferred into the 1 ml of fresh medium in a 2 ml centrifuge tube and pre-incubated for 30 minutes on a thermomixer shaker at 750 rpm. After pre-incubation, (GlcNAc)₈ was separately added to the culture medium in the absence or presence of Slp1. For gene expression studies using qRT-PCR, total RNA was prepared from each rice cultivar (40 mg) using an RNeasy plant mini kit (Qiagen) and subjected to cDNA synthesis using a QuantiTect reverse transcription kit (Qiagen). qRT-PCR was performed using TaqMan gene expression assay reagent using a model 7500 Fast Real-Time

PCR system (Applied Biosystems). The 18S rRNA was used as an internal control to normalize the amount of mRNA.

3.2.7.1 Yeast-two hybrid screen

A yeast two-hybrid screen was performed to confirm dimerisation of Slp1 protein. To perform yeast two-hybrid analysis, the Matchmaker™ GAL4 Two-Hybrid System 3 (Clontech Laboratories Ltd.) was employed according to manufacturer's instructions. The Matchmaker GAL4 Two-hybrid system utilises four reporter genes: *lacZ*, *HIS3*, *ADE2* and *MEL1*. To test whether two proteins interact, the cDNA encoding the proteins of interest are cloned into bait and prey vectors. Upon transformation into yeast, the genes are expressed as fusion proteins, one as a fusion to the *GAL4* activation domain (AD) and the other to the DNA-binding domain. During a positive interaction between two proteins, the DNA-BD and AD components are drawn into close proximity, thereby inducing the transcription of the reporter genes described above. In the Matchmaker™ system, the pGBKT7 and pGADT7 vectors carry the DNA-BD and AD respectively.

3.2.7.2 Small scale yeast transformation

Constructs were simultaneously transformed into the yeast host strain AH109 (*MAT α* , *trp1-901*, *leu2-3, 112*, *ura3-52*, *his3-200*, *gal4 Δ* , *gal80 Δ* , *LYS2::GAL1_{UAS}-GAL1_{TATA}-HIS3*, *GAL2_{UAS}-GAL2_{TATA}-ADE2*, *URA3::MEL1_{UAS}-MEL1_{TATA}-lacZ*) using a small-scale lithium-acetate (LiOAc)-mediated yeast transformation protocol (Ito *et al.*, 1983; Schiestl and Gietz, 1989; Hill *et al.*, 1991; Gietz *et al.*, 1992). 1 ml of YPDA (20 g L⁻¹ peptone, 20 g L⁻¹ glucose, 10 g L⁻¹ yeast extract, 0.003% (v/v) adenine hemisulfate, pH 6.5) was inoculated with a single two-week old colony of AH109 yeast strain. The solution was pipetted up and down vigorously to remove any visible clumps before being transferred to 50 ml of YPDA and incubated at 30°C with shaking (200 rpm) for 17 hours. The culture was transferred to a flask containing 300 ml of YPDA before being incubated at 30°C with shaking (200 rpm) for a further 2-3 hours. Cells were recovered by decanting the culture into 50 ml falcon tubes before being centrifuged at 1000 x g for 5 minutes at room temperature. The supernatant was removed and the cells collected by resuspension in 50 ml sterile distilled H₂O. Cells were pooled and centrifuged for a

further 5 minutes 1000 x g at room temperature. The supernatant was discarded and the pellets resuspended in 1.5 ml of freshly prepared 1 x TE/LiOAc diluted from 10 x stocks (10 TE buffer: 0.1 M Tris-HCl, 10 mM EDTA, pH 7.5 and 10 x LiOAc: 1 M Lithium Acetate, pH 7.5). In a 1.5 ml microfuge tube, 100 ng of each plasmid, 10 μ l denatured herring sperm DNA and 100 μ l of yeast cells were combined and vortexed for 30 seconds. To the solution, 600 μ l of sterile PEG/LiOAc solution (40% (w/v) PEG 4000, 1 x TE buffer, 1 x LiOAc) was added. Samples were vortexed for 10 seconds and incubated at 30°C with shaking (200 rpm) for 30 minutes after which 70 μ l of DMSO was added. Samples were inverted gently to ensure the solutions were sufficiently mixed and heat-shocked by placing at 42°C for 15 minutes and then transferred to ice for 2 minutes. Cells were pelleted at 9000 x g for 5 seconds and resuspended in 600 μ l of sterile 1 x TE buffer before being plated out.

3.2.7.3 Plating and screening of yeast transformants

Aliquots of cells were plated out onto SD/Dropout (DO) agar plates (6.7 g L⁻¹ yeast nitrogen base without amino acids, 20 g L⁻¹ glucose, 20 g L⁻¹ agar), Dropout solution (20 mg L⁻¹ adenine hemisulfate), arginine HCl (20 mg L⁻¹), histidine HCl monohydrate (20 mg L⁻¹), isoleucine (30 mg L⁻¹), leucine (100 mg L⁻¹), lysine HCl (30 mg L⁻¹), methionine (20 mg L⁻¹), phenylalanine (50 mg L⁻¹), threonine (200 mg L⁻¹), tryptophan (20 mg L⁻¹), tyrosine (30 mg L⁻¹), uracil (20 mg L⁻¹), valine (150 mg L⁻¹), with specific nutrients omitted to select for transformants containing the introduced plasmids. Aspartic acid (100 mg L⁻¹) was also added to selection media lacking methionine. For α -galactosidase assays, X- α -Gal (Clontech) was dissolved in DMF (20mg ml⁻¹) and added to DO agar medium (20 g ml⁻¹). Plates were inverted and incubated at 30°C for 2-6 days until colonies appeared.

3.3 Results

3.3.1 Chitin in the fungal cell wall is exposed to the plant during intracellular growth

In order to determine the extent to which chitin within the fungal cell wall is exposed to the host plant cell during invasive growth, staining of intracellular biotrophic hyphae was performed using calcofluor white (CFW). CFW is a non-specific fluorochrome which binds to both β -1,3 and β -1,4 polysaccharides including chitin and cellulose, and is used routinely in the diagnosis and identification of chitinaceous fungal parasites in clinical mycology (Choi and O'Day, 1984; Harrington and Hageage, 1991; Rasconi *et al.*, 2009). CFW is also a useful tool to stain tissue elements such as keratin, collagen and elastin (Monheit *et al.*, 1984). CFW has previously been employed as a suitable dye for staining of *M. oryzae* tissues to visualise the septa within conidia and vegetative mycelia (Veneault-Forrey *et al.*, 2006; Chen *et al.*, 2008; Saunders *et al.*, 2010). Upon staining of CFW of infected rice plant cells, chitin within the cell wall of biotrophic fungal hyphae (FCW) and cellulose within plant cell wall (PCW) were labelled, as shown in Figure 3.1. This figure demonstrates that during biotrophic intracellular growth, chitin within the fungal cell wall of *M. oryzae* is exposed to the plant EIHM.

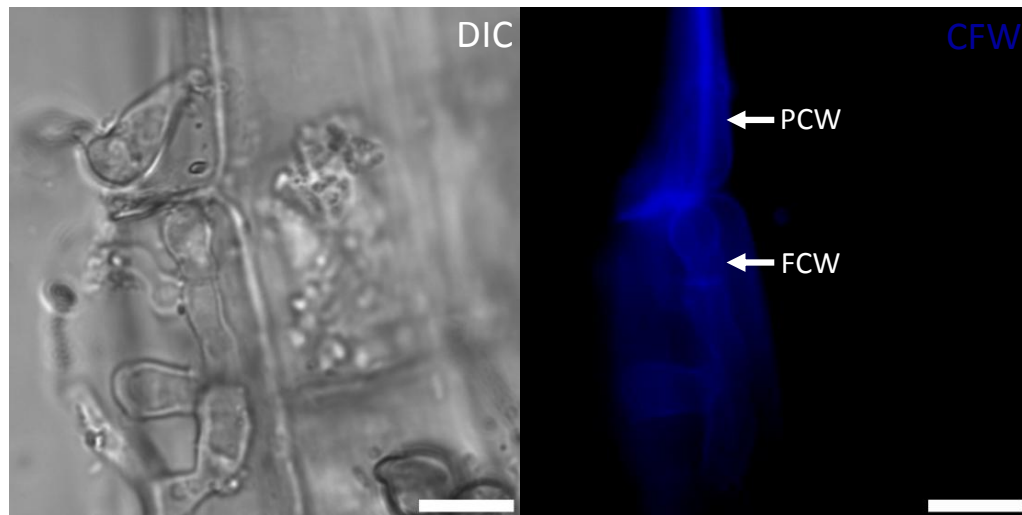


Figure 3.1 Chitin within the fungal cell wall is exposed to the plant during biotrophic growth. To visualise chitin within the fungal cell wall during intracellular growth, conidia of the wild-type *M. oryzae* Guy11 strain were inoculated onto rice leaf tissue and incubated at 24°C in a moist chamber. At 24 hours post-inoculation (hpi), rice leaf tissue was dissected and stained with the non-specific fluorochrome Calcofluor White (CFW, blue) and visualised by epifluorescence microscopy. CFW staining was non-specific and labelled both chitin in the fungal cell wall (FCW) and cellulose within the plant cell wall (PCW). CFW was applied at a concentration of 10 µg/ml and samples were excited at 350 nm for 200 ms. Scale bars represent 10 µm

3.3.2. Identification of *M. oryzae* secreted LysM effector proteins

Having demonstrated that chitin in the *M. oryzae* cell wall becomes exposed to the plant during biotrophic growth, we wanted to identify *M. oryzae* chitin-binding proteins that mediate the release of chitin oligosaccharides by hyphal tips, that might otherwise initiate PAMP-triggered immune responses in the rice cell (Jones and Dangl, 2006). An interrogation of the *M. oryzae* genome identified 9 genes encoding predicted LysM proteins, which have previously been shown to serve peptidoglycan-binding functions, including the binding of chitin (Buist *et al.*, 2006; De Jonge *et al.*, 2010). In *M. oryzae*, a type-III CVNH-LysM lectin containing a putative LysM domain protein was recently identified and was shown to have a role in binding carbohydrates (Koharudin *et al.*, 2011). Two hypothetical secreted proteins containing LysM proteins were identified by examining the *M. oryzae* genome sequence database (<http://www.broad.mit.edu/annotation/fungi/magnaporthe/>), and are referred to as Secreted LysM Proteins 1 and 2 (*SLP1* and *SLP2*). The *SLP1* ORF (Accession number MGG_10097) is 581 nucleotides long with an intron of 81 nucleotides in length, as shown in Figure 3.2. *SLP1* encodes a protein of 162 amino acids in length with two LysM domains and a predicted N-terminal secretion motif of 27 amino acids (based on Signal P3.0 analysis). *SLP2* (Accession number MGG_03468) is 858 nucleotides long and encodes a protein of 286 amino acids, as shown in Figure 3.3. Slp2 also contains two putative LysM domains within its secondary protein structure and a predicted N-terminal secretion signal of 21 amino acids (based on SignalP3.0 analysis). Interestingly, both Slp1 and Slp2 were similar in structure to the *Cladosporium fulvum* LysM effector Ecp6, which contains three LysM domains (Bolton *et al.*, 2006; de Jonge *et al.*, 2010), as well as to the *Mycosphaerella graminicola* LysM effectors MgLysM1, MgLysM2 and MgLysM3 (Marshall *et al.*, 2011). Slp1 and Slp2 were also previously identified as putative orthologues of the *C. fulvum* LysM effector Ecp6 (de Jonge and Thomma, 2009). Both Slp1 and Slp2 are cysteine rich proteins with 6 cysteine residues predicted in their primary structures, a feature which is typical of secreted apoplastic effector proteins in other plant pathogenic fungi (Hogenhout *et al.*, 2009).

```

1:   ATG CAG TTC GCT ACC ATC ACC ACC CTC CTC TTT GCC GGC GTT GCC GCC GCC
1:   M  Q  F  A  T  I  T  T  L  L  F  A  G  V  A  A  A

51:  ATG CCT gtaagcagagcaccgcccgatattcatcccacttcccaactcacacgtccaacgatccac
18:  M  P

116: tgataacctcaacttttttacaccgcaaaaacag CAG GCA ACC CCC ACC AGC GCC GCC CCT
20:                                     Q  A  T  P  T  S  A  A  P

175: CCC TCG GCG ACC TCG ACC TGC ACG CCG GGC CCC GTG GTC GAC TAC ACG GTG
29:  P  S  A  T  S  T  C  T  P  G  P  V  V  D  Y  T  V

226: CAG GGC AAC GAC ACG CTG ACC ATC GTG TCG CAG AAG CTC AAC TCG GGC ATC
46:  Q  G  N  D  T  L  T  I  V  S  Q  K  L  N  S  G  I

277: TGC AAC ATC GCG ACG CTC AAC AAC CTG GCC AAC CCC AAC TTC ATC GCG CTG
63:  C  N  I  A  T  L  N  N  L  A  N  P  N  F  I  A  L

328: GGC GCC GTG CTC AAG GTG CCG ACC GCC CCC TGC GTC ATC GAC AAC ATC TCC
80:  G  A  V  L  K  V  P  T  A  P  C  V  I  D  N  I  S

379: TGC CTG GCC AAG CAG AGC GAC AAC AAC ACG TGC GTC AGC GGC GTC TCC CCC
97:  C  L  A  K  Q  S  D  N  N  T  C  V  S  G  V  S  P

430: TAC TAC ACC ATC GTC TCG GGC GAC ACC TTC TTC CTG GTC GCC CAA AAG TTC
114: Y  Y  T  I  V  S  G  D  T  F  F  L  V  A  Q  K  F

481: AAC CTC AGC GTC GAC GCC CTC CAG GCC GCC AAC GTC GGC GCC GAC CCC CTC
131: N  L  S  V  D  A  L  Q  A  A  N  V  G  A  D  P  L

532: CTG CTC CAG CTC AAC CAG GTC ATC AAC ATC CCC ATC TGC AAG AAC TAG
148: L  L  Q  L  N  Q  V  I  N  I  P  I  C  K  N  *

```

Figure 3.2 Nucleotide sequence and putative amino acid sequence of the *M. oryzae* *SLP1* gene. The DNA sequence of the *SLP1* gene (Accession number MGG_10097) was retrieved from the *M. oryzae* genome database (www.broad.mit.edu/annotation/fungi/magnaporthe/) (Dean *et al.*, 2005). Putative derived amino acid sequences are listed below each codon using the standard one letter code. Nucleotide bases in lower case represent introns within the *SLP1* ORF. Introns all followed GT-AG rule and contained consensus sequences associated with fungal introns (Gurr *et al.*, 1987).


```

1:  ATG TTG CCC ATT ACT GTT GTT ACT CTG TTT GCG GCC CTC GCC GCC GCT GCG
1:  M   L   P   I   T   V   V   T   L   F   A   A   L   A   A   A   A

52:  CCC GCC TCC GTC TCC ATG GAA AAG CGT CGT GTG GAG GGC GAG CTG GTC GTA
18:  P   A   S   V   S   M   E   K   R   R   V   E   G   E   L   V   V

103: CGG GCG GAT GCT GCC CCC CCG GCG GTG TTG ACT GAG TTG TCC TCG CCC GTC
35:  R   A   D   A   A   P   P   A   V   L   T   E   L   S   S   P   V

154: GCG TCT GCT CCT GCG GCC GAG GCT TCC AAG GCA GGT GAT GCG GCC AAG GCA
52:  A   S   A   P   A   A   E   A   S   K   A   G   D   A   A   K   A

205: GGT GAT GCG GCC AAG GCA GGC GAT GCG GCC AAG GCA GGC GAT GCG GCC AAA
69:  G   D   A   A   K   A   G   D   A   A   K   A   G   D   A   A   K

256: GGA GGC GAT GCC AAA GGA GGC GAT GCC AAA GGA GGC GAT GCC AAA GGA GGC
86:  G   G   D   A   K   G   G   D   A   K   G   G   D   A   K   G   G

307: GAT GCC AAA GGA GGC AAA GGA GGC GAT GCC AAA GGA GGC AAA GGA GGG GAT
103: D   A   K   G   G   K   G   G   D   A   K   G   G   K   G   G   D

358: GCG GCC AAA GGA GGC AAA GGA GGG GAT GCG GCC AAA GGA GGC AAA GGA GGG
120: A   A   K   G   G   K   G   G   D   A   A   K   G   G   K   G   G

409: GAT GCA GCC AAA GGA GGC AAT GTC CGC GGC TGC GCA GAC CTC AAG ACC AAC
137: D   A   A   K   G   G   N   V   R   G   C   A   D   L   K   T   N

460: GGG CCC GTG GTC GAG CAC AAG GTG GTC CAG GGC GAC ACG CTG GGC AAG CTG
154: G   P   V   V   E   H   K   V   V   Q   G   D   T   L   G   K   L

511: ACG GCG ACG TTC CAG TCA GGC ATC TGC AAT ATC GCC AAG GAG AAC AAC ATC
181: T   A   T   F   Q   S   G   I   C   N   I   A   K   E   N   N   I

562: GCC GAC CCG GAC AAG ATC GAC GTC GGC CAG GTG CTC AAG ATC CCC ACC GGC
198: A   D   P   D   K   I   D   V   G   Q   V   L   K   I   P   T   G

613: CTC TGC ACG CAA AAC GTC GAC AAC AAT TCG TGT ATC AAG GCT GCA GTT GTC
215: L   C   T   Q   N   V   D   N   N   S   C   I   K   A   A   V   V

664: AAC CCC AAC ACC GAT GAA AAG GGC ACC TGC CTC AAG ACG GGC CCC TTC ACG
232: N   P   N   T   D   E   K   G   T   C   L   K   T   G   P   F   T

715: CGC GTC ATC AAG AAG GGC GAC AGC TTC GTT GGT ATT GCC AAG GAG CTG GGC
249: R   V   I   K   K   G   D   S   F   V   G   I   A   K   E   L   G

766: TTG CAG GAG CAG GCC GTG GTT GAT GTT AAC CCT GGC GTC GAC CGC TTC AAT
266: L   Q   E   Q   A   V   V   D   V   N   P   G   V   D   R   F   N

817: TTG CTG CCC GAA CAG ACC ATC AAC TTG CCC AAG TGC AAA TAA
283: L   L   P   E   Q   T   I   N   L   P   K   C   K   *

```

Figure 3.3 Nucleotide sequence and putative amino acid sequence of the *M. oryzae* *SLP2* gene. The DNA sequence of the *SLP2* gene (Accession number MGG_03468) was retrieved from the *M. oryzae* genome database (www.broad.mit.edu/annotation/fungi/magnaporthe/)(Dean *et al.*, 2005). Putative derived amino acid sequences are listed below each codon using the standard one letter code.

3.3.3 Multiple amino acid sequence alignment of Slp1 and Slp2 demonstrates shared homology with other fungal LysM proteins

To determine the relatedness of the *M. oryzae* Slp1 and Slp2 proteins, amino acid sequences of Slp1 and Slp2 were aligned with other putative LysM proteins from related fungi using ClustalW (Thompson *et al.*, 1994; Chenna *et al.*, 2003). Amino acid sequences of Slp1 and Slp2 proteins were retrieved from the *M. oryzae* genome sequence database <http://www.broad.mit.edu/annotation/fungi/magnaporthe/>). A BLASTP search (Altschul *et al.*, 1990) was performed and amino acid sequences of a number of related fungal LysM proteins were retrieved based on a homology support value of 1×10^{-10} with Slp1 and Slp2. Included in the alignment were the fungal LysM proteins, from *Colletotrichum lindemuthiana* (Cih1), *Cladosporium fulvum* (Ecp6), *Mycosphaerella fijiensis* (Myfi212004), *Mycosphaerella graminicola* (Mygr111221), *Mycosphaerella graminicola* (Mygr105487), *Aspergillus carbonarius* (Asca397243), *Aspergillus niger* (Asni137703), *Aspergillus niger* (Asni46084), *Aspergillus flavus* (AFL06185), *Aspergillus nidulans* (ANID_04644), *Aspergillus carbonarius* (Asca11079), *Aspergillus niger* (Asni45667), *Cryptonectria parasitica* (Crpa331312), *Botrytis cinerea* (BC1G_13975), *Sclerotinia sclerotiorum* (SS1G_03535), *Aspergillus niger* (Asni40209), *Aspergillus flavus* (AFL08011), *Aspergillus oryzae* (A124000032), *Aspergillus carbonarius* (Asca10397), *Aspergillus niger* (Asni38961), and *Cochliobolus heterostrophus* (Coh32914), as shown in Figure 3.4.

3.3.4 Phylogenetic tree of fungal LysM effector proteins

Phylogenetic analysis of LysM containing effector proteins was carried out using amino acid sequences from a range of fungal plant pathogens. A phylogenetic tree was constructed using the Maximum Likelihood algorithm (Felsenstein, 1981) using the phylogenetic analysis program PhyML (Dereeper *et al.*, 2008), as shown in Figure 3.5. The phylogeny was supported with a bootstrap value of 100 resampling of data. Amino acid sequences of fungal LysM proteins were sourced based on homology to the *Magnaporthe oryzae* LysM protein Slp1 (1×10^{-10}).

Slp1_M. oryzae	21	YTVQGN	DTEITISQKLNS---	GICNATLNLNLANPNFIALGAVIKPTAPACVI--	DNIS
CtH1_C. lindemuthiana	64	HKVKSGE	ESITITIAEKYDT--	GICNLAIRLNLDLPNIIDLNQDITPDCACEK--	DNTS
Ecp6_C. fulvum	17	YTVVKGD	DTTITSIAKKFKS-	GICNHVSVNKLNPILIELGATIIIPDNCSNK--	DNKS
Myfi212004_M. fijiensis	181	YTVKSGD	STTTIAKNFSS---	GICDIAAYNKLTPNPFILNGQAQLPLNCTKP--	DNT
Mygr111221_M. graminicola	18	YTVKAGD	TTLGAIAQYNS--	GVCDIARVNGIDNPDIKPDQVLSIPANCVTPT--	DNTS
Mygr105487_M. graminicola	17	YVARSGD	TTLTKIAQEYIHDDVV	GVCDIARANLLADPNRIDAGTPYTIPINCQTY--	DRNS
Asca397243_A. carbonarius	13	-----	TTVFDEARTNR---	GVCDIGRONLMADVTLVPNVGSFFIIPPEVCE--	PDNST
Asn137703_A. niger	13	-----	TTVFDEARATNR---	GVCDIGRONLMADVTLVPNVGEYFIIPPEVCE--	PDNST
Asni46084_A. niger	12	-----	TTVFDEARKTNR---	GVCDIGRNHLMDVTLPPNIGEYFIIPGETCT--	PONES
AFL06185_A. flavus	13	-----	TTVFDEARITKR---	GVCDIGRONLMADVTLPPNVGETFIIPAEEVD--	PDNST
ANID_04644_A. nidulans	13	-----	TTLFSIATATNR---	GVCDIGRONLMADVTLIPNVGEQIIIPPECH--	TDNDS
Ascal1079_A. carbonarius	13	-----	TTVFDEAKATNR---	GVCDIGRYNLMDVTLIPNVGQTLPPIPEEVD--	PDSST
Asni45667_A. niger	13	-----	TTVFDEAKATNR---	GVCDIGRONLMADVTLIPNVGQTLPPIPAEVE--	PDNST
Crpa331312_C. parasitica	13	-----	TTTHADVANATGR---	GICNIAARYNFMAQALLPNVGQEIAPAEWCPDEID	DTT
BC1G_13975_A. cinerea	12	-----	DTIFSLAAATNR---	GVCDIARASRPDAEY-IDTGFTLIIPAECVN--	PONES
SslG_03535_S. sclerotiorum	12	-----	DTIFSLAAATNR---	GVCDIARASRPDAEY-IDTCMLIIPAQCVCN--	PDES
Asni40209_A. niger	12	-----	DTIASVSNVSVNR---	GICDIARLRNMADAMIPFLTGEQLHIPPETCT--	PDNST
AFL08011_A. flavus	12	-----	DTIYSIATTILNR---	GVCPILARYNHLSDPELLYPG-EVLYPEACNTNAADS	
A12400032_A. oryzae	12	-----	DTIYSIATTILNR---	GVCPILARYNHLSDPELLYPG-EVLYPEACNTNAADS	
Ascal0397_A. carbonarius	17	HTVQPNE	TITETIAHKYSI---	GACDLARLVNLDLPNFIYVDEPHIPSHTLP--	SDTS
Asn38961_A. niger	17	YTVQEN	DTTITIAKYNS---	GACDLARLVNLDLPNFIYANETHPRARATFP--	DDYS
Slp2_M. oryzae	20	DAAKAGD	DAAKAGDAKGDDAKGGDAKGDAGKGGDAKGGKGGDA		GGDA
Cohc32914_C. heterostrophus	14	YTIIVAG	DTTITTDKFGS---	GACNLAAYNNINSPNLIIPFEVTVTPANTCGA-IDFN	NS

Slp1_M. oryzae	75	CLAKQSDNNCTCVG---VSPYYTIVSGDTFFLVAQ-KFNLSVTEALQAAAN-VGADP--
CiH1_C. lindemuthiana	118	CHKPGDGTATCVKDGKK---DGKIDIVSVVSGDITSTIAQ-ALCITSLSKPDAN-PGVVVP--
Ecp6_C. fulvum	72	CVSTP-AEPTETCVPG---LFGSYTIVSGDITTNISQ-DFNITLDSLIAANTQIQENP--
Myfi212004 M. fijiensis	235	CLPPSPNATATCVAG---LENAYNIRSGDITTAIAAK-DFNITLASILAANPNITNP--
Mygr11221 M. graminicola	72	CKMPV-PVITNTCVG---VGSTYFVKSGDSFSATAT-SFNITLASLEARNPQIPNY--
Mygr105487 M. graminicola	74	CL---
Asca397243 A. carbonarius	62	CLLPDTN---TRTICLY---GGPRLYTYTVRGDITYEVIAR-RLNITVESLMHVDGSPNETLV
Asni137703 A. niger	62	CLLPNVN---ATRTICLY---GGPRLYTYTVRGDITYEVIAR-RLNITVESLMHVDGSPNETLV
Asni146084 A. niger	61	CLIKIDVG---RTRICLY---GGPRLYTYTVRGDITYEKIAL-RLNITVESLSGGQ----
AFL06185 A. flavus	62	CLLSGN---ATNTICLY---GGPRLYTYTVNGDITYEKIAQ-RLNITVEALMGNTTEG----
ANID 04644 A. nidulans	62	CLLPNTT---RTRICVS---GGPNRYTYTVNGDITYEILAR-RLNITVESLTAALAGDETTG-
Asca11079 A. carbonarius	62	CLLSSVT---RTRICIN---GGPRLYTYTVNGDITDIVAQ-RLNITASLSMSDDTAFT---
Asi45667 A. niger	62	CLLPNTT---RTRICIN---GGPRLYTYTVNGDITDIYAK-RLNITITESMSDDTSFT---
Crpa331312 C. parasitica	64	CWIDNYN---STNICLI---GGPRLYTYTVNGDITYATAN-RLNIAVATLSTGD-----
BC1G_13975 B. cinerea	60	CLLTAS---EDTTSCLY---GGPHTYTYTVRNDITYTKIAM-KFNIDVSA SADVIS----ML
SS1G 03535 S. sclerotiorum	60	CLLTAS---NDTTLCLY---GGPHTYTYTVRNDITYTKIAT-KFNIDVSVLSTNTTQ----ML
Asca140209 A. niger	61	CLLFPSPNTNDYACVS---GGPHTYTYTVRGDITRTIAL-RLNITVEALSAATG-----
AFL08011 A. flavus	62	CLLSLQN-STTNDCLF---GGPHTYRTTFEGDITRKIALGKFNITLEALNSSVGRMAG---
Al24000032 A. oryzae	62	CLLSLQN-STTNDCLF---GGPHTYRTTFEGDITRKIALGKFNITLEALNSSVGRMAG---
Asca10397 A. carbonarius	71	CFSPNLT-LTTNCLCP---GGPHVYITLPGDTLOKIANERFNITAEBSLNQIAQTGYIAA
Asni38961 A. niger	71	CFSTNNT-DATACLY---GGPHVYITLPGDTLOKIANERYNITIDSLSFTAQTYGYIAA
Slp2 M. oryzae	80	AKGGKGGDAAGKGNV---GCADLTKNGPVEHKVWGDTLGLKLTALFGSGCINIAKEN-
Coh232914 C. heterostrophus	69	CVNTIQTATGTDQCKGLSVSNPTQVLPDPTDTTLTAN-NFDKLTALENAGQRFAN-

Slp1_M. oryzae	125	----	LLIQLNQVNIIP	ICKN----
CIH1_C. lindemuthiana	171	----	HHINLVGQKINVP	VC-----
Ecp6_C. fulvum	124	----	DAIDVGIITV	VCPSSQCEAVGTYNIVG-DIFVDLATATVHTITGOIKALN
Myfi212004_M. fijiensis	288	----	DLIQVGGQIKIT	VCPNSRCDSVGSYIIKSG-DIFVDLATKYKATVGOIKALN
Mygr11221_M. graminicola	124	----	DLIFPGQVINTP	HCPSNVCDISGTYVIESG-DIFYNLAQSNNVTVGOIESLN
Mygr105487_M. graminicola		-----		
Asca397243_A. carbonarius	116	NPVSATAEINVGQFVKVFP	QCDPSOCITCPYRETNG	----VYKDLAQYDITVGOIMLS
Asn137703_A. niger	116	NPISPTAEIDVGQFKVFP	QCDPSOCVTCPPYSEKNG	----VYKDLAIKYGTITVGOIMMS
Asn146084_A. niger	107	-----SANETIPVGQFKVFP	ECSPSOCIICPPYVKG	----VYKDLAIKYGTITVGOIMLS

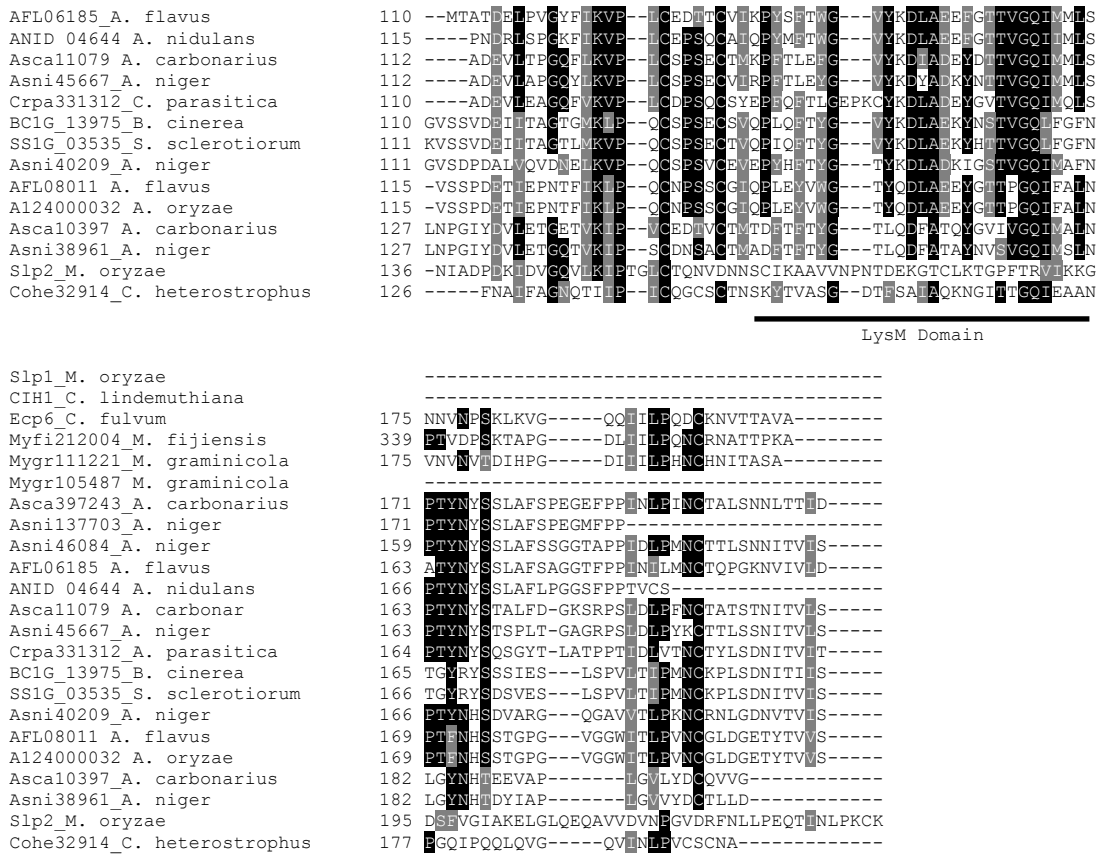


Figure 3.4 Multiple amino acid sequence alignment of fungal LysM proteins. Protein sequences were sourced from publically available databases based on homology ($1e^{-10}$) to *M. oryzae* Slp1 and Slp2. Fungal LysM domains were predicted using the LysM hmmer model developed by de Jonge and Thomma (2009), and are highlighted under the sequence alignment. Only *M. graminicola* (Mygr111221), *C. heterostrophus*, *C. fulvum*, *M. fijiensis*, *A. flavus* (AFL08011) and *A. oryzae* species were predicted to have three LysM domains under the hmmer model. The fungal species *A. niger* (Asni45667), *A. carbonarius*, *A. flavus* (AFL06185), *A. nidulans*, *A. niger* (Asni46084), *A. carbonarius* (Asca397243) and *M. graminicola* contain one LysM domain. All other fungal species included in the alignment contain two putative LysM domains. Sequences were aligned using CLUSTALW (Thompson *et al.*, 1994), and shaded using BOXSHADE 3.21. Identical amino acid residues are shaded in black, similar residues in grey, and non-identical residues are unshaded.

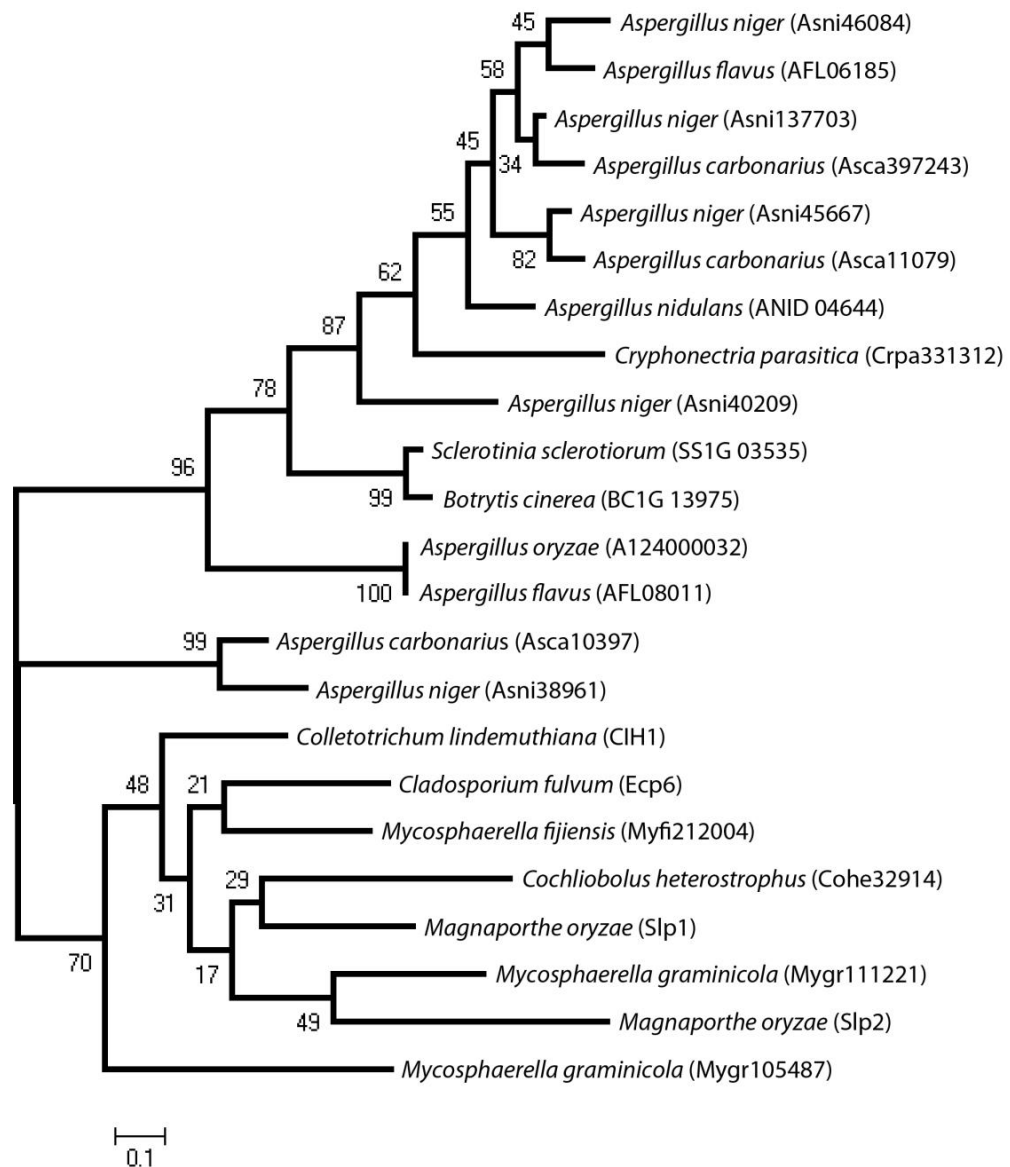


Figure 3.5 Phylogenetic analysis of LysM amino acid sequences from a range of fungal organisms. A maximum likelihood tree (Felsenstein, 1981) was constructed from a range of fungal organisms. Amino acid sequences were sourced from publicly available genome databases, and were selected based on their homology (1×10^{-10}) to the LysM-domain containing protein Slp1. Accession numbers of the proteins can be found in parentheses. The phylogenetic analysis was supported with a re-sampling bootstrap value of 100. Branch strength support is indicated with a bootstrap re-sampling value of 100.

3.3.5 Generation of the *SLP1* targeted gene replacement vector

In order to determine and assess the role of *SLP1*, targeted gene replacement of *SLP1* was performed using a PCR-based split marker deletion method, as shown in Figure 3.6 (Yu *et al.*, 2004; Kershaw and Talbot, 2009). In a first round PCR, primers were designed to amplify a 1 kb genomic region both upstream and downstream of the *SLP1* ORF. Primers were designed to contain 5' and 3' overhanging regions complementary in sequence to the hygromycin phosphotransferase resistance gene cassette (*Hph*). These overhanging regions were required to create a fusion between the upstream and downstream flanking regions of the *SLP1* ORF to the *Hph* resistance cassette during a second-round PCR. In the second round PCR, two constructs were amplified. The first construct contained a 1 kb upstream genomic fragment of *SLP1* fused at the 3' to the initial 1 kb coding region of the 1.4 kb *Hph* cassette. The second construct contained a 1kb downstream genomic fragment of the *SLP1* stop codon fused at the 5' end with the terminal 1 kb coding region of the *Hph* resistance cassette. The two constructs were simultaneously introduced into the *M. oryzae* Guy11 strain. Successful integration of the two constructs at the *SLP1* locus occurred when three independent homologous recombination events occur between the constructs and the chromosomal DNA (Kershaw and Talbot, 2009). The primers used for the targeted gene replacement of *SLP1*, as shown in Figure 3.6, can be found in Table 3.1.

Table 3.1 Oligonucleotide primers used in the targeted gene deletion of *SLP1*

Primer Name	Nucleotide sequence (5' - 3')
MGG10097.1	GTCTCCATCCCGCGCAATGCAGTA
MGG10097.2	GTCGTGACTGGGAAAACCCCTGGCGAGTTGTTTGAGAGCGAATGGCT
MGG10097.3	TCCTGTGTGAAATTGTTATCCGCTTGGCCGCGAGGACTTGGAGAGGC
MGG10097.4	CAGTTAGCAAAAACAATCTATTGCGCA
HY split	GGATGCCTCCGCTCGAAGTA
YG split	CGTTGCAAGACCTGCCTGAA
M13F	CGCCAGGGTTTTCCCAGTCACGAG
M13R	AGCGGATAACAATTTTCACACAGGA

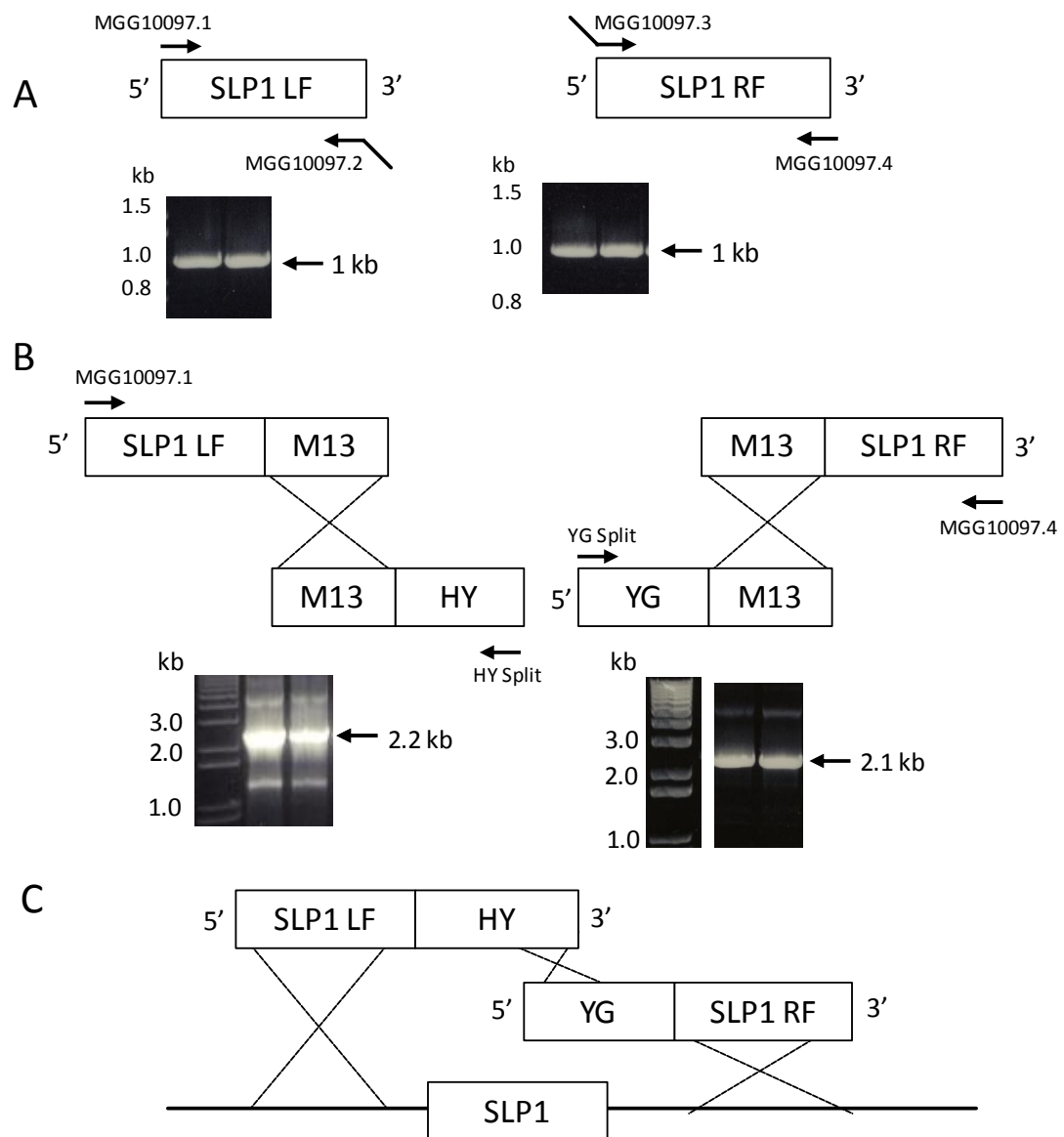


Figure 3.6 Schematic representation of the targeted deletion of *SLP1* using a PCR-based split-marker deletion method. A. Amplification of a 1 kb flanking region either side of the *SLP1* ORF was performed using the primers shown. Primers MGG10097.2 and MGG10097.3 contain an M13 overhanging nucleotide sequence which is complementary to the hygromycin Hph resistance marker. **B.** A second round PCR was performed in which the *SLP1* LF was fused to the initial 1 kb coding sequence of the *Hph* cassette and the *SLP1* RF was fused to the terminal 1 kb coding region of the *Hph* cassette. **C.** Upon introduction of the two constructs into *M. oryzae*, three independent homologous recombination events occur, resulting in the replacement of the *SLP1* ORF with the *Hph* cassette and bestowing resistance of putative transformants to hygromycin B.

3.3.6 Analysis of putative $\Delta slp1$ transformants

Putative $\Delta slp1$ transformants were selected based on their resistance to the antibiotic hygromycin B (200 $\mu\text{g ml}^{-1}$). More than fifty putative transformants were selected and genomic DNA extracted. Genomic DNA was digested with the restriction enzyme *Eco* RI and fractionated by agarose gel electrophoresis before being transferred to a Hybond-N membrane (Amersham). The membrane was probed with either a 500 bp fragment of the *SLP1* ORF, a 1 kb fragment upstream of the *SLP1* start codon or a 500 bp fragment of the hygromycin phosphotransferase (*Hph*) resistance cassette, as shown in Figure 3.7. Initial probing with a 500 bp fragment of the *SLP1* locus identified one transformant, T19, in which the *SLP1* probe failed to hybridise successfully, but was present in the WT control lane, as shown in Figure 3.7B. Further analysis of T19 was performed in which a 1 kb upstream flanking region of the *SLP1* locus was used as a probe, as shown in Figure 3.7A. This probe hybridised successfully to a 5.5 kb fragment in T19 and to a 4.5 kb fragment in the Guy11 control lane, as shown in Figure 3.7B. A size difference of 1 kb was expected between the native *SLP1* locus and the larger *Hph* cassette in $\Delta slp1$ mutants, and suggested that the *SLP1* locus of T19 had been replaced with the *Hph* cassette. Finally, a 1 kb *Hph* fragment was used as a probe to check for ectopic integration of the construct in T19. As shown in Figure 3.7B, the presence of a hybridising band at 5.5 kb, which was absent in the Guy11 control lane, suggested that the *SLP1* locus had been replaced with the *Hph* resistance cassette in T19. T19 was assumed to be a $\Delta slp1$ null mutant and was selected for further phenotypic analysis.

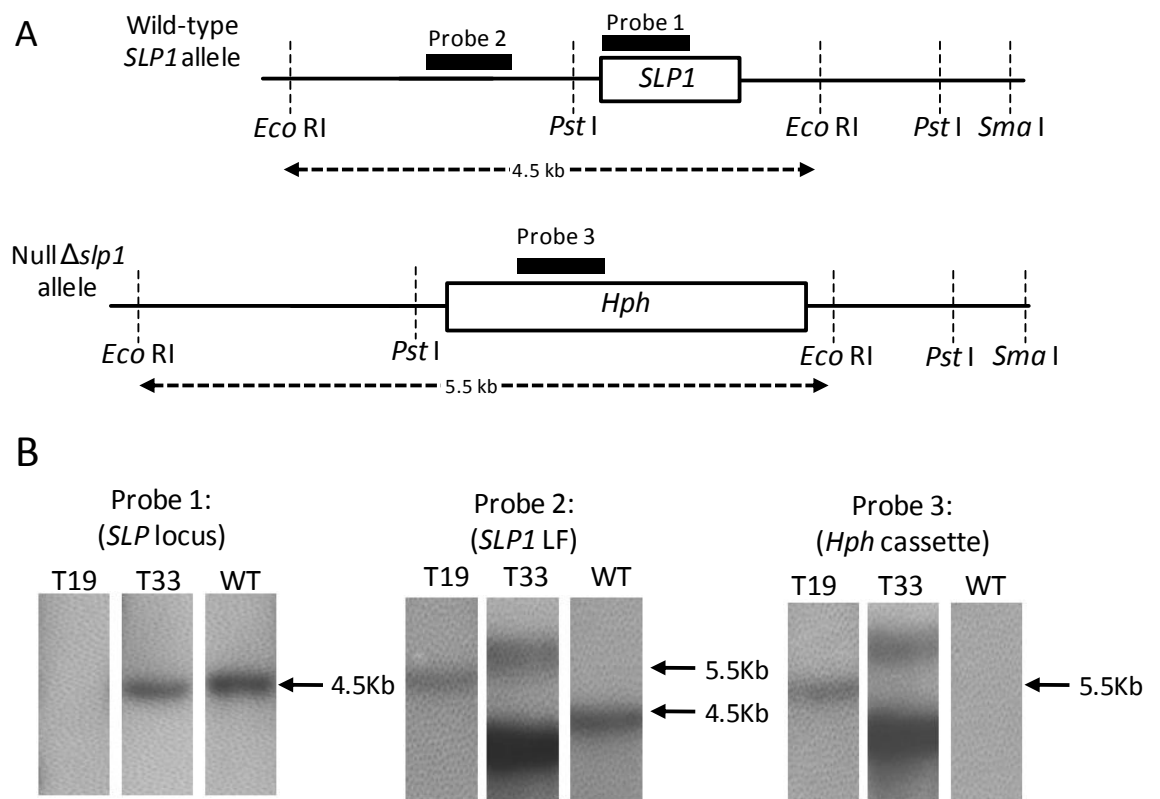


Figure 3.7 Targeted gene replacement of *SLP1* and confirmation by Southern Blotting analysis. **A.** Targeted gene replacement of *SLP1* was carried out using a PCR-based split marker method (Kershaw & Talbot, 2009) resulting in replacement of the *SLP1* allele with a hygromycin phosphotransferase resistance cassette (*Hph*). The restriction sites used for confirmation of putative $\Delta slp1$ null mutants and the probes used in Southern blotting analysis are shown. **B.** Confirmation of the $\Delta slp1$ null mutant. Two transformants, T19 and T33, are shown along with the wild-type Guy11 (WT) DNA. Transformant T19 is a putative $\Delta slp1$ replacement mutant, and T33 is a putative ectopic transformant. Genomic DNA was isolated from transformants and was digested with the restriction enzyme *Eco* RI before being fractionated by agarose gel electrophoresis and transferred a Hybond-N membrane (Amersham). Probing with a 500 bp fragment of the *SLP1* locus (Probe 1) failed to hybridise to DNA from transformant T19, but can be seen hybridising at the expected 4.5 kb in T33 and WT control lanes. Probing with a 1 kb promoter fragment upstream of the *SLP1* locus (Probe 2) hybridises at the expected 5.5 kb in T19 and at 4.5 kb in WT DNA. Probing with a 500bp fragment of the hygromycin resistance gene (Probe 3) shows only a single integration of the resistance cassette in T19 and hybridises at the expected size of 5.5 kb. The multiple hybridisation of probe 3 in T33 is consistent with ectopic integration of the *Hph* resistance cassette in this transformant. As expected, probe 3 failed to hybridise in the WT control lane.

3.3.7 Generation of the *SLP2* targeted gene replacement vector

In order to determine and assess the role of *SLP2*, targeted gene replacement of *SLP2* was performed using a PCR-based split marker deletion method, as shown in Figure 3.8 (Yu *et al.*, 2004; Kershaw and Talbot, 2009). In a first round PCR, primers were designed to amplify a 1 kb genomic region both upstream and downstream of the *SLP2* ORF. Primers were designed to contain 5' and 3' overhanging regions that were complementary in sequence to the hygromycin phosphotransferase resistance gene cassette (*Hph*), which were required to create a fusion between the upstream and downstream flanking regions of the *SLP2* ORF to the *Hph* resistance cassette during a second-round PCR. In the second round PCR, two constructs were amplified. The first construct contained a 1 kb upstream genomic fragment of *SLP2* fused at the 3' end to the initial 1 kb coding region of the 1.4 kb *Hph* cassette. The second construct contained a 1kb downstream genomic fragment of the *SLP2* stop codon fused at the 5' end with the terminal 1 kb coding region of the *Hph* resistance cassette. The two constructs were simultaneously introduced into the *M. oryzae* $\Delta ku70$ strain which lacks the non-homologous DNA end-joining pathway (Krappmann *et al.*, 2006) and reduces the frequency of ectopic integration of the resistance cassette (Kershaw and Talbot, 2009). Successful integration of the two constructs at the *SLP2* locus occurred when three independent homologous recombination events occurred between the constructs and the chromosomal DNA (Kershaw and Talbot, 2009). The primers used to generate the *SLP2* gene replacement construct can be found in Table 3.2.

Table 3.2 Oligonucleotides primers used in the targeted gene deletion of *SLP2*

Primer Name	Nucleotide sequence (5' - 3')
MGG03468.1	GAGAAACAACCTAACCCAAAAGCT
MGG03468.2	GTCGTGACTGGGAAAACCCTGGCGGCTGTCAAAGCTGTATACGAT
MGG04368.3	TCCTGTGTGAAATTGTTATCCGCTGGCGCTTAAATGCATTTTCTG
MGG03468.4	GCTCGTTCCACTAGACAGTGGTTA
HY split	GGATGCCTCCGCTCGAAGTA
YG split	CGTTGCAAGACCTGCCTGAA
M13F	CGCCAGGGTTTTCCAGTCACGAG
M13R	AGCGGATAACAATTCACACAGGA

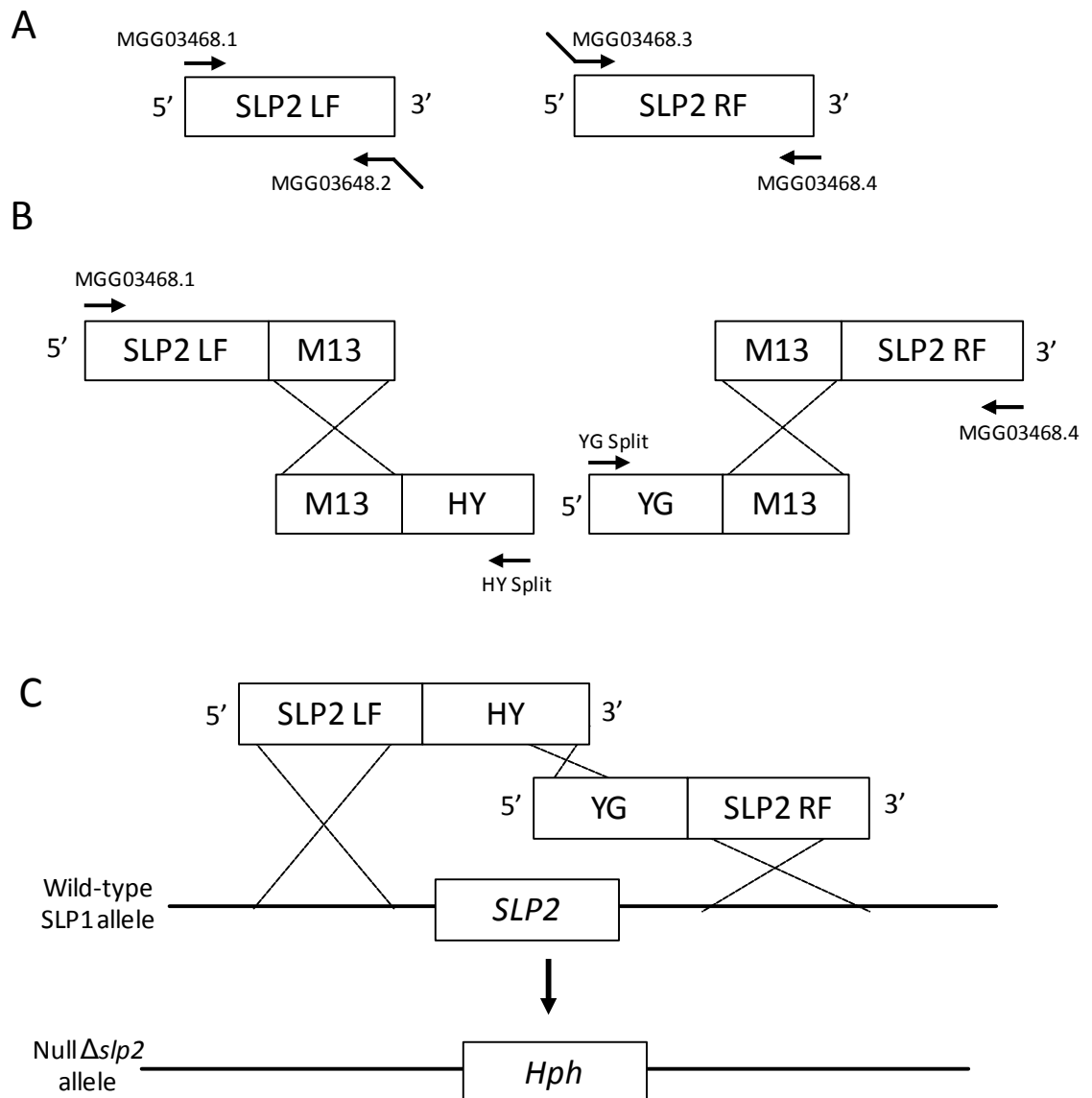


Figure 3.8 Schematic representation of the targeted deletion of *SLP2* using a PCR-based split-marker deletion method. **A.** Amplification of a 1 kb flanking region either side of the *SLP2* ORF was performed using the primers shown. Primers MGG03468.2 and MGG03468.3 contain an M13 overhanging nucleotide sequence which is complementary in sequence to the hygromycin *Hph* resistance marker. **B.** A second round PCR was performed in which the *SLP2* LF and was fused to the initial 1 kb coding sequence of the *Hph* cassette and the *SLP2* RF was fused to the terminal 1 kb coding region of the *Hph* cassette. **C.** Introduction of the two fragments into *M. oryzae* results in three independent homologous recombination events between the flanking regions and the chromosomal DNA, resulting in the replacement of the *SLP2* ORF with the *Hph* cassette bestowing resistance of putative transformants to hygromycin B.

3.3.8 Analysis of putative $\Delta slp2$ transformants

Putative $\Delta slp2$ transformants were selected based on their resistance to the antibiotic hygromycin B (200 $\mu\text{g ml}^{-1}$). Genomic DNA was extracted from transformants, digested with *Xba* I and fractionated by agarose gel electrophoresis. The gel was transferred to a Hybond-N membrane (Amersham) and probed with either an 850 bp fragment from the *SLP2* locus, or the 5' *SLP2* LF flanking region, as shown in Figure 3.9. The absence of a hybridising band in lanes 1, 2, 3, 4, 5, 7 and 8, indicated that a targeted gene replacement event had occurred in these transformants, as shown in Figure 3.9C. One transformant, transformant 6, contained the *SLP2* ORF, suggesting that an ectopic integration of the *Hph* resistance cassette had occurred. To confirm successful integration of the replacement construct at the *SLP2* locus in positive transformants, the membrane was further probed with a 1 kb *SLP2* flanking region, as shown in Figure 3.9A and Figure 3.9D. Using this strategy, the LF probe, as shown in Figure 3.9A, should hybridise at 3.8 kb in the wild-type locus and 4.4 kb in successful $\Delta slp2$ mutants as a result of integration of the larger *Hph* cassette at the *SLP2* locus. As shown in Figure 3.9D, transformants 1, 2, 3, 4, 5, 7 and 8 appeared to be putative $\Delta slp2$ replacement mutants, consistent with results gained from probing with the *SLP2* locus. In contrast, the *SLP2* LF hybridised at 3.8 kb in lane 6 containing transformant 6, an ectopic $\Delta slp2$ mutant, and lane 9 containing Guy11 genomic DNA.

To further confirm correct integration of the *Hph* cassette at the *SLP2* locus, PCR was performed on genomic DNA extracted from these transformants. Using primers upstream and downstream of the *SLP2* locus, as shown in Figure 3.10A, a 3.5 kb fragment would be amplified from genomic DNA extracted from wild-type Guy11 DNA and ectopic transformants, whereas a 4.5 kb fragment would be amplified in putative $\Delta slp2$ mutants, as shown in Figures 3.10A and 3.10B. Additionally, *Hph*-specific primers were used to confirm the presence of the *Hph* cassette at the *SLP2* locus, as shown in Figures 3.10C and 3.10D.

Transformants 1 and 2 were putative $\Delta slp2$ mutants by Southern analysis and PCR and were selected for phenotypic analysis.

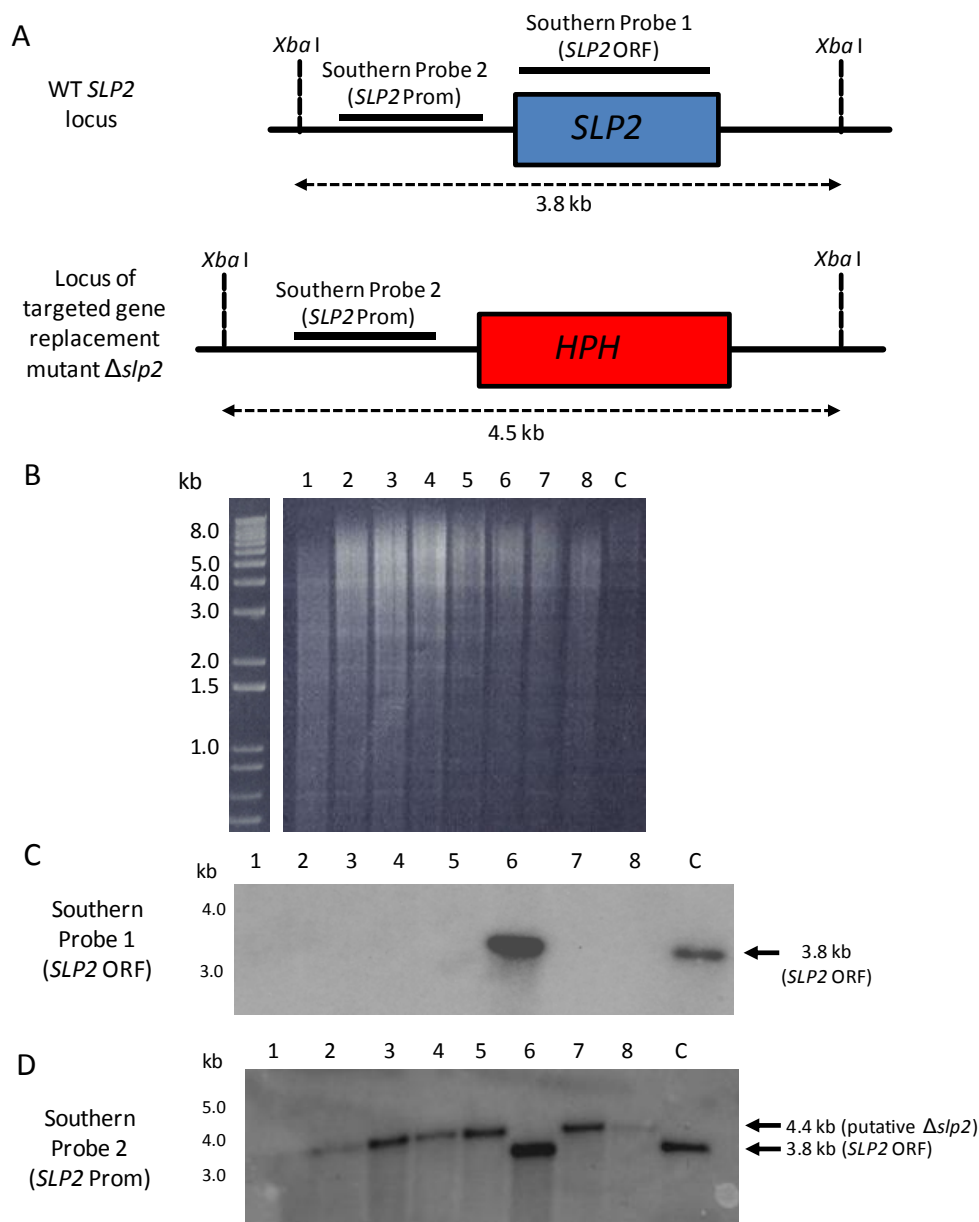


Figure 3.9 Southern blotting analysis of putative $\Delta slp2$ transformants. **A.** Schematic representation of the *M. oryzae* wild-type locus *SLP2* and the targeted gene replacement locus highlighting the *Xba* I restriction sites used for Southern analysis. **B.** A number of hygromycin-resistant transformants were selected and genomic DNA extracted. DNA was restriction digested with *Xba* I and fractionated by agarose gel electrophoresis before being transferred to a Hybond-N membrane (Amersham). **C.** Southern analysis hybridised with a 850 bp fragment of the *SLP2* ORF. Transformants 1, 2, 3, 4, 5, 7, 8 failed to hybridise, suggesting successful integration of *Hph* resistance cassette at the *SLP2* locus. **D.** Southern blot analysis hybridised with a 1 kb fragment of the *SLP2* upstream promoter region. Transformants 1, 2, 3, 4, 5, 7, 8 hybridised at 4.4 kb, suggesting successful integration of *HPH* resistance cassette at the *SLP2* locus.

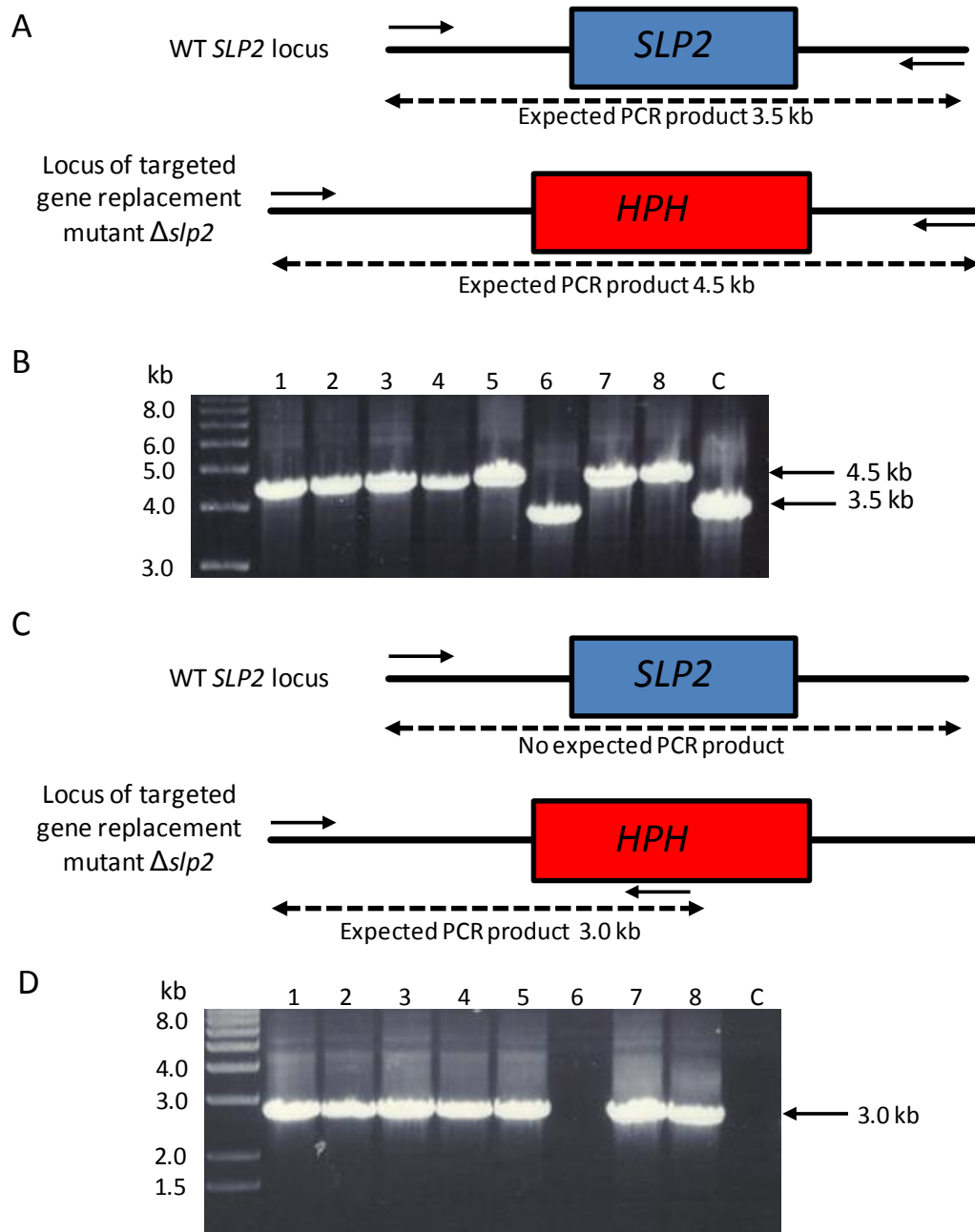


Figure 3.10 Confirmation of putative $\Delta slp2$ transformants by PCR. **A.** Schematic representation of wild-type *SLP2* locus and expected locus of targeted gene replacement $\Delta slp2$ mutants. Primers used to confirm $\Delta slp2$ transformants by PCR are shown. **B.** Using primers upstream and downstream of the locus, PCR confirms 7 putative $\Delta slp2$ mutants (1, 2, 3, 4, 5, 7, 8), in which the expected 4.5 kb PCR product is amplified. Transformant number 6 contains an ectopic integration of the *Hph* resistance cassette, and amplification yields the same 3.0 kb product as the control Guy11 (C). **C.** Schematic representation of the wild-type *SLP2* locus and the expected locus of the targeted gene replacement mutants. The primers used are shown as arrows. **D.** Amplification of 3.0 kb product confirms integration of the *Hph* resistance cassette in transformants 1, 2, 3, 4, 5, 7, and 8. No products could be amplified from either Transformant number 6 or from Guy11 control DNA (C), confirming correct integration of the *Hph* cassette at the *SLP2* genomic locus. All transformations were introduced into a $\Delta ku70$ genetic background which lacks the non-homologous DNA end-joining pathway (Krappmann *et al.*, 2006) and reduces the frequency of ectopic integration of the resistance cassette (Kershaw and Talbot, 2009).

3.3.9 $\Delta slp1$ vegetative growth and colony morphology

In order to assess the effect of targeted gene replacement of *SLP1* on colony morphology and vegetative growth, mycelial plugs of the $\Delta slp1$ mutant and the wild-type *M. oryzae* Guy11 strain were inoculated onto CM agar plates and colony growth measurements were taken over a ten-day period, as shown in Figure 3.11. All $\Delta slp1$ mutants displayed normal patterns of vegetative growth and exhibited normal diurnal patterns of growth with distinctive light and dark concentric rings as a result of diurnal patterns of conidiation (Figure 3.11). After ten days post-inoculation, the $\Delta slp1$ mutant colony had grown significantly more than Guy11 (two-tailed t-test, $p < 0.05$).

3.3.10 $\Delta slp2$ vegetative growth and colony morphology

In order to assess the effect of targeted gene replacement of *SLP2* on colony morphology and vegetative growth, mycelial plugs of the $\Delta slp2$ mutant and the wild-type *M. oryzae* Guy11 strain were inoculated onto CM agar plates and colony growth measurements were taken over a ten-day period, as shown in Figure 3.12. All $\Delta slp2$ mutants displayed normal patterns of vegetative growth and exhibited normal diurnal patterns of growth with distinctive light and dark concentric rings as a result of diurnal patterns of conidiation (Figure 3.12). After ten days post-inoculation, the $\Delta slp2$ mutant colony had grown significantly more than Guy11 (two-tailed t-test, $p < 0.05$).

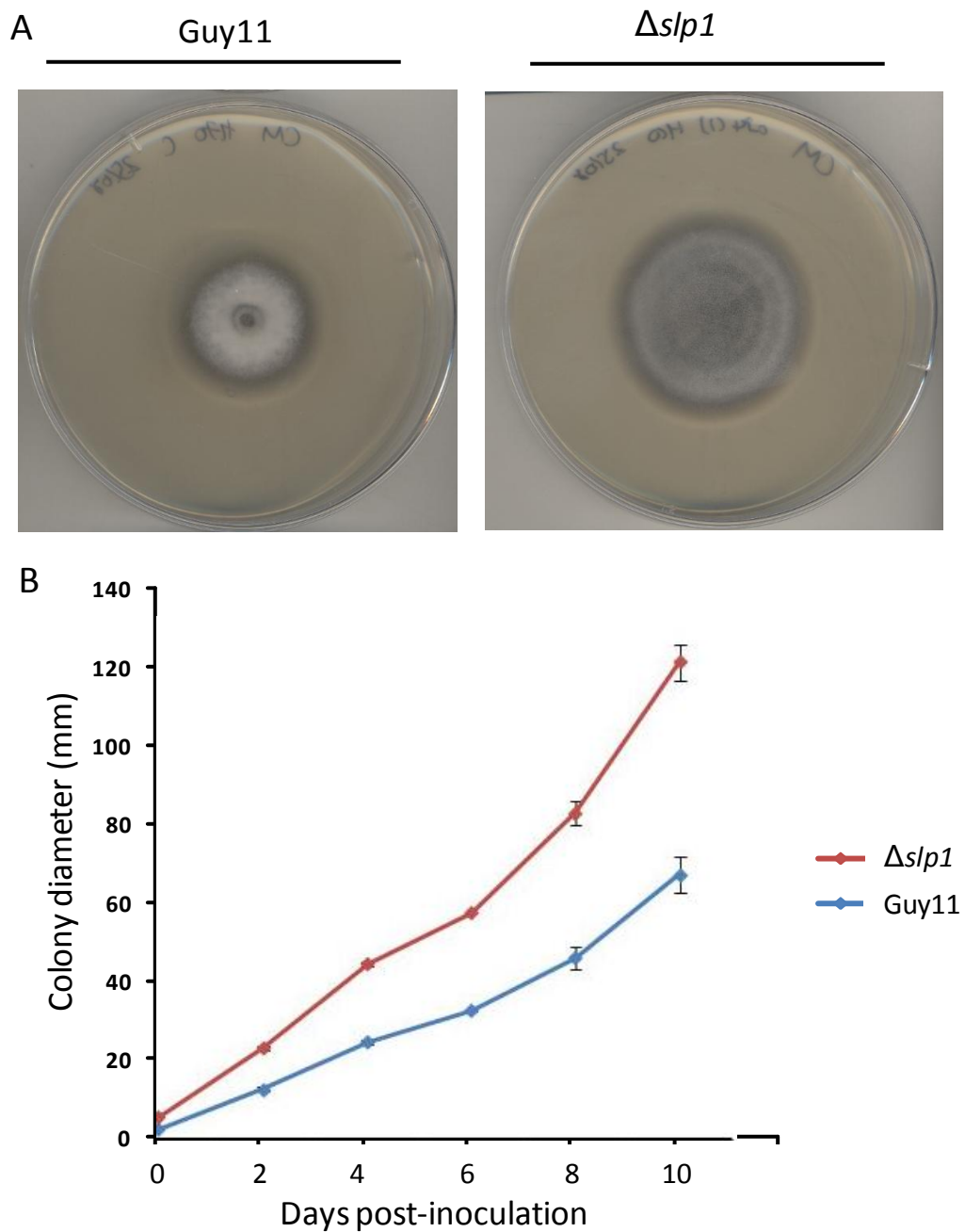


Figure 3.11 Vegetative growth and colony morphology of $\Delta slp1$ mutants. **A.** A 4 mm mycelial plug of the Guy11 and the $\Delta slp1$ mutant was inoculated onto CM agar plates and incubated for 6 days at 26°C. Colony images were captured using an Epson Expression 1680 Pro scanner. **B.** Over a period of ten days, the $\Delta slp1$ displayed an accelerated growth phenotype compared to the Guy11 control. Error bars represent 1 standard deviation from three independent replicates.

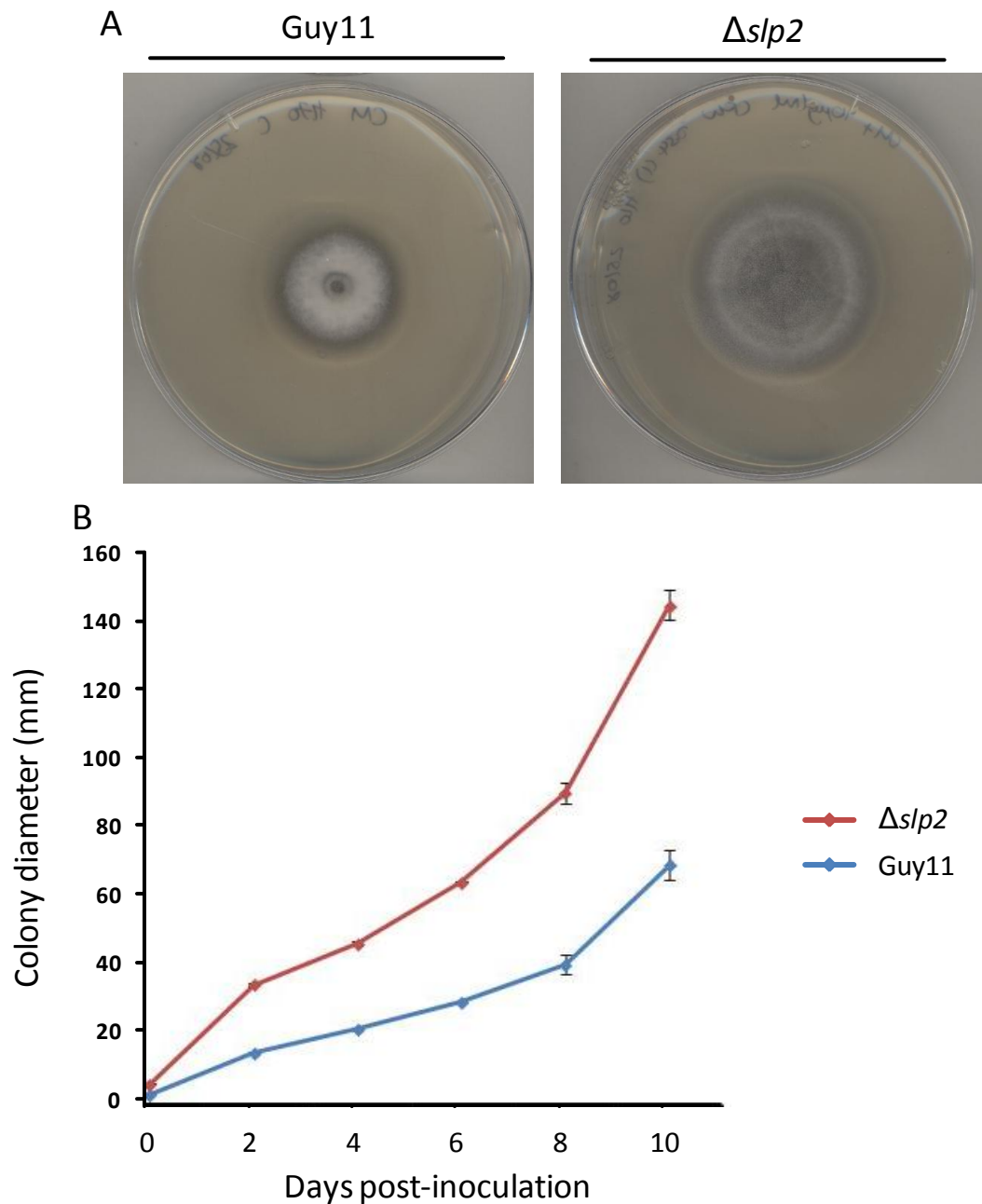


Figure 3.12 Vegetative growth and colony morphology of $\Delta slp2$ mutants. **A.** A 4 mm mycelial plug of the Guy11 and $\Delta slp2$ mutant was inoculated onto CM agar plates and incubated for 6 days at 26°C. Colony images were captured using an Epson Expression 1680 Pro scanner. **B.** Over a period of ten days, the $\Delta slp2$ displayed an accelerated growth phenotype compared to the Guy11 control. Error bars represent 1 standard deviation from three independent replicates.

3.3.11 The $\Delta slp1$ mutant is reduced in virulence

To investigate the role of *SLP1* in causing plant disease, three-week old seedlings of the blast-susceptible rice cultivar, CO-39 were spray inoculated with the $\Delta slp1$ mutant and the wild-type Guy11 strain. Although pathogenic, the $\Delta slp1$ mutant appeared to be significantly reduced in its capacity to cause plant disease, as shown in Figure 3.13A. In order to quantify this reduction in virulence, both lesion density and lesion size were analysed using image analysis software (ImageJ), as shown in Figure 3.13B and 3.13C. Both lesion size and lesion density were significantly reduced compared to Guy11 lesions, as shown in Figure 3.13B and 3.13C. The mean lesion size for Guy11 was calculated to be 1.15 mm^2 (\pm SE 0.049, $n > 100$ lesions), whilst the mean lesion size of the $\Delta slp1$ mutant was calculated to be 0.31 mm^2 (\pm SE 0.025, $n > 100$), which was calculated to be statistically significant (t-test, $p < 0.01$). Additionally, the mean lesion density per unit area of the $\Delta slp1$ mutant (11.1 ± 5.7 , $n = 49$) was found to be significantly lower than that of the wild-type (40.7 ± 10.8 , $n = 28$) (t-test, $p < 0.01$).

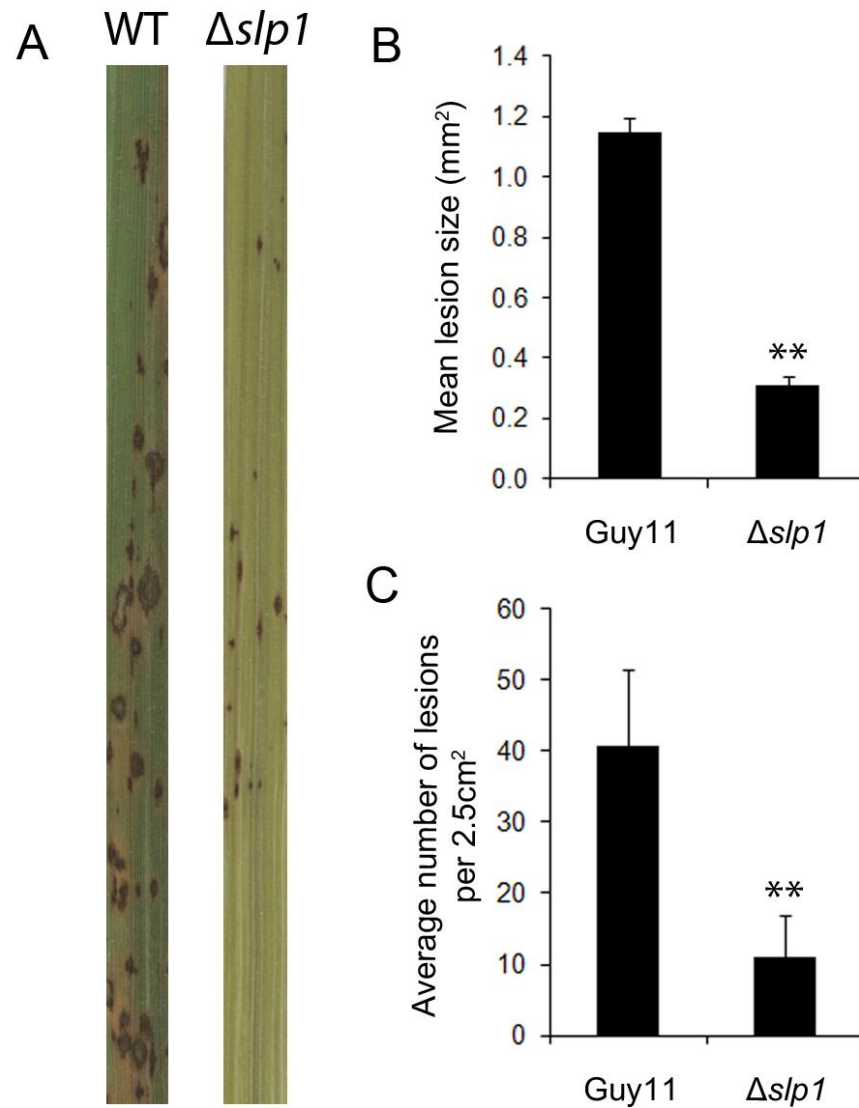


Figure 3.13 The $\Delta slp1$ mutant is reduced in virulence. **A.** Three week-old seedlings of the blast susceptible rice cultivar CO-39 were spray inoculated with the $\Delta slp1$ mutant and the Guy11 strain at a density of 5×10^4 spores ml⁻¹ and incubated for 7 days. **B.** The mean lesion size of the $\Delta slp1$ mutant is significantly reduced compared to that of the Guy11 strain. **C.** The mean number of lesions per 2.5 cm² of the $\Delta slp1$ strain was significantly reduced compared to that of the Guy11 strain. ** denotes $p < 0.05$.

3.3.12 The $\Delta slp2$ mutant is fully pathogenic

To assess the role of *SLP2* in causing plant disease, three-week old seedlings of the blast-susceptible cultivar, CO-39, were spray inoculated with the $\Delta slp2$ mutant and the wild-type $\Delta ku70$ strain. In order to investigate the functionality of *SLP2*, targeted gene replacement was performed in the $\Delta ku70$ mutant strain. This mutant strain has previously been shown to be fully pathogenic on rice leaves and is a useful molecular tool which reduces the frequency of non-homologous recombination during transformation of targeted gene replacement DNA constructs (Kershaw *et al.*, 2009). After 7 days post-inoculation, the disease symptoms of both the $\Delta slp2$ mutant and the wild-type $\Delta ku70$ strain appeared to be identical, with characteristic necrotic lesions visible on rice leaves inoculated with both the $\Delta slp2$ mutant and the $\Delta ku70$ strain, as shown in Figure 3.14A. In order to statistically compare the $\Delta slp2$ mutant and the $\Delta ku70$ strain, the lesion density of the $\Delta slp2$ mutant and $\Delta ku70$ strain was quantified, as shown in Figure 3.14B. The mean lesion density per 100 mm² of the $\Delta slp2$ mutant was calculated to be 0.43 lesions per 100mm² (SD \pm 0.097), whereas the mean lesion density of the $\Delta ku70$ strain was found to be 0.51 lesions per 100mm² (SD \pm 0.087). Statistically, no significant difference between the mean lesion density of the $\Delta slp2$ mutant and the wild-type $\Delta ku70$ strain could be determined (n>100, two-tailed t-test, p>0.05). As there was no significant virulence phenotype of the $\Delta slp2$ mutant, we conclude that the role of *SLP2* to cause plant disease is negligible. We therefore focussed our research efforts on the characterisation of *Slp1* and the role of the *SLP2* was not characterised further for this reason.

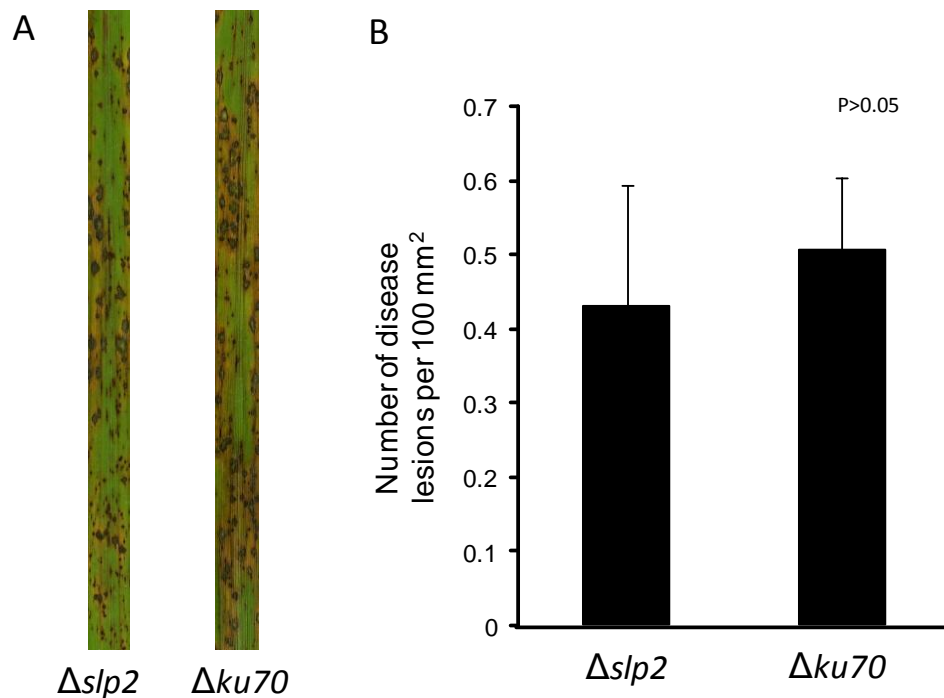


Figure 3.14 *SLP2* is dispensible for plant infection. **A.** Three-week old seedlings of the blast susceptible cultivar CO-39 were spray inoculated with the $\Delta slp2$ mutant and the wild-type $\Delta ku70$ strain at a concentration of 5×10^4 spores ml⁻¹. The $\Delta ku70$ genetic background is fully pathogenic and is a useful high-throughput molecular tool to reduce the frequency of non-homologous recombination (Kershaw *et al.*, 2009). The disease symptoms of the $\Delta slp2$ mutant is identical to that of the $\Delta ku70$ wild-type strain. **B.** Quantification of disease severity of the $\Delta slp2$ mutant compared to the wild-type $\Delta ku70$ strain. The number of lesions per 100 mm² of the $\Delta slp2$ and $\Delta ku70$ was calculated and no significant difference could be found between the mean number of lesions per unit area (two-tailed t-test, $p > 0.05$). Error bars represent one standard deviation.

3.3.13 The $\Delta slp1$ mutant exhibits normal patterns of appressorium-mediated development

Having demonstrated that the $\Delta slp1$ mutant was reduced in virulence, we reasoned that $\Delta slp1$ might be impaired in its ability to form functional infection structures. To investigate this, conidia of the $\Delta slp1$ mutant and the Guy11 strain were harvested, inoculated onto borosilicate glass coverslips and incubated in a moist chamber at 24°C before being visualised microscopically. The $\Delta slp1$ mutant conidia were of a normal morphology, germinated at a similar rate as the Guy11 strain and formed fully mature appressoria after a period of 24 hours. From this, we conclude that the reduction in disease virulence of the $\Delta slp1$ mutant is not due to impaired appressorium morphogenesis.

3.3.14 The $\Delta slp1$ mutant is less able to colonise epidermal host cells

Having ruled out the possibility that the loss of virulence associated with the $\Delta slp1$ mutants is due to an inability to form functional appressoria, we wanted to test whether the virulence phenotype of $\Delta slp1$ was instead due to a reduced ability to colonise epidermal host cells. To test this idea, conidia of the $\Delta slp1$ mutant and Guy11 strain were harvested and inoculated on rice leaf epidermis and incubated in a moist chamber at 24°C for 48 hours. After 48 hours post-inoculation, rice leaf tissue was dissected and infection sites were examined microscopically, as shown in Figure 3.16. Significantly, after 48 hours the number of host epidermal cells occupied by fungal hyphae of the $\Delta slp1$ mutant was significantly lower than the Guy11 strain ($n = 15$, two-tailed t-test, $p = 0.014$), as shown in Figure 3.16B. After 48 hours post-inoculation, the mean number of host epidermal cells occupied by $\Delta slp1$ hyphae was found to be 4.29 cells ($SD \pm 2.5$), while the mean number of cells occupied by Guy11 fungal hyphae was 7.33 ($SD \pm 3.6$). At this stage of colonisation, the Guy11 strain had become well established within host tissues. In contrast, the $\Delta slp1$ mutant has only just started to colonise epidermal host cells. We conclude that Slp1 is required for efficient invasion by *M. oryzae* to bring about rice blast disease.

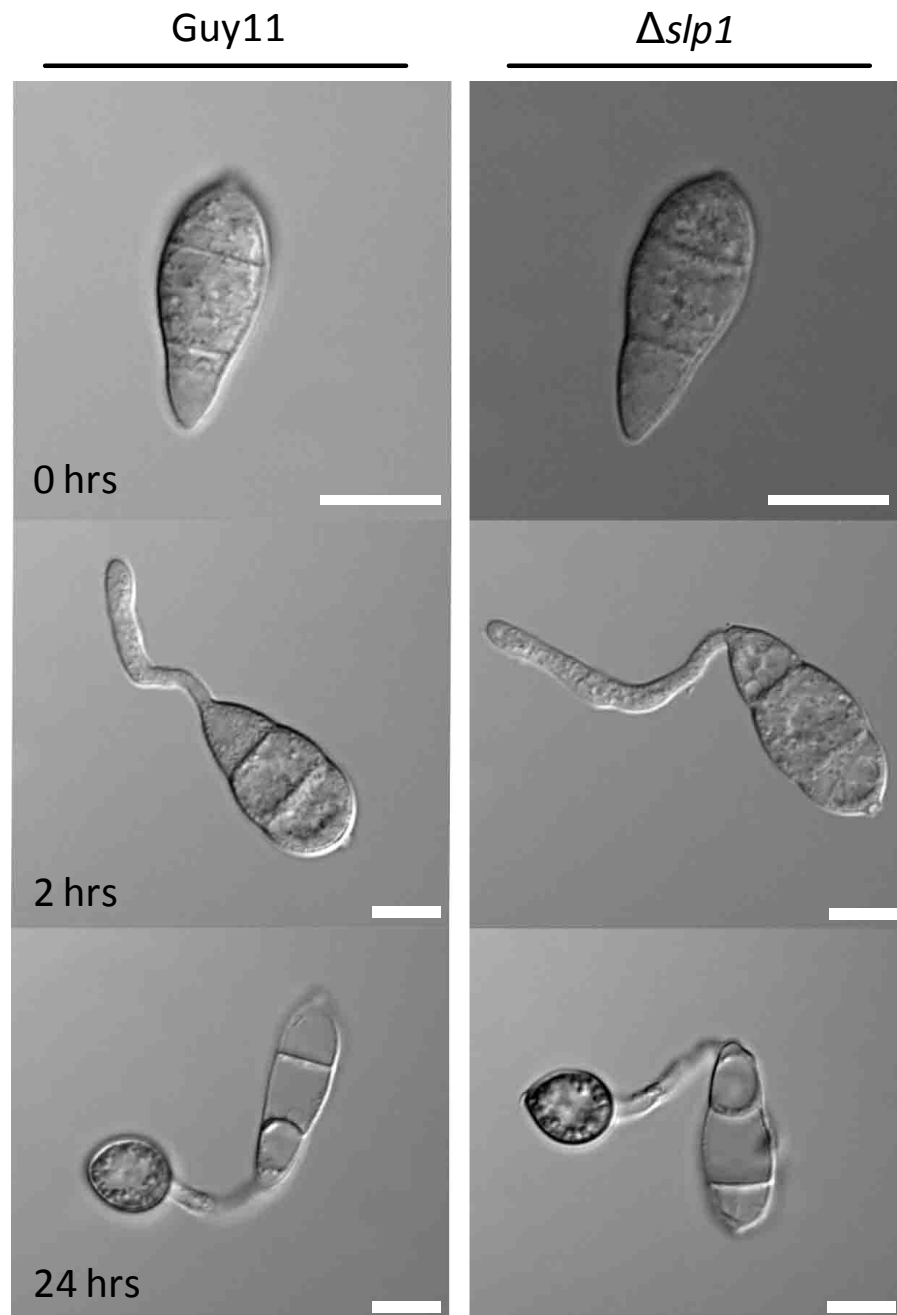


Figure 3.15 Appressorium-mediated morphogenesis is unaltered in the $\Delta slp1$ mutant. Conidia of the $\Delta slp1$ mutant and the Guy11 strain were harvested, inoculated onto borosilicate glass coverslips and incubated in a moist chamber at 24°C. Conidia of the $\Delta slp1$ mutant were similar to that of the Guy11 strain (0 hrs). After 2 hours post-inoculation, conidia of the $\Delta slp1$ mutant had produced germ tubes which were similar in morphology to that of the Guy11 strain. After 24 hours post-inoculation, mature and fully melanised appressoria had developed in the $\Delta slp1$ mutant in a similar manner to that of the Guy11 strain. Strains were visualised using an Olympus IX81 microscope. Scale bars represent 10 μ m

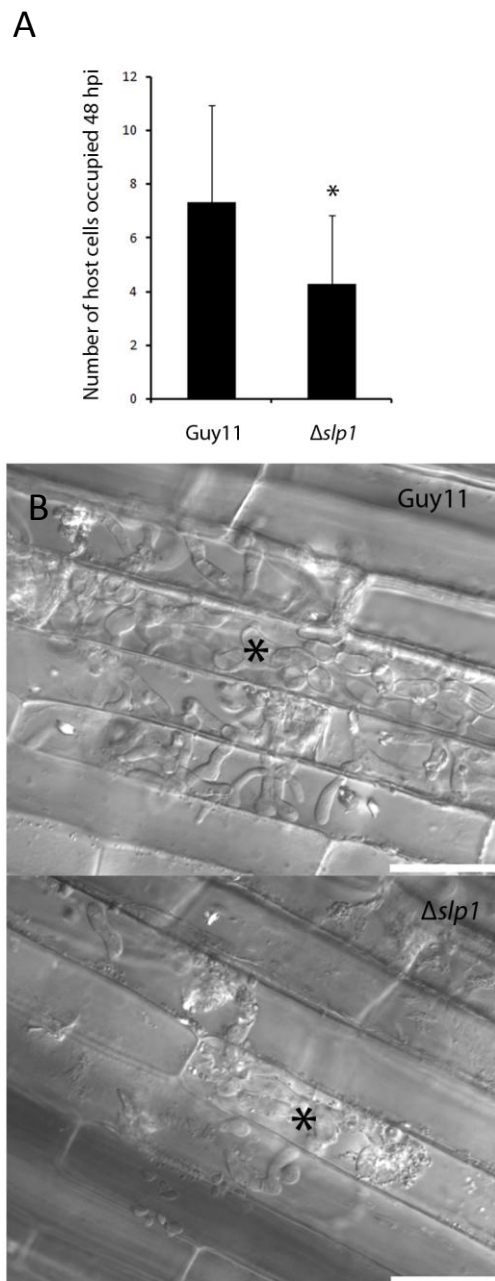


Figure 3.16 The $\Delta slp1$ mutant is reduced in its ability to colonise host cells. **A.** The number of host cells occupied by $\Delta slp1$ fungal hyphae is significantly lower than Guy11 after 48 hours post-inoculation ($n = 15$, two-tailed t-test, $p=0.014$). **B.** Micrographs showing typical infection sites of the $\Delta slp1$ mutant and the Guy11 strain at 48 hours post-inoculation. * denotes $p<0.05$. Black asterix mark the site of appressorium-mediated penetration into the epidermal host cell. Scale bars represent 30 μm

3.3.15 Slp1 co-precipitates specifically with chitin but not other cell-wall polysaccharides

Slp1 is predicted to contain two putative LysM protein domains that have previously been shown to bind peptidoglycans, including chitin (Buist *et al.*, 2006; de Jonge *et al.*, 2010). We were interested to test which polysaccharides Slp1 could bind to, if any. To do this, recombinant Slp1 protein was generated. A 486 bp *SLP1* cDNA fragment was amplified, and cloned into the *Pichia pastoris* over-expression system (Kombrink, 2012). Using this system, recombinant Slp1 protein was isolated, extracted and purified. To test if Slp1 was able to bind peptidoglycans, purified Slp1 protein was incubated with a number polysaccharides including insoluble crab shell chitin, chitin beads (Sigma), chitosan (de-acetylated chitin), cellulose and xylan. During affinity precipitation experiments, Slp1 was found to specifically co-precipitate with insoluble crab shell chitin, and chitin beads, and was detected in the insoluble pellet fraction (P) following SDS-PAGE and Coomassie staining, as shown in Figure 3.17 (P). Slp1 did not, however, precipitate with chitosan, cellulose or xylan, and instead remained in the supernatant fraction (S) following affinity precipitation, as shown in Figure 3.17 (S). Interestingly, as well as precipitating specifically with chitin and not other tested polysaccharides, several Slp1 protein bands were evident in both the pellet and supernatant fractions, suggesting that Slp1 may have the capacity to dimerise. To ensure that these fractionated protein bands were not contaminants from the protein over-expression system, we isolated, extracted and purified these individual fractionated protein bands and carried out mass-spectrometry analysis. Slp1 was detected in all of these experiments, confirming that the bands were not in fact due to over expression artefacts.

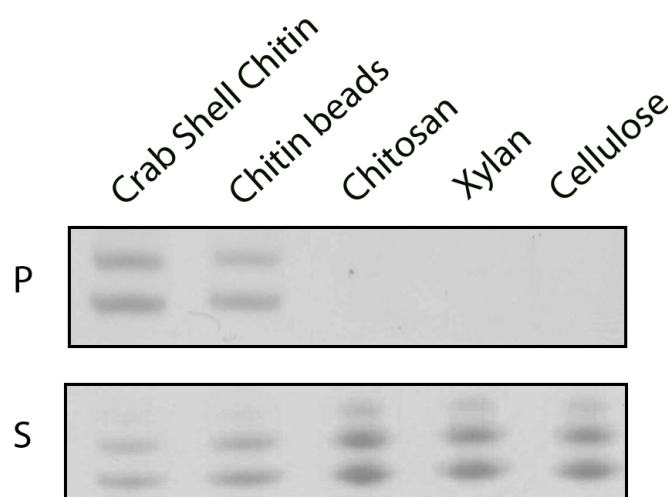


Figure 3.17 Slp1 co-precipitates with chitin but not other insoluble cell wall polysaccharides. Slp1 was incubated with the polysaccharides insoluble crab shell chitin, chitin beads, chitosan, xylan and cellulose and affinity precipitation was performed. After incubation with chitin and chitin beads, recombinant Slp1 could be detected in the insoluble pellet fraction (P) after SDS-PAGE and Coomassie blue staining. However, Slp1 protein could not be detected in the pellet fraction when precipitated with chitosan, xylan and cellulose. Slp1 protein could be detected in the supernatant fractions (S) after affinity precipitation with all polysaccharides.

3.3.16 Slp1 does not protect fungal hyphae from hydrolysis by plant-derived chitinases

3.3.16.1 *M. oryzae* is insensitive to crude-extract of plant-derived chitinase enzymes

Having demonstrated that Slp1 co-precipitated with insoluble chitin during affinity precipitation assays, we wanted to define the precise biological and functional role of Slp1. We hypothesised that Slp1 might bind chitin in the fungal cell wall and thereby shield fungal hyphae from the hydrolysing effects of chitinase enzymes which are released by the plant. Previously, the *Cladosporium fulvum* Avr4 effector was shown to bind to chitin within fungal cell walls and shield fungal hyphae from hydrolysis by chitinase enzymes (Van den Burg *et al.*, 2006), and we reasoned that Slp1 might serve a similar function. However, germination of conidia of *C. fulvum* were not inhibited by crude extracts of chitinases and β -1,3-glucanases from plants, most likely due to the complex nature of the *C. fulvum* cell wall matrix impeding accessibility of chitinases and glucanase enzymes to the site of action. To test whether *M. oryzae* was sensitive to crude extract of intracellular chitinase enzymes from plants (ChiB), conidia of the *M. oryzae* Guy11 strain were harvested and inoculated onto glass coverslips. Immediately after inoculation, crude extract of intracellular chitinases was applied (Joosten *et al.*, 1990, 1995), as shown in Figure 3.18. After 2-4 hours post-inoculation, conidia of the Guy11 strain were able to germinate in the presence of basic intracellular chitinases (ChiB) at a similar rate to the control. We conclude that *M. oryzae* is not susceptible to disruption by crude extract of chitinases and is therefore not suitable to test if Slp1 shields fungal hyphae from hydrolysing chitinase enzymes.

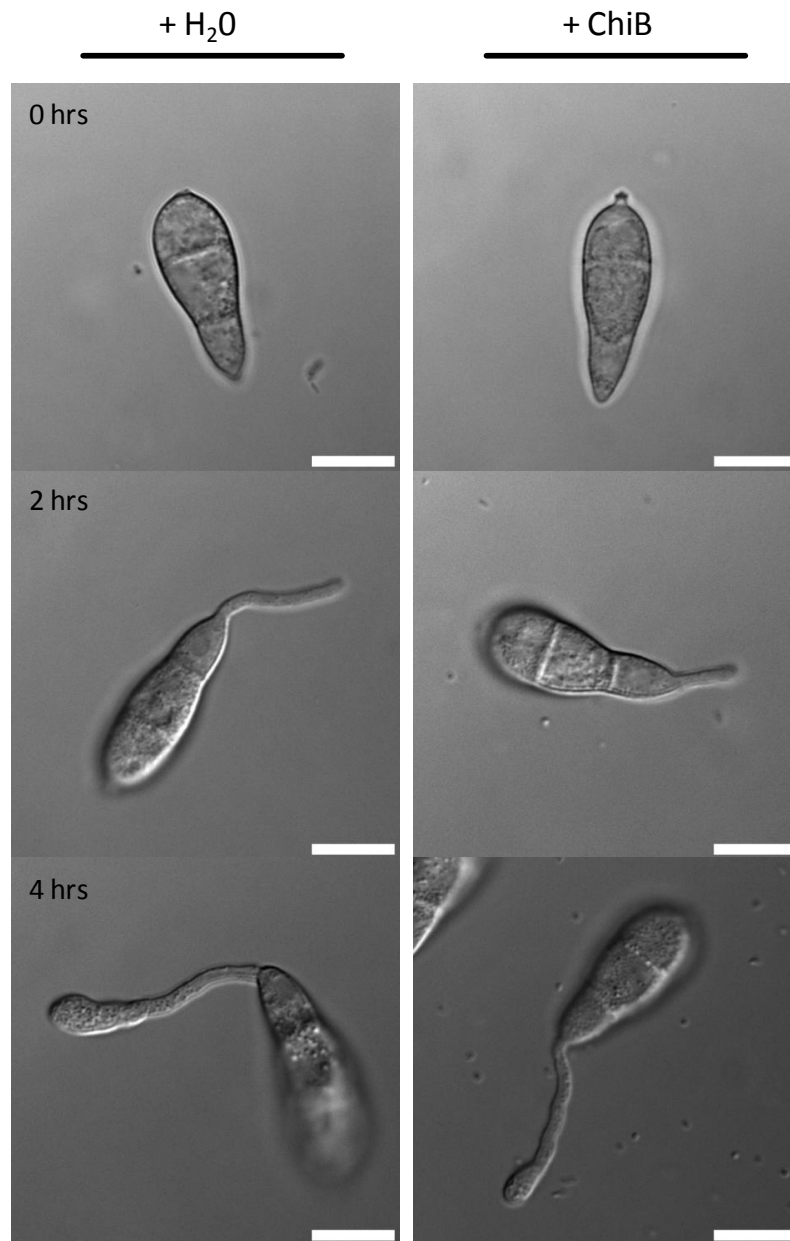


Figure 3.18 *M. oryzae* spores exhibit normal appressorium-mediated changes in morphology in the presence of basic intracellular chitinases. To determine if *M. oryzae* is sensitive to crude extract of basic intracellular chitinases (Joosten *et al.*, 1990, 1995), conidia of the *M. oryzae* Guy11 strain were harvested and inoculated onto glass coverslips. Immediately after inoculation, crude extract of intracellular chitinases was added (+ChiB treatment). After two hours post-inoculation, *M. oryzae* conidia were able to germinate in the presence of ChiB, suggesting that *M. oryzae* is not sensitive to disruption by intracellular chitinases. Images are representative of three independent replicate experiments. Scale bars represent 10 μ m

3.3.16.2 Using *Trichoderma viride* as a model species demonstrates that Slp1 does not shield fungal hyphae from hydrolysis by chitinases

M. oryzae appeared to be insensitive to disruption by hydrolysis from basic intracellular chitinases (Figure 3.18), and so a suitable model species was required which was sensitive to chitinases. We focused our attention on using *Trichoderma viride* as a model species which has previously been used to test susceptibility of fungal hyphae to chitinases (Van den Burg *et al.*, 2006; van Esse *et al.*, 2007; de Jonge *et al.*, 2010). To investigate this, we incubated *Trichoderma viride* spores with crude extract of chitinase enzymes from tomato leaves in the presence or absence of purified Slp1 protein, as shown in Figure 3.19. The *C. fulvum* effector protein Avr4 has previously been shown to protect fungal hyphae from hydrolysis by chitinases (Van den Burg *et al.*, 2006; van Esse *et al.*, 2007) and was included here as a control. In contrast to Avr4, however, Slp1 was unable to provide protection to *T. viride* spores from hydrolysis by chitinases. Previous studies have demonstrated that concentrations as low as 10 μ M of Avr4 are sufficient to prevent tip hydrolysis by intracellular chitinases (de Jonge and Thomma, 2009; de Jonge *et al.*, 2010). In all experiments performed, concentrations as high as 100 μ M of purified Slp1 protein was not sufficient to protect spores of *T. viride* from chitinase-related hyphal tip hydrolysis. We therefore conclude that Slp1 is not likely to be involved in shielding fungal hyphae from chitinases (Mentlak *et al.*, 2012a). To this end, Slp1 behaves in a similar manner to that of the *C. fulvum* Ecp6, but not Avr4.

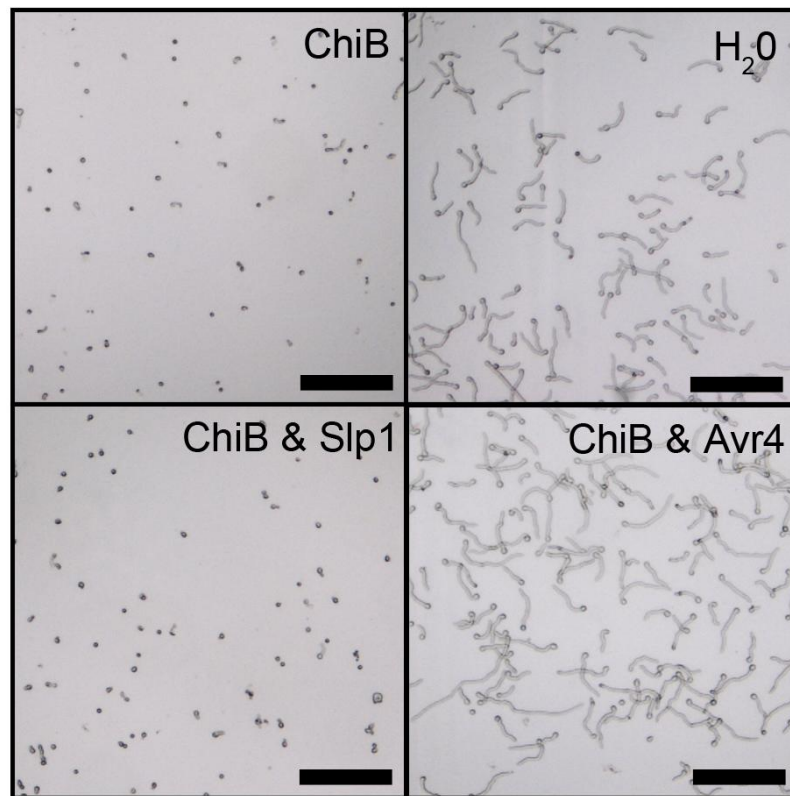


Figure 3.19 Slp1 is unable to protect fungal hyphae from crude extract of plant-derived chitinases. *Trichoderma viride* spores were harvested and inoculated onto a 96-well plate. After 2-4 hours, basic intracellular chitinases (ChiB) extracted from tomato leaves (Joosten *et al.*, 1990; 1995) was applied. In the presence of ChiB, *T. viride* spores were unable to germinate, but were able to do so in the H₂O control. When 100 µM of Slp1 was incubated in addition to ChiB, *T. viride* spores were unable to germinate, suggesting that Slp1 is unable to prevent cell wall hydrolysis by ChiB. As a control, Avr4 was included in experiments, which has previously been shown to protect fungal hyphae from chitinases (Van den Burg *et al.*, 2006; van Esse *et al.*, 2007; de Jonge *et al.*, 2010). Pre-treatment of 10 µM Avr4 with ChiB results in the germination of *T. viride*, confirming that Avr4 is able to shield fungal hyphal tips from hydrolysis by ChiB. Images are representative of three independent replicate experiments. Scale bars represent 10 µm

3.3.17 Slp1 inhibits medium alkalinisation of tomato cell suspensions

We were unable to confirm a role for Slp1 in the protection of fungal hyphal from chitinases, so we wanted to see if Slp1 could instead suppress chitin-induced immune responses. During infection, chitin oligosaccharides can be released from the tips of fungal hyphae, which can act as PAMPs thereby aiding pathogen perception and recognition. We hypothesised that Slp1 might be involved in sequestering these chitin oligosaccharides and suppression of chitin-induced immune responses. In the presence of nanomolar concentrations of chitin oligosaccharides [(GlcNAc)₆], plant cell suspensions have previously been shown to react with medium alkalinisation (Felix *et al.*, 1993; de Jonge *et al.*, 2010). During medium alkalinisation, the pH of a plant cell suspension increases significantly over a period of 3-4 minutes (de Jonge *et al.*, 2010; Marshall *et al.*, 2011). We wanted to see whether Slp1 could disrupt and potentially suppress chitin-based immune responses, and so we tested whether Slp1 could suppress this chitin-induced pH shift of tomato cell suspensions (de Jonge *et al.*, 2010). Indeed, in the presence of a ten-fold molar excess of Slp1 (10 nM), medium alkalinisation of tomato suspensions cells was inhibited, as shown in Figure 3.20. In this way, we conclude that Slp1 behaves similarly to that of the *C. fulvum* Ecp6 effector, in that it is capable of suppressing chitin-induced immune responses in tomato cell suspensions.

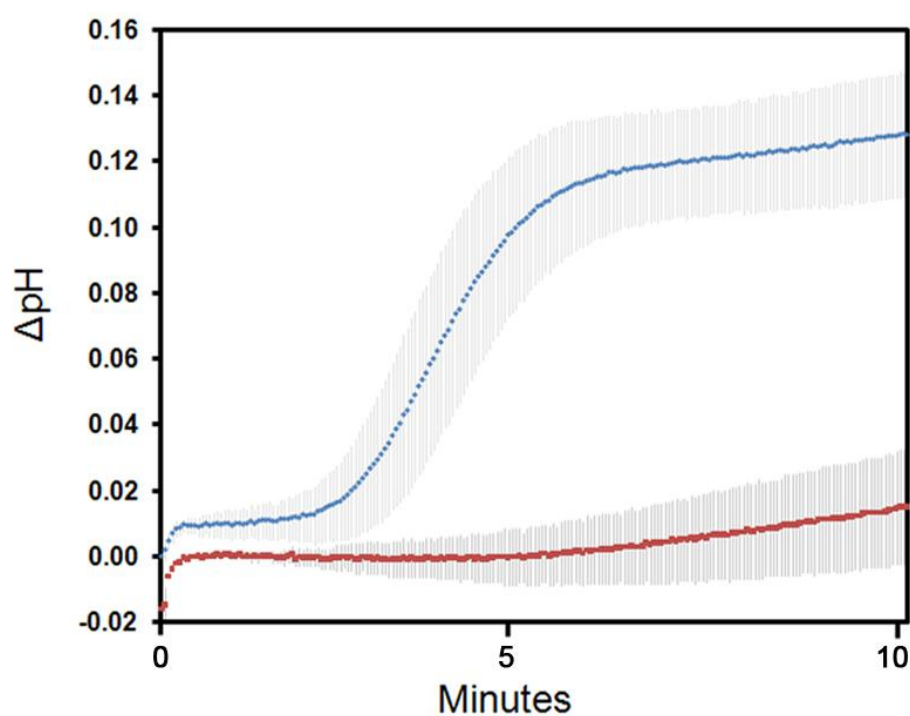


Figure 3.20 Medium alkalisation of tomato cell suspensions is suppressed in the presence of Slp1. After treatment with a 1 nM concentration of chitin oligosaccharides [(GlcNAc)₈], the pH of the cell suspension increases dramatically after a period of 2-3 minutes (blue line). However, upon incubation with 1 nM GlcNAc₈ and a ten-fold molar excess of Slp1 (10 nM) (red line), medium alkalisation was inhibited. Error bars represent ± 1 SD of three independent replicate experiments.

3.3.18 Slp1 inhibits the chitin-induced oxidative burst by rice cells

Having confirmed a role for Slp1 in the suppression of chitin-triggered medium alkalisation in tomato cell suspensions, we wanted to further understand the mechanism by which Slp1 suppresses chitin-triggered plant immune responses. Specifically, we wanted to see if these suppression characteristics could extend to its native rice host. In the presence of nanomolar concentrations of chitin oligosaccharides [(GlcNAc)₈], rice cell suspensions react by undergoing an oxidative burst (Yamaguchi *et al.*, 2005). During the chitin-induced oxidative burst, reactive oxygen species (ROS) such as H₂O₂ and O₂⁻ are released, which can be measured using luminol-dependent chemiluminescence. We were interested in testing whether Slp1 could suppress the chitin-induced oxidative burst in rice cells. Upon incubating rice suspension cells with 1 nM (GlcNAc)₈, chemiluminescence could be detected after 20 minutes, as shown in Figure 3.21. This oxidative burst is suppressed, however, in the presence of a ten-fold or 100-fold molar excess of Slp1 (10 nM or 100 nM), as shown in Figure 3.21. After 120 minutes, suppression of the oxidative burst could still be observed in the presence of 10 nM Slp1, although suppression was much greater in the presence of a 100-fold molar excess of Slp1. A 100-fold molar excess of Slp1 was capable of suppressing the chitin-induced oxidative burst across all time points examined. We conclude that the *M. oryzae* Slp1 protein is able to suppress chitin-induced immune responses in both its native rice plant and in non-host species.

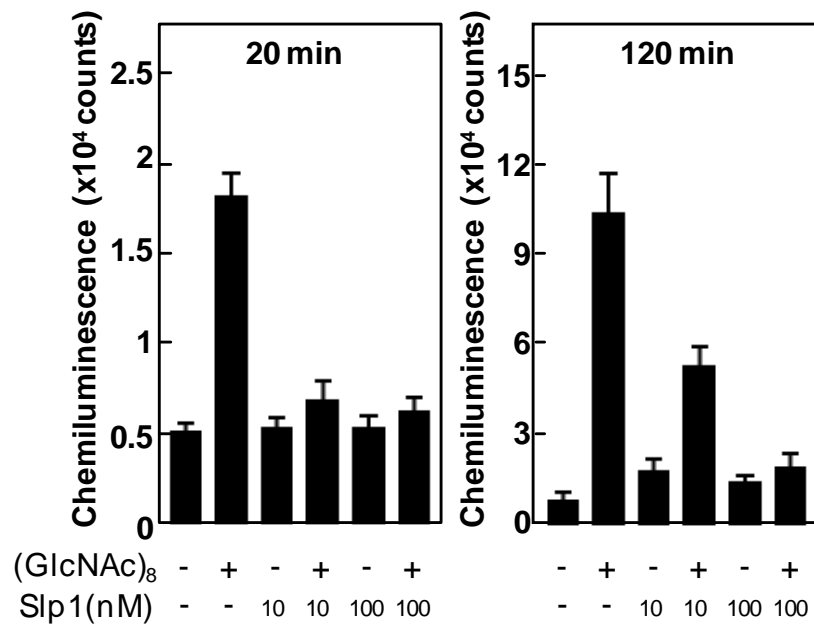


Figure 3.21 Slp1 inhibits the chitin-induced oxidative burst in rice suspension cells. Production of ROS 20 min or 120 min after induction with 1 nM (GlcNAc)₈ was determined in the absence or presence of Slp1 (10 and 100 nM) using luminol-dependent chemiluminescence, as described previously (de Jonge *et al.*, 2010). The experiment was performed twice with similar results. Mean with the SE of three independent replicate experiments is shown and asterisks indicate significant differences ($p < 0.01$) when compared with the 1 nM (GlcNAc)₈ treatment. Assays were carried out by Tomonori Shinya, Ippei Otomo, Yoko Nishizawa and Naoto Shibuya at the Faculty of Agriculture, Meiji University, Japan.

3.3.19 Slp1 inhibits chitin-induced expression of defence genes in rice cells

Chitin-triggered immunity is known to result in induction of pathogenesis-related genes, and we therefore sought to determine the effect of the Slp1 effector on induction of rice defense gene expression. We therefore performed quantitative RT-PCR (qRT-PCR) and examined changes in expression of the rice Phenylalanine ammonia lyase gene, *PAL1*, and the β -glucanase-encoding gene, *rBG*. In the presence of 1 nM (GlcNAc)₈, expression of both *PAL1* and *rBG* genes increased significantly, as shown in Figure 3.23. However, the increase in gene expression was suppressed when a 100-fold molar excess of Slp1 was also included, consistent with the role of Slp1 in preventing chitin-triggered immunity responses in rice.

3.3.20 Slp1 competes with the rice PRR CEBiP

We were interested to how Slp1 interacts with plant membrane receptors that detect chitin helping to establish the chitin-induced oxidative burst (Shibuya *et al.*, 1996). In rice, the pattern recognition receptor LysM protein CEBiP (for Chitin Elicitor and Binding Protein) resides at the rice plasma membrane and is able to bind chitin oligosaccharides (Shibuya *et al.*, 1996; Kaku *et al.*, 2006). We hypothesized that Slp1 might therefore function to compete with the CEBiP recognition receptor residing at the invaginated rice cell membrane. CEBiP is a LysM domain-containing protein and interacts with the LysM receptor-like kinase protein CERK1 to bring about plant defense responses (Shimizu *et al.*, 2010). CEBiP has also been shown to contribute to rice blast disease resistance (Kishimoto *et al.*, 2010). We therefore performed a competition assay in which a microsomal membrane preparation containing the receptor protein CEBiP was isolated from rice suspension cells. When this membrane fraction was incubated with 0.4 mM biotinylated N-acetylchito-octaose (GlcNAc)₈, labelling of CEBiP occurred, as shown in Figure 3.24. When an equimolar amount of Slp1 (0.4 mM) was added, a significant portion of biotinylated (GlcNAc)₈ became bound to the effector, suggesting that Slp1 is capable of competing with CEBiP for chitin binding in this assay. When a 10-fold molar excess of Slp1 (4 mM) was added, however, binding of biotinylated (GlcNAc)₈ to the membrane fraction containing CEBiP was almost entirely blocked and resulted in the almost exclusive labelling of Slp1, as shown in Figure 3.24.

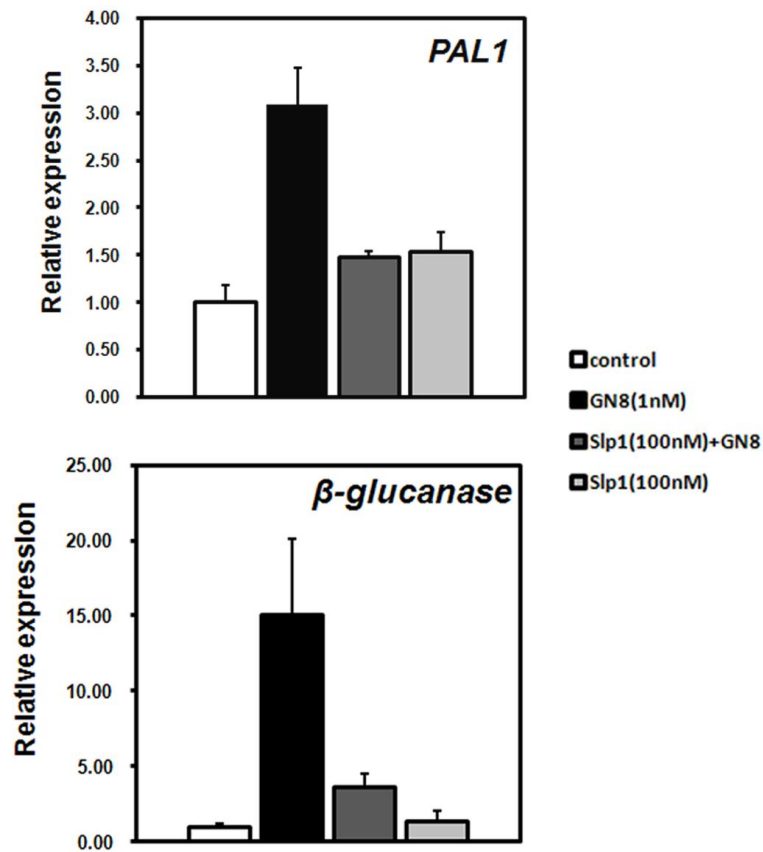


Figure 3.23 Expression of rice defense genes *PAL1* and *rBG* induced by (GlcNAc)₈ is suppressed in the presence of Slp1. The bars display the relative transcript level of the chitin-responsive genes normalized to the constitutively expressed ubiquitin gene. The mean with SE of two replicate experiments is shown, and asterisks indicate significant differences ($P < 0.05$) when compared with the 1 mM (GlcNAc)₈ treatment. Assays were carried out by Tomonori Shinya, Ippei Otomo, Yoko Nishizawa and Naoto Shibuya at the Faculty of Agriculture, Meiji University, Japan.

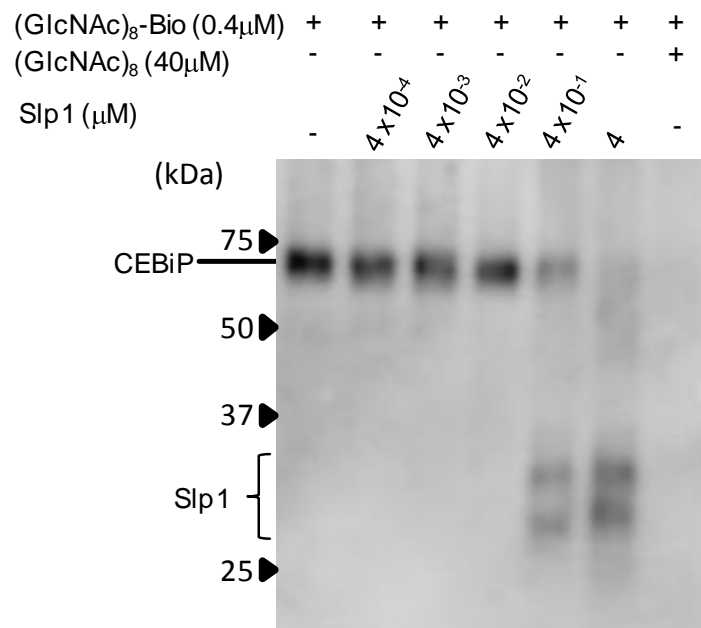


Figure 3.24 Slp1 competes with the plant membrane PRR CEBiP for chitin-binding. Protein gel blot analysis using an antibiotin antibody showing affinity labeling of a microsomal membrane preparation (rice MF) from suspension cultured rice cells containing the PRR CEBiP, with biotinylated (GlcNAc)₈ [(GlcNAc)₈-Bio], in the presence or absence of Slp1 and nonbiotinylated (GlcNAc)₈. The experiment was performed twice with similar results. Assays were carried out by Tomonori Shinya, Ippei Otomo, Yoko Nishizawa and Naoto Shibuya at the Faculty of Agriculture, Meiji University, Japan.

3.3.21 Targeted gene silencing of CEBiP in rice restores the ability of $\Delta slp1$ mutants of *M. oryzae* to cause rice blast disease

We were interested in establishing whether the ability of the Slp1 effector to act as a competitive inhibitor of CEBiP, thereby suppressing PAMP-triggered immunity, was the reason why *M. oryzae* $\Delta slp1$ mutants showed a significant reduction in their ability to cause rice blast disease. We therefore obtained transgenic rice lines of cultivar Nipponbare, in which the CEBiP encoding gene had been silenced using RNA interference (RNAi; Kishimoto *et al.*, 2010). These rice lines have previously been shown to lack chitin-triggered immune responses and to exhibit increased susceptibility to rice blast disease (Kishimoto *et al.*, 2010). We inoculated the CEBiP RNAi plants, and corresponding wild-type Nipponbare rice lines, with the *M. oryzae* $\Delta slp1$ mutant and Guy11 strain, as shown in Figure 3.25. Strikingly, we observed that the $\Delta slp1$ mutant was as virulent as Guy11 when inoculated onto CEBiP RNAi plants, as shown in Figure 3.25. On CEBiP RNAi plants, the mean number of host cells occupied by the fungus at 48 hours post-inoculation by the Guy11 and $\Delta slp1$ strain was 9.4 (SD \pm 3.21) and 10.2 (SD \pm 2.83), respectively. Furthermore, on CEBiP RNAi plants, no significant difference in host tissue colonization was observed between Guy11 and the $\Delta slp1$ mutant (two-tailed t test, $n = 34$ infection sites, $P = 0.322$). By contrast, when nonsilenced Nipponbare rice lines were inoculated, the mean number of host cells occupied by Guy11 and the $\Delta slp1$ mutant was 8.1 (SD \pm 2.63) and 3.7 (SD \pm 1.78), respectively. The mean number of host cells colonized by the $\Delta slp1$ mutant was significantly lower than the wildtype Guy11 (two-tailed t test, $P < 0.01$), as shown in Figure 3.25. We conclude that it is the ability of Slp1 to act as a competitive inhibitor of CEBiP that is its principal function during rice blast disease and that this role is highly significant in determining the outcome of the host–pathogen interaction.

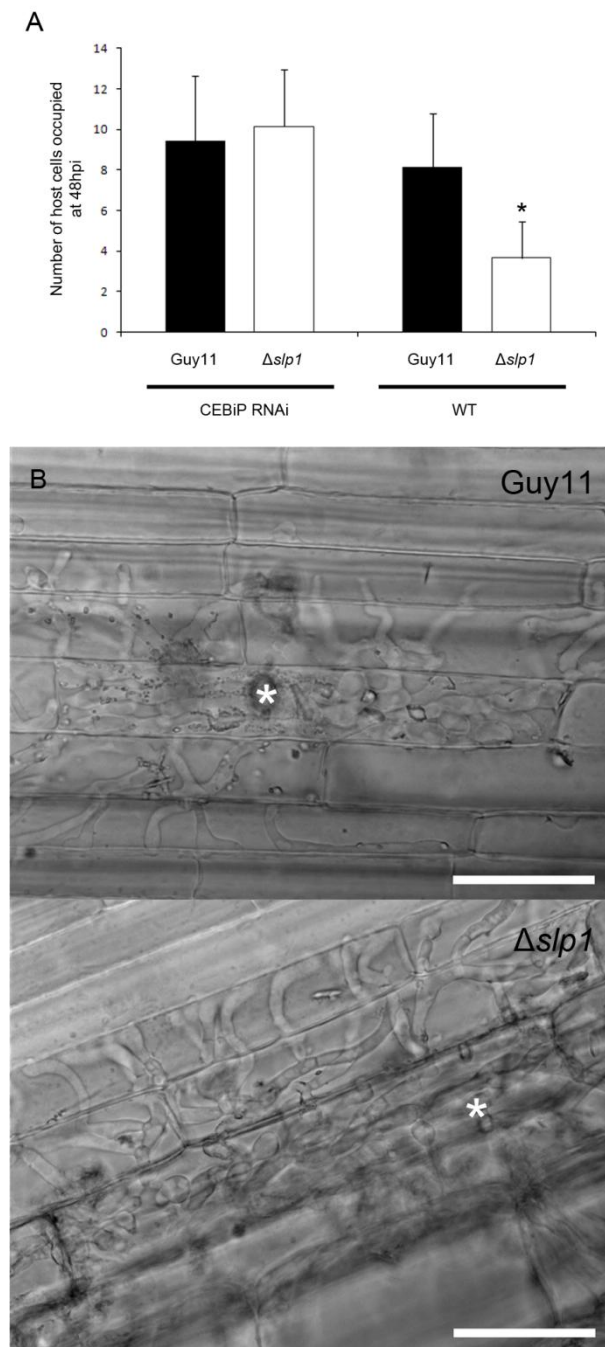


Figure 3.25 The ability of a $\Delta slp1$ mutant to cause rice blast disease is restored when inoculated onto a rice cultivar in which CEBiP has been silenced by RNAi. **A.** At 48 hours post-inoculation, host cell colonization of the $\Delta slp1$ mutant was similar to that of Guy11 on a CEBiP RNAi line of cultivar Nipponbare (two-tailed t-test, $P = 0.323$). On wild-type non-transformed Nipponbare, the $\Delta slp1$ mutant was significantly reduced in its ability to colonize host tissue (two-tailed t test, $P < 0.01$). Error bars represent 1 SD. **B.** Micrographs of typical infection sites of Guy11 and $\Delta slp1$ on leafsheath tissue from the CEBiP RNAi line. White asterisks mark the initial site of host cell entry. Scale bars represent 35 μm .

3.3.22 Employing a yeast two-hybrid screen for detection of Slp1-Slp1 interactions

In section 3.3.14, Slp1 was shown to co-precipitate specifically with insoluble chitin during affinity precipitation assays. Interestingly, however, multiple bands were present in the chitin pull-down assay (Figure 3.3.17), and so we hypothesised that, in addition to chitin, Slp1 might have a capacity to bind to itself thereby forming a multi-protein complex. A yeast two-hybrid screen was therefore performed to confirm any potential Slp1-Slp1 interaction.

3.2.23 Construction of DNA-BD and AD gene fusions

The gene fusion vectors pGBKT7 and pGADT7 were used as part of the Matchmaker Gold yeast two-hybrid kit (Clontech). A schematic representation of the restriction sites within the pGADT7 and pGBKT7 vectors used in this assay can be found in Figure 3.26A. To assay any putative Slp1-Slp1 interactions, primers were designed to amplify an *SLP1* cDNA made from RNA extracted from infected leaf tissue (144 hours post inoculation). cDNA was used in this instance due to the presence of an 81 nucleotide-long intron within the *SLP1* ORF. The forward (5') PCR primer 5'SLP1-EcoRI was designed to include a 5' restriction site *Eco* RI, whilst the reverse (3') primer 3'SLP1-BamHI was designed to include a *Bam* HI restriction site at the 3' end of the amplicon. Inclusion of these restriction sites was required to perform directional cloning of the *SLP1* cDNA into the pGADT7 and pGBKT7 vectors. Following amplification, the *SLP1* cDNA was ligated into the intermediary TA cloning vector pGEM-T (Promega) to create the vector pSLP1EB, as shown in Figure 3.26B. Restriction digest with the restriction enzymes *Eco* RI and *Bam* HI released a 489 bp *SLP1* cDNA fragment out of the pSLP1EB vector. This fragment was gel purified and ligated into *Eco* RI / *Bam* HI digested pGADT7 and pGBKT7. Positive clones of the *SLP1* cDNA fragment were confirmed in both pGADT7 and pGBKT7 by restriction digest with the restriction enzymes *Eco* RI and *Bam* HI which yielded a 489 bp fragment out of the pGADT7 and pGBKT7. Vectors were also independently verified by DNA sequencing to ensure an in frame fusion of *SLP1* to the BD and AD domains in pGBKT7 and pGADT7 respectively. The completed pGADT7 and pGBKT7 vectors containing the *SLP1* cDNA were named pGAD-SLP1 and pGBK-SLP1. A schematic representation of the cloning

strategy used to clone the *SLP1* cDNA into the pGADT7 and pGBKT7 vectors can be found in Figure 3.26B. The oligonucleotide primers used for the amplification of *SLP1* can be found in Table 3.3.

Table 3.3 Oligonucleotide primers used in the amplification of *SLP1* cDNA. The *Eco* RI and *Bam* HI restriction sites are underlined.

Primer Name	Nucleotide sequence (5' - 3')
SLP1-EcoRI	AAGAATTCATGCAGTTCGCTACCATC
SLP1-BamHI	AAGGATCCCTAGTTCTTGCAGATGGG

3.3.24 Slp1 interacts with itself in a yeast two-hybrid screen

During initial control experiments, the pGAD-SLP1 and pGBK-SLP1 fusion vectors did not independently activate the reporter genes in the absence of their respective binding partners. The pGAD-SLP1 and pGBK-SLP1 fusion vectors were independently transformed into the yeast strain AH109 and plated onto SD/-Leu/X- α -Gal and SD/-Trp/X- α -Gal, respectively, and assayed for growth according to the manufacturer's instructions (Clontech). The lack of growth on these respective plates demonstrates that each vector does not independently autoactivate their respective reporter genes, as shown in Figure 3.26. To assay for Slp1-Slp1 interactions, the pGBK-SLP1 and pGAD-SLP1 vectors were simultaneously transformed into the yeast strain AH109. As a positive control, the vectors AD-Bck1 and BD-Mkk1 were also simultaneously transformed (Penn, 2011). Transformants were plated out onto SD/-Leu/-Trp medium (low stringency), SD/-His/-Leu/-Trp medium (medium stringency) and SD/-Ade/-His/-Leu/-Trp/-X- α -Gal media (high stringency). Plating onto low stringency media enables the detection of weak protein-protein interactions, whilst plating out onto high stringency media enables the detection of protein-protein interactions that have higher affinity, as discussed previously (Wilson *et al.*, 2010). Plates were inverted and incubated at 30°C until yeast colonies appeared, which typically occurred after 3-5 days.

Upon simultaneous co-transformation of the pGBK-SLP1 and pGAD-SLP1, all four reporter genes were activated when plated onto high-stringency medium, including activation of the *MEL1* reporter gene, leading to the activation of the β -galactosidase enzyme and formation of

blue yeast colonies after 3-4 days, as shown in Figure 3.27. The ability of yeast transformants to grow on this high stringency media is evidence of a strong protein-protein interaction between Slp1 and itself (Wilson *et al.*, 2010). The observation that Slp1 can bind to itself in a yeast-two hybrid screen is consistent with earlier observations during affinity precipitation assays in which multiple Slp1 protein bands were identified, as discussed in Section 3.3.14.

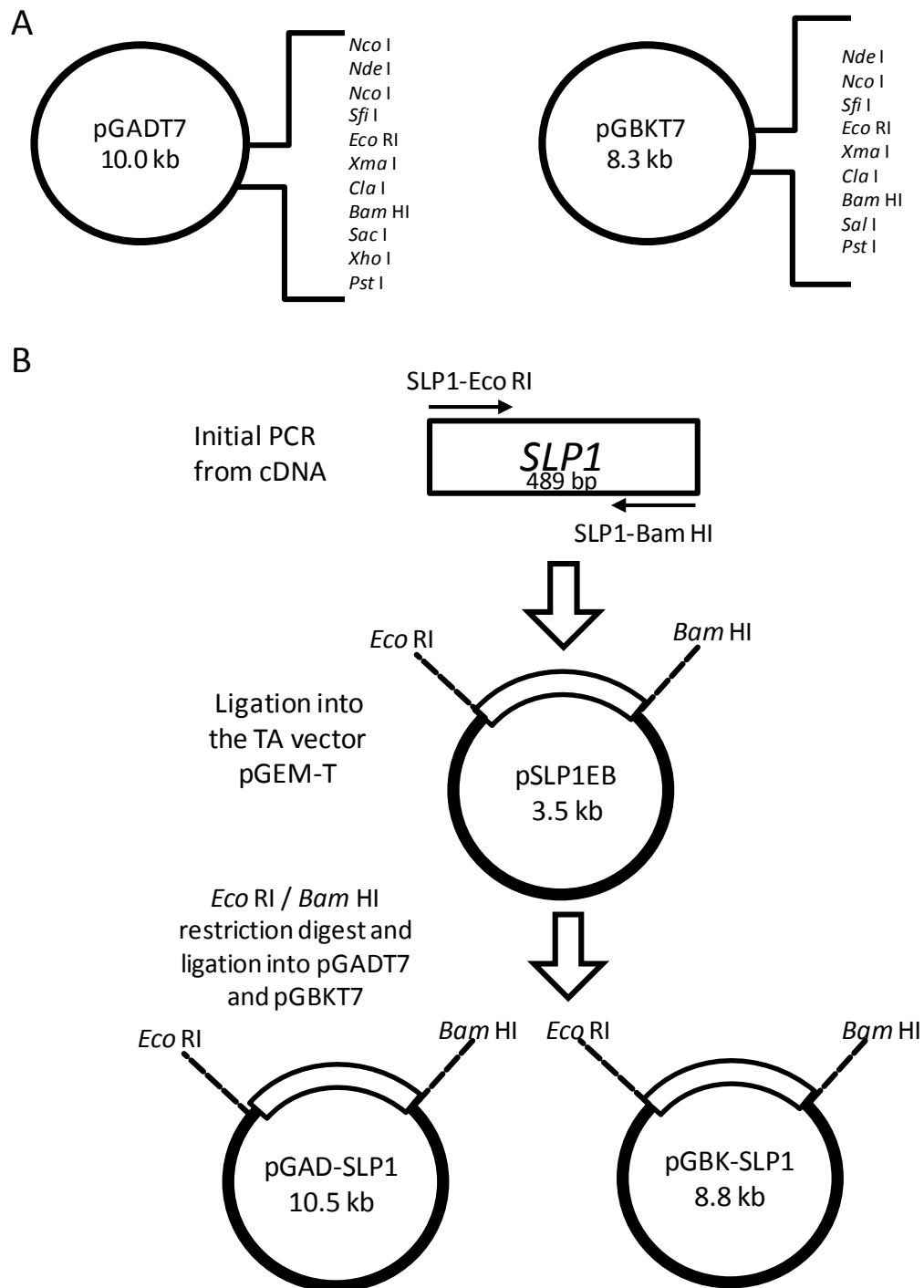


Figure 3.26 Schematic representation of the cloning strategy to perform yeast two-hybrid analysis. **A.** Schematic of the pGADT7 and pGBKT7 cloning vectors used to perform yeast two-hybrid analysis using the Matchmaker Gold yeast-two hybrid kit (Clontech). Restriction sites within the multiple cloning site are shown. **B.** Schematic representation of the cloning strategy for amplification of an *SLP1* cDNA and subsequent ligation in to the pGADT7 and pGBKT7 vectors.

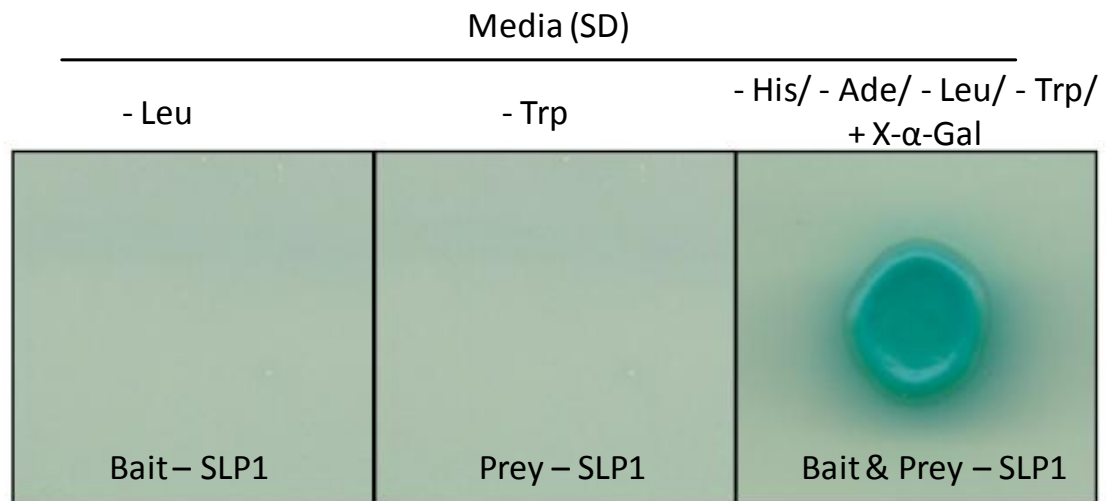


Figure 3.27 A yeast two-hybrid screen reveals an Slp1-Slp1 interaction. During preliminary control experiments, the pGAD-SLP1 (Bait – SLP1) and pGBK-SLP1 (Prey – SLP1) were independently transformed into the yeast strain AH109 before being plated out onto SD/-Leu and SD/-Trp respectively. The lack of growth on these media demonstrate that neither the pGBK-SLP1 or pGAD-SLP1 vectors are capable of autoactivating the reporter genes. Simultaneous co-transformation of the pGAD-SLP1 (Bait – SLP1) and pGBK-SLP1 (Prey – SLP1) vectors into the yeast strain AH109 results in the activation of all four reporter genes and growth on high stringency media (-His/-Ade/-Leu/-Trp/+X- α -Gal). Co-transformation also activates MEL1 expression in which the enzyme α -galactosidase is secreted into the medium resulting in the hydrolysis of X- α -Gal in the medium and turning the yeast colony blue. Growth on such high stringency media strongly supports the hypothesis that Slp1 can dimerise.

3.4 Discussion

One of the earliest defence strategies employed by plant cells to fungal invasion is the localised release of reactive oxygen species (ROS), including hydroxyl species as well as superoxide radicals and its dismutation product, hydrogen peroxide (Wojtaszek *et al.*, 1997; Mellersh *et al.*, 2002; Torres *et al.*, 2006). In addition to having anti-microbial properties (Levine *et al.*, 1994), ROS have also been demonstrated to strengthen plant cell walls by oxidative cross-linking of (hydroxy)proline-rich structural proteins (Bradley *et al.*, 1992). Indeed, one of the earliest manifestations of plants to *M. oryzae* infection includes the release of reactive oxygen species such as superoxide at the site of conidial attachment to the leaf surface (Pasechnik *et al.*, 1998). Conversely, an oxidative burst is also required by the rice blast fungus to initiate plant disease, and two putative superoxidase generating NADPH-oxidase genes (*NOX1* and *NOX2* genes) have been shown to be indispensable for rice blast infection (Egan *et al.*, 2007). It is not currently known, however, how fungal pathogens overcome the damaging effects of plant-derived ROS to cause disease. The binding of highly conserved pathogen associated molecular patterns (PAMPs) to host pattern recognition receptors (PRRs) is thought to establish immune signalling cascades which lead to this oxidative burst (Yamaguchi *et al.*, 2005). Chitin is an example of such a PAMP, which can be detected upon binding to the PRR CEBiP (Shibuya *et al.*, 1995; Kaku *et al.*, 2006). A number of other highly conserved molecular motifs have been documented to act as plant pathogen PAMPs. The conserved N-terminal amino acid sequence of bacterial flagellin (flg22), for example, can act as an elicitor and is recognised by the *Arabidopsis thaliana* membrane receptor *FLS2*. In an analogous manner to their response with chitin oligosaccharides, plant cells react with a strong medium alkalinisation response upon binding of flg22 to *FLS2* (Felix *et al.*, 1999).

A central paradigm in the study of plant pathogen effector biology was provided by the zigzag model, which was initially proposed to explain innate immune responses during plant pathogen interactions (Jones and Dangl, 2006). Under this model, PRRs provide the first line of plant defence which detect conserved PAMPs such as chitin and flg22. PRRs are also able to detect and bind MAMPs, or microbe-associated molecular patterns, a term which was coined to extend

to those molecular motifs derived from non-pathogenic microorganisms (Boller and Felix, 2009). Upon binding of PAMPs to PRRs, a plant immune response is activated, known as PAMP-triggered immunity (PTI). An example of such PTI is the oxidative burst and expression of defence genes which occurs when the rice membrane receptor CEBiP binds chitin oligosaccharides (Kaku *et al.*, 2006). To overcome PTI, plant pathogenic organisms secrete host cytoplasmic effectors which disrupt and suppress plant PTI immune responses, resulting in effector-triggered susceptibility (ETS). Effector-triggered immunity (ETI) occurs when the plant deploys cytoplasmic resistance (R) gene products which bind either directly or indirectly to the plant pathogen cytoplasmic effectors. This typically results in a hypersensitive response (HR) in which the host cell undergoes programmed cell death limiting the pathogen in its dissemination to host tissues distal from the initial site of infection (Jones and Dangl, 2006).

In this chapter, the function of Slp1, a putative apoplastic rice blast effector protein was investigated. Slp1 binds chitin, is able to compete with the rice PRR CEBiP and is capable of suppressing chitin-triggered immune responses, including suppression of the chitin-triggered oxidative burst and expression of rice defense genes. To this end, Slp1 appeared to behave in a similar manner to that of the *C. fulvum* apoplastic effector protein Ecp6 which has similar characteristics as it appears to interfere with PAMP recognition of apoplastic effectors (de Jonge *et al.*, 2010). It has recently been proposed that the ability of both Slp1 and Ecp6 to directly suppress PTI requires that the ETI/PTI model needs re-analysing (Thomma *et al.*, 2011). The ability of both Slp1 and Ecp6 to circumvent ETS and suppress PTI directly without the deployment of cytoplasmic Avr gene products strongly supports this notion (Thomma *et al.*, 2011). In contrast to work reported by de Jonge *et al.*, (2010) and Marshall *et al.*, (2011), we were able to demonstrate here for the first time that the $\Delta slp1$ virulence phenotype is a direct consequence of competition of Slp1 with the CEBiP receptor. In order to confirm this, inoculation of $\Delta slp1$ mutants onto CEBiP RNAi lines restored the virulence phenotype of $\Delta slp1$. On CEBiP RNAi lines, the ability of the plant to detect fungal chitin during infection is reduced, suppressing the chitin-triggered oxidative burst, meaning CEBiP RNAi lines are more susceptible to rice blast infection (Kaku *et al.*, 2006; Kishimoto *et al.*, 2011). Therefore, during

rice blast infection on CEBiP RNAi suppression lines, *M. oryzae* no longer requires a functional Slp1 protein to suppress a PTI-associated oxidative burst. Although the reason for dimerisation of Slp1 is not clear at this stage, the *C. fulvum* Ecp6 effector has also been shown to have a capacity to bind to itself (B. Thomma, personal communication). Further characterisation and analysis of the crystal structure of Slp1 may help to elucidate if there is a functional significance to this dimerisation.

Slp1 is a small cysteine rich protein containing a predicted N-terminal secretion peptide. *SLP1* is also up-regulated during intracellular growth compared with growth in axenic culture (Mosquera *et al.*, 2009). To this end, Slp1 contains the hallmarks of a secreted effector protein. In the next chapter, I explore the likelihood of Slp1 as an apoplastic effector protein deployed specifically during biotrophic intracellular growth.

Chapter 4. Slp1 is a putative apoplastic effector secreted by the rice blast fungus *M. oryzae* specifically during biotrophic growth

Abstract

In the previous chapter, Slp1 was shown to play a crucial role in the suppression of chitin-triggered immunity during the biotrophic stages of rice blast disease. In this chapter, the expression and localisation of *SLP1* is investigated and results suggest that Slp1 is a putative apoplastic effector protein which is secreted specifically by intracellular fungal hyphae during biotrophic growth. We show that Slp1 has a similar localisation pattern to that of the *M. oryzae* effector protein Bas4, and accumulates around the hyphal tips of invasively growing hyphae. In contrast to Bas4, however, Slp1 does not accumulate with effector molecules that have putative host cytoplasmic targets at the Biotrophic Interfacial Complex (BIC). Further to this, we show that the initial 27 amino acids of Slp1, which encodes a predicted N-terminal secretion peptide, is required for delivery and secretion of Slp1 into the apoplastic space. This secretion signal is further shown to be critical for complementation of the $\Delta slp1$ mutant, suggesting that Slp1 is functional at the plant-fungal interface, most likely in the apoplastic space.

4.1 Introduction

Intercellular fungal pathogens, such as the leaf mould fungus *Cladosporium fulvum*, grow and proliferate within the intercellular spaces of leaf tissue. Here, a suite of apoplastic effector proteins are secreted by the pathogen which can act to suppress plant defence responses such as PAMP-triggered immunity (PTI) (Jones and Dangl, 2006), which is activated upon binding and recognition of pathogen-associated molecular patterns (PAMPs) to host pattern recognition receptors (PRRs). These apoplastic effectors can have diverse and distinct functions ranging from the suppression of PAMP-triggered immunity, such as that of the *C. fulvum* effector Ecp6 (De Jonge *et al.*, 2010), to proteins that have protease inhibitor functions, such as the oomycete *Phytophthora infestans* effectors EPIC1 and EPIC2B, which inhibit tomato cysteine proteases (Song *et al.*, 2008).

In contrast to intercellular fungal plant pathogens, *M. oryzae* grows intracellularly during early biotrophic growth phases. At this time, a plant-derived plasma membrane known as the Extra-Invasive Hyphal Membrane (EIHM) (Kankanala *et al.*, 2007) is thought to become invaginated and surround fungal hyphae during biotrophic growth. It is not currently known, however, whether the space between the fungal cell wall and the EIHM is a discrete environment from the bulk apoplastic space, which is defined as the space between the plant cell membrane and plant cell wall (Kankanala *et al.*, 2007; Hoefle and Hückelhoven 2008).

The earliest evidence that *M. oryzae* delivers effector proteins with host cytoplasmic targets was provided by Jia *et al.*, (2000) where the *M. oryzae* protein Avr-Pita was shown to bind directly to the rice cytoplasmic resistance (R) gene product Pita in a yeast-two hybrid screen. More recently, *M. oryzae* avirulence effector proteins have been detected directly by epifluorescence microscopy within the rice host cytoplasm, providing further support that *M. oryzae* effector molecules are delivered across the EIHM into the host cytoplasm (Khang *et al.*, 2010). There is, however, a lack of examples of *M. oryzae* effector proteins that have apoplastic targets, and only one putative apoplastic effector has thus far been described. Referred to as Biotrophy Associated Protein 4 (Bas4), this small cysteine-rich protein is highly expressed during

biotrophic growth, and has been shown to accumulate uniformly around hyphal tips during biotrophic growth (Mosquera *et al.*, 2009). Plasmolysis assays, in which infected rice tissue was placed in a hyperosmotic solution, demonstrated that fluorescently-labelled Bas4:GFP becomes freely diffusible in the space generated between the fungal cell wall and EIHM of the shrinking rice protoplast (Khang *et al.*, 2010). Attempts to attach a host nuclear localisation signal (NLS) to fluorescently labelled BAS4:GFP did not result in the accumulation of a fluorescent signal at the host nucleus, in contrast to delivered effectors such as Pwl2:mRFP, suggesting that BAS4 is not translocated across the host membrane into the host cytosol (Khang *et al.*, 2010; Valent and Khang, 2010). Little is known, however, regarding the function of Bas4 as the predicted protein has no significant homology to any known protein (Mosquera *et al.*, 2009).

During infection by oomycete plant pathogens, such as *Hyaloperonospora arabidopsidis* and *Phytophthora infestans*, a plant-derived membrane known as the Extra Haustorial Membrane (EHM) becomes invaginated and surrounds specialised hyphal feeding structures, known as haustoria, that form during biotrophic growth (Koh *et al.*, 2005; O'Connell and Panstruga, 2006; Micali *et al.*, 2011; Lu *et al.*, 2012). Tethering of the EHM to the neck band that forms at the site of host cell entry, results in a sealed compartment which is separate to that of the bulk apoplast and is referred to as the Extra Haustorial Matrix (EHMx) (Bushnell, 1972). During oomycete infections, a battery of apoplastic effectors are delivered into the EHMx and at least seven classes of oomycete apoplastic effectors have been identified (van Damme *et al.*, 2012). These apoplastic effectors have diverse functions ranging from cysteine-rich proteins that are similar to phytotoxins (Liu *et al.*, 2005), to cell-death inducing effector molecules such as the *P. infestans* NPP1.1 which induces non-specific necrosis and cell death upon transient expression of PiNPP1.1 in *Nicotiana benthamiana* (Kanneganti *et al.*, 2006). As stated, several lines of evidence point to the *M. oryzae* effector protein Bas4 as having an apoplastic target and initial experiments in which Bas4:GFP was demonstrated as being incapable of diffusing from the site of secretion into the bulk apoplast raise the possibility that the invaginated EIHM forms a similar separate compartment as the oomycete EHMx (Mosquera *et al.*, 2009).

In this chapter, I report on the localisation and expression of the effector protein *M. oryzae* Slp1 that was characterised in Chapter 3. The expression and localisation of Slp2 was not examined because $\Delta slp2$ mutants were shown to be fully pathogenic. Using a fluorescently-labelled *SLP1:GFP* strain, Slp1 is shown to accumulate at the hyphal tips of invasively growing fungal hyphae. The secretion and localisation pattern of Slp1 during biotrophic growth is observed and compared to that of other *M. oryzae* effector proteins. Further to this, the molecular mechanisms of Slp1 secretion are investigated and the potential role of the N-terminal signal peptide of Slp1 is described.

4.2 Methods

4.2.1 Construction of the C-terminal GFP fusion vector *SLP1:GFP*

To generate the *SLP1:GFP* vector, primers were designed to amplify a 2.5 kb *SLP1* (Accession number MGG_10097) fragment from *M. oryzae* total genomic DNA. A forward (5') primer (5'SLP1-Prom) was designed approximately 2 kb upstream of the *SLP1* start codon to include the promoter sequence of the *SLP1* gene. The 5'SLP1-Prom primer was engineered to include a 30 bp overhang complementary in nucleotide sequence to the pYSGFP-1 vector (Saunders *et al.*, 2010). The reverse (3') primer (3'SLP1-GFP) was designed at the 3' end of the *SLP1* ORF and was designed to exclude the predicted *SLP1* translational stop codon. The 3'SLP1-Prom primer also included a 30 bp overhang, which is complementary in nucleotide sequence to GFP at the 5' end of the primer. The nucleotide sequences of the primers used to construct the *SLP1:GFP* vector are listed below:

5'SLP1-Prom

5' GATTATTGCACGGGAATTGCATGCTCTCACGAGGAAGATAGCCCAGCCC 3'

3'SLP1-GFP

5' GGTGAACAGCTCCTCGCCCTTGCTCACCATGTTCTTGCAGATGGGGATGTT 3'

The 2.5 kb *SLP1* genomic fragment was amplified using an Applied Biosystems GeneAmp® PCR System 9700 using *Taq* polymerase (Promega). The PCR was performed using an initial denaturation step of 94°C for 5 minutes followed by the PCR cycling parameters; 94°C for 30 seconds, 58°C for 30 seconds, 65°C for 3 minutes (35 cycles), 65°C for 10 minutes. PCR products were analysed by gel electrophoresis, as discussed in Chapter 2. The 2.5 kb genomic fragment was co-transformed with *Hind* III-digested pYSGFP-1 into *S. cerevisiae* (Saunders *et al.*, 2010). The *SLP1* genomic fragment became integrated into pYSGFP-1 fragment by gap-replacement cloning (Oldenburg *et al.*, 1997) as a result of homologous recombination between the complementary sequence of the pYSGFP-1 vector and the sequence overhang of the PCR amplicon. Positive yeast clones were confirmed by PCR and the construct independently verified and checked for errors by DNA sequencing. The resulting *SLP1:GFP* plasmid was

subsequently introduced into *M. oryzae* by transformation of the *M. oryzae* Guy11 strain (Leung *et al.*, 1988; Nottegham and Silue, 1992).

4.2.2 Construction of the *SLP1*²⁷⁻¹⁶²:*GFP* fusion vector

To generate the *SLP1*²⁷⁻¹⁶²:*GFP* vector, primers were designed to amplify a 2.0 kb *SLP1* promoter fragment upstream of the *SLP1* gene (*SLP1-Prom* fragment) and a 468 bp fragment (*SLP1*²⁷⁻¹⁶² fragment) from *M. oryzae* genomic DNA. To amplify the *SLP1-Prom* fragment, a forward (5') primer (5'SLP1-Prom) was used (as described in Section 4.2.1) with a reverse (3') primer (3'SLP1-Prom), which was designed at the 3' end of the *SLP1* promoter, and was designed to include a 30 bp overhang complementary in sequence to the 5' region encoding the Slp1²⁷⁻¹⁶² peptide. Additionally, a 468 bp *SLP1*²⁷⁻¹⁶² fragment which codes for the Slp1²⁷⁻¹⁶² peptide was amplified. A forward (5') primer (5'SLP1²⁷) was designed downstream of the *SLP1* start codon. The forward (5') primer 5'SLP1²⁷ primer was used with the reverse (3') primer 3'SLP1-GFP, as described in Section 4.2.1. The nucleotide sequences of the primers used to construct the *SLP1*²⁷⁻¹⁶²:*GFP* vector are listed below:

5'SLP1-Prom

5' GATTATTGCACGGAATTGCATGCTCTCACGAGGAAGATAGCCCAGCCC 3'

3'SLP1-Prom

5'GTGCAGGTCGAGGTCGCCGAGGGAGGGGCCAGTTTGACGGTTTGAGAGACGGT 3'

5'SLP1²⁷

5'AAATGGCCCCTCCCTCGGCGACCTCG 3'

3'SLP1-GFP

5'GGTGAACAGCTCCTCGCCCTTGCTCACCATGTTCTTGCAGATGGGGATGTT 3'

Both the 2 kb *SLP1-Prom* and 468 bp *SLP1*²⁷⁻¹⁶² genomic fragments were amplified using an Applied Biosystems GeneAmp® PCR System 9700 using *Taq* polymerase (Promega). The PCR was performed using an initial denaturation step of 94°C for 5 minutes followed by the PCR cycling parameters; 94°C for 30 seconds, 58°C for 30 seconds, 65°C for 1 or 2 minutes (for amplifying *SLP1*²⁷⁻¹⁶² coding and *SLP1-Prom* fragments respectively) (35 cycles), 65°C for 10 minutes. PCR products were analysed by gel electrophoresis, as discussed in Chapter 2. Both the 2 kb and 468 bp genomic fragments were simultaneously transformed into *S. cerevisiae* with

Hind III-digested pYSGFP-1 (Saunders *et al.*, 2010). The *SLP1* genomic fragment became integrated into pYSGFP-1 fragment by gap-replacement cloning (Oldenburg *et al.*, 1997) as a result of homologous recombination between the complementary sequence of the pYSGFP vector and the sequence overhang of the PCR amplicons. Positive yeast clones were confirmed by PCR and the construct was independently confirmed and checked for errors by DNA sequencing. The resulting *SLP1*²⁷⁻¹⁶²:*GFP* plasmid was subsequently introduced into *M. oryzae* by transformation of Guy11 (Leung *et al.*, 1988; Nottegham and Silue, 1992).

4.2.3 Generating the *SLP1*¹⁻²⁷:*GFP* fusion vector

To generate the *SLP1*¹⁻²⁷:*GFP* vector, primers were designed to amplify a 2.1 kb *SLP1* promoter fragment upstream of the *SLP1* gene containing the first 81 nucleotides of the *SLP1* ORF from *M. oryzae* genomic DNA. The resulting 2.1 kb fragment is referred to here as the *SLP1*¹⁻²⁷ fragment. To amplify the *SLP1*¹⁻²⁷ fragment, a forward (5') primer (5'SLP1-Prom) was used (as described in Section 4.2.1) with a reverse (3') primer (3'SLP1¹⁻²⁷), which was designed at the 3' end of the predicted *SLP1* signal peptide coding region. The *SLP1*¹⁻²⁷ primer included a 30 bp overhang complementary in sequence to the codon region of the *GFP* allele. The nucleotide sequences of the primers used to construct the *SLP1*¹⁻²⁷:*GFP* vector are listed below:

5'SLP1-Prom
 5' GATTATTGCACGGAATTGCATGCTCTCACGAGGAAGATAGCCCAGCCC 3'
 3'SLP1¹⁻²⁷
 5' GTGAACCAGCTCCTCGCCCTTGCTCACCATCAGGCAACCCCCACCAGCGCC 3'

The 2.1 kb *SLP1* genomic fragments were amplified using an Applied Biosystems GeneAmp® PCR System 9700 using *Taq* polymerase (Promega). The PCR was performed using an initial denaturation step of 94°C for 5 minutes followed by the PCR cycling parameters; 94°C for 30 seconds, 58°C for 30 seconds, 65°C for 2 minutes (35 cycles), 65°C for 10 minutes. PCR products were analysed by gel electrophoresis, as discussed in Chapter 2. The *SLP1*¹⁻²⁷ genomic fragments were transformed into *S. cerevisiae* with *Hind* III-digested pYSGFP-1 (Saunders *et al.*, 2010). The *SLP1*¹⁻²⁷ genomic fragment became integrated into pYSGFP-1 fragment by gap-replacement cloning (Oldenburg *et al.*, 1997) as a result of homologous recombination between

the complementary sequence of the pYSGFP vector and the sequence overhangs of the PCR amplicons. Positive yeast clones were confirmed by PCR and the construct was independently confirmed and checked for errors by DNA sequencing. The resulting *SLP1*¹⁻²⁷:*GFP* plasmid was subsequently introduced into *M. oryzae* by transformation of Guy11 (Leung *et al.*, 1988; Nottegham and Silue, 1992).

4.2.4 Generating the *AVR-Pia*¹⁻¹⁹:*SLP1*²⁷⁻¹⁶²:*GFP* fusion vector

To generate the *AVR-Pia*¹⁻¹⁹:*SLP1*²⁷⁻¹⁶²:*GFP* vector, a 2 kb fragment containing the active promoter of the *SLP1* gene was amplified. The forward (5') primer 5'SLP1-Prom was used, as described in Section 4.2.1, with a reverse (3') primer 3'SLP1-Pia, which was designed at the 3' end of the active SLP1 promoter and included a 5' 30 bp overhang complementary in sequence to the *AVR-Pia* signal peptide (Yoshida *et al.*, 2009). To generate the *AVR-Pia*¹⁻¹⁹:*SLP1*²⁷⁻¹⁶²:*GFP* vector, the nucleotide coding region for the *Avr-Pia*¹⁻¹⁹:*Slp1*²⁷⁻¹⁶² peptide was synthesised (MWG Eurofins Operon). To amplify the 500 bp *AVR-Pia*¹⁻¹⁹:*SLP1*²⁷⁻¹⁶² fragment, a forward (5') primer (5'*AVR-Pia*) was designed and used with the reverse (3') primer 3'SLP-GFP, as described in Section 4.2.1. The nucleotide sequences of the primers used to construct the *AVR-Pia*¹⁻¹⁹:*SLP1*²⁷⁻¹⁶²:*GFP* vector are listed below:

5'SLP1-Prom
 5' GATTATTGCACGGGAATTGCATGCTCTCACGAGGAAGATAGCCCAGCCC 3'

3'SLP1-Pia
 5' AAAGGGGATGAAAATTGTCGAAAAATGCATTTTGACGGTTTGAGAGACGGT 3'

5'*AVR-Pia*
 5' ATGCATTTTTCGACAATTTTC 3'

3'SLP1-GFP
 5' GGTGAACAGCTCCTCGCCCTTGCTCACCATGTTCTTGCAGATGGGGATGTT 3'

The 2.0 kb *SLP1* promoter and 500 bp *AVR-Pia*¹⁻¹⁹:*SLP1*²⁷⁻¹⁶² fragments were amplified using an Applied Biosystems GeneAmp® PCR System 9700 using *Taq* polymerase (Promega). The PCR was performed using an initial denaturation step of 94°C for 5 minutes followed by the PCR cycling parameters; 94°C for 30 seconds, 58°C for 30 seconds, 65°C for 1 or 2 minutes (to amplify the *SLP1* promoter or *AVR-Pia*¹⁻¹⁹:*SLP1*²⁷⁻¹⁶² fragment respectively) (35 cycles), 65°C

for 10 minutes. PCR products were analysed by gel electrophoresis, as discussed in Chapter 2. The *SLP1* promoter and *AVR-Pia*¹⁻¹⁹:*SLP1*²⁷⁻¹⁶² fragments were simultaneously transformed into *S. cerevisiae* with *Hind* III-digested pYSGFP-1 (Saunders *et al.*, 2010). The *SLP1* promoter and *AVR-Pia*¹⁻¹⁹:*SLP1*²⁷⁻¹⁶² fragments became integrated into pYSGFP-1 fragment by gap-replacement cloning (Oldenburg *et al.*, 1997) as a result of homologous recombination between the complementary sequence of the pYSGFP vector and the sequence overhangs of the PCR amplicons. Positive yeast clones were confirmed by PCR and the construct was independently confirmed and checked for errors by DNA sequencing. The resulting *AVR-Pia*¹⁻¹⁹:*SLP1*²⁷⁻¹⁶²:*GFP* plasmid was subsequently introduced into *M. oryzae* by transformation of Guy11 expressing the BIC-localised avirulence effector *AVR-Pia*¹⁻¹⁹:*mRFP* (Yoshida *et al.*, 2009).

4.3 Results

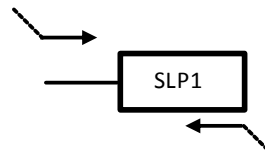
4.3.1 Slp1 is secreted into the apoplastic space

4.3.1.1 Generating and construction of a C-terminal *SLP1:GFP* fusion vector

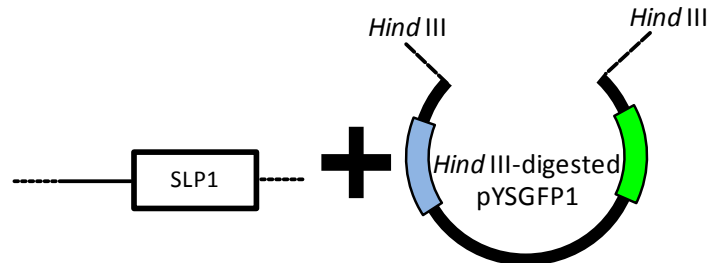
To visualise the sub-cellular localisation of *SLP1:GFP* by epifluorescence microscopy, a C-terminal translational fusion of the *SLP1* gene under the control of its native upstream promoter was fused to the reporter gene Green Fluorescent Protein (GFP) to generate the *SLP1:GFP* vector, as shown in Figure 4.1. A 2.5 kb genomic fragment containing the 568 bp *SLP1* ORF and a 2 kb upstream region incorporating the *SLP1* promoter was PCR amplified and cloned into *Hind* III-digested vector pYSGFP1 (Saunders *et al.*, 2010). An in frame fusion of the *SLP1* ORF to *GFP* was generated by homologous recombination upon co-transformation into *S. cerevisiae* by gap replacement cloning (Oldenburg *et al.*, 1997). A diagrammatic representation of the cloning strategy using homologous recombination to generate the *SLP1:GFP* gene fusion vector is shown in Figure 4.1. Positive clones of the *SLP1:GFP* vector were confirmed by PCR using *SLP1*-specific primers, and independently verified by DNA sequencing. The *SLP1:GFP* fusion vector was introduced into the Guy11 *M. oryzae* strain (Nottingham and Silue, 1992) and a number of putative sulfonylurea-resistant transformants were selected. Resistance to sulfonylurea was bestowed upon these transformants based on the presence of the *ILV1* allele in the pYSGFP-1 vector which encodes acetolactate synthase encoding resistance to sulfonylurea (Sweigard *et al.*, 1997). DNA was isolated from ten putative transformants and digested with *Eco* RI and fractionated by agarose gel electrophoresis. The gel was transferred to a Hybond-N membrane (Amersham) and probed with a 1.5 kb *GFP:trpC* fragment, as shown in Figure 4.2. Two transformants were shown to have a single copy ectopic integration of the *SLP1:GFP* vector, as shown in Figure 4.2, and were selected for further analysis.

A

1). PCR amplification. Both 5' and 3' oligonucleotides have overlapping complementary sequence to *ILV1* and *GFP* alleles respectively



2). Co-transformation of amplicon with *Hind* III-digested pYSGFP1 into *S. cerevisiae*



3). Yeast mediates homologous recombination between overlapping nucleotide sequence of the 5' and 3' ends of the amplicon with the vector

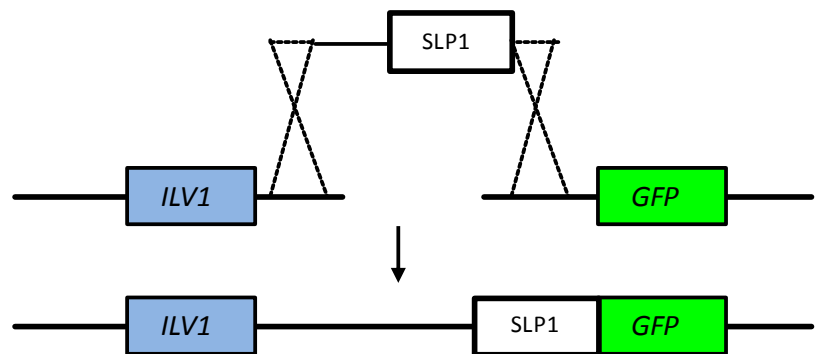
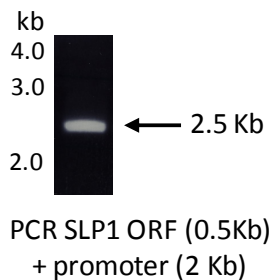
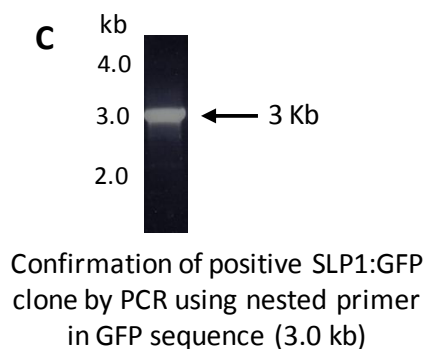
**B****C**

Figure 4.1 Schematic representation of the construction of the C-terminal *SLP1:GFP* fusion vector. **A.** Cloning strategy using homologous recombination in yeast for fusion of *GFP* to the C-terminus of the *SLP1* gene. **B.** PCR amplification of the *SLP1* ORF plus a 2 kb promoter sequence (2.5 kb). **C.** Confirmation of positive *SLP1:GFP* clones in yeast by PCR using *SLP1* and *GFP*-specific primers.

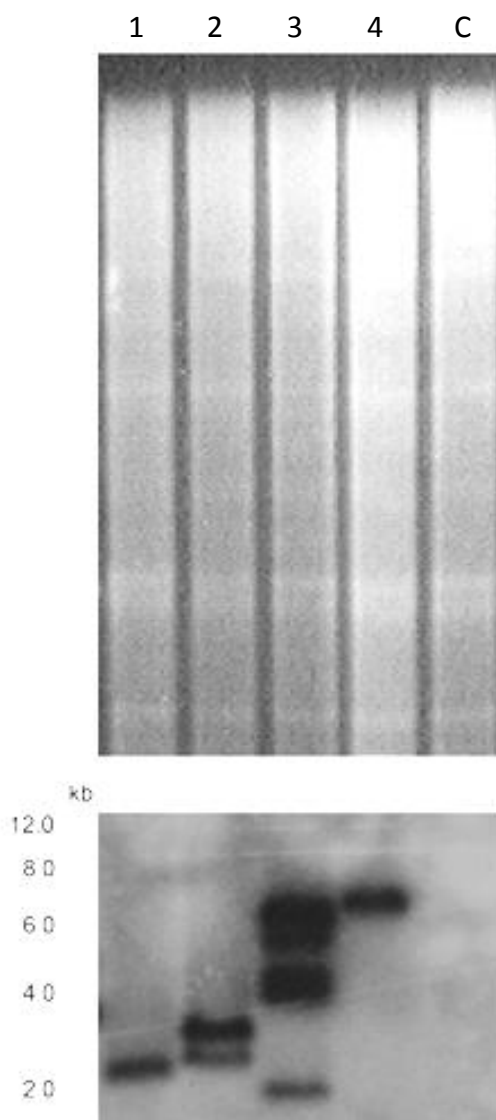


Figure 4.2 Southern blot analysis of putative *SLPI:GFP* transformants. Genomic DNA was extracted from ten sulfonylurea-resistant transformants, restriction digested with *Eco* RI, gel fractionated and transferred to a Hybond-N membrane (Amersham). A subset of DNA extracted from 4 transformants is displayed here. The Southern blot was probed with a 1.5 kb *GFP:trpC* fragment, which did not hybridise with the non-transformed Guy11 control (Lane C). Transformants 1 and 4 were selected as single copy transformants and used for further experiments.

4.3.1.2 Expression and localisation of *SLP1:GFP* during infection-related development of *M. oryzae*

In order to investigate the sub-cellular localisation of *SLP1* during infection-related development, *M. oryzae* conidia expressing *SLP1:GFP* were harvested and inoculated onto borosilicate glass coverslips and incubated in a moist chamber at 24°C. Examination by epifluorescence microscopy was performed at 0, 4, 12 and 24 hours post-inoculation (Figure 4.3). No fluorescence could be observed in conidia, incipient germ tubes or mature appressoria of the *SLP1:GFP* expressing strain, whereas fluorescence could be consistently detected in the Guy *M. oryzae* strain expressing the autophagosome marker *ATG8:GFP* (Kershaw and Talbot, 2009), which was included in the assay as a positive control. At 24 hours post-inoculation, autofluorescence can be seen in the *SLP1:GFP* expressing strain. This background fluorescence is consistent with previous studies (Kershaw *et al.*, 2009). As a control, the Guy11 strain was also observed under similar epifluorescent conditions and had a similar level of fluorescence emanating from the appressorium (data not shown).

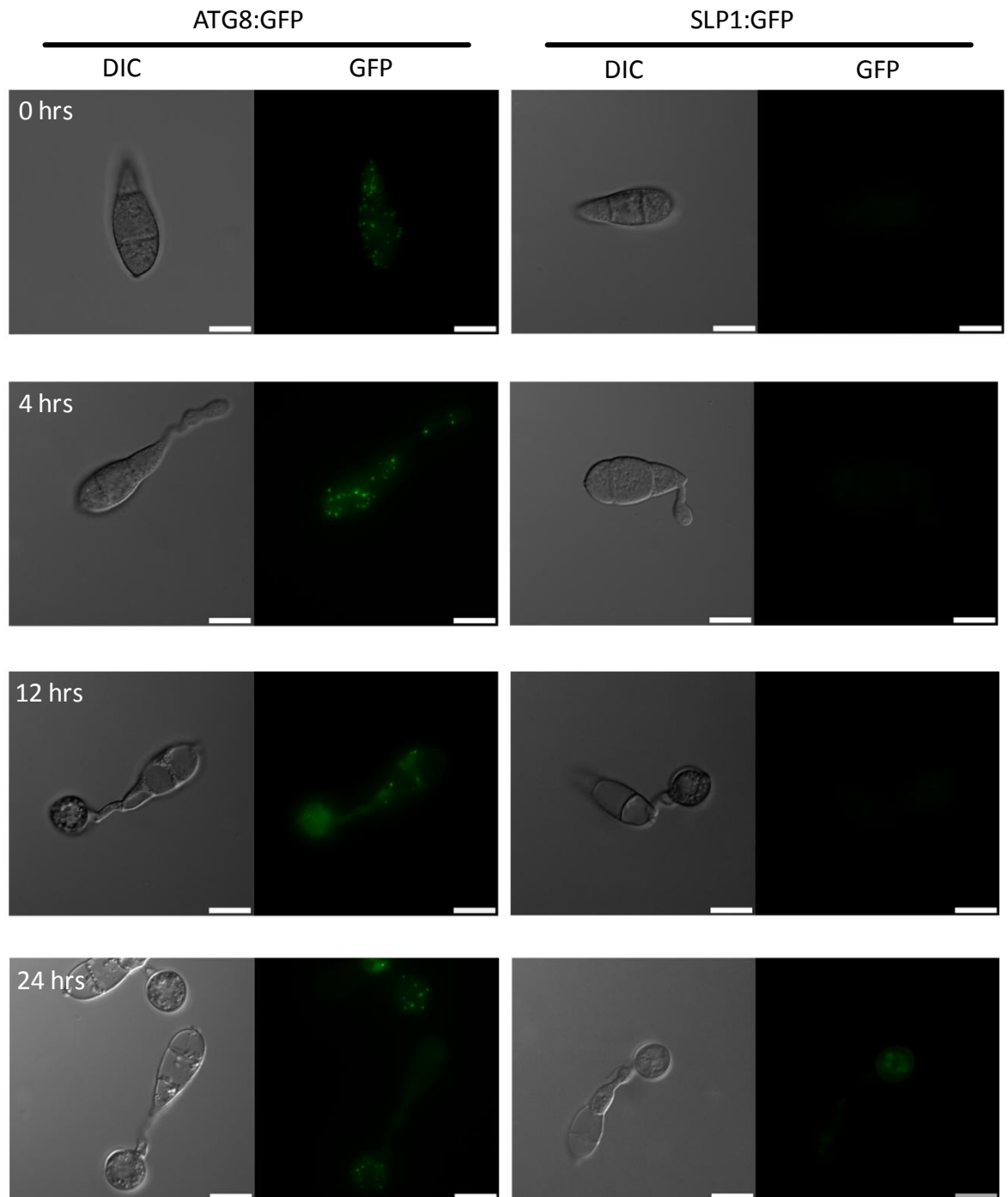


Figure 4.3 *SLP1* is not expressed during appressorium-mediated morphogenesis. Conidia of a putative *SLP1:GFP* transformant and Guy11 *ATG8:GFP* (Kershaw and Talbot, 2009) strain were harvested, inoculated onto glass coverslips and incubated in a moist chamber at 26°C. Fluorescence from the *SLP1:GFP* strain could not be detected in conidia, germ tubes or incipient appressoria. The *ATG8:GFP* strain was included here as a positive control, and fluorescence could be detected in autophagosomes at all time points. Both strains were excited at 488 nm for 400 ms. Scale bars represent 10 μ m.

4.3.1.3 Expression and localisation of *SLP1:GFP* cannot be detected during *in vitro* vegetative growth

Having demonstrated that localisation of Slp1:GFP could not be detected during appressorium-mediated development of *M. oryzae*, we were interested to see if expression of *SLP1:GFP* could be detected during *in vitro* growth of vegetative hyphae. A mycelial plug of the *SLP1:GFP* and *FIM:GFP* strains were inoculated onto liquid CM and incubated in a moist chamber at 24°C. The *FIM:GFP* strain, which expresses a C-terminal GFP fusion to the actin-binding protein fimbrin and localises the actin cytoskeleton of *M. oryzae* (Browsers *et al.*, 1995; Dean *et al.*, 2005), was included in the assay as a positive control. After 24 hours post-inoculation, vegetative hyphae were examined by epifluorescence microscopy, as shown in Figure 4.4. Fluorescence could not be detected in vegetative hyphae of the *SLP1:GFP* strain, whereas the actin patches, as identified by expression of *FIM:GFP* were clearly visible by epifluorescence microscopy and localised discrete actin puncta (Figure 4.4).

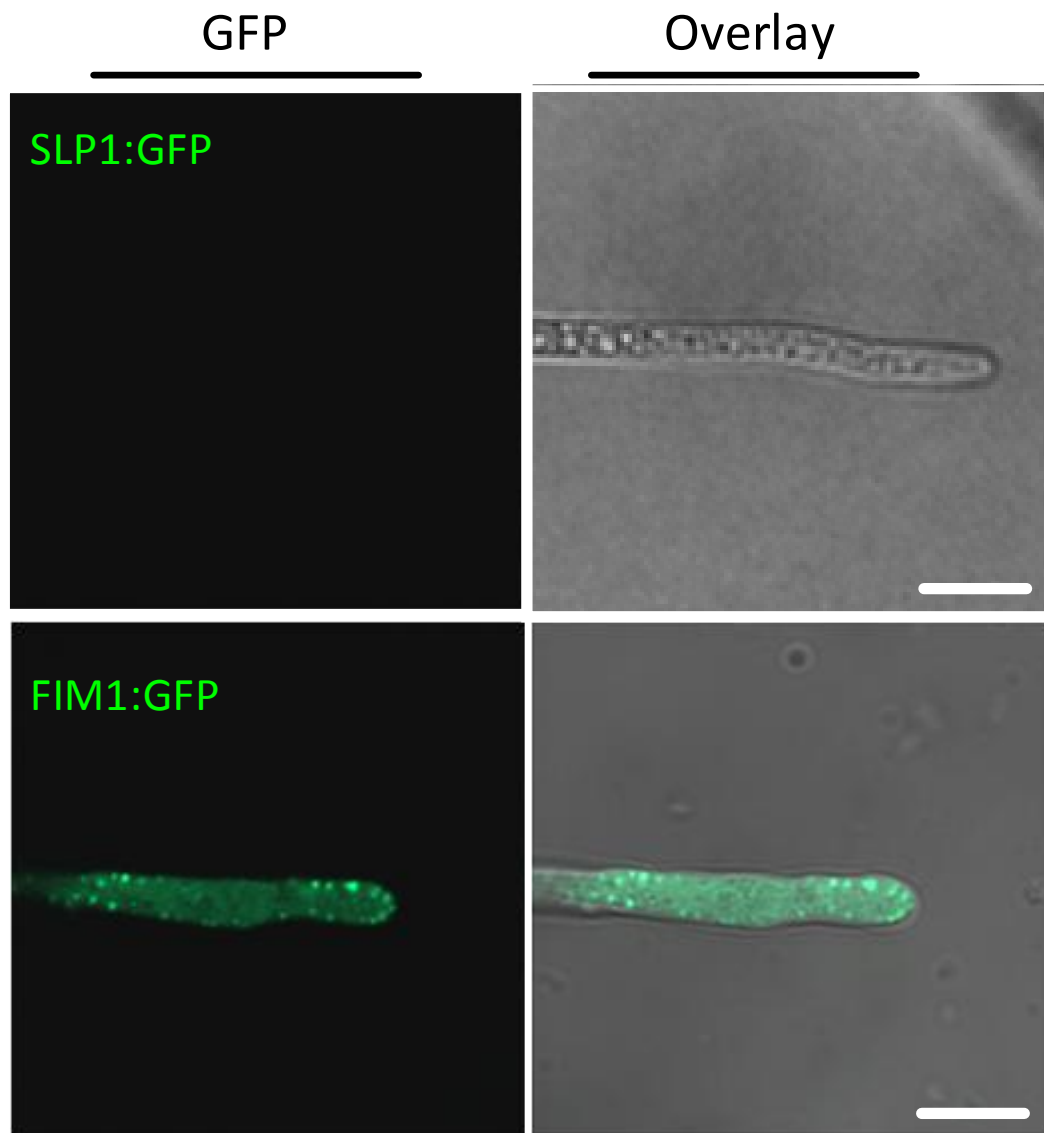


Figure 4.4 *SLP1:GFP* is not expressed *in vitro*. A mycelial plug of a putative Guy11 *SLP1:GFP* transformant and a Guy11 strain expressing the Fimbrin marker *FIM:GFP* was inoculated onto a drop of liquid CM and incubated for 24 hours. The *FIM:GFP* marker was included as a positive control. Hyphal tips were examined by epifluorescence microscopy, and no fluorescence could be observed in the putative Guy11 *SLP1:GFP* transformant (top). In contrast, GFP fluorescence could be seen to accumulate at actin patches in the *FIM:GFP* expressing strain (bottom). Both images were taken at the same exposure to 488 nm (0.2 s). Scale bars represent 10 μ m.

4.3.1.4 *SLP1:GFP* accumulates at the plant-fungal interface during intracellular biotrophic growth

Expression and localisation of *SLP1:GFP* could not be determined in *M. oryzae* growing in axenic culture, as shown in Figures 4.3 and 4.4. As the *SLP1* ORF encodes a predicted N-terminal secretion signal, we reasoned that *SLP1* might only be expressed during intracellular biotrophic growth, a characteristic shared by a number of putative effector proteins (Mosquera *et al.*, 2009). A number of genes encoding proteins with predicted effector function have previously been shown to be expressed at low levels during vegetative growth but are highly expressed during intracellular biotrophic growth (Mosquera *et al.*, 2009). To investigate the sub-cellular localisation of *SLP1:GFP* during biotrophic growth, we inoculated the *SLP1:GFP* strain onto epidermal leaf tissue using the leaf sheath method, as described previously (Kankanala *et al.*, 2007; Mosquera *et al.*, 2009; Khang *et al.*, 2010). After 24 hours post-inoculation (hpi), infected leaf tissue was dissected and examined by epifluorescence microscopy, as shown in Figure 4.5A. At 24 hpi *Slp1:GFP* could be seen to accumulate at the tips of invasive fungal hyphae and localised at the plant-fungal interface. At a later stage of infection, when invasive hyphae had begun colonising neighbouring host cells (36 hpi), *Slp1:GFP* could be seen accumulating at the tips of invasive filamentous hyphae that were moving into adjacent host cells. At this time, *Slp1:GFP* ceased accumulating in the initially invaded host cell and fluorescence could only be observed in those hyphal cells that were colonising new host cells, as shown in Figure 4.5B. Expression of *SLP1* appeared to be specific to the intracellular growth phase of the fungus and localised to the plant-fungal interface.

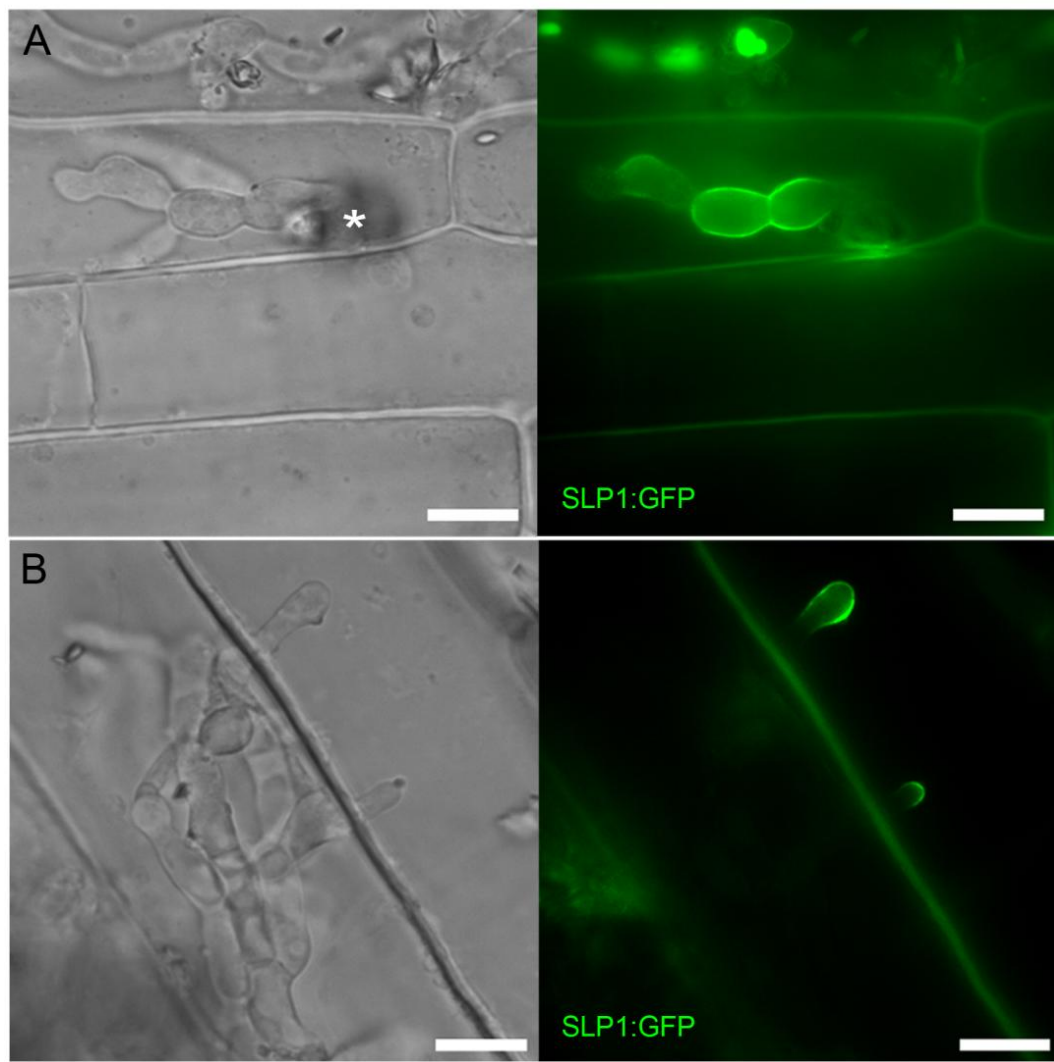


Figure 4.5 *Slp1:GFP* accumulates at the plant fungal interface. **A.** Conidia of a *M. oryzae* transformant expressing the *SLP1:GFP* fusion vector was inoculated onto rice leaf sheath tissue. At 24 hpi, expression of *GFP* was observed in invasively growing fungal hyphae and fluorescence accumulated at the plant-fungal interface. **B.** At a later stage of infection (36 hpi), invasive pseudohyphae moved into adjacent host cells. At this time, *SLP1:GFP* was highly expressed in fungal hyphae that were moving into neighbouring host cells and accumulated at the plant-fungal interface. As hyphae colonised adjacent host cells, fluorescence could no longer be observed at the plant-interface of the initially infected epidermal host cell. White asterisk marks the site of appressorium formation. Scale bars represent 10 μm .

4.3.1.5 *SLP1* is only expressed during *in planta* growth

Having noted that GFP fluorescence could not be detected in the *SLP1:GFP* expressing *M. oryzae* strain, we hypothesised that *SLP1* might be expressed at low levels in vegetative culture, hindering the detection of GFP fluorescence. To investigate and confirm this, a more sensitive method of detecting *SLP1* transcripts was required and so the expression profile of *SLP1* during growth *in planta* was compared with mycelial growth of vegetative hyphae using qualitative RT-PCR. To do this, 3-week old rice leaves were sprayed with conidia from the *M. oryzae* Guy11 strain and total RNA extracted from infected leaf tissue after 7 days post-inoculation. Total RNA was also extracted from *M. oryzae* Guy11 mycelium grown in axenic culture, cDNA from both infected leaf tissue and mycelia RNA samples was generated, and RT-PCR performed using *SLP1*-specific primers, as shown in Figure 4.6. *SLP1* was expressed specifically during invasive growth *in planta* and an *SLP1* cDNA was amplified from infected tissue and confirmed by DNA sequencing. However, we were unable to amplify an *SLP1* cDNA from the mycelial cDNA sample, as shown in Figure 4.6. To confirm the viability of mycelial cDNA, RT-PCR of *SLP2* was performed alongside amplification of *SLP1* cDNA as a positive control. The differential expression pattern of *SLP1* is consistent with a role for Slp1 because a putative effector protein as a number of rice blast effector proteins, including the avirulence effector protein *AVR-Pita*, are only expressed during growth on host tissues and are expressed at low levels or are absent when the fungus is grown in axenic culture (Mosquera *et al.*, 2009).

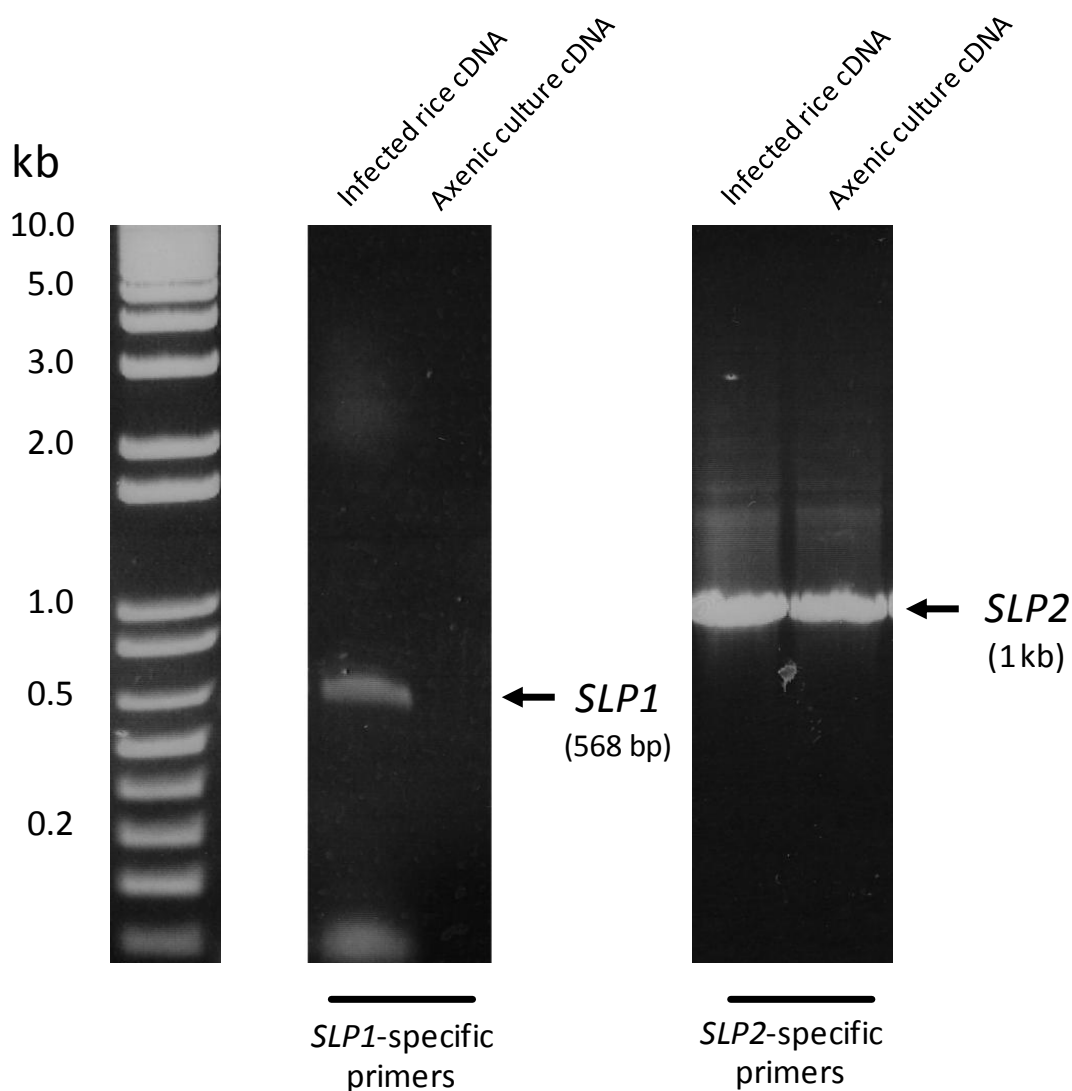


Figure 4.6 *SLP1* is only expressed during in planta growth. Total RNA was extracted from both infected plant tissue after inoculation with *M. oryzae* Guy11 conidia and *M. oryzae* vegetative hyphae grown in axenic culture and cDNA was generated. RT-PCR was performed on infected rice tissue and axenic culture cDNA using *SLP1*-specific primers. An *SLP1* cDNA could not be amplified from axenic culture cDNA but could be amplified from infected leaf tissue cDNA. As a positive control to confirm the viability of the cDNA generated from mycelial RNA, *SLP2* could be amplified from both infected leaf tissue and axenic culture.

4.3.2 Slp1:GFP does not accumulate at the Biotrophic Interfacial Complex (BIC)

Live-cell imaging suggested that Slp1 is an apoplastic effector protein which accumulates at the plant-fungal interface. We were interested to investigate how the localisation pattern of Slp differs from that of previously described *M. oryzae* effector proteins (Mosquera *et al.*, 2009; Khang *et al.*, 2010). Specifically, we were interested to understand how the Slp1:GFP localisation differs from that of avirulence effector proteins which are thought to be translocated into the host cytoplasm and accumulate at the Biotrophic Interfacial Complex (BIC) (Mosquera *et al.*, 2009; Khang *et al.*, 2010). In order to understand how Slp1:GFP differs in its localisation to that of BIC-localised effectors, we generated a *M. oryzae* strain that simultaneously expressed *SLP1:GFP* and a fluorescently-labelled BIC-localised effector. The *SLP1:GFP* fusion vector was introduced into a *M. oryzae* Guy11 strain expressing the BIC-localised *PWL2:mRFP* (Khang *et al.*, 2010), obtained from Dr. Barbara Valent, Kansas State University. Similarly, the *SLP1:GFP* vector was also introduced into a *M. oryzae* Guy11 strain expressing *AVR-Pia:mRFP* (Yoshida *et al.*, 2009), obtained from Dr. Ryohei Terauchi, Iwate Biotechnology Research Centre, Japan. Strains were inoculated onto rice leaf epidermis and incubated in a moist chamber at 24°C before visualising the localisation using epifluorescence microscopy. Slp1:GFP did not co-localise with either Pwl2:mRFP, as shown in Figure 4.7A, or Avr-Pia:mRFP, as shown in Figure 4.7B. More than fifty ($n = 53$) infection sites were examined and co-localisation between Slp1:GFP and BIC-labelled effectors was only observed at three infection sites. The lack of co-localisation between Slp1:GFP and the BIC-localised effectors Pwl2:mRFP and Avr-Pia:mRFP suggests that the Slp1 effector is a distinct effector from previously described rice blast effectors that have cytoplasmic targets.

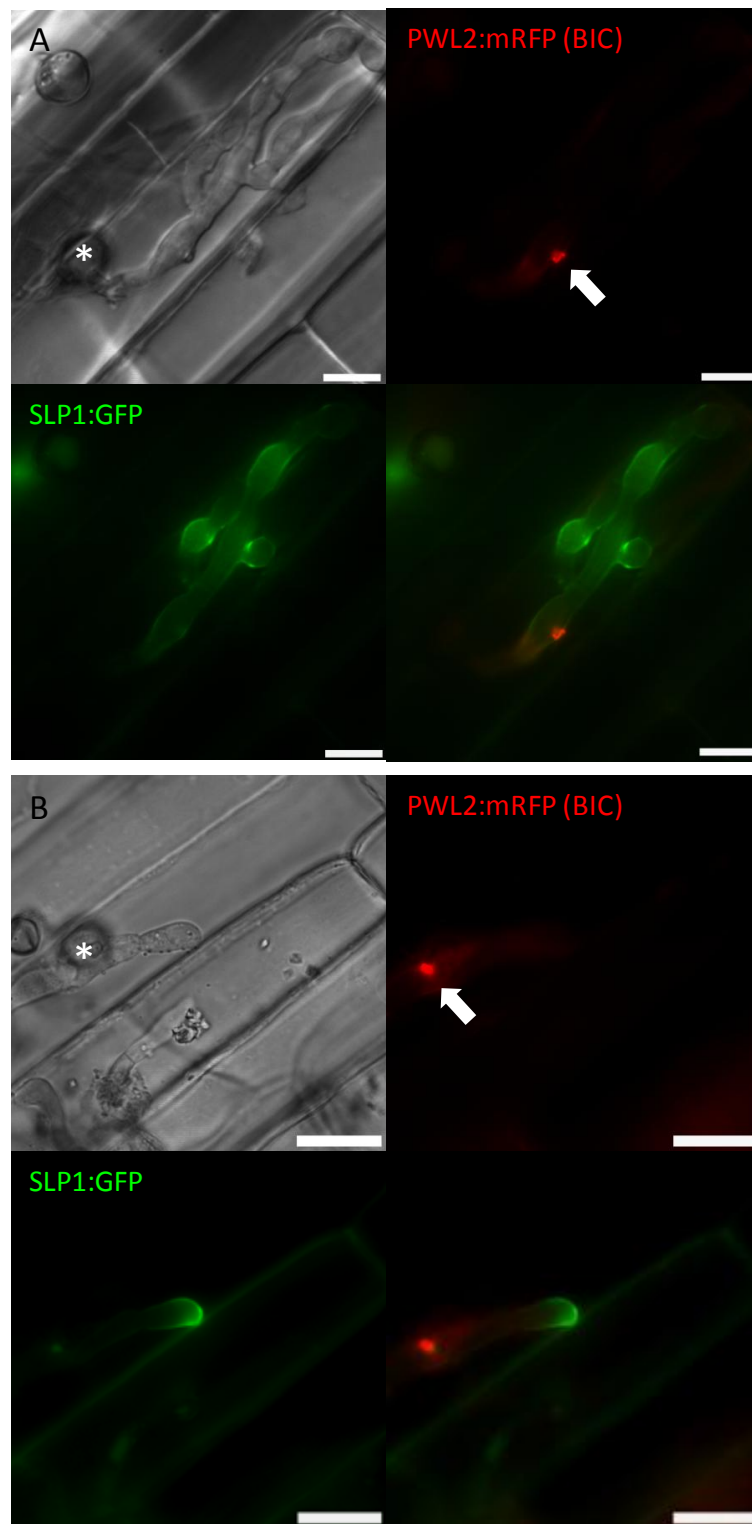


Figure 4.7 Slp1:GFP does not co-localise with BIC-localised avirulence effectors. A. Conidia of a *M. oryzae* Guy11 strain expressing *SLP1:GFP* and *PWL2:mRFP* were harvested and inoculated onto rice leaf tissue. At 24 hpi, Slp1:GFP accumulated at the plant-fungal interface, whilst PwL2:mRFP accumulated at the sub-apical Biotrophic Interfacial Complex (BIC). **B.** Conidia of a *M. oryzae* Guy11 strain expressing *SLP1:GFP* and *AVR-Pia:mRFP* were harvested and inoculated onto rice leaf tissue. At 24 hpi, Slp1:GFP accumulated at the hyphal tips of invasive whilst Avr-Pia:mRFP accumulated at the sub-apical BIC. White arrows indicate the BIC. White asterix marks the site of appressorium formation. Scale bars represent 10 μm

4.3.3 Slp1:GFP co-localises with the putative apoplastic effector protein Bas4:mRFP

Having established that Slp1 has a different pattern of localisation to *M. oryzae* avirulence proteins, we were then interested to examine how Slp1:GFP localisation pattern compared with that of *M. oryzae* putative apoplastic effectors. To date, only one other *M. oryzae* effector protein, Bas4, has been described, which is thought to be secreted into the apoplastic space by *M. oryzae* during intracellular biotrophic growth (Mosquera *et al.*, 2009; Khang *et al.*, 2010). In order to establish how the pattern of localisation of Bas4 is different to that of Slp1, the *SLP1:GFP* fusion vector was introduced into a *M. oryzae* strain expressing *BAS4:mRFP* (Khang *et al.*, 2010), donated by Dr. Barbara Valent, Kansas State University. As shown in Figure 4.8, Slp1:GFP co-localises with the Bas4:mRFP marker. Although there was significant co-localisation between the Slp1:GFP and Bas4:mRFP markers, there were a number of areas surrounding the fungal hyphae where Slp1:GFP accumulated but Bas4:mRFP did not.

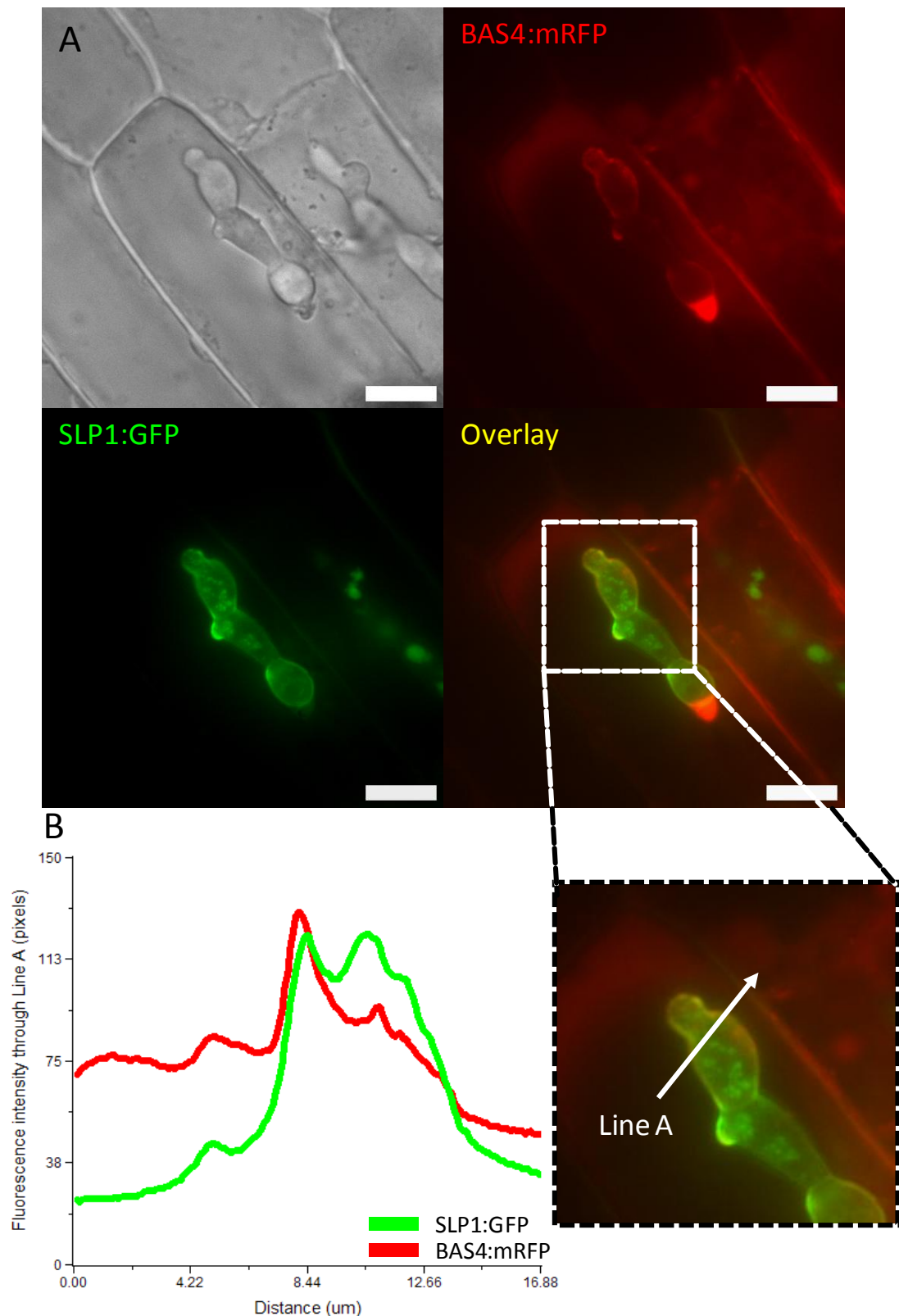


Figure 4.8 Slp1:GFP and Bas4:mRFP partially co-localise. **A.** A *M. oryzae* Guy11 strain which co-expresses the markers *SLP1:GFP* and *BAS4:mRFP* were inoculated onto rice leaf epidermis and incubated in a moist chamber at 24°C. At 24 hours post inoculation, the GFP (Green) and mRFP (Red) fluorescent signals co-localised, although there were locations in which Slp1:GFP accumulated whilst Bas4:mRFP did not. **B.** The intensity of fluorescent signals through line A were observed to partially co-localise. Scale bars represent 10 µm

4.3.4 The N-terminal Slp1 signal peptide is required for secretion at the plant-fungal interface

4.3.4.1 Construction of the *SLP1*²⁷⁻¹⁶²:*GFP* vector

Slp1:GFP appeared to accumulate in the apoplastic space at the plant-fungal interface, and so we were interested in characterising the molecular mechanisms of its secretion. *SLP1* encodes a small secreted protein of 162 amino acids, which contains a predicted N-terminal secretion signal of 27 amino acids (based on SignalP 3.0 analysis). We wanted to understand whether the removal of the predicted signal peptide disrupted protein secretion and subsequent delivery of Slp1 to the plant-fungal interface. To investigate this, we constructed the *SLP1*²⁷⁻¹⁶²:*GFP* plasmid in which the nucleotide coding region for the first 27 amino acids of the Slp1 protein was removed. A 2.0 kb genomic fragment containing the *SLP1* promoter region and a 0.4 kb genomic fragment encoding Slp1²⁷⁻¹⁶² was amplified. A new translational start codon was introduced and the stop codon of the 0.4 kb *SLP1* amplicon removed by primer engineering. The 2.0 kb *SLP1* promoter and 0.4 kb *SLP1*²⁷⁻¹⁶² genomic fragments were co-transformed with *Hind* III-digested pYSGFP1 vector (Saunders *et al.*, 2010) into the yeast *S. cerevisiae*. Primers were engineered to contain 30 bp overhangs at both the 5' and 3' ends of the 2.0 kb *SLP1* promoter fragment, and to include a 30 bp overhang at the 3' end of the *SLP1*²⁷⁻¹⁶² fragment. These overhanging regions were important to generate an in-frame fusion of *SLP1*²⁷⁻¹⁶² to *GFP* with the *SLP1* promoter by homologous recombination between the PCR fragments and the pYSGFP-1 vector (Oldenburg *et al.*, 1997). A schematic representation explaining the process and strategy of gap replacement cloning by homologous recombination is shown in Figure 4.1. Positive clones of the *SLP1*²⁷⁻¹⁶²:*GFP* vector were confirmed by PCR using SLP1-specific primers, and independently verified by DNA sequencing. The resulting *SLP1*²⁷⁻¹⁶²:*GFP* plasmid was used for transformation into the *M. oryzae* Guy11 strain and a number of putative sulfonylurea-resistant transformants were selected. Resistance to sulfonylurea was bestowed upon these transformants due to the *ILVI* allele encoding acetolactate synthase in the pYSGFP-1 vector, which encodes resistance to sulfonylurea (Sweigard *et al.*, 1997). Putative

transformants were subsequently screened for expression of *SLPI*²⁷⁻¹⁶²:*GFP* by epifluorescence microscopy and positive transformants were selected for further analysis.

4.3.4.2 Expression and localisation of the *SLPI*²⁷⁻¹⁶²:*GFP* construct

To determine the contribution of the putative Slp1 signal peptide for secretion, the *M. oryzae* Guy11 strain expressing the *SLPI*²⁷⁻¹⁶²:*GFP* construct was inoculated onto rice leaf tissue and incubated in a moist chamber at 24°C. After 24 hours post-inoculation, Slp1:GFP was prevented from reaching the tips of invasively growing hyphae and Slp1 localisation was longer observed accumulating in the apoplastic space, as shown in Figure 4.9. Interestingly, the resultant intracellular Slp1²⁷⁻¹⁶²:GFP instead appeared to accumulate as aggregates in the fungal cytoplasm. This cellular mislocalisation of *SLPI*²⁷⁻¹⁶²:*GFP* is consistent with the hypothesis that Slp1 is an apoplastic effector, the secretion of which is dependent on the signal peptide sequence within the initial 27 amino acids of the coding sequence.

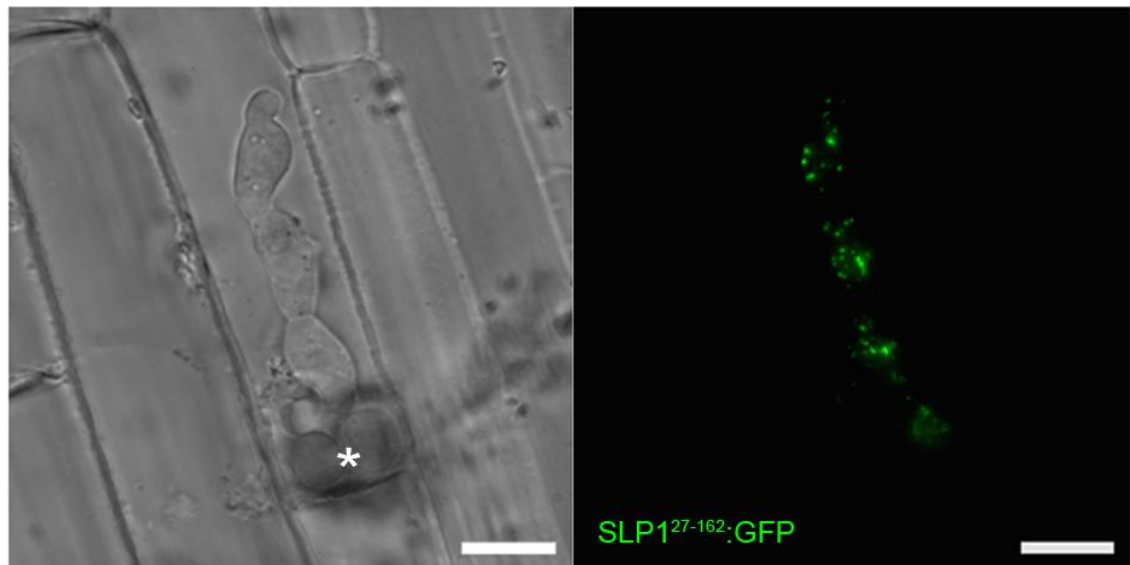


Figure 4.9 The N-terminal 27 amino acids of Slp1 is required for secretion at the plant-fungal interface. A *M. oryzae* Guy11 transformant expressing *SLP1*²⁷⁻¹⁶²::*GFP* was inoculated onto rice leaf epidermis and examined 24 hours post-inoculation. Visualisation of infection sites by epifluorescence microscopy revealed that fluorescence failed to accumulate at the plant-fungal interface and instead was apparent in the fungal cytoplasm as punctate aggregates. White asterix marks the site of appressorium formation. Scale bars represent 10 μm

4.3.5 Using GFP gene fusion vectors to complement the $\Delta slp1$ mutant

4.3.5.1 Complementation of the $\Delta slp1$ mutant with the *SLP1:GFP* vector

We were interested to see if we could complement the $\Delta slp1$ mutant generated in Chapter 3 with the *SLP1:GFP* gene fusion vector. The most striking phenotype of the $\Delta slp1$ mutant was a reduction in disease severity, and we were interested to see if we could restore the virulence of *M. oryzae* $\Delta slp1$ mutants upon introduction of the *SLP1:GFP* vector. This was critical to confirm the virulence phenotype of $\Delta slp1$ is associated with a loss of the *SLP1* gene, but also to establish the functionality of the GFP fusion protein. *SLP1:GFP* was introduced into the $\Delta slp1$ mutant and a number of putative sulfonylurea-resistant transformants were selected. Transformants were screened based on the expression of *SLP1:GFP* during biotrophic growth. The resulting transformant that was selected for complementation analysis is referred to as $\Delta slp1:SLP1:GFP$.

Seedlings of the blast resistant rice cultivar, CO-39 were spray-inoculated with a *M. oryzae* Guy11 strain, $\Delta slp1$ and $\Delta slp1:SLP1:GFP$ (Figure 4.10). As shown in Figure 4.10, the $\Delta slp1$ mutant was highly reduced in virulence and was unable to cause significant disease symptoms. In contrast, similar disease symptoms were visible on plants inoculated with both the Guy11 and $\Delta slp1:SLP1:GFP$ strains, confirming that the reduction in disease virulence of $\Delta slp1$ is a direct result of the targeted replacement of the *SLP1* gene. Restoration of disease symptoms also confirms the functionality of the GFP fusion protein and the likely localisation pattern of Slp1 at the plant fungal interface.

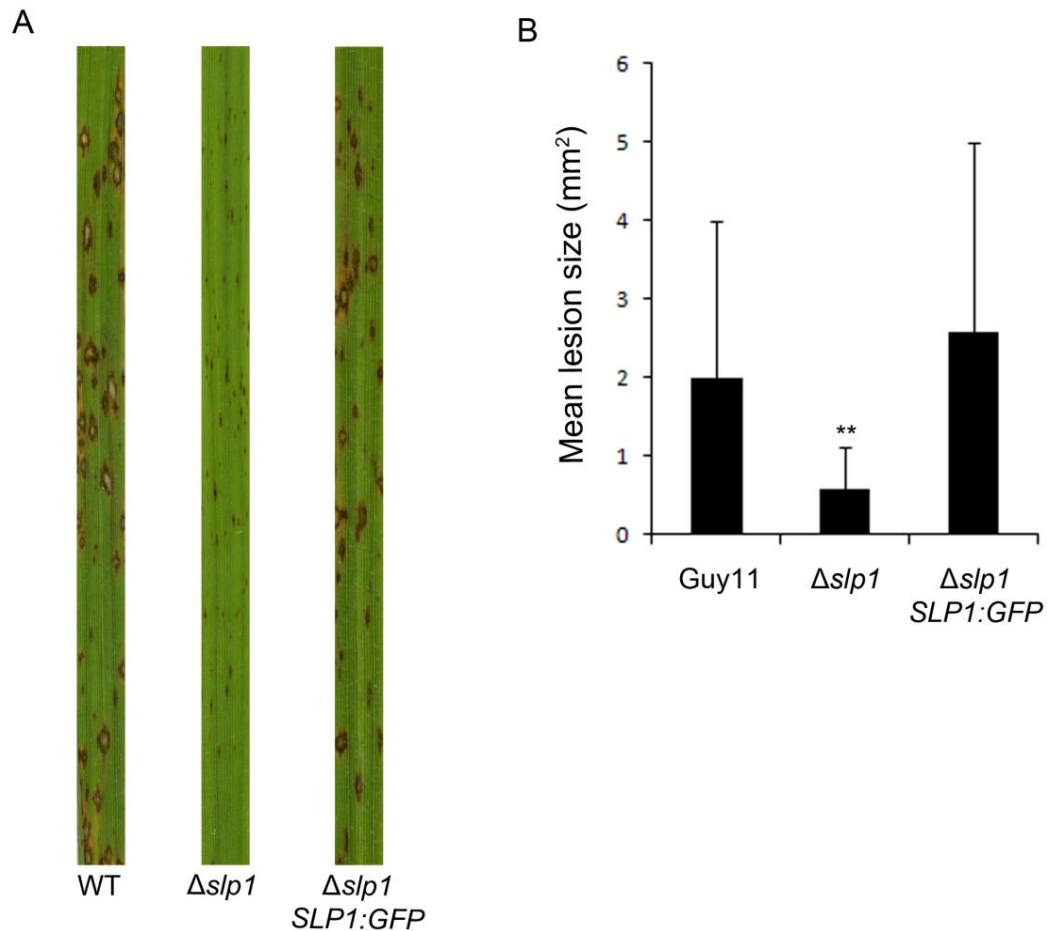


Figure 4.10 Complementation analysis of $\Delta slp1$ mutants using the *SLP1:GFP* vector. A. The *SLP1:GFP* vector was introduced into the $\Delta slp1$ mutant and a number of putative transformants were selected based on the expression of *SLP1:GFP*. The resulting complemented strain is referred to as $\Delta slp1:SLP1:GFP$. A *M. oryzae* Guy11 strain, the $\Delta slp1$ mutant and the complemented $\Delta slp1:SLP1:GFP$ strains were spray inoculated onto 2-3 week old seedlings of the rice blast susceptible rice cultivar CO-39 at a density of 5×10^4 spores ml^{-1} . Introduction of the *SLP1:GFP* construct is able to restore symptoms of the $\Delta slp1$ mutant to that of the wild-type Guy11 strain, with typical disease symptoms developing after 7 days post inoculation. **B.** Mean lesion size is significantly reduced in the $\Delta slp1$ mutant strain (two-tailed t-test, $p < 0.001$, $n = 53$ lesions) but is restored to that of the wild-type strain in the complemented mutant (two-tailed t-test, $p = 0.09$, $n = 73$ lesions). ** represents a p-value of less than 0.001. Error bars represent 1 standard deviation.

4.3.5.2 The N-terminal Slp1 secretion peptide signal is required for complementation of the $\Delta slp1$ mutant

We hypothesised based on our observations that Slp1 is an apoplastic effector, required at the plant-fungal interface (Figure 4.5). We were interested to see if the $SLP^{27-162}:GFP$ vector could complement the $\Delta slp1$ null mutant generated in Chapter 3 as expression of $SLP^{27-162}:GFP$ resulted in cellular mislocalisation. Removal of the predicted Slp1 signal peptide prevented mature Slp1 from reaching the plant-fungal interface (Figure 4.9) and we therefore hypothesised that the $SLP^{27-162}:GFP$ vector would not complement the $\Delta slp1$ mutant. We reasoned that the virulence phenotype of $\Delta slp1$ would not be restored upon introduction of the $SLP^{27-162}:GFP$ vector because a functional Slp1 would fail to be delivered into the apoplastic space. $SLP^{27-162}:GFP$ was introduced into the $\Delta slp1$ mutant and a number of putative sulfonylurea-resistant transformants were selected. Introduction and expression of the $SLP^{27-162}:GFP$ vector was confirmed by epifluorescence imaging of an $\Delta slp1:SLP^{27-162}:GFP$ strain during intracellular biotrophic growth.

Seedlings of the blast-susceptible cultivar CO-39 were spray-inoculated with a *M. oryzae* Guy11 strain, $\Delta slp1$ and $\Delta slp1:SLP^{27-162}:GFP$ as shown in Figure 4.11. Whilst the Guy11 strain was able to cause severe disease symptoms with characteristic lesions visible at 7 days post-inoculation, only small lesions were visible on leaves inoculated with both the $\Delta slp1$ and $\Delta slp1:SLP^{27-162}:GFP$ strains. The inability of the $SLP^{27-162}:GFP$ vector to restore and complement the virulence phenotype of $\Delta slp1$ supports a role for Slp1 being secreted at the plant-fungal interface.



Figure 4.11 Introduction of the *SLPI*²⁷⁻¹⁶²:*GFP* fails to restore the virulence phenotype of $\Delta slp1$. A. The *SLPI*²⁷⁻¹⁶²:*GFP* vector was introduced into the $\Delta slp1$ mutant and a number of putative transformants were selected based on the expression of *SLPI*²⁷⁻¹⁶²:*GFP*. The resulting complemented strain is referred to as $\Delta slp1$: *SLPI*²⁷⁻¹⁶²:*GFP*. A *M. oryzae* Guy11 strain, the $\Delta slp1$ mutant and the complemented $\Delta slp1$: *SLPI*²⁷⁻¹⁶²:*GFP* strains were spray inoculated onto 2-3 week old seedlings of the rice blast susceptible rice cultivar CO-39 at a density of 5×10^4 spores ml⁻¹. Introduction of the *SLPI*²⁷⁻¹⁶²:*GFP* construct is unable to restore symptoms of the $\Delta slp1$ mutant to that of the wild-type Guy11 strain, with disease symptoms similar to that of $\Delta slp1$ forming 7 days post-inoculation.

4.3.6 The mature Slp1 protein is not required for secretion and delivery into the apoplasmic space

4.3.6.1 Construction of the *SLP1*¹⁻²⁷:GFP vector

Having demonstrated that the Slp1 signal peptide is required for secretion by intracellular hyphae, we were interested in further investigating the molecular mechanism of secretion of Slp1. Specifically, we wanted to test if a peptide signal within the mature Slp1 protein contributed to the secretion of Slp1. To do this, we generated the *SLP1*¹⁻²⁷:GFP fusion vector in which a 2.1 kb genomic fragment containing the *SLP1* promoter and the nucleotide sequence coding for the N-terminal Slp1 signal peptide was fused to GFP. Based on SignalP(3.0) analysis, and results obtained from Section 4.3.4, we assumed in this instance that the peptide secretion signal of Slp1 is contained within the initial 27 amino acids of the protein. A 2.1 kb genomic fragment containing the *SLP1* promoter region and the initial 81 nucleotides of *SLP1* was amplified. This 2.1 kb fragment, which we refer to as *SLP1Prom:SLP1*¹⁻²⁷, was co-transformed with *Hind* III-digested pYSGFP1 vector (Saunders *et al.*, 2010) into the yeast *S. cerevisiae*. Primers were engineered to contain 30 bp overhangs at both the 5' and 3' ends of the 2.1 kb *SLP1Prom:SLP1*¹⁻²⁷ fragment. These 5' and 3' overhanging regions were complementary in nucleotide sequence to the pYSGFP1 vector and mediated an in frame fusion of *SLP1Prom:SLP1*¹⁻²⁷ to GFP upon homologous recombination between the 2.1 kb *SLP1Prom:SLP1*¹⁻²⁷ fragment and the pYSGFP1 fragment (Oldenburg *et al.*, 1997). The cloning strategy used to generate this *SLP1*¹⁻²⁷:GFP vector by homologous recombination was adapted from that described in Section 4.3.1.1 and Figure 4.1. Positive clones of the *SLP1*¹⁻²⁷:GFP vector were confirmed by PCR using *SLP1*-specific primers and independently verified by DNA sequencing. The resulting *SLP1*¹⁻²⁷:GFP plasmid was used for subsequent transformation into the *M. oryzae* Guy11 strain and a number of putative sulfonylurea-resistant transformants were selected. Resistance to sulfonylurea was bestowed upon these transformants due to the presence of the *ILV1* allele encoding acetolactate synthase contained within the pYSGFP1 vector which encodes resistance to sulfonylurea (Sweigard *et al.*, 1997). Putative transformants were screened

for expression of *SLP1*¹⁻²⁷:*GFP* by epifluorescence microscopy and positive transformants were selected for further investigation.

4.3.6.2 Localisation of Slp1¹⁻²⁷:GFP in invasive hyphae

To determine if the mature Slp1 protein contains a peptide sequence required for secretion, conidia from a *M. oryzae* Guy11 strain expressing *SLP1*¹⁻²⁷:*GFP* were inoculated onto rice leaf tissue and incubated in a moist chamber at 24°C. At 24 hpi, fluorescence could be seen accumulating at the tips of intracellular invasive hyphae, as shown in Figure 4.12. The pattern of localisation of Slp1¹⁻²⁷:GFP resembled that of Slp1:GFP (Figure 4.5) suggesting that Slp1¹⁻²⁷:GFP is still secreted at hyphal tips into the apoplastic space. We therefore conclude that the mature Slp1 protein does not contain a peptide sequence which contributes to the secretion at hyphal tips of intracellular fungal hyphae.

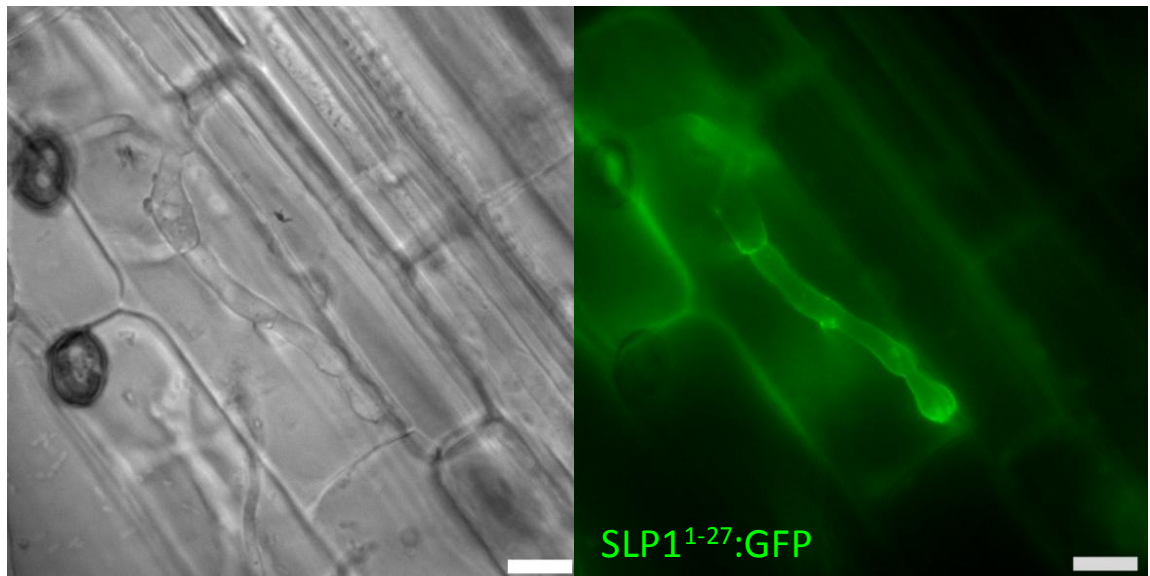


Figure 4.12 The initial 27 amino acids of Slp1 is sufficient to guide secretion. In order to determine if the mature Slp1 protein is required for secretion a *M. oryzae* transformant expressing *SLP1*¹⁻²⁷:*GFP* was inoculated onto rice epidermal leaf tissue. At 24 hours post-inoculation, GFP could be seen accumulating at the plant fungal interface, suggesting that Slp1¹⁻²⁷ is sufficient to bring about secretion of GFP. Scale bars represent 10 μ m

4.3.7 Replacement of the Slp1 signal peptide with the BIC-localised Avr-Pia signal peptide fails to re-direct Slp1 to the BIC

4.3.7.1 Construction of the *AVR-Pia*¹⁻¹⁹:*SLP1*²⁷⁻¹⁶²:*GFP* vector

The Slp1 signal peptide appeared to be crucial for secretion, and so we were interested in further characterising the genetics of this secretion mechanism. Based on previous results (Section 4.3.4), we concluded that the N-terminal Slp1 signal peptide was at least partially responsible for directing Slp1 to hyphal tips and we wanted to see if we could disrupt the normal secretion pattern by genetic manipulation. Specifically, we hypothesised that replacement of the Slp1 signal peptide with a signal peptide from a BIC-localised effector protein would re-direct Slp1 through an alternative secretion pathway and result in the accumulation of Slp1 at the BIC. To investigate this, we constructed the *AVR-Pia*¹⁻¹⁹:*SLP1*²⁷⁻¹⁶²:*GFP* vector in which the nucleotide coding region for the first 19 amino acids of the BIC-localised effector protein Avr-Pia (Yoshida *et al.*, 2009) was fused to the mature Slp1 protein to create *AVR-Pia*¹⁻¹⁹:*SLP1*²⁷⁻¹⁶². This fragment was subsequently fused to GFP to create the vector *AVR-Pia*¹⁻¹⁹:*SLP1*²⁷⁻¹⁶²:*GFP*, as shown in Figure 4.13. Significantly, expression of this *AVR-Pia*¹⁻¹⁹:*SLP1*²⁷⁻¹⁶²:*GFP* fragment was driven by the native 2.0 kb *SLP1* promoter fragment. To do this, a 468 bp DNA fragment encoding the *Avr-Pia*¹⁻¹⁹:*Slp1*²⁷⁻¹⁶² peptide was synthesised (MWG Eurofins Operon, London), as shown in Figure 4.13. This DNA fragment contains the nucleotide sequence encoding *AVR-Pia*¹⁻¹⁹:*Slp1*²⁷⁻¹⁶² protein. A 2.0 kb genomic fragment encoding the *SLP1* promoter and the 468 bp *AVR-Pia*¹⁻¹⁹:*SLP1*²⁷⁻¹⁶² fragment were co-transformed with *Hind* III-digested pYSGFP1 vector (Saunders *et al.*, 2010) into the yeast *S. cerevisiae*. Primers were engineered to contain 30 bp overhangs at both the 5' and 3' ends of the 2.0 kb *SLP1* promoter fragment, and to include a 30 bp overhang at the 3' end of the *AVR-Pia*¹⁻¹⁹:*SLP1*²⁷⁻¹⁶² fragment. These complementary overhanging regions were important to generate an in frame fusion of *SLP1*^{Pro}:*AVR-Pia*¹⁻¹⁹:*SLP1*²⁷⁻¹⁶² to GFP by homologous recombination between the PCR fragments and the pYSGFP-1 vector (Oldenburg *et al.*, 1997). The process and strategy of gap replacement cloning by homologous recombination was adapted from that shown in Figure 4.1. Positive clones of the *AVR-Pia*¹⁻¹⁹:*SLP1*²⁷⁻¹⁶²:*GFP* vector were confirmed by PCR using *SLP1*-specific

primers, and independently verified by DNA sequencing. The resulting *AVR-Pia*¹⁻¹⁹:*SLPI*²⁷⁻¹⁶²:*GFP* plasmid was used for transformation into a *M. oryzae* Guy11 strain expressing *AVR-Pia:mRFP* and a number of putative sulfonylurea-resistant transformants were selected. Resistance to sulfonylurea was bestowed upon these transformants due to the presence of the *ILV1* allele encoding acetolactate synthase in the pYSGFP-1 vector which encodes resistance to sulfonylurea (Sweigard *et al.*, 1997). Putative transformants were subsequently screened for expression of *AVR-Pia*¹⁻¹⁹:*SLPI*²⁷⁻¹⁶²:*GFP* by epifluorescence microscopy and positive transformants were selected for further analysis.

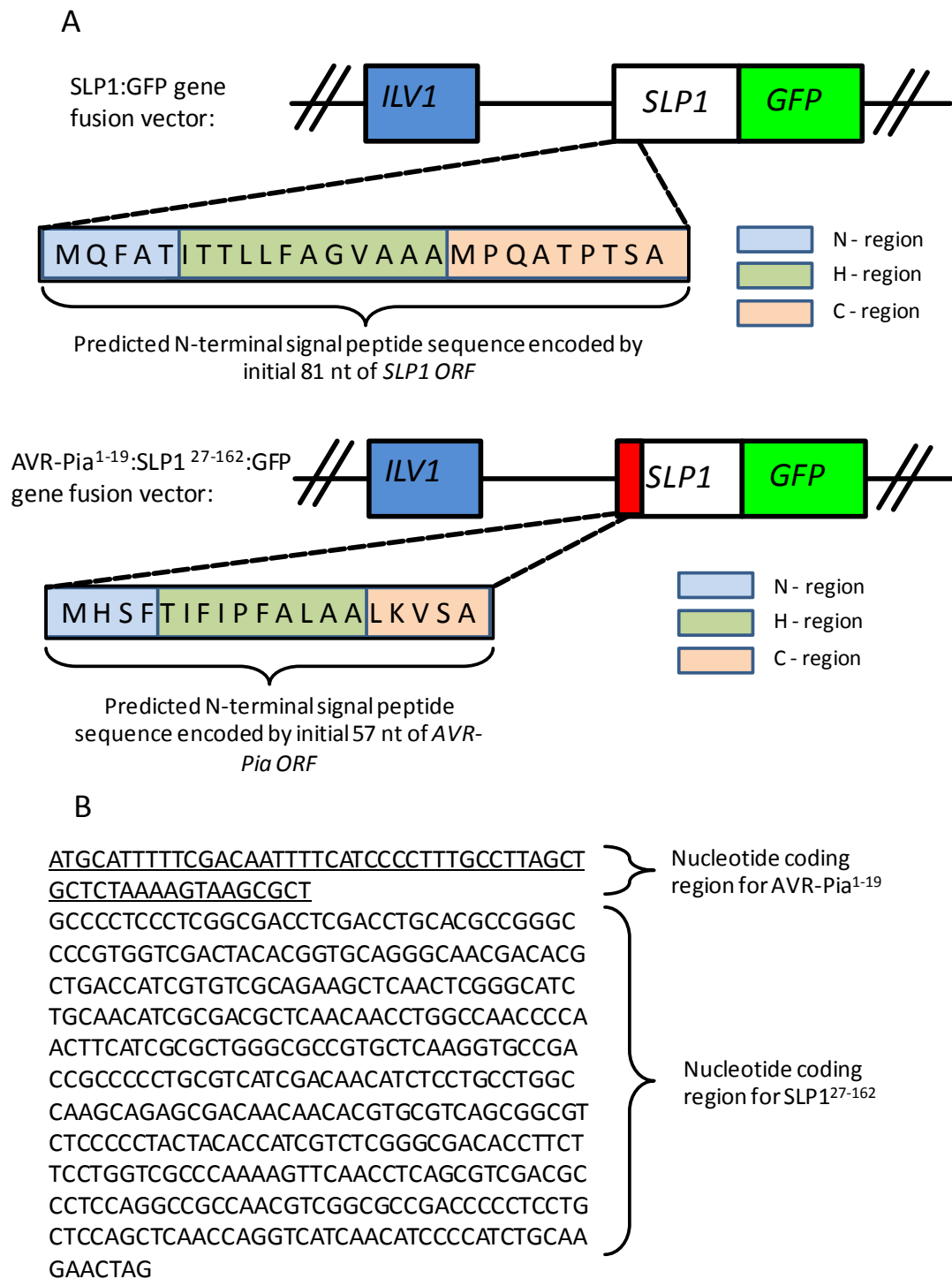


Figure 4.13 Schematic representation of the AVR-Pia¹⁻¹⁹SLP1²⁷⁻¹⁶²:GFP vector. **A.** To generate the AVR-Pia¹⁻¹⁹:SLP1²⁷⁻¹⁶²:GFP vector, the N-terminal nucleotide sequence encoding the initial 27 amino acids was removed from the SLP1:GFP fusion vector and replaced with the nucleotide sequence encoding the N-terminal secretion signal of Avr-Pia (Yoshida *et al.*, 2009). **B.** Nucleotide coding sequence of AVR-Pia¹⁻¹⁹:SLP1²⁷⁻¹⁶²

4.3.7.2 Avr-Pia¹⁻¹⁹:Slp1²⁷⁻¹⁶²:GFP localises to the plant-fungal interface and not to the BIC

To determine if we could re-direct the secretion of Slp1 by genetic manipulation of the Slp1 signal peptide coding region, conidia from a *M. oryzae* Guy11 strain expressing AVR-Pia¹⁻¹⁹:SLP1²⁷⁻¹⁶²:GFP and AVR-Pia:mRFP were inoculated onto rice leaf tissue and incubated in a moist chamber at 24°C. At 24 hpi, fluorescence could be seen accumulating at the tips of intracellular invasive hyphae and GFP fluorescence (associated with Avr-Pia¹⁻¹⁹:Slp1²⁷⁻¹⁶²:GFP) did not appear to co-localise with the RFP fluorescence associated with the BIC (Avr-Pia:mRFP), as shown in Figure 4.14. The pattern of localisation of Avr-Pia¹⁻¹⁹:Slp1²⁷⁻¹⁶²:GFP resembled that of Slp1:GFP and Avr-Pia¹⁻¹⁹:Slp1²⁷⁻¹⁶²:GFP continued to be secreted by hyphal tips into the apoplastic space, but was not observed at the BIC. We conclude that replacement of the Slp1 signal peptide with the Avr-Pia signal peptide is not sufficient to re-direct the Slp1 via an alternative secretion pathway to the BIC, as shown in Figure 4.14. Although dependent on the Slp1 signal peptide, secretion of Slp1 might also be dependent on a nucleotide sequence within the *SLP1* promoter fragment, most likely in the 5' Untranslated Region (5'UTR). Alternatively, any generic fungal signal peptide may be sufficient to drive Slp1 secretion to the hyphal tips instead of the BIC.

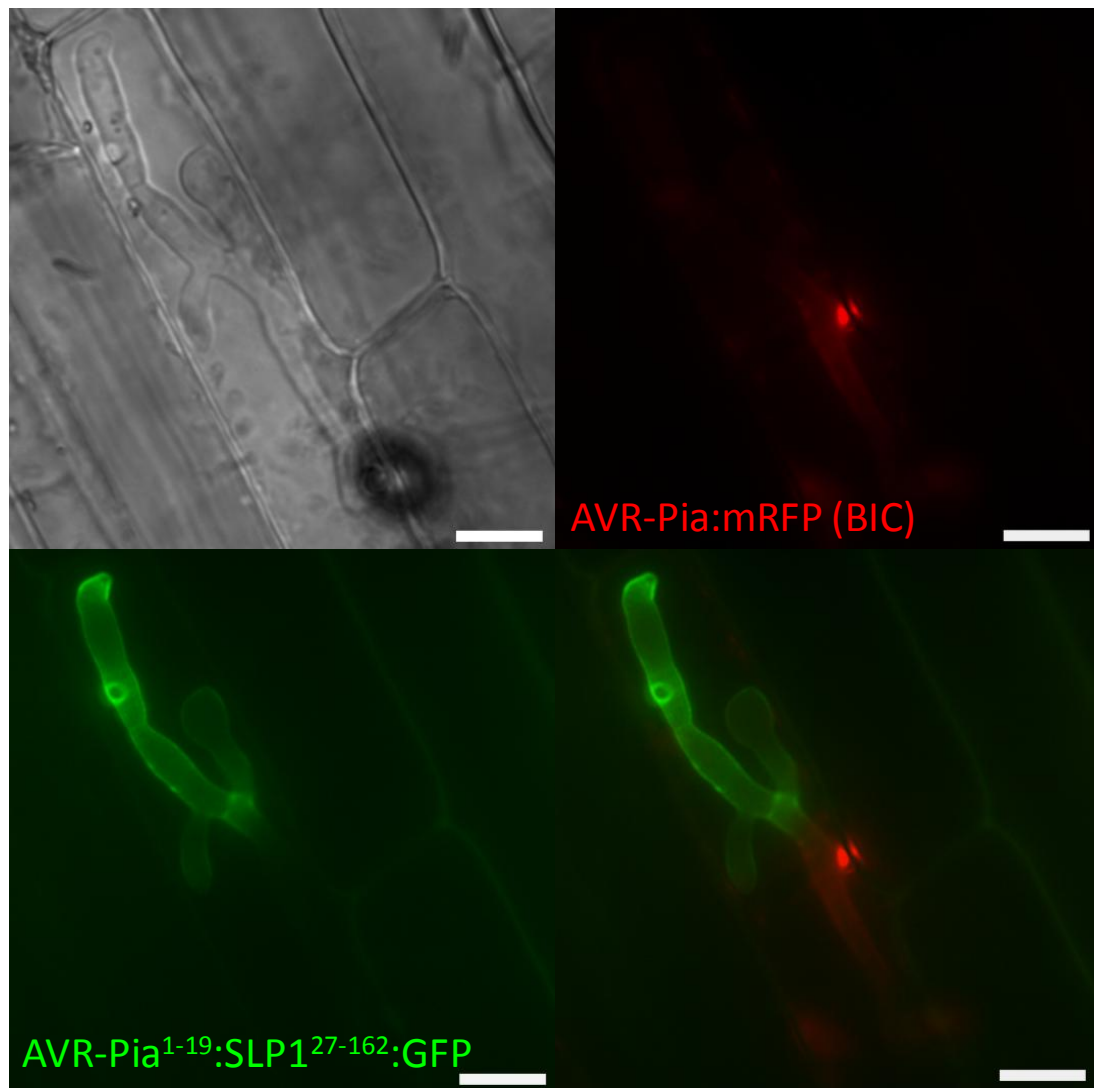


Figure 4.14 Replacing the Slp1 signal peptide with the N-terminal Avr-Pia signal peptide fails to re-direct the protein to the Biotrophic Interfacial Complex (BIC). A *M. oryzae* strain expressing both *AVR-Pia*:mRFP (Red) and *AVR-Pia*¹⁻¹⁹:*SLP1*²⁷⁻¹⁶²:GFP (Green) was inoculated onto rice leaf epidermis and visualised by epifluorescence microscopy after 24 hours post-inoculation. Replacement of the Slp1 signal peptide with the N-terminal signal peptide from AVR-Pia failed to re-direct the GFP signal to the BIC and fluorescence continued to accumulate at the plant-fungal interface. Scale bars represent 10 μ m

4.4 Discussion

During biotrophic growth, apoplastic effector molecules are deployed by oomycete and intercellular fungal pathogens, and a number of classes of these apoplastic effectors with varying functions have been described in the literature (for reviews see Stergiopoulus and de Wit, 2009; van Damme *et al.*, 2012). In oomycete pathogens, apoplastic effectors are secreted into the Extra Haustorial Matrix (EHMx) which is the space generated between haustoria and the plant-derived Extra Haustorial Membrane (EHM) (O'Connell and Panstruga, 2006; Micali *et al.*, 2011; Lu *et al.*, 2012). Oomycete apoplastic effector molecules are delivered into this EHMx, and have been shown to have a diverse set of functions ranging from protease inhibitors that target serine and cysteine proteases (Tian *et al.*, 2005), to cell-death inducing factors such as that of the *Phytophthora infestans* NPP1.1 (Kanneganti *et al.*, 2006; van Damme *et al.*, 2012).

Apoplastic effectors are also deployed by intercellular fungal pathogens, including the tomato leaf mold fungus *Cladosporium fulvum*. During infection by *C. fulvum*, for example, the cysteine-rich apoplastic effector proteins Avr2, Avr4 and Ecp6 are secreted (van Esse *et al.*, 2007; de Jonge *et al.*, 2010). Avr2 is a small protein of 58 amino acids and induces a hypersensitive response (HR) on tomato plants carrying the cognate R gene *Cf-2* (Dixon *et al.*, 1996; Luderer *et al.*, 2002). Avr2 is known to inhibit the function of the tomato papain-like cysteine endoprotease Rcr3 and is required for suppression of autonecrosis (Krüger *et al.*, 2002). In contrast, Avr4, which also contains eight cysteine residues, possesses chitin-binding motifs in its protein structure, and protects fungal cell walls from degradation by plant-derived chitinases (Van Den Burg *et al.*, 2006). Further to this, Avr4 is only expressed during infection on its host when the fungus is most likely to be exposed to the hydrolysing effects of plant chitinases (van Esse *et al.*, 2007).

Of the 12, 841 predicted proteins in the *M. oryzae* genome (Dean *et al.*, 2005), approximately 12 % (1,546) are thought to be secreted based on the presence of an N-terminal secretion peptide and combination of bioinformatic algorithms based on SignalP3.0 and WOLFPSORT

analysis (Soanes *et al.*, 2008). Although the deployment of apoplastic effectors has been well described in the oomycetes and intercellular fungal plant pathogens, there are few examples of rice blast apoplastic effectors from this large predicted pool of secreted proteins. To date, only one secreted *M. oryzae* apoplastic effector, Bas4, has been localised, and was shown to accumulate between the invaginated plant plasma membrane (EIHM) and the fungal cell wall (Kankanala *et al.*, 2007; Mosquera *et al.*, 2009; Khang *et al.*, 2010; Valent and Khang, 2010). *BAS4* is highly expressed during intracellular growth, and was initially identified as being more than 50-fold over-expressed compared with its expression *in vitro* (Mosquera *et al.*, 2009). In addition to accumulation around hyphal tips, Bas4:GFP was also shown to accumulate with delivered effector proteins at the Biotrophic Interfacial Complex (BIC) (Mosquera *et al.*, 2009; Khang *et al.*, 2010). We were able to confirm the expression of *SLP1:GFP* which was shown to be secreted by intracellular hyphal tips and accumulated at the plant-fungal interface. The pattern of localisation of Slp1:GFP was similar to that of Bas4, and we were able to show partial co-localisation between fluorescently-labelled Bas4:mRFP and Slp1:GFP (Mosquera *et al.*, 2009). In contrast to fluorescently-labelled Bas4, however, Slp1:GFP was not observed accumulating at the sub-apical BIC which accumulates fluorescently-labelled avirulence effectors during biotrophic growth (Mosquera *et al.*, 2009; Khang *et al.*, 2010; Valent and Khang, 2010). Interestingly, *SLP1:GFP* was not expressed *in vitro*, nor could *SLP1* cDNA transcripts be cloned using RT-PCR. This provides evidence that *SLP1* is only expressed during the intracellular biotrophic growth phases of the *M. oryzae* life cycle, a characteristic which is ubiquitous among both *M. oryzae* and other fungal effectors (van Esse *et al.*, 2007; Mosquera *et al.*, 2009). Although Slp1:GFP appeared to be apoplastic in its pattern of localisation, at this stage we cannot fully exclude the possibility that Slp1:GFP is able to bind chitin within the fungal cell wall and become integrated into the fungal cell wall matrix.

In this chapter, the contribution of the N-terminal signal peptide of Slp1 was investigated and was shown to be required for secretion of Slp1, as fungal hyphae expressing *SLP1*²⁷⁻¹⁶²:*GFP* failed to accumulate a fluorescent GFP signal at the plant-fungal interface (Figure 4.9). Interestingly, the accumulation of mis-localised Slp1²⁷⁻¹⁶²:*GFP* is consistent with previous

observations using Yeast-Two-Hybrid analysis and chitin precipitation assays that Slp1 has the capacity to form multimers (Chapter 3). Further analysis of the N-terminal peptide signal revealed that only the *SLP1* promoter fragment and the signal peptide are required for secretion at the intracellular hyphal tips, and mature Slp1 fails to contribute to the localisation of Slp1. This has signal peptide and promoter region have previously been shown for the *M. oryzae* effectors Bas1, Bas2, Bas3 and Bas4 to show preferential BIC localisation (Mosquera *et al.*, 2009).

Although we were able to demonstrate that the Slp1 signal peptide is required for secretion, we were unable to re-direct Slp1 via an alternative secretion pathway to the BIC. This raises a number of questions about the secretion mechanisms of both Slp1 and BIC-localised effectors. We were able to confirm that the mature Slp1 protein does not contribute to its secretion or sub-cellular location, which was previously demonstrated for a number of other *M. oryzae* BIC-localised effectors (Mosquera *et al.*, 2009). A major question that still needs to be answered is whether a nucleotide sequence upstream of the start codon contributes to the secretion mechanism. Due to time constraints, this could not be pursued here. One experiment that is likely to aid in this discussion is whether Slp1 can be re-directed to the BIC when placed under the control of a BIC-localised promoter fragment or using a BIC-localised signal peptide instead of the native Slp1 signal peptide.

In the previous chapter, Slp1 was shown to bind both soluble and insoluble forms of chitin. In contrast to the apoplastic *C. fulvum* effector Avr4 (Van Den Burg *et al.*, 2006), Slp1 was unable to protect fungal hyphae from the hydrolysing effects of plant-derived chitinase enzymes. Instead, Slp1 was able to suppress the effects of chitin-induced PAMP-triggered immune responses in both tomato cell suspensions and rice cells. The secreted apoplastic *C. fulvum* effector Ecp6 and the *Mycosphaerella graminicola* Mg3LysM effector were previously shown to have similar functions to Slp1, although an understanding of their *in planta* sub-cellular localisation remains to be determined, and how they accumulate at the plant-fungal interface is unknown (de Jonge *et al.*, 2010; Marshall *et al.*, 2011). The accumulation of Slp1 at the plant-fungal interface is consistent with a role for Slp1 in the sequestration of chitin oligosaccharides

at the plant-fungal interface which can otherwise be perceived by plant PRRs and trigger resistance responses (Kaku *et al.*, 2006; Miya *et al.*, 2007; Kishimoto *et al.*, 2010).

Although a number of *M. oryzae* effector proteins have been shown to localise to the BIC (Mosquera *et al.*, 2009; Khang *et al.*, 2010), the role of these molecules in perturbing host cellular machinery has not yet been examined. In the next chapter I raise these issues using a suite of transgenic rice lines in which GFP is localised to the rice cellular machinery. By doing so, I explore and demonstrate how the host plasma membrane and endoplasmic reticulum are altered during rice blast infection.

Chapter 5. Investigating biotrophic growth of *M. oryzae* and dissecting the structure of the Biotrophic Interfacial Complex (BIC)

Abstract

The rice blast fungus *M. oryzae* is a hemibiotrophic fungus, meaning the fungus undergoes an initial period of biotrophic growth in which the pathogen grows within living host tissue, which is later followed by a period of necrotrophic growth in which host tissue is destroyed during which the fungus sporulates which is required for completion of the life cycle. Relatively little is understood about the symptomless biotrophic growth phase and, in particular, almost nothing is known about how infection disrupts host cell structure and causes organelle re-arrangement. In this study, several marker genes were transformed to generate stable transgenic rice plants in which GFP was targeted to both the plant plasma membrane and the endoplasmic reticulum. By doing this it became possible to understand and visualise how these cellular components change as *M. oryzae* grows and invades host cells. Using a combination of plant and fungal cellular markers, the nature and structure of the Biotrophic Interfacial Complex (BIC), an infection structure that forms during biotrophy and which accumulates fluorescently labelled pathogen effector molecules was investigated. Results obtained from this study suggest that the BIC structure is composed of plant-derived cellular organelles and resides outside of the fungal cell wall.

5.1 Introduction

To initiate disease and enter a host plant cell, *M. oryzae* generates an elaborate infection structure called the appressorium. The dome-shaped appressorium develops high internal turgor, enabling a narrow penetration peg, that develops at the appressorial base, to rupture the tough host cuticle commencing disease. The genetic determinants of appressorium formation have been well-characterised, but there is currently a paucity of data available on the subsequent infection cycle and how the fungus grows within host cells (for reviews see Talbot, 2003; Caracuel-Rios and Talbot, 2008; Wilson and Talbot, 2009; Mentlak *et al.*, 2012).

After rupture of the host cuticle has occurred, a period of intracellular biotrophic growth commences, during which the fungus grows asymptotically within host tissue. After appressorium formation, the short, narrow penetration peg differentiates into a primary filamentous hypha. At this stage, it is thought that the plant plasma membrane is not breached, but instead becomes invaginated and surrounds the filamentous primary hypha to establish the Extra-Invasive Hyphal Membrane (EIHM) (Kankanala *et al.*, 2007). Inability of the membrane tracker dye FM4-64 to reach and label the EIHM at this time provides strong evidence that the EIHM is a sealed compartment and is spatially separated from the apoplastic space (Kankanala *et al.*, 2007), which is defined as the space between the plant cell membrane and plant cell wall (Hoefle and Hückelhoven, 2008). Primary hyphae grow initially within the host, beneath the site of appressorium formation, before differentiating into secondary pseudohyphae, which are thicker and more bulbous in morphology (Heath *et al.*, 1990; Khang *et al.*, 2010). During this time, it is thought that the EIHM continues to encase intracellular hyphae, growing to accommodate the fungus as hyphal growth continues (Kankanala *et al.*, 2007). However, it is still not known whether the EIHM extends around the entire intracellular fungal hyphae (Kankanala *et al.*, 2007). Plasmolysis assays in which infected cells are treated with a hyperosmotic sucrose solution have demonstrated that the EIHM remains intact during this infection stage, confirming that the fungus is growing biotrophically and host cells remain viable (Kankanala *et al.*, 2007). Secondary pseudohyphae continue to grow which fill the initial

epidermal host cell before colonising adjacent host cells. Live-cell imaging of secondary pseudohyphae at this time suggest that these hyphae undergo extreme constriction, leading to the suggestion that hyphae exploit plasmodesmata to move into neighbouring host cells. Consistent with this hypothesis is the observation that transiently expressed GFP-labelled TMV:MP co-localises with fungal membrane stained with FM4-64 (Kankanala *et al.*, 2007). Only after 3-4 days post-inoculation do disease symptoms become apparent in the form of large necrotic lesions. At this time, the fungus has switched to a necrotrophic lifestyle, secreting cell wall-degrading enzymes to utilise host tissue as an energy source to fuel sporulation from expanding lesions (Talbot *et al.*, 2003; Talbot and Wilson, 2009).

During biotrophic growth, *M. oryzae* is thought to secrete a number of effector proteins which are thought to act to downregulate and perturb host cell defence responses (Sweigard *et al.*, 1995; Soanes *et al.*, 2008; Khang *et al.*, 2010). Although relatively little is understood about the mechanism by which rice blast effectors are trafficked into plant cells, significant advances have occurred in recent years (Mosquera *et al.*, 2007; Khang *et al.*, 2010). Studies which use translational fusions of effector genes to the Green Fluorescent Protein (GFP) marker, and its allelic variants such as Red Fluorescent Protein (RFP), have greatly accelerated our understanding of the pattern of localisation of rice blast effectors and how these are delivered into host cytoplasm (Valent and Khang, 2010). Studies using such genetically engineered marker strains have revealed a characteristic localisation pattern of avirulence effectors in which fluorescently-labelled effectors accumulate in the Biotrophic Interfacial Complex (BIC), a bulbous infection structure that develops at the plant-fungal interface (Mosquera *et al.*, 2009; Khang *et al.*, 2010; Valent and Khang, 2010). Although relatively little is known about the nature of the BIC, a number of avirulence effectors including Avr-Pita, Pwl2, Bas (Biotrophy Associated Secreted) proteins (Bas1-4), Avr-Pia and Avr-Pii have all been shown to accumulate at the BIC (Mosquera *et al.*, 2009; Yoshida *et al.*, 2009; Khang *et al.*, 2010). As stated, biotrophic growth commences when a primary filamentous hypha forms at the base of the appressorium. The BIC forms at the apical tip of this filamentous primary hypha, and starts to accumulate fluorescently-labelled effectors at approximately 18 – 22 hours post-inoculation

(Figure 5.1). At this time, secretion of effectors into the BIC appears to occur in a polarized manner, a feature characteristic of hyphal tip secretion from filamentous fungi, and thereby implicating a role for the Spitzenkörper, polarisome and exocyst components in the secretion of effectors (Harris *et al.*, 2005; Virag and Harris, 2006; Steinberg, 2007; Brand and Gow, 2009). However, as the primary hypha differentiates into secondary pseudohyphae at approximately 24 – 30 hours post-inoculation, fluorescently-labelled effectors continue to accumulate at the BIC, which now occupies a subapical position attached to the side of the intracellular hypha (see Figure 5.1). Although a number of rice blast effectors have been shown to accumulate at the BIC, relatively little is known about the nature of the host and pathogen membrane structure around BICs, how the structure develops, or its precise biological relevance as a portal for the secretion of effector molecules.

In this chapter, I set out to investigate the biotrophic growth of the rice blast fungus. To do this, I generated genetically-stable transgenic rice lines that localise GFP to both the plant plasma membrane and the endoplasmic reticulum, in collaboration with Dr. Hiromasa Saitoh and Dr. Ryohei Terauchi at the Iwate Biotechnology Research Centre, Iwate, Japan. This enabled both the host plasma membrane and the endoplasmic reticulum to be visualised by epifluorescence microscopy, allowing the nature of the plant-fungal interface to better defined. In particular, I was interested to test the hypothesis that the EIHM is continuous around an entire intracellular fungal hypha. The use of fungal cellular markers, in combination with these transgenic plant markers, enabled a deeper understanding of the membrane structure around the BIC, which I show here co-localises with both the plant plasma membrane and ER and is located outside the boundaries of the fungal invasive hypha.

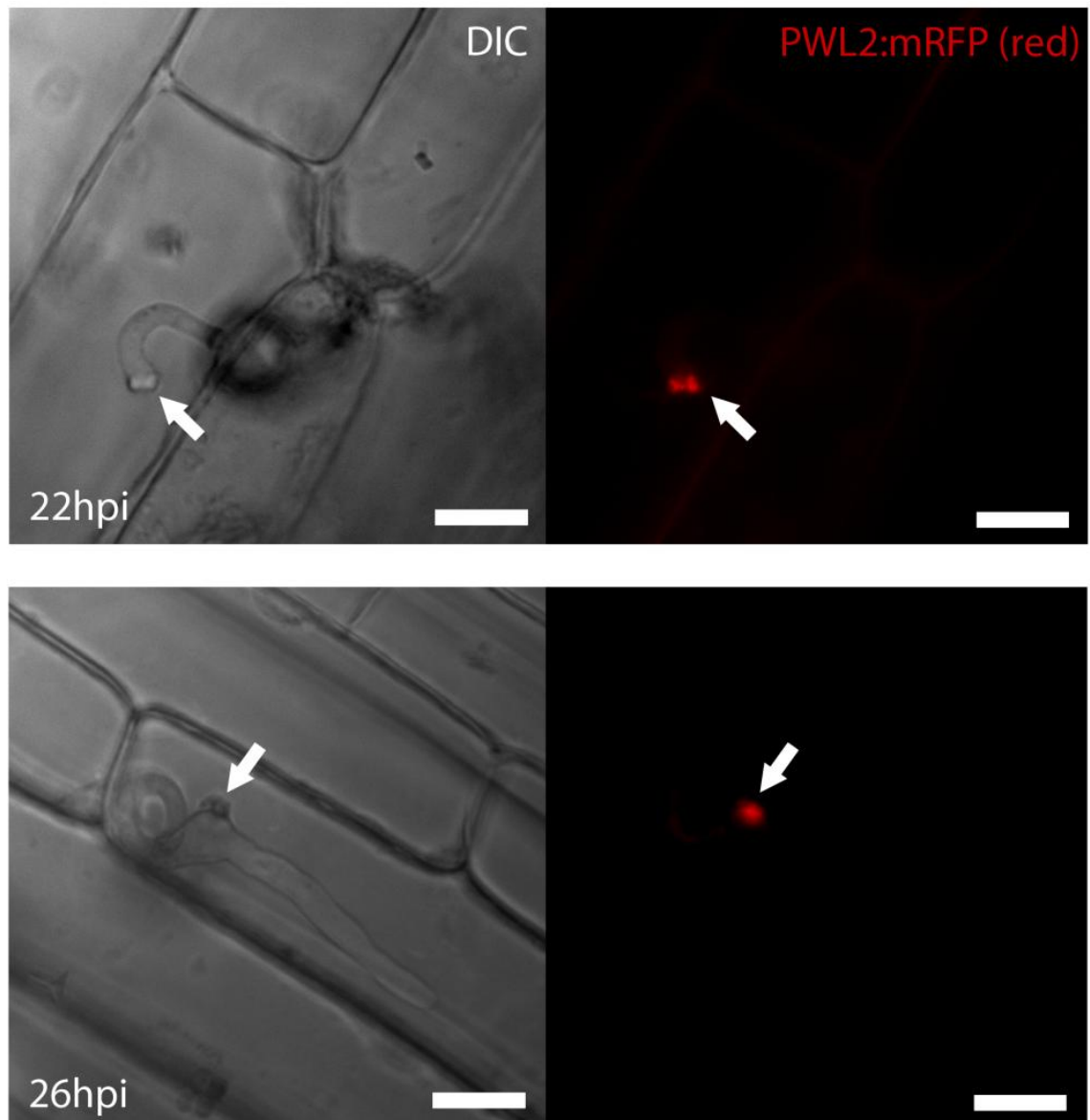


Figure 5.1 *Magnaporthe oryzae* avirulence effectors localise to the Biotrophic Interfacial Complex (BIC). At 22 hours post-inoculation (hpi), *PWL2:mRFP* (Red) is highly expressed and accumulates at the apical tips of filamentous hyphae (top). At 26 hpi, fungal hyphae have continued to ramify within the initial host cell and have started to form bulbous secondary hyphae. As this occurs, *PWL2:mRFP* expression is still visible in the bulbous BIC structure, which is now at a subapical position located on the side of invasive pseudohyphal cells (bottom). Scale bars represent 10 μ m. White arrows highlight the BIC. Image taken, with permission, from Mentlak *et al.*, (2012).

5.2 Methods

5.2.1 Construction of the *toxA*:RFP vector

Primers were designed to amplify a 1.8 kb *HYG:toxA* fragment using the *toxA:GFP* vector previously generated (Badaruddin, 2012). The *toxA* promoter encoding fragment has previously been shown to cause constitutive expression of the downstream DNA fragment (Badaruddin, 2012). A forward (5') primer (5' HYG) was designed with the reverse (3') primer (3' *toxA*) engineered to include an *Eco* RI restriction site. Primers were also designed to amplify a 2.1 kb *RFP:trpC* amplicon from the *H1:RFP* vector previously generated by Saunders *et al.*, 2010. To amplify an *RFP:trpC* DNA fragment, a forward (5') primer (5' RFP) was designed to include an *Eco* RI restriction site, whilst the reverse (3') primer was engineered to include a *Spe* I restriction site (3' *trpC*). These restriction sites are highlighted below:

5' HYG	5' ACTGGTTC CCCGGTCGGCATCTACT 3'
3' <i>toxA</i>	5' AAGAATTC CCTATATTCATTCAATGT 3'
5' RFP	5' AAGAATTC ATGGTGAGCAAGGGCG 3'
3' <i>trpC</i>	5' AA ACTAGTAAGCTTGCATGCCTGC 3'

All PCR amplifications were performed using an Applied Biosystems GeneAmp® PCR System 9700 using *Taq* polymerase (Promega). The PCR was performed using an initial denaturation step of 94°C for 5 minutes followed by the PCR cycling parameters; 94°C for 30 seconds, 58°C for 30 seconds, 65°C for 2 minutes (35 cycles), 65°C for 10 minutes. PCR products were analysed by gel electrophoresis as discussed in Chapter 2. The *HYG:toxA* fragment was amplified and cloned into the TA cloning vector pGEM-T. Positive clones were identified by restriction digest with *Eco* RI and *Sac* I which liberated the *HYG:toxA* fragment out of pGEM-T. The resulting vector containing the *HYG:toxA* fragment in pGEM-T is referred to hereafter as pHYG-T. Similarly, the 2.1 kb *RFP:trpC* fragment was cloned into pGEM-T and positive clones were identified by restriction digest with the enzymes *Eco* RI and *Spe* I. The 2.1 kb *RFP:trpC* fragment was subsequently restriction digested with *Eco* RI and *Spe* I, isolated by gel electrophoresis and ligated directionally into the pHYG-T vector as an *Eco* RI / *Spe* I fragment. Positive clones were identified by restriction digest with *Eco* RI and *Spe* I which yielded a 4.8

kb fragment (linearised pHYG-T) and a 2.1 kb fragment (*RFP:trpC*). The resulting vector is referred to as *toxA:RFP* and this plasmid was used to transform the *M. oryzae* Guy11 strain and stored at -20°C in the laboratory of N.J. Talbot (University of Exeter).

5.2.2 Construction of the C-terminal *PIP2a:GFP* gene fusion in the plant binary expression vector pCAMBIA 1302

Primers were designed to amplify the 0.8 kb rice *PIP2a* coding sequence from rice leaf cDNA and the *sGFP* codon-optimised allele, which was amplified from the *toxA:GFP* vector (Badaruddin, 2012). An initial first round PCR amplification was performed to amplify *PIP2a* using a forward (5') primer (5'PIP2a), which was designed to include a *Spe* I restriction site. The reverse (3') primer (3'PIP2a) was designed to include a complementary overhanging sequence with the *sGFP* allele, permitting the *PIP2a* gene to be fused to the *GFP* gene during a second round PCR amplification. Primers were also used to amplify a 0.75 kb *GFP* fragment from the *toxA:GFP* vector (Badaruddin, 2012). A forward (5') primer (5'GFP) was designed to be used with a reverse (3') primer (3'GFP-PmlI) which had been designed to include a 3' *Pml* I restriction site. The primers used to amplify the rice *PIP2a* gene and *GFP* can be found below (restriction sites underlined and GFP overhang on 3' *PIP2a* gene in bold).

5'PIP2a	5'	AA <u>ACTAGT</u> ATGGCGAAAGACATTGAGG	3'
3'PIP2a-GFP	5'	GCCCTTGCTCACCATGGCGTTGCTCCGGTAGGACC	3'
5'GFP	5'	ATGGTGAGCAAGGGAGAGG	3'
3'GFP-Pml I	5'	AACACGTGTTACTTGACAGCTCGTCCAT	3'

The 0.8 kb *PIP2a* gene was amplified from rice leaf cDNA using an Applied Biosystems GeneAmp® PCR system using *Taq* polymerase (Promega). The first round PCR was performed using an initial denaturation step of 94°C for 5 minutes followed by the PCR cycling parameters; 94°C for 30 seconds, 58°C for 30 seconds, 70°C for 1 minute (35 cycles), 65°C for 10 minutes. PCR products were analysed by gel electrophoresis as discussed in Chapter 2. An initial first round PCR was performed in which a 0.8 kb *PIP2a* gene was amplified from rice leaf cDNA. A 0.75 kb *GFP* allele was also independently PCR amplified. A second round PCR was then performed using the forward (5') primer 5'PIP2a and the reverse primer 3'GFP-PmlI

using both the 0.8 kb *PIP2a* gene and 0.75 kb *GFP* gene as template DNA. PCR for the second round amplification was performed using an initial denaturation step of 94°C for 5 minutes followed by the PCR cycling parameters; 94°C for 30 seconds, 65°C for 30 seconds, 70°C for 2 minutes (35 cycles), 65°C for 10 minutes. The resulting 1.5 kb *PIP2a:GFP* fusion was separated by gel electrophoresis, as described in Chapter 2 and ligated into the cloning vector pGEM-T (Promega). Positive clones were identified by restriction digest with the enzymes *Spe* I and *Pml* I, which liberated the 1.5 kb *PIP2a:GFP* fragment out of pGEM-T. The plant expression vector pCAMBIA 1302 was restriction digested with *Spe* I and *Pml* I. The 1.5 kb *PIP2a:GFP* fragment was restriction digested with the restriction enzymes *Spe* I and *Pml* I and ligated into pCAMBIA 1302. Positive clones were identified by restriction digest with the restriction enzymes *Spe* I and *Pml* I which liberated a 1.5 kb fragment from pCAMBIA 1302. The resulting *PIP2a:GFP* pCAMBIA 1302 vector was confirmed by DNA sequencing and sent to Dr. Ryohei Terauchi and Dr. Hiromasa Saitoh at the Iwate Biotechnology Research Centre, Iwate, Japan.

5.2.3 *Agrobacterium* - mediated transformation of rice

All plant vectors used in this study were transformed into the rice background *Oryza sativa* cv. *sasanishiki* by Dr. Hiromasa Saitoh and Dr. Ryohei Terauchi at the Iwate Biotechnology Research Centre, Iwate, Japan. Plasmids electroporated into *Agrobacterium tumefaciens* EHA105 were transformed into rice callus using *Agrobacterium*-mediated transformation, according to the method described by Heie *et al.*, (1994) and Heie and Komari (2008). Rice seeds were de-husked and sterilized by placing in 0.05% hypochlorite solution, 70 % ethanol for 5 minutes with gentle shaking and rinsed thoroughly three times in sterilised deionised water. Rice callus was induced by placing sterile scutella onto 2N6 media (N6 Major Salts, N6 Minor salts, N6 vitamins, 1 g L⁻¹ casamino acids, 30 g L⁻¹ sucrose, 2 mg L⁻¹ 2,4-D, 2 g L⁻¹ Gelrite, pH 8.0) and placed in the dark for 5 days. Actively growing calli (1-2 mm) appeared after approximately 5 days and were used in transformation experiments. Prior to transformation, actively growing pieces of rice calli were resuspended in 2N6L media (2N6 media without Gelrite) and grown in darkness at 25°C on a rotary shaker (125 rpm) for at least 24 hours.

Agrobacterium tumefaciens EHA105 was grown for 5 days on AB medium (Chilton *et al.*, 1974) supplemented with 50 mg L⁻¹ hygromycin and 50 mg L⁻¹ kanamycin. Bacteria were collected and resuspended in AAM media (AA salts and amino acids (Toriyama and Hinata, 1985), MS vitamins (Murashige and Skoog, 1962), 500 mg ml⁻¹ casamino acids, 68.55 g L⁻¹ sucrose, 36 g L⁻¹ glucose, 100 µM acetosyringone, pH 5.2) until the bacteria had reached a density of 3-5 x 10⁹ cells ml⁻¹. For transformation, rice tissue as described above was placed in the bacterial suspension and transferred without rinsing to 2N6-AS media (2N6 media described above plus 10g L⁻¹ glucose and 100 µM acetosyringone, pH 5.2) and incubated in the darkness at 25°C for 3 days. After co-cultivation, calli were rinsed with 250 mg L⁻¹ cefotaxime in sterilized deionised water and placed on 2N6-CH media (2N6 media plus 250 mg L⁻¹ cefotaxime and 50 mg L⁻¹ hygromycin) and cultured for 3 weeks. Actively growing calli were transferred to 2N6-7-CH medium (N6 major salts, N6 minor salts, N6 vitamins, 2 g L⁻¹ casamino acids, 20 g L⁻¹ sucrose, 30 g L⁻¹ sorbitol, 1 mg L⁻¹ 2,4-D, 0.5 mg L⁻¹ 1-1 6-benzyladenine, 100 mg L⁻¹ hygromycin, 250 mg L⁻¹ cefotaxime, 2 g L⁻¹ Gelrite, pH 5.8) for ten days. Proliferated colonies were placed on regeneration medium N6S3-CH (Half-strength N6 major salts, N6 minor salts, N6 vitamins, AA amino acids, 1g L⁻¹ casamino acids, 20 g L⁻¹ sucrose, 0.2 mg L⁻¹ 1-1 naphthaleneacetic acid, 1 mg L⁻¹ kinetin, 250 mg L⁻¹ cefotaxime, 50 mg L⁻¹ hygromycin, 3 g L⁻¹ Gelrite pH 5.8) at 25°C and incubated under continuous light. Regenerated plants (T₀) were acclimatized and the transferred to soil before being grown to maturity. Expression and presence of GFP was confirmed using Western blot analysis and epifluorescence microscopy. Several vector markers were transformed into rice, although a number were found to be unstable and fluorescence could not be confirmed. A list of the vectors transformed into rice can be found in Table 5.1.

5.2.4 Total protein extraction and Western blotting of rice transformants

Total protein was extracted from 50 mg of leaf tissue of each plant by homogenization in extraction buffer (250 mM Tris-HCl [pH 7.5], 2.5 mM EDTA, 0.1% ascorbic acid, 1 mM PMSF). The samples were centrifuged at 6000 x g for 10 minutes. The supernatant was

collected and 15 µl of sample was separated on an e-Pagel® 10 – 20% (ATTO) and the proteins transferred to an Immobilon™ Transfer Membrane (Millipore). Blots were blocked in 5 % non-fat milk powder suspended in TTBS (10 mM Tris-HCl [pH 7.5], 100 mM NaCl, 0.1 % (v/v) Tween 20) for 1 hour at room temperature with gentle rocking. For immuno-detection, blots were probed with Living Colors® A.v monoclonal antibody (JL-8) (Clontech) in a fresh 1:10,000 dilution in TTBS for 2 hours. The membrane was washed three times by placing in TTBS for 10 minutes with gentle rocking. An Anti-mouse IgG HRP conjugate (Promega) freshly prepared as a 1:10,000 dilution in TTBS was used as a secondary antibody and incubated with the membrane for 1 hour at room temperature with gentle rocking. After washing the membrane with TTBS three times, reactions were captured using an ECL Western blotting detection kit (GE Healthcare) and a Luminescent Image Analyzer LAS-4000 (Fujifilm).

Table 5.1 Plant expression vectors used for transformation in this study

Name	Pattern of Localisation	Reference	Notes
LTi6B:GFP	Plasma membrane	Kurup <i>et al.</i> , 2005	-
PIP2a:GFP	Plasma membrane	This study	-
GFP:HDEL	Endoplasmic reticulum	Runions <i>et al.</i> , 2006	-
AtFIM:GFP	Fimbrin	Voigt <i>et al.</i> , 2004	Fluorescence not observed / Unstable
fABD2:GFP	Fimbrin	Ketelaar <i>et al.</i> , 2004	Fluorescence not observed / Unstable
sec:GFP	Apoplastic space	Runions <i>et al.</i> , 2006	Fluorescence not observed / Unstable
LifeAct:GFP	Fimbrin	Deeks <i>et al.</i> , 2010	Currently being transformed

5.2.4 Construction of the *PMA1:GFP* fusion vector

To generate the plasma membrane targeting *PMA1:GFP* vector, primers were designed to amplify a 5.2 kb *PMA1* (Accession number MGG_04994) genomic fragment from *M. oryzae* DNA encoding a putative membrane-bound H⁺ATPase protein pump and a 2 kb upstream promoter sequence. A forward (5') primer (5'ATPase) was designed approximately 2 kb

upstream of the ATPase start codon to include the promoter sequence of the gene. The 5'ATPase forward primer was designed to include a 30 bp overhang which is complementary in sequence to the pYSGFP-1 vector (Saunders *et al.*, 2010). The reverse (3') primer (3'ATPase) was designed to include a 30 bp overhang which was complementary in sequence to GFP. The reverse (3'ATPase) primer was designed to exclude the translational stop codon of the *PMA1* gene. The sequences of the primers used to construct the *PMA1:GFP* vector are listed below:

5'ATPase:

5' GATTATTGCACGGGAATTGCATGCTCTCACCAAGTGCAATCACGTATTACA 3'

3'ATPase:

5' GGTGAACAGCTCCTCGCCCTTGCTCACCATCTCCTCCTCGACAATCTG 3'

The 5.2 kb *PMA1* genomic fragment was amplified using an Applied Biosystems GeneAmp® PCR System 97000 using *Taq* polymerase (Promega). The PCR was performed using an initial denaturation step of 94°C for 5 minutes followed by the PCR cycling parameters; 94°C for 30 seconds, 58°C for 30 seconds, 65°C for 5 minutes (35 cycles), 65°C for 10 minutes. PCR products were analysed by gel electrophoresis as discussed in Chapter 2. The 5.2 kb *PMA1* genomic fragment was transformed into *S. cerevisiae* with *Hind* III-digested pYSGFP-1 (Saunders *et al.*, 2010). The *PMA1* genomic fragment became integrated into pYSGFP-1 fragment by gap-replacement cloning (Oldenburg *et al.*, 1997) as a result of homologous recombination between the complementary sequence of the pYSGFP vector and the sequence overhang of the *PMA1* genomic fragment. Positive yeast clones were confirmed by PCR and the construct was independently verified by DNA sequencing. The resulting *PMA1:GFP* plasmid was subsequently introduced into *M. oryzae* by transformation of Guy11 expressing *PWL2:mRFP*.

5.3 Results

5.3.1.1 The *toxA*:*RFP* vector as a suitable marker for visualising fungal cytoplasm

To examine biotrophic growth of the rice blast fungus, a suitable fungal reporter strain was required to visualise fungal cytoplasm by epifluorescence microscopy. To do this, the *tdtom* allelic variant of *RFP* was amplified and cloned in frame at the 3' end of the constitutive *toxA* promoter to create the vector *toxA*:*RFP*. This construct was transformed into *M. oryzae* and used to define the limits of fungal cytoplasm during intracellular growth.

5.3.1.2 Construction and introduction of the *toxA*:*RFP* vector

A schematic representation of the construction of the *toxA*:*RFP* vector is shown in Figure 5.2. A 1.8 kb *HYG*:*toxA* fragment was amplified and cloned into the cloning vector pGEM-T to generate the vector pHYG-T (Figures 5.2 and 5.3). The *HYG* fragment encodes the hygromycin resistance cassette encoding hygromycin phosphotransferase gene enabling selection of putative *M. oryzae* transformants using the antibiotic hygromycin B (Leung *et al.*, 1988). The *toxA* fragment encodes a constitutive promoter sequence and was selected to drive the expression of *RFP*. Positive clones of the *HYG*:*toxA* fragment in pGEM-T were identified by restriction digest with the enzymes *Eco* RI and *Sac* I, as shown in Figure 5.3A. Similarly, a 2.1 kb *RFP*:*trpC* fragment encoding the *tdtom* allelic variant of *RFP* fused to the *Aspergillus nidulans* *trpC* terminator sequence was amplified and cloned into the cloning vector pGEM-T. Positive clones were identified and selected by restriction digest with *Eco* RI and *Spe* I, as shown in Figure 5.3B. The *RFP*:*trpC* fragment was cloned directionally into the vector pHYG-T as an *Eco* RI / *Spe* I fragment to create *toxA*:*RFP*. Positive clones of the *toxA*:*RFP* construct were confirmed by restriction digest with the enzymes *Eco* RI and *Spe* I. The *toxA*:*RFP* vector was introduced into the wild type strain of *M. oryzae*, Guy11. Putative transformants were selected based on their resistance to hygromycin and were examined for expression of *RFP* visualised by epifluorescence microscopy. DNA was isolated from transformants, digested with *Eco*RI and subjected to Southern blot analysis using a 1.4 kb fragment of the hygromycin phosphotransferase resistance cassette (see Chapter 2). Three transformants were selected that

had a single integration of the tox:RFP construct and were used for further investigations (Figure 5.4).

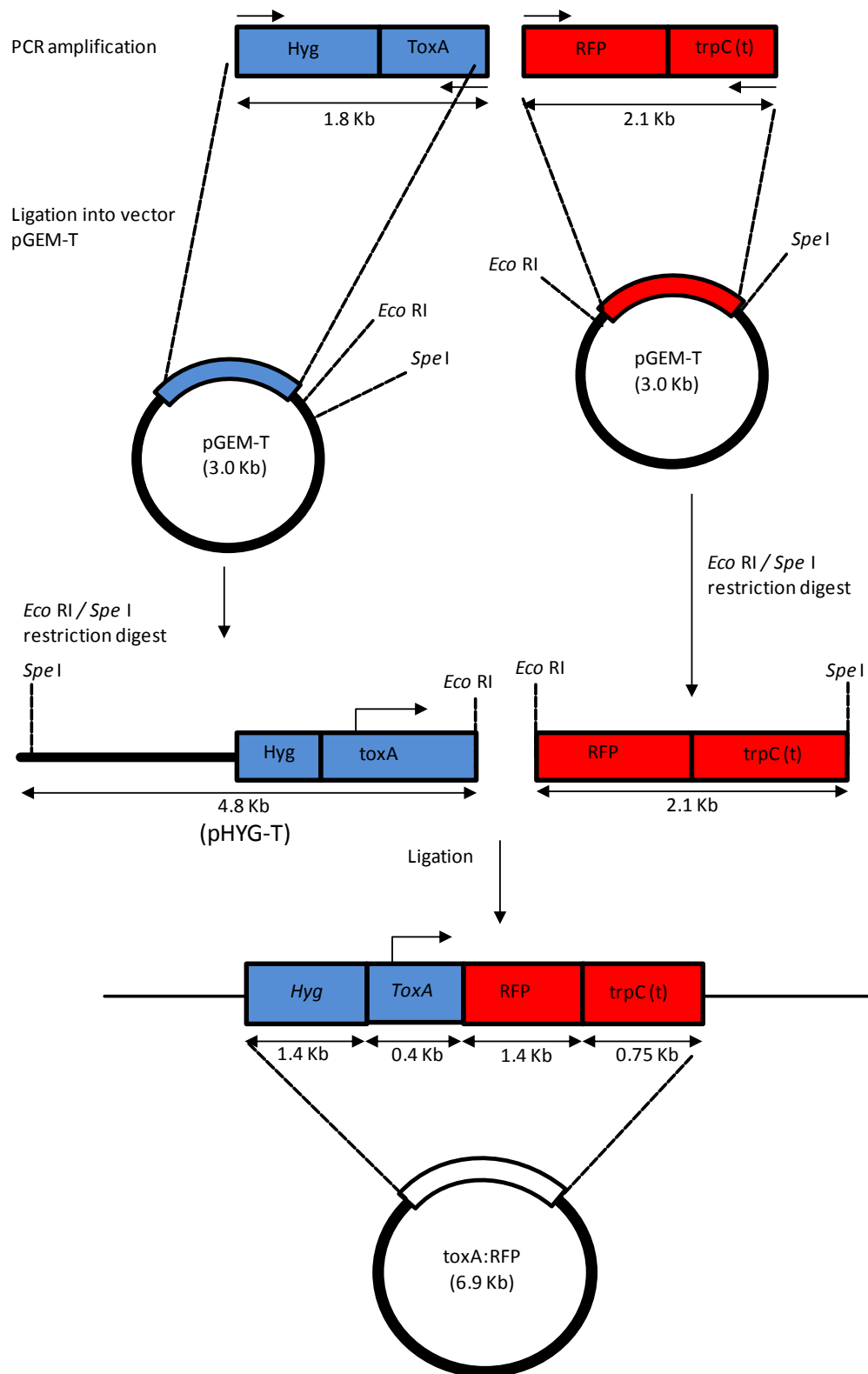


Figure 5.2 Schematic representation of the strategy used to generate the *toxA*:RFP vector

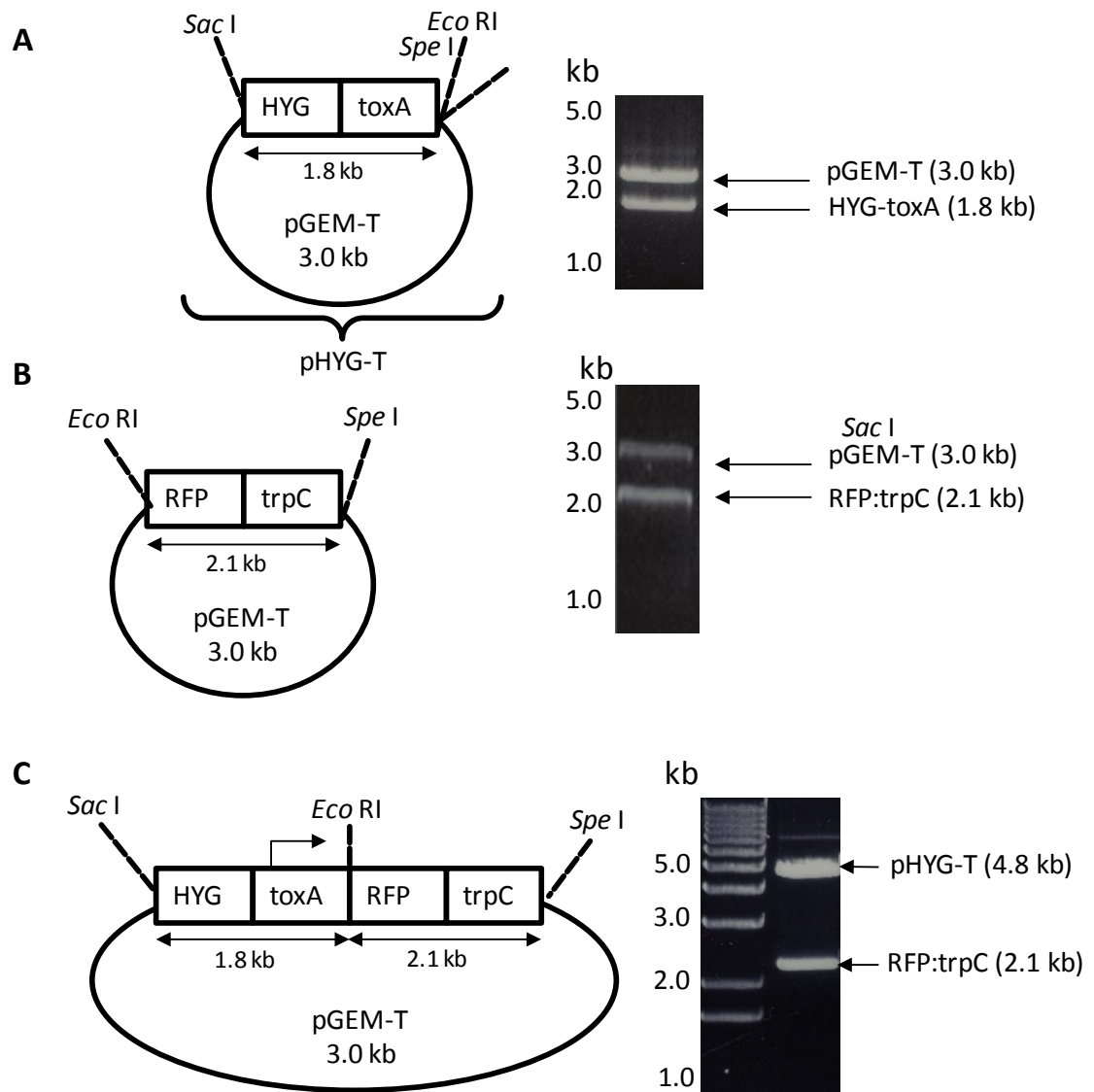


Figure 5.3 Construction and confirmation of the *toxA*:RFP vector

A. A 1.8 kb fragment containing the *HYG:toxA* cassette was ligated into the TA vector pGEM-T. Positive clones were identified by restriction digest with *Eco* RI and *Sac* I, which liberates the 1.8 kb *HYG:toxA* cassette from the 3.0 kb cloning vector. The resulting *HYG:toxA* construct in pGEM-T was named pHYG-T.

B. A 2.1 kb fragment coding for *RFP:trpC* (*tdtomato* variant *RFP*) and cloned into the vector pGEM-T. Positive clones were identified by restriction digest with *Eco* RI and *Spe* I, which liberates the 2.1 kb *RFP:trpC* fragment from the 3.0 kb vector.

C. The 2.1 kb *RFP:trpC* digested with *Eco* RI and *Spe* I was cloned directionally into pHYG-T, which had been digested with the restriction enzymes *Eco* RI and *Spe* I. Positive clones were identified by restriction digest with *Eco* RI and *Spe* I to yield a 4.8 kb fragment (pHYG-T) and the 2.1 kb *RFP:trpC* fragment.

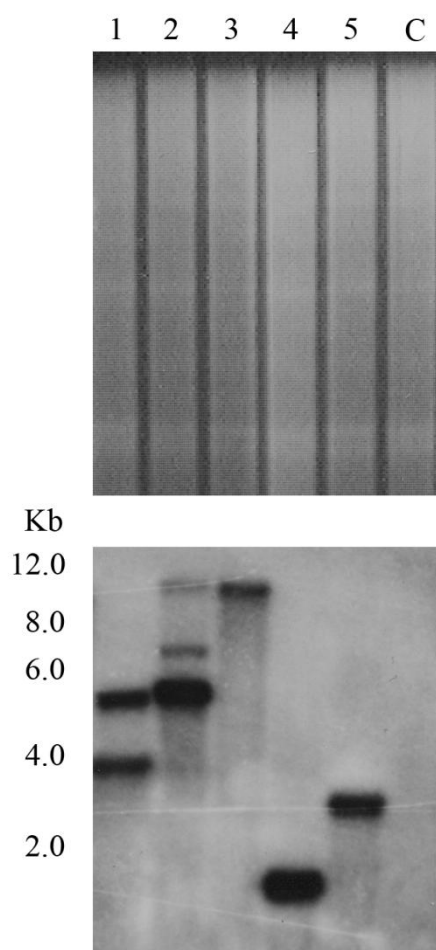


Figure 5.4 Southern blot analysis of putative *toxA*:RFP transformants. Transformants were initially screened by epifluorescence for RFP expression. Based on this, five transformants were selected and subjected to Southern Blotting analysis, in which genomic DNA was extracted, restriction digested with the restriction enzyme *Eco*RI, gel fractionated and transferred to Hybond-N. The Southern blot was probed with a 1.4 kb HYG cassette, which did not hybridise with the non-transformed Guy11 control (Lane C). Transformants 3, 4, and 5 were selected as single copy transformants and were used for further experiments.

5.3.2 Expression of LTi6B:GFP in transgenic plants localises GFP to the plant plasma membrane

To visualise the plant plasma membrane by epifluorescence microscopy, the cell membrane marker LTi6B:GFP (Kurup *et al.*, 2005) was transformed into rice (*Oryza sativa* cv. *sasanishiki*) to generate transgenic rice that constitutively localise GFP to the plasma membrane. The LTi6B gene encodes a 67 amino acid low temperature, salt responsive protein, and expression of the LTi6B:GFP vector (under the control of the 35S constitutive promoter) has previously been shown to localise GFP to the plant cell membrane in *Arabidopsis thaliana* (Kurup *et al.* 2005). To confirm the transformation and expression of LTi6B:GFP in rice cells, total protein was extracted from 2-3 week old leaves of transgenic T1 LTi6B:GFP and wild-type plants. Equal volumes of the samples were initially run out on 1-dimensional PVDF membranes and stained with coomassie blue to confirm the LTi6B:GFP and wild-type samples contained an equal concentration of protein, as shown in Figure 5.5A. Protein concentrations of samples from both LTi6B:GFP and wild-type extracts was also calculated independently using a nano-drop (data not shown). Western blot analysis was performed using an anti-GFP antibody as a probe (Roche), and plants transformed with LTi6B were confirmed to express GFP protein (25 kD), as shown in Figure 5.5B. To confirm localisation of LTi6B:GFP to the plant cell membrane, epidermal leaf tissue was plasmolysed by exposure to 0.75 M sucrose. When plant cells are placed in a hyperosmotic solution, such as 0.75 M sucrose, the plant protoplast can be seen to shrink, causing the plasma membrane to recede away from the rigid plant cell wall. In LTi6B:GFP plants, the plant plasma membrane could be seen receding from the plant cell wall following plasmolysis (Figure 5.5B). In non-plasmolysed tissue, the GFP signal was retained at the cell boundary confirming that LTi6B:GFP localises to the plant plasma membrane.

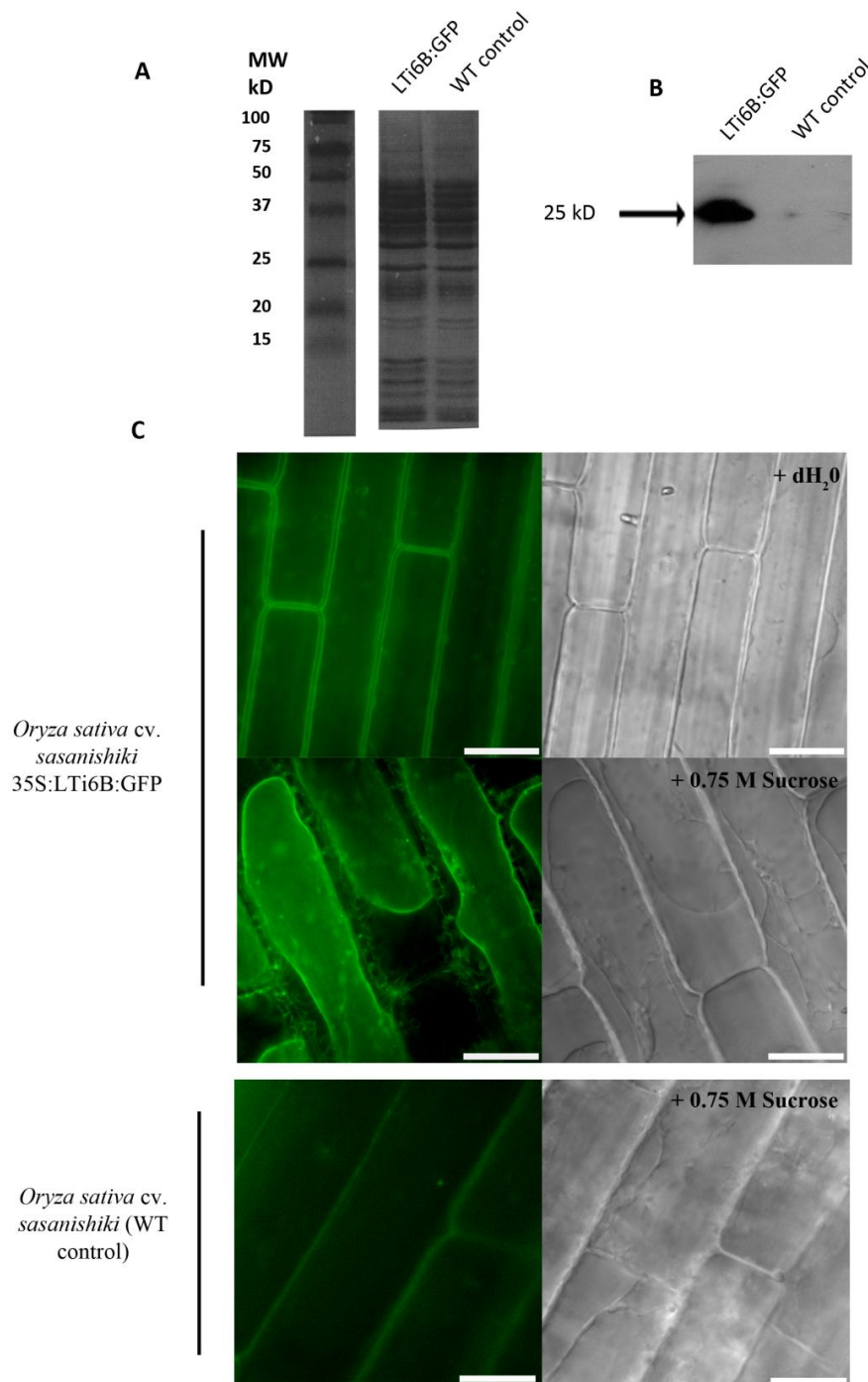


Figure 5.5 Plants expressing the LTi6B:GFP vector localise GFP to the plant plasma membrane. **A.** Loading control of protein samples extracted from LTi6B:GFP and wild-type (WT) plants. Approximately 10 μ l of each sample was loaded and protein concentrations of LTi6B:GFP and wild-type (WT) samples were found to be equal upon coomassie staining. **B.** Western blotting analysis probing with an anti-GFP antibody confirms the expression of GFP protein in transgenic plants expressing the LTi6B:GFP construct. GFP protein could not be observed in non-transgenic wild-type plant tissue. **C.** Plasmolysing plant cells expressing LTi6B:GFP in the presence of 0.75 M sucrose confirms that GFP is directed to the cell membrane. Both LTi6B-transformed and wild-type (WT) cells were viewed using an Olympus IX81 epifluorescent microscope and exposed to 500 ms at 488 nm. Scale bars represent 15 μ m.

5.3.3.1 Construction of the PIP2a:GFP plant expression vector

Having confirmed the localisation of LTi6B:GFP to the cell membrane, other gene fusions were required as plant membrane markers to understand if the EIHM (Kankanala *et al.*, 2007) is a distinct membrane from the bulk plant plasma membrane. In previous studies, the family of PIP (Plasma membrane Intrinsic Protein) proteins have been shown to localise to the plant cell membrane and are thought to act as aquaporins which contain Membrane Intrinsic Protein domains (Cutler *et al.*, 2000; Malz and Sauter, 1999). To investigate whether the EIHM is distinct from the bulk plasma membrane, the PIP2a:GFP plant expression vector was generated (Figure 5.6). In order to do this, *PIP2a*, a rice gene encoding a plasma membrane targeted protein, was cloned and fused to the C-terminus of GFP. The strategy used to construct the PIP2a:GFP plant expression vector is outlined in Figure 5.6. A first round PCR was initially performed to amplify a rice 860 bp *PIP2a* cDNA and a 750 bp *GFP* fragment, with primers engineered to remove the translational stop codon from the *PIP2a* gene. This was followed by a second round PCR to fuse *GFP* to the C-terminus of *PIP2a*. The resulting PIP2a:GFP fusion fragment was cloned into the cloning vector pGEM-T. Positive clones were identified by restriction digestion with *Spe* I / *Pml* I, which had been engineered into the 5' and 3' ends of *PIP2a* and *GFP* respectively to liberate a 1.6 kb PIP2a:GFP fragment from the vector (Figure 5.7). This 1.6 kb fragment was cloned directionally into the plant binary expression vector pCAMBIA 1302, which had been digested with restriction enzymes *Spe* I and *Pml* I. Positive clones were selected by *Spe* I and *Pml* I restriction digestion and confirmed by diagnostic digest (Figure 5.7) and independently verified by DNA sequencing. Expression of the PIP2a:GFP construct in plant cells was made possible by the presence of a dual 35S constitutive promoter which is present upstream of the multiple cloning site of pCAMBIA 1302. The final PIP2a:GFP construct in pCAMBIA 1302 was sent to Dr. Hiromasa Saitoh and Dr. Ryohei Terauchi at the Iwate Biotechnology Research Council, Iwate, Japan, for transformation into rice.

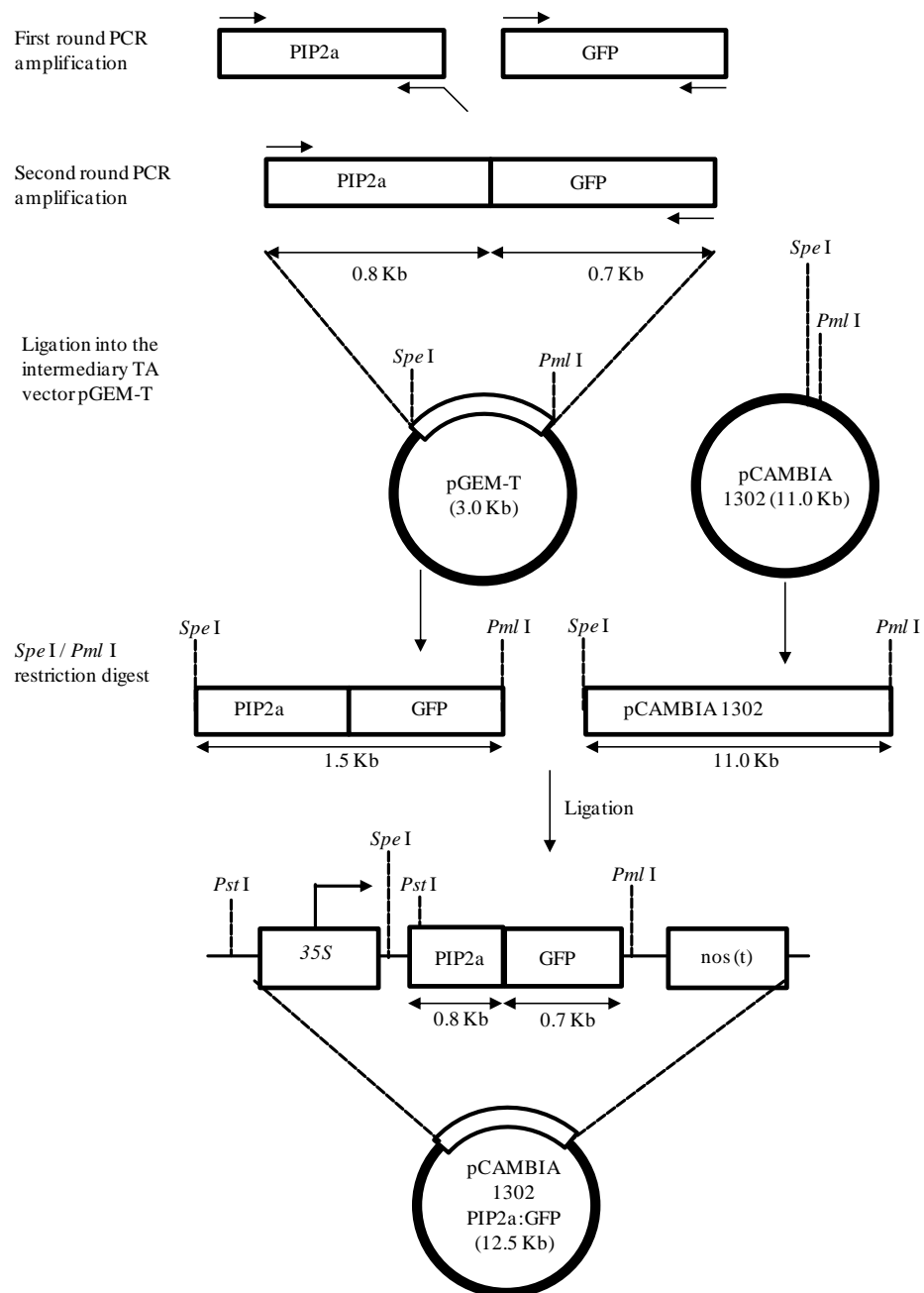


Figure 5.6 Schematic representation of the cloning strategy for generating the PIP2a:GFP fusion vector in the pCAMBIA 1302 plant expression vector.

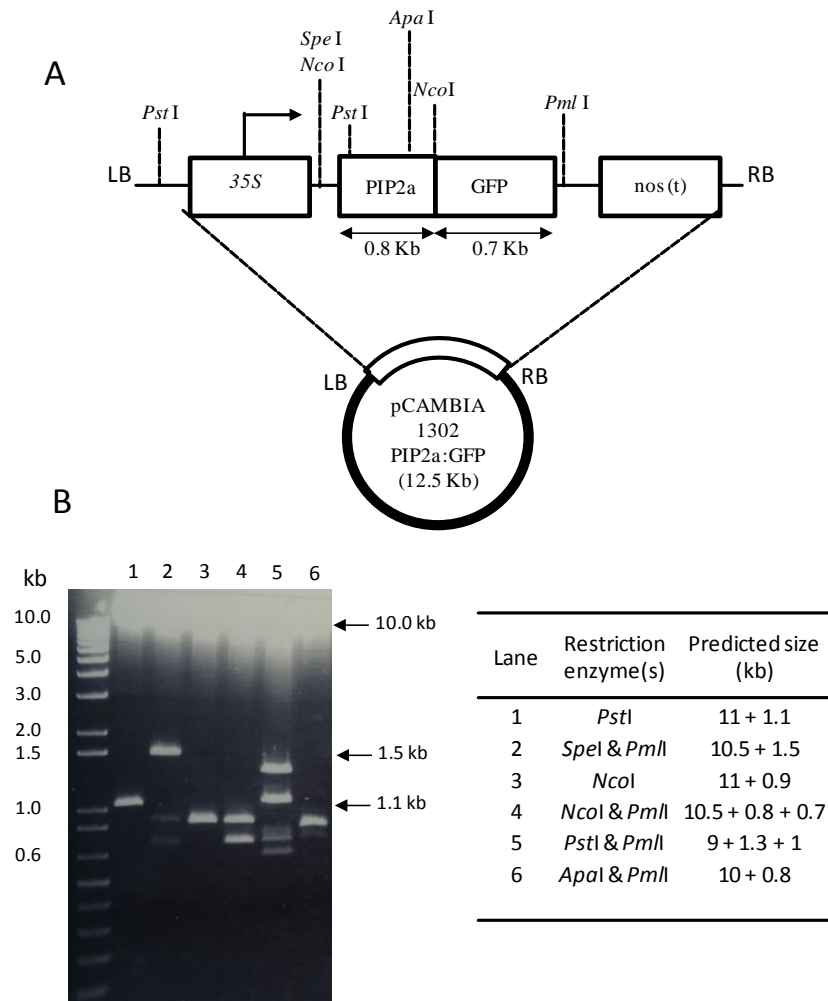


Figure 5.7 Confirmation of the PIP2a:GFP fusion construct in the plant expression vector pCambia 1302 by diagnostic digests. **A.** Schematic representation of the C-terminal PIP2a:GFP fusion construct in the plant expression vector pCambia 1302 highlighting restriction enzymes used for diagnostic digest. **B.** Insertion of the PIP2a:GFP construct in pCambia was confirmed by diagnostic restriction digest, as listed.

5.3.3.2 Stable transgenic plants expressing the PIP2a:GFP construct localise GFP to the plant plasma membrane

Following transformation of rice with the PIP2a:GFP (pCAMBIA 1302) vector, expression of PIP2a:GFP was confirmed. Confirmation of PIP2a:GFP expression was initially provided by Western blot analysis. Total protein was extracted from T1 rice leaves transformed with PIP2a:GFP and wild-type plants. Equal volumes of the samples were initially run out on 1-dimensional PVDF membranes and stained with coomassie blue to confirm that the PIP2a:GFP and wild-type samples contained equal concentrations of protein, as shown in Figure 5.8. Western blot analysis was performed in which equal concentrations of the PIP2a:GFP and WT samples were probed with an anti-GFP antibody. As shown in Figure 5.8A, expression of GFP was confirmed in leaf tissue expressing PIP2a:GFP, but was absent in wild-type tissue that had not undergone transformation. The localisation of PIP2a:GFP was subsequently confirmed by epifluorescence microscopy. Using plasmolysis assays in which epidermal leaf tissue was exposed to 0.75 M sucrose, a GFP signal could be seen receding away from the plant cell wall (Figure 5.8B). The pattern of localisation of PIP2a:GFP transgenic plants was identical to that of plants expressing LTI6B:GFP that had previously been confirmed to localise to the cell membrane (Figure 5.5). The pattern of localisation of PIP2a:GFP is consistent with the reported function of rice *PIP2a* as an integral membrane-bound aquaporin (Cutler *et al.*, 2000).

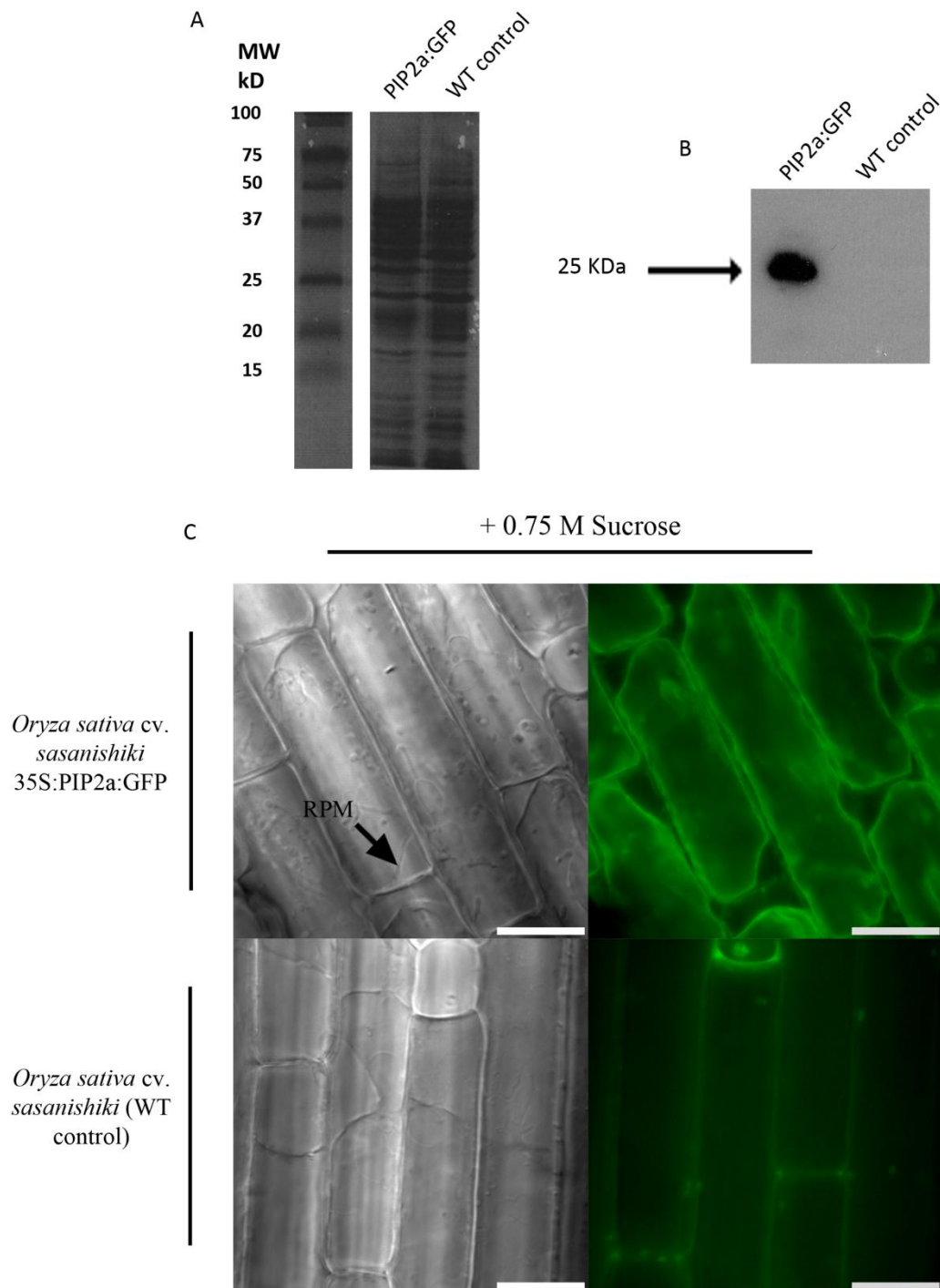


Figure 5.8 Plants expressing the PIP2a:GFP vector localise GFP to the plant plasma membrane. **A.** Loading control of protein samples extracted from PIP2a:GFP and wild-type (WT) plants. Approximately 10 μ l of each sample was loaded and protein concentrations of PIP2a:GFP and wild-type (WT) samples were found to be equal **B.** Western blotting analysis probing with an anti-GFP antibody confirms the expression of GFP protein in transgenic plants expressing the PIP2a:GFP construct. GFP protein could not be observed in non-transgenic wild-type plant tissue. **C.** Plasmolysing plant cells expressing PIP2a:GFP in the presence of 0.75 M sucrose confirms that GFP is directed to the cell membrane. Both LTi6B-transformed and wild-type (WT) cells were exposed to 500 ms at 488 nm. Scale bars represent 15 μ m.

5.3.4 Stable transgenic plants expressing GFP:HDEL localise GFP to an intricate and dynamic endoplasmic reticulum structure

To understand how the plant endoplasmic reticulum (ER) is altered in response to *M. oryzae* infection, the ER-resident marker GFP marker GFP:HDEL was obtained (Zheng *et al.*, 2005) and transformed into rice (*Oryza sativa* cv. *sasanishiki*) to generate stable transgenic plants that constitutively express the ER marker in all tissue types. The GFP:HDEL vector encodes a C-terminal codon-modified GFP (Haseloff and Siemerign, 1997) fusion to the 63 nucleotide secretion signal from the *Arabidopsis thaliana* chitinase gene. Additionally, the construct harbours a C-terminal HDEL ER-retention signal for retention of GFP within the ER lumen (Denecke *et al.*, 1992; Pagney *et al.*, 2000; Runions *et al.*, 2006). The gene fusion was expressed under the control of the constitutive 35S promoter and cloned into the plant binary vector pVKH18En6 series (Runions *et al.*, 2006). Plants were grown for 3-4 weeks and epidermal leaf tissue dissected before being examined by epifluorescence and total internal reflection (TIRF) microscopy (Figure 5.9). As show in Figure 5.9A, transgenic plants expressing GFP:HDEL localise GFP to the plant ER, enabling visualisation of a dynamic and intricate ER structure. Time-lapse epifluorescence imaging demonstrates the dynamic nature of the ER in rice cells. Further to this, using confocal Z-stacking microscopy, the ER could be observed around the plant nucleus, consistent with perinuclear ER (Baluška *et al.*, 1999), as shown in Figure 5.9B.

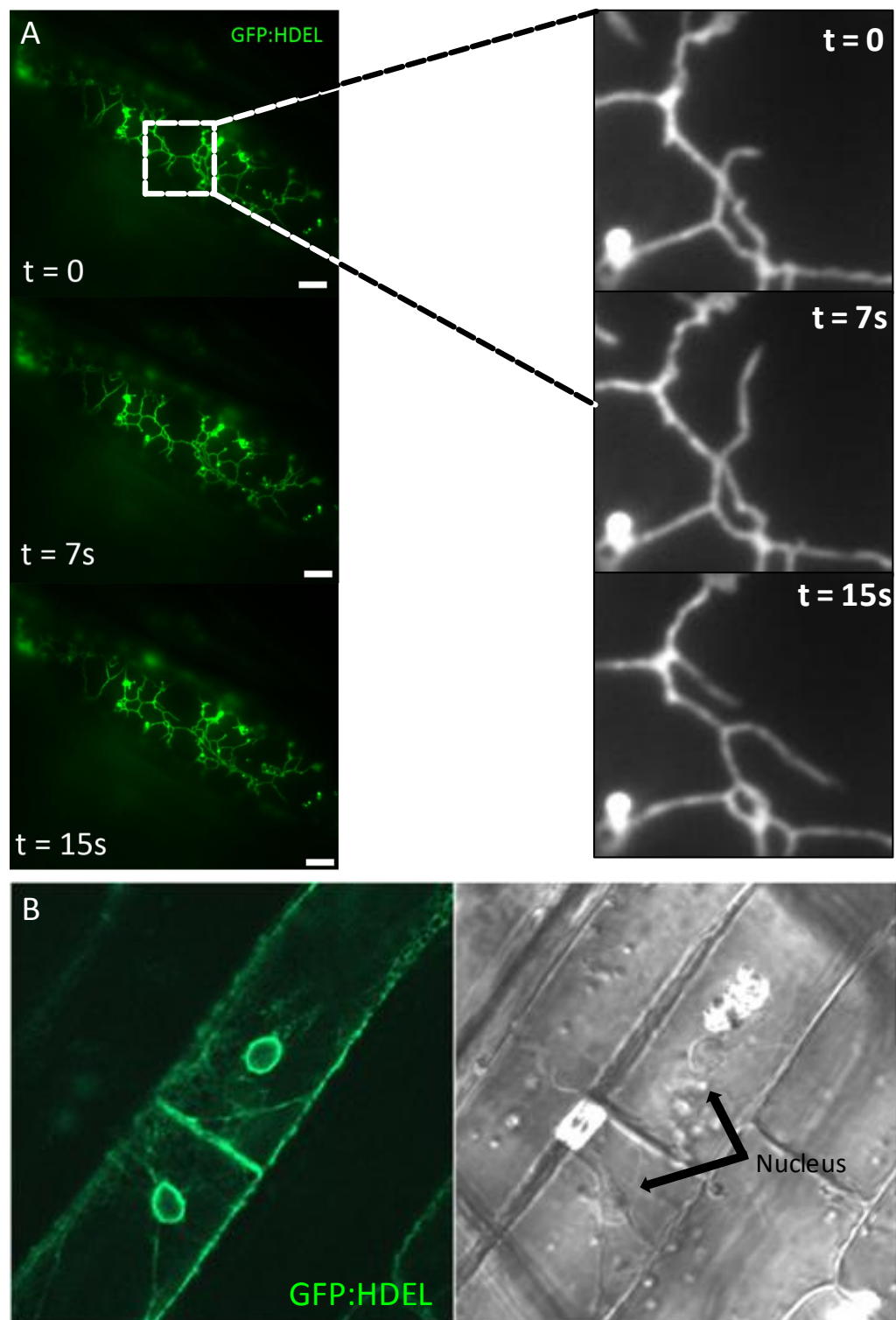


Figure 5.9 Epidermal plant cells expressing the GFP:HDEL construct enables the visualisation of a highly dynamic and intricate network of plant endoplasmic reticulum. **A.** Using time lapse epifluorescence imaging over a period of 15 seconds, the structure of the plant ER could be seen to change shape and re-model itself (inset). Epidermal plant tissue was dissected from 3-4 week old plants using the leaf sheath assay and mounted onto microscope slides. Images were captured using total internal reflection microscopy (TIRF). **B.** GFP:HDEL localises to perinuclear ER and can be seen to surround the host cell nucleus, which is visible by DIC. Scale bars represent 10 μm

5.3.5 During intracellular growth of *M. oryzae*, the host plant plasma membrane becomes invaginated

During intracellular growth of *M. oryzae* on host tissue, it is thought that the plant plasma membrane becomes invaginated and that invasive hyphae become surrounded by a host-derived plasma membrane referred to as the Extra-Invasive Hyphal Membrane (EIHM) (Kankanala *et al.*, 2007). Although an EIHM has previously been observed by transmission electron microscopy (Kankanala *et al.*, 2007), the presence of the EIHM had not subsequently been confirmed to exist around an entire fungal hypha. To test this experimentally, a *M. oryzae* strain expressing *toxA::RFP* was inoculated onto transgenic rice leaves expressing LTi6B:GFP. At 24 hpi, epidermal leaf tissue was dissected and *M. oryzae* was observed growing within host cells. At this time point, the plant plasma membrane was observed by epifluorescence microscopy (determined by using the LTi6B:GFP marker) and could be seen surrounding intracellular fungal hyphae and thereby establishing the EIHM (Figure 5.10). The host membrane was intact at more than 50 (n = 53) infection sites which were examined when intracellular growth was limited to one epidermal host cell (24 hpi). At later stages of infection (approximately 36 hpi), fungal hyphae had completely ramified within the initial host cell, and fungal hyphae could be seen to colonise adjacent cells. At this stage, the host membrane remained intact and was observed to invaginate around fungal hyphae moving into neighbouring cells, as shown in Figure 5.10B. At this stage, however, it was not clear whether the membrane remained intact in the initial host cell, as the host membrane could no longer be observed within this cell (Figure 5.10B). This supports and confirms the hypothesis that during the initial biotrophic intracellular growth phase of rice blast infection, the plant plasma membrane remains intact.

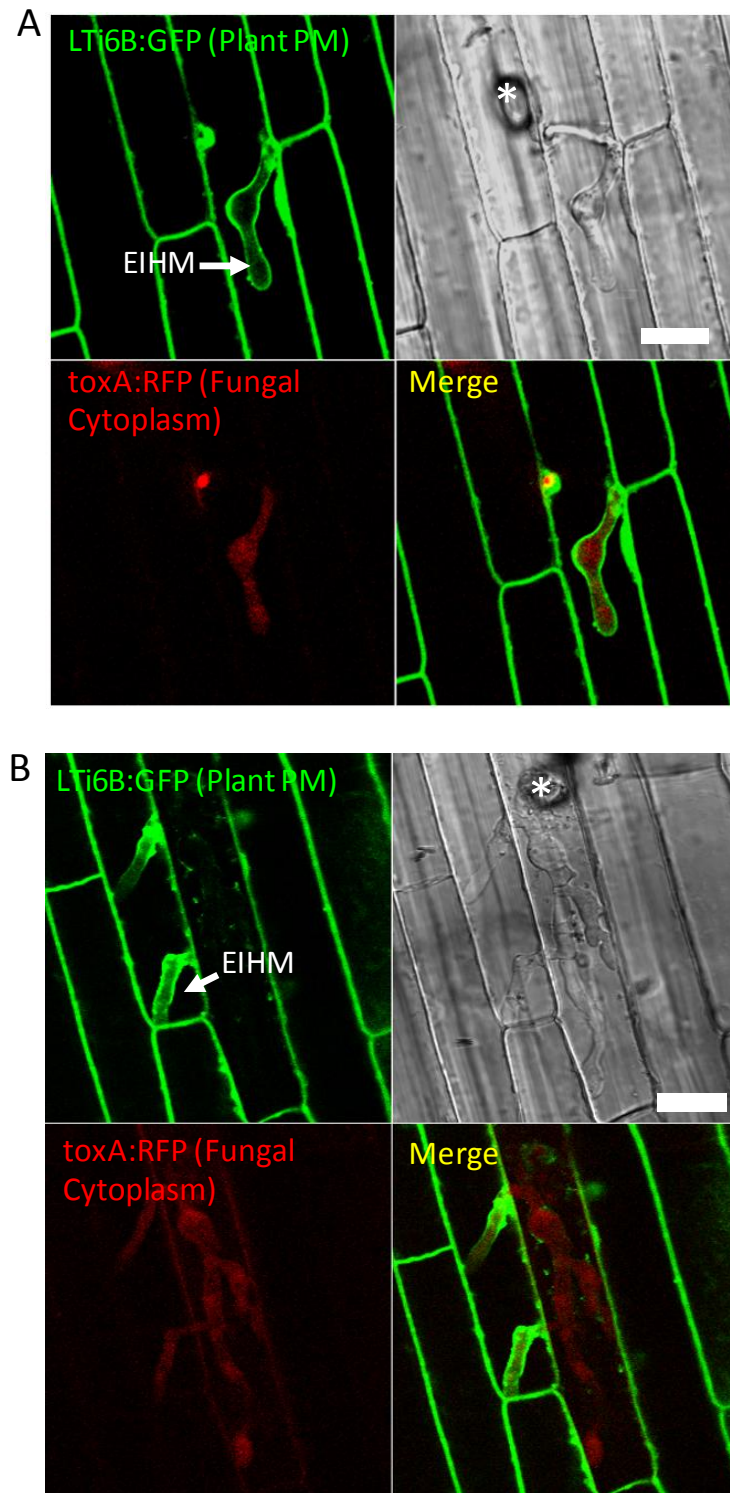
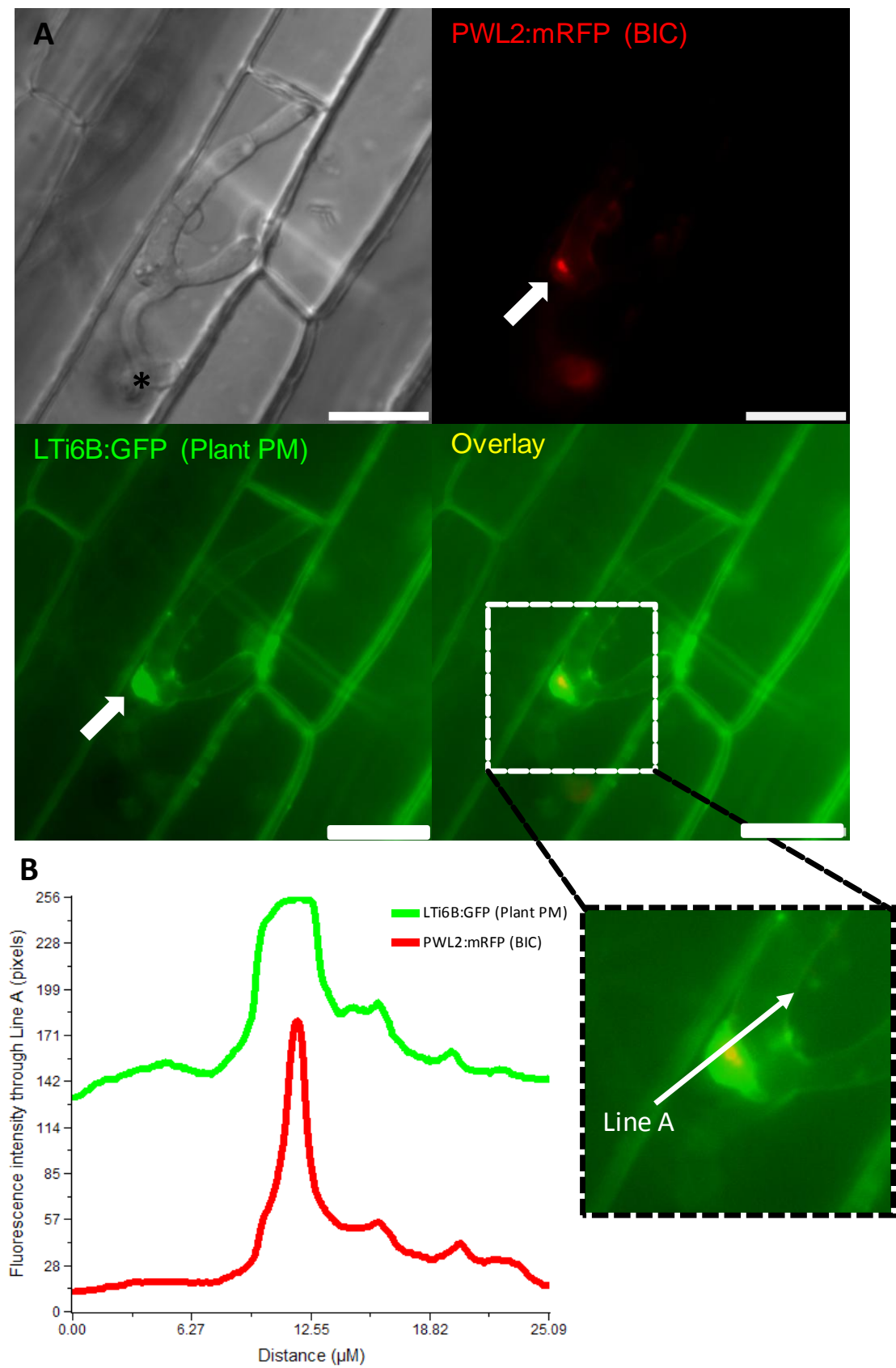


Figure 5.10 The host membrane becomes invaginated during rice blast disease. Plants expressing LTi6B:GFP were inoculated with a Guy11 *toxA*:RFP strain and incubated in a moist chamber. **A.** At 24 hours post inoculation (hpi), the rice cell membrane becomes invaginated around the intracellular growing hypha. The plant plasma membrane (LTi6B:GFP, Green) can be seen to completely surround an intracellular fungal hypha (*toxA*:RFP, Red), establishing the Extra-Invasive Hyphal Membrane (EIHM). **B.** At 36 hpi, the plant plasma membrane can be seen to surround fungal hyphae that are starting to colonise neighbouring host cells. At this time, the plant plasma membrane can no longer be observed in the initial host cell and it is not clear if the host membrane is still intact. White asterix marks the site of appressorium formation. Scale bars, 10 μm

5.3.6 Host plasma membrane accumulates at the Biotrophic Interfacial Complex (BIC)

LTi6B:GFP-expressing transgenic plants were used to examine the structure of the host membrane around the Biotrophic Interfacial Complex (BIC), the putative site of avirulence effector delivery into host cells. Although invagination of the host plasma membrane and establishment of the EIHM during rice blast disease had been confirmed, it was not clear where the host membrane resided in relation to the BIC structure. A Guy11 strain of *M. oryzae* expressing the BIC reporter gene *PWL2:mRFP* (Khang *et al.*, 2010) was used to inoculate transgenic rice plants expressing LTi6B, permitting simultaneous visualisation of the host plasma membrane and BIC by epifluorescence microscopy in live infected cells. As shown in Figure 5.11A, LTi6B:GFP appeared to accumulate at the BIC, as demonstrated by the co-localisation of fluorescence signals from the expression of *LTi6B:GFP* and *PWL2:mRFP*. It has previously been suggested that the BIC is a membrane-rich structure, but this data provides the first direct evidence that the BIC structure is composed at least partly of plant-derived plasma membrane. Interestingly, more than twenty (n=21) infection sites were examined where a BIC was clearly visible. Complete co-localisation between the LTi6B:GFP and *PWL2:mRFP* signals could be seen at all of these infection sites confirming that this observation is a consistent characteristic of the BIC, as shown in Figure 5.11C.



C

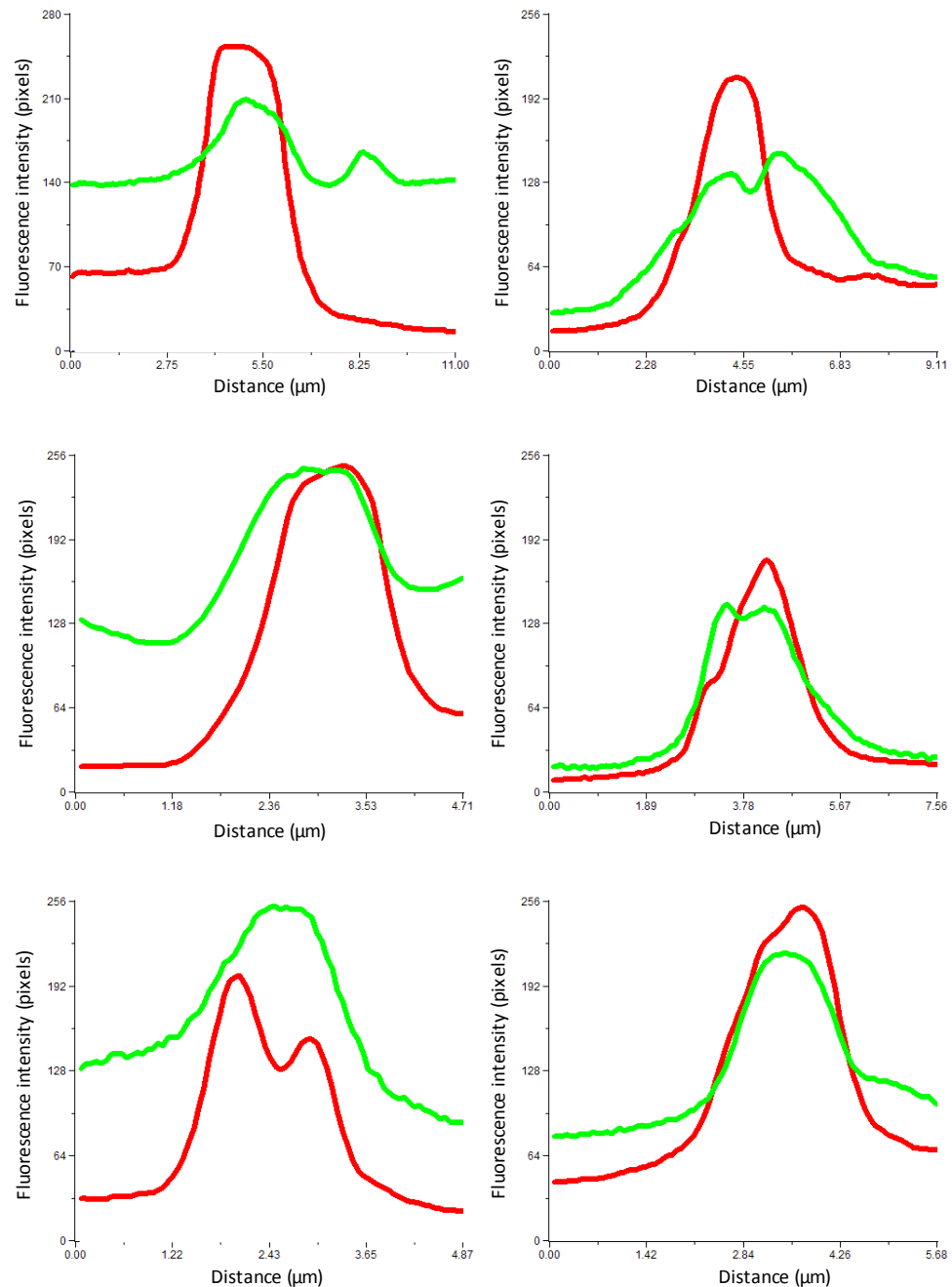


Figure 5.11 The BIC co-localises with the host plant plasma membrane (PM). **A.** Transgenic plants expressing the *LTi6B:GFP* plasma membrane marker (Green) were inoculated with a fungal strain expressing the BIC marker *PWL2:mRFP* (Red). At 24hpi on epidermal leaf tissue, co-localisation between the plant PM and the BIC was observed. **B.** Co-localisation as demonstrated by a fluorescence intensity distribution through Line A which dissects fluorescence derived from *PWL2:mRFP* (Fungus) and *LTi6B:GFP* (Plant). Co-localisation demonstrates that the BIC structure is comprised of material derived from plant plasma membrane. **C.** Representative fluorescence intensity distributions from 6 other infection sites shows that co-localisation between *LTi6B:GFP* and *PWL2:mRFP* is consistent. Black asterisk in DIC image highlights the site of appressorium formation. White arrows indicate the BIC. Scale bars represent 10 μm

5.3.7 Visualisation of transgenic GFP:HDEL plants reveals that host Endoplasmic Reticulum accumulates at the BIC

Plants expressing the GFP:HDEL construct were used to examine the structure of host endoplasmic reticulum (ER) around the BIC. A Guy11 strain of *M. oryzae* expressing the BIC reporter gene *PWL2:mRFP* was used to inoculate T2 rice plants expressing the GFP:HDEL construct. As shown in Figure 5.12, rice ER could be seen to accumulate at the BIC, as demonstrated by co-localisation between fluorescence signals from the GFP:HDEL and BIC markers. More than 20 infection sites ($n = 25$) were examined where putative BICs could be observed clearly, and complete co-localisation between the BIC and the host ER was observed. This provides evidence that the structure of the BIC is at least partly composed of host-derived ER.

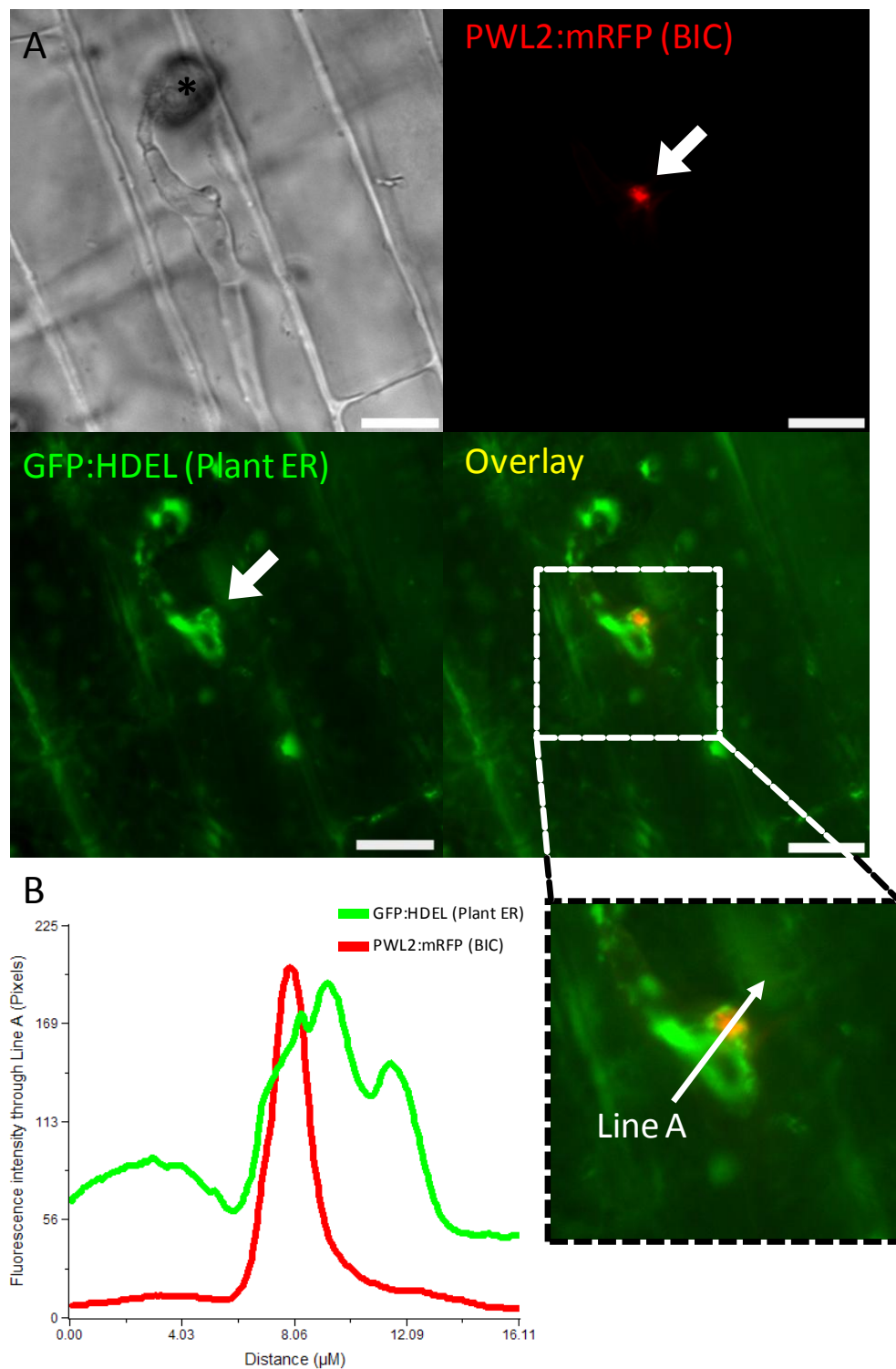


Figure 5.12 The BIC partially co-localises with plant endoplasmic reticulum (ER). **A.** Transgenic plants expressing the GFP:HDEL ER marker (Green) were inoculated with a *M. oryzae* strain expressing the BIC marker PWL2:mRFP (Red). At 24 hpi on epidermal leaf tissue, co-localisation between the ER and the BIC was observed. **B.** Co-localisation as demonstrated by a fluorescence intensity distribution through Line A which dissects fluorescence derived from PWL2:mRFP (Fungus) and GFP:HDEL (Plant). Co-localisation demonstrates that the BIC structure is comprised of material derived from plant ER. Black asterisk in DIC image highlights the site of appressorium formation. Scale bars 10 μm

5.3.8 Fungal cytoplasm is unable to diffuse into the BIC

Having shown that the BIC is composed mostly of plant plasma membrane and ER, I reasoned that the BIC was therefore likely to be a plant structure as opposed to a fungal-derived structure (Kankanala *et al.*, 2007). In order to investigate this idea further, a *M. oryzae* strain was generated in which the BIC and the fungal cytoplasm could be visualised simultaneously by epifluorescence microscopy. The *toxA::GFP* strain was used in this instance which is a marker of fungal cytoplasm (Badaruddin, 2012), and was introduced a Guy11 *M. oryzae* strain expressing the BIC-localised effector *PWL2::mRFP*. As shown in Figure 5.13, fungal cytoplasm was incapable of diffusing into the BIC during intracellular growth as demonstrated by the lack of co-localisation between GFP (defining the fungal cytoplasm) and RFP (defining the BIC) signals. Approximately fifty infection sites were examined and co-localisation between the *toxA::GFP* and *PWL2::mRFP* was never observed.

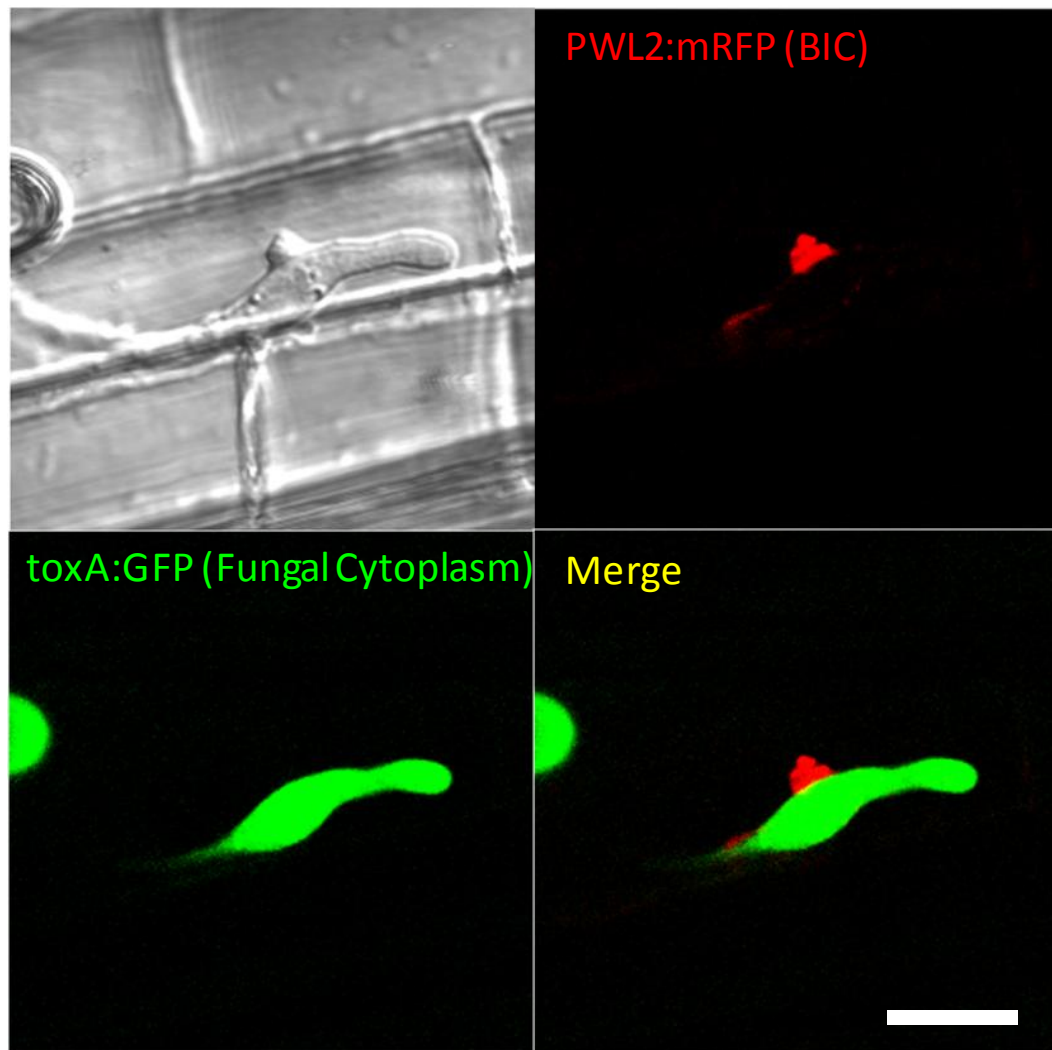
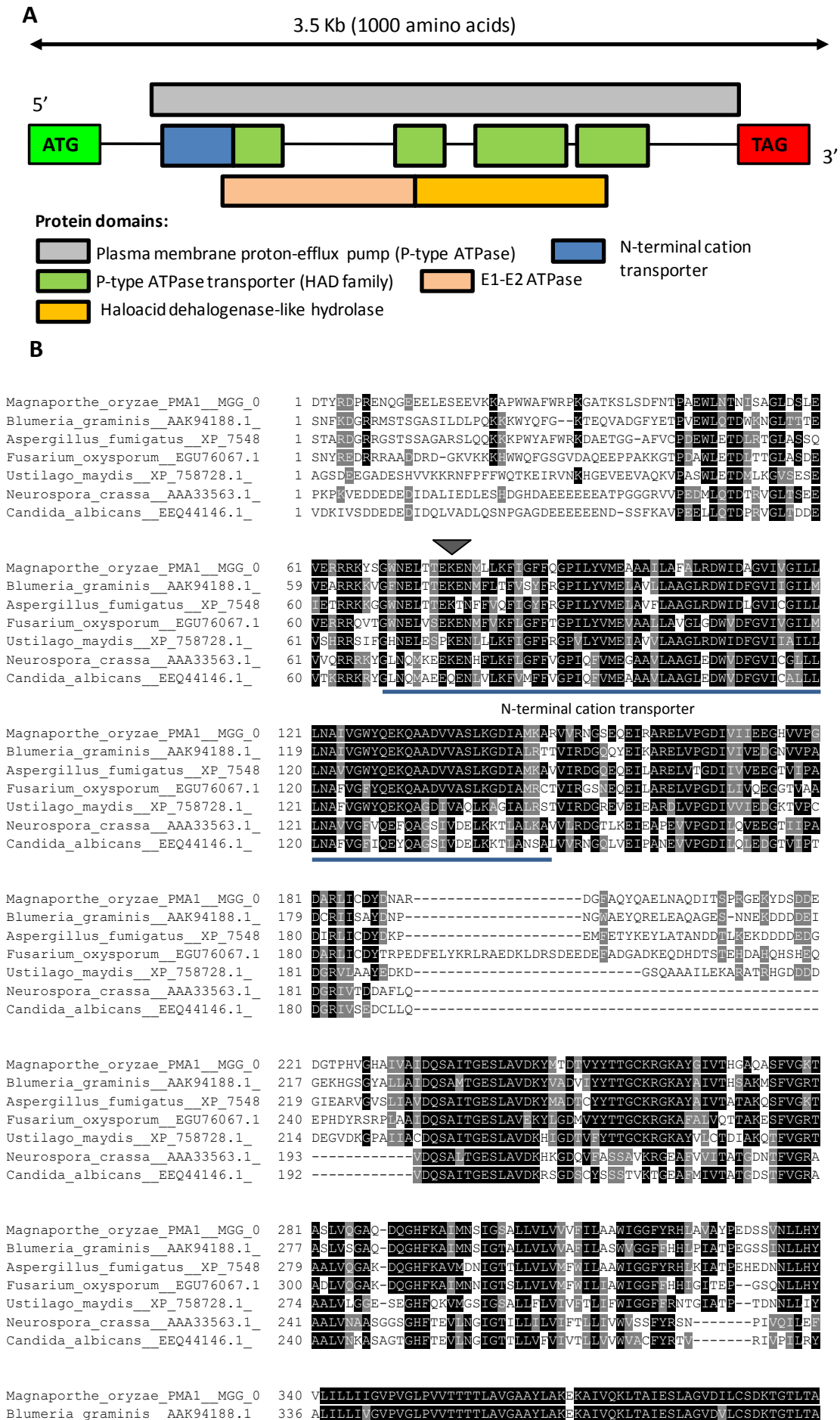


Figure 5.13 Fungal cytoplasm is incapable of diffusing into the BIC. A *M. oryzae* strain simultaneously expressing the BIC localised effector *PWL2:mRFP* (Red) and the fungal cytoplasmic marker *toxA:GFP* (Green) was inoculated onto CO-39 rice plants. At 24 hpi, the lack of co-localisation between fungal cytoplasm and the BIC suggest they are spatially and structurally separated. Images taken on 3-week old rice leaves at 24 hpi. Scale bars represent 10 μm .

5.3.9.1 Generating a fungal plasma membrane marker *PMA1::GFP*

In order to define and visualise the boundaries of fungal hyphae during biotrophic growth by live-cell imaging, a fungal plasma membrane marker was required, which localised GFP to the fungal plasma membrane. Generating a fungal plasma membrane marker would enable the fungal cell membrane and hyphal periphery to be positionally defined in relation to the BIC. Having previously demonstrated that the BIC-localised effector Pwl2:mRFP localised to the plant host membrane, the position of the fungal plasma membrane in relation to this structure was still unknown. A preliminary search of the *M. oryzae* genome (Dean *et al.*, 2005) database (www.broad.mit.edu/annotation/fungi/magnaporthe/) identified a putative membrane targeted protein encoding a membrane-bound H⁺ATPase domain and was named Plasma Membrane ATPase (*PMA1*) (Accession number MGG_04994). Figure 5.14A shows a diagrammatic representation of the structure of the *PMA1* gene which encodes a putative membrane-bound H⁺ATPase pump of 1000 amino acids. The *M. oryzae* predicted *Pma1* amino acid sequence (MGG_04994) was aligned with orthologous H⁺ATPase protein pumps from *Blumeria graminis* (AAK94188.1), *Aspergillus fumigatus* (XP_754847.1), *Fusarium oxysporum* (EGU76067.1), *Neurospora crassa* (AAA33563.1), *Candida albicans* (EEQ44146.1) and *Ustilago maydis* (XP_758728.1), as shown in Figure 5.14B. Sequences were obtained using a BLASTP search against the *M. oryzae* Pma1 (Altschul *et al.*, 1990) and aligned using the CLUSTALW alignment (Thompson *et al.*, 1994). The Pma1 protein was highly conserved across the fungal kingdom, and sequence homology between the amino acid sequence of *M. oryzae* Pma1 ranged from 72 % with that of the *Blumeria graminis* H⁺ATPase (AAK94188.1) to 59 % sequence homology with *Ustilago maydis* H⁺ATPase (XP_758728.1), as shown in Figure 5.14B.



```

Aspergillus_fumigatus_XP_7548 338 TLILLIIGVPVGLPVVTTTTLAVGAAYLAEQKAIVQKLTAIESLAGVDILCSDKTGTLTA
Fusarium_oxysporum_EGU76067.1 357 ALVLLIIGVPVGLPVVTTTTLAVGAAYLAKQKAIVQKLTAIESLAGVDILCSDKTGTLTA
Ustilago_maydis_XP_758728.1 331 TLLELIIGVPVGLPVVTTTTLAVGAAYLAKQKAIVQKLTAIESLAGVDILCSDKTGTLTA
Neurospora_crassa_AAA33563.1 294 TLAITIIIGVPVGLPVVTTTTLAVGAAYLAKQKAIVQKLTAIESLAGVDILCSDKTGTLTK
Candida_albicans_EEQ44146.1 293 TLAITIIIGVPVGLPVVTTTTLAVGAAYLAKQKAIVQKLTAIESLAGVDILCSDKTGTLTK

Magnaporthe_oryzae_PMA1_MGG_0 400 NQLSVREFFVMEGVDTNWMMAVAALASSHNKSLDPIDKVTILTTLKRYPKAKEITLSEGW
Blumeria_graminis_AAK94188.1 396 NQLSIREFFVAVGVDVNWMMVAALASSHNKSLDPIDKVTILTTLKRYPKAKEITLSEGW
Aspergillus_fumigatus_XP_7548 398 NQLSIREFFVYNEGVDVNWMMVAALASSHNKSLDPIDKVTILTTLKRYPKAKEITLSEGW
Fusarium_oxysporum_EGU76067.1 417 NKLSIRDPNIAEGQDVNWMMAVAALASSHNKSLDPIDKVTILTTLKRYPKAKEITLSEGW
Ustilago_maydis_XP_758728.1 391 NKLSIREFFVTEGVDTNWMMAVAALASSHNKSLDPIDKVTILTTLKRYPKAKEITLSEGW
Neurospora_crassa_AAA33563.1 354 NKLSIREFFVTVAGVDPEDIMLTACLAASRKKKGLDAIDKAFKSLKYVPRAKSVLSK-YK
Candida_albicans_EEQ44146.1 353 NKLSIREFFVTVAGVDPEDIMLTACLAASRKKKGLDAIDKAFKSLINYPRAKAAEPK-YK

Magnaporthe_oryzae_PMA1_MGG_0 460 TEKFTPFDPVSKRITS-CNY-KGVKYTCCKGAPNAVLAISNCTE----EQKRLFEKATE
Blumeria_graminis_AAK94188.1 456 TEKFTPFDPVSKRITAVIK-EGVTYTCAGKAPKALINISNCSK----EDAEMYKSKVTE
Aspergillus_fumigatus_XP_7548 458 TEKFTPFDPVSKRITITCTC-EGVRYTCAGKAPKALINISNCSK----EEAAKFEKAAE
Fusarium_oxysporum_EGU76067.1 477 TESFTPFDPVSKRITACRL-GNDKTCVKGAPKAVLKASGSE----DESRIYKEKQD
Ustilago_maydis_XP_758728.1 451 THKFTPFDPVSKRITAEVEK-EGQVYTAAGKAPNAVLKLCAPDA----ETAQYFKVAGD
Neurospora_crassa_AAA33563.1 413 VLOSHFFDPVSKKVVAVESPOCEBITCVKGAPLFLVLTVEEDHPIPEVDQAYKKNVAE
Candida_albicans_EEQ44146.1 412 VIBEQPFDPVSKKVTAVESPEGERIICVKGAPLFLVLTVEEDHPIPEVDVHENYQNTVAE

Magnaporthe_oryzae_PMA1_MGG_0 515 FARRGFRSLGVAVQEGEPWOLGMLSLFDPFPREDTACTIAEAQALGLSVKMLTGDAIAI
Blumeria_graminis_AAK94188.1 511 FARRGFRSLGVAVKKGQGDWOLGMLPMFDPFPREDTASTIAEAQVGLGLSVKMLTGDAIAI
Aspergillus_fumigatus_XP_7548 513 FARRGFRSLGVAVQEGEPWOLGMLPMFDPFPREDTASTIAEAQALGLSVKMLTGDAIAI
Fusarium_oxysporum_EGU76067.1 532 FARRGFRSLGVAVKKNDGPWVILGLSLMFPDPFPREDTACTIIEAGHLGLPVKMLTGDAIAI
Ustilago_maydis_XP_758728.1 506 FARRGFRSLGVAVN-TDQWKLGMLPMFPFPREDTACTIAEAQSLGLSVKMLTGDAIAI
Neurospora_crassa_AAA33563.1 473 FATRGFRSLGVARKRGEGSWELGLMPCMDPPREDTYKTVCEAKTLGLSLKMLTGDAVGI
Candida_albicans_EEQ44146.1 472 FARRGFRSLGVARKRGEGSWELGLMPCMDPPREDTACTIENARRLGLRVKMLTGDAVGI

Magnaporthe_oryzae_PMA1_MGG_0 575 AKETCKMLALMGTKVYNSDKLHLS---DMAGSAIHDLCEADGFAEVFPEHKYQVVEMLQQ
Blumeria_graminis_AAK94188.1 571 AKETCKMLALMGTKVYNSERLIHG---GLSGITCQHDLEKADGFAEVFPEHKYQVVEMLQQ
Aspergillus_fumigatus_XP_7548 573 AKETCKMLALMGTKVYNSERLIHG---GLSGITCQHDLEKADGFAEVFPEHKYQVVEMLQQ
Fusarium_oxysporum_EGU76067.1 592 AKETCKMLALMGTKVYNSERLIHG---GLSGITCQHDLEKADGFAEVFPEHKYQVVEMLQQ
Ustilago_maydis_XP_758728.1 565 AKETCKMLALMGTKVYNSERLIHG---GLSGITCQHDLEKADGFAEVFPEHKYQVVEMLQQ
Neurospora_crassa_AAA33563.1 533 AKETCKMLALMGTKVYNSERLIHG---GLSGITCQHDLEKADGFAEVFPEHKYQVVEMLQQ
Candida_albicans_EEQ44146.1 532 AKETCKMLALMGTKVYNSERLIHG---GLSGITCQHDLEKADGFAEVFPEHKYQVVEMLQQ

Magnaporthe_oryzae_PMA1_MGG_0 632 RGHLTAMTGDGVNDAPSLKKS-DCGIAVEGATEAAQAAADIVFLAPGLSTIVSAIKTSRQI
Blumeria_graminis_AAK94188.1 628 RGHLTAMTGDGVNDAPSLKKS-DCGIAVEGATEAAQAAADIVFLAPGLSTIVSAIKTSRQI
Aspergillus_fumigatus_XP_7548 630 RGHLTAMTGDGVNDAPSLKADCGIAVEGATEAAQAAADIVFLAPGLSTIVSAIKTSRQI
Fusarium_oxysporum_EGU76067.1 649 RGHLTAMTGDGVNDAPSLKADCGIAVEGATEAAQAAADIVFLAPGLSTIVSAIKTSRQI
Ustilago_maydis_XP_758728.1 623 RGHLTAMTGDGVNDAPSLKADCGIAVEGATEAAQAAADIVFLAPGLSTIVSAIKTSRQI
Neurospora_crassa_AAA33563.1 593 RGYIVAMTGDGVNDAPSLKADTGIAGEGSDAARSADIVFLAPGLSTIVSAIKTSRQI
Candida_albicans_EEQ44146.1 592 RGYIVAMTGDGVNDAPSLKADTGIAGEGSDAARSADIVFLAPGLSTIVSAIKTSRQI

Magnaporthe_oryzae_PMA1_MGG_0 692 FORMKAYIQYRIALCLHLEIYLV-TSMIINETVRVDLIVFALFADLATIAYAYDNAHYE
Blumeria_graminis_AAK94188.1 688 FORMKAYIQYRIALCLHLEIYLV-TSMIINETVRVDLIVFALFADLATIAYAYDNAHYE
Aspergillus_fumigatus_XP_7548 690 FORMKAYIQYRIALCLHLEIYLV-TSMIINETVRVDLIVFALFADLATIAYAYDNAHYE
Fusarium_oxysporum_EGU76067.1 709 FORMKAYIQYRIALCLHLEIYLV-TSMIINETVRVDLIVFALFADLATIAYAYDNAHYE
Ustilago_maydis_XP_758728.1 683 FHRMKAYIQYRIALCLHLEIYLV-TSMIINETVRVDLIVFALFADLATIAYAYDNAHYE
Neurospora_crassa_AAA33563.1 653 FHRMYAYVYRIALCLHLEIYLV-TSMIINETVRVDLIVFALFADLATIAYAYDNAHYE
Candida_albicans_EEQ44146.1 652 FHRMYAYVYRIALCLHLEIYLV-TSMIINETVRVDLIVFALFADLATIAYAYDNAHYE

Magnaporthe_oryzae_PMA1_MGG_0 752 RRPVEWQLPKIWIISVVLGLLAGTWILRGTMWLE--NGGIIONFGSQEILFLQISLT
Blumeria_graminis_AAK94188.1 748 RRPVEWQLPKIWIISVVLGLLAGTWILRGTMWLE--NGGIIONFGSQEILFLQISLT
Aspergillus_fumigatus_XP_7548 750 RRPVEWQLPKIWIISVVLGLLAGTWILRGTMWLE--NGGIIONFGSQEILFLQISLT
Fusarium_oxysporum_EGU76067.1 769 RRPVEWQLPKIWIISVVLGLLAGTWILRGTMWLE--NGGIIONFGSQEILFLQISLT
Ustilago_maydis_XP_758728.1 743 RRPVEWQLPKIWIISVVLGLLAGTWILRGTMWLE--NGGIIONFGSQEILFLQISLT
Neurospora_crassa_AAA33563.1 713 QTPVKWNLPLKWIISVVLGLLAGTWILRGTMWLE--NGGIIONFGSQEILFLQISLT
Candida_albicans_EEQ44146.1 712 RRPVKWNLPLKWIISVVLGLLAGTWILRGTMWLE--NGGIIONFGSQEILFLQISLT

Magnaporthe_oryzae_PMA1_MGG_0 810 ENWLIFVTRGFN-----TFPSWQLIGAIFGVDILASLHAGFGWFSGGGLGEPALPASLAKN
Blumeria_graminis_AAK94188.1 806 ENWLIFVTRGDE-----TFPSWQLIGAIFGVDILASLHAGFGWFSGGGLGEPALPASLAKN
Aspergillus_fumigatus_XP_7548 808 ENWLIFVTRGDK-----TFPSWQLIGAIFGVDILASLHAGFGWFSGGGLGEPALPASLAKN
Fusarium_oxysporum_EGU76067.1 827 ENWLIFVTRGDK-----TFPSWQLIGAIFGVDILASLHAGFGWFSGGGLGEPALPASLAKN
Ustilago_maydis_XP_758728.1 801 ENWLIFVTRGDK-----TFPSWQLIGAIFGVDILASLHAGFGWFSGGGLGEPALPASLAKN
Neurospora_crassa_AAA33563.1 773 ENWLIFVTRGDK-----TFPSWQLIGAIFGVDILASLHAGFGWFSGGGLGEPALPASLAKN
Candida_albicans_EEQ44146.1 770 ENWLIFVTRGDK-----TFPSWQLIGAIFGVDILASLHAGFGWFSGGGLGEPALPASLAKN

```

```

Magnaporthe_oryzae_PMA1_MGG_0 865 LSENGAVDVTIVVWYISLAVIIVIGIVVYVMTGWKRLDGLGRKKRSAQDT---MMENI
Blumeria_graminis__AAK94188.1_ 861 LSTDGRISIVTVIVVWCYSIAVTIVIAIVYHIMNKAAWLDNLGRFTRSKADT---QMENI
Aspergillus_fumigatus__XP_7548 861 FSVNGDVIDVTVVVIMGYSTGVTLIIAVVYVLTIIIPALDNLGRFTRSKADT---KIENM
Fusarium_oxysporum__EGU76067.1 880 QSSNGWVDIVTVVIVVWLYSFGVTIVIAIVYFVLAKLSDLNLGRKDRKKRDT---KLENI
Ustilago_maydis__XP_758728.1_ 855 APHGGWTDIVTIVVYIYSMGVTAITCAVYVYVLAKWDWLNNLGRFTRSKQKNP---LLEDF
Neurospora_crassa__AAA33563.1_ 819 -----DLSIVAVVRVIRWISFGIFCLMGGVYVYLLDSVGFNDLMHGKSPKGNQKQRSLEDF
Candida_albicans__EEQ44146.1_ 816 -----WTDIVTVVVRTIIVSFGVFCVLMGAYVYVLTSTSEAFDIFCNGRKPPQQHIDKRSLEDF

```

Figure 5.14 The *M. oryzae* Plasma Membrane ATPase (*PMA1*) gene encodes an H⁺ATPase membrane pump. A. Representation of the Guy11 genomic locus of the *PMA1* gene (Accession number MGG_04994). **B.** Amino acid alignment of fungal H⁺ ATPase proteins. The *M. oryzae* Pma1 protein was aligned using CLUSTALW (Thompson *et al.*, 1994) with the fungal H⁺ ATPase protein pumps from *Blumeria graminis* (AAK94188.1), *Aspergillus fumigatus* (XP_754847.1), *Fusarium oxysporum* (EGU76067.1), *Neurospora crassa* (AAA33563.1), *Candida albicans* (EEQ44146.1) and *Ustilago maydis* (XP_758728.1). Area highlighted in blue denotes the conserved N-terminal cation transporter. The dark grey triangles above the alignment denotes the start and finish of the amino acid sequences encoding the plasma-membrane bound P-type ATPase domains of the H⁺ATPase proteins. Shading of the alignments was performed using BoxShade 3.21 (http://www.ch.embnet.org/software/BOX_form.html). Identical amino acid residues are shaded in black, similar residues in grey, and non-identical residues are unshaded.

5.3.9.2 Construction and introduction of the *PMA1:GFP* gene fusion vector

To define the boundaries of the fungal plasma membrane by epifluorescence microscopy, a C-terminal *PMA1:GFP* gene fusion vector was generated. The *PMA1* gene encodes a 3.5 kb ORF coding for a protein of 1000 amino acids in length, containing an N-terminal cation transporter domain and plasma membrane proton-efflux P-type ATPase domain (Figure 5.14). The construction of the *PMA1:GFP* gene fusion vector can be seen in a diagrammatic representation in Figure 5.15. A 5.2 kb genomic fragment containing the *PMA1* ORF and a 2 kb upstream region incorporating the promoter sequence was amplified and cloned into *Hind* III-digested vector pYSGFP-1. Primers were engineered to contain 30 bp overhangs at both the 5' and 3' end of the *PMA1* PCR amplicon to allow an in frame fusion of the *PMA1* gene to GFP by homologous recombination upon transformation into *S. cerevisiae* (as shown in Figure 5.14). The translational stop codon in the *PMA1* ORF was removed by primer engineering. Positive clones of the *PMA1:GFP* vector were confirmed by PCR and independently verified by DNA sequencing through the gene fusion to check the in frame gene fusion had been successful and errors had not been introduced. The *PMA1:GFP* fusion vector was introduced into the *M. oryzae* *PWL2:mRFP*-expressing strain and putative transformants selected based on their resistance to sulfonylurea, bestowed upon by the *ILV1* allele which encodes acetolactate synthase which is present within the pYSGFP-1 vector (Sweigard *et al.*, 1997). Several putative transformants were obtained and selected for further analysis based on screening by epifluorescence microscopy (Figure 5.16). Consistent with the role of *PMA1* as a membrane bound P-type H⁺ATPase pump, localisation of GFP could be observed *in vitro*, and was observed localising to the fungal plasma membrane, as shown in Figure 5.16.

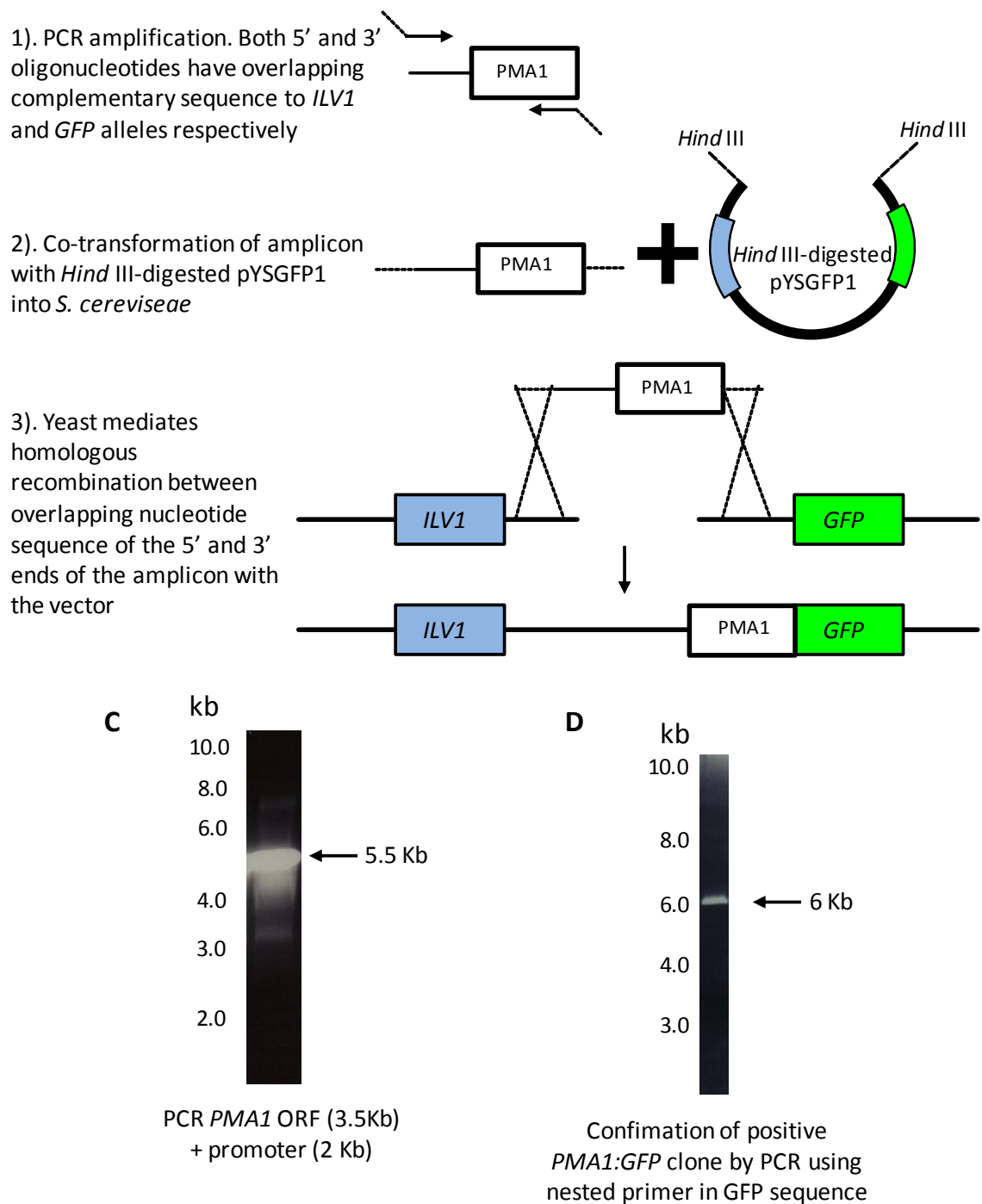


Figure 5.15. Schematic representation of the cloning strategy used to generate the *PMA1:GFP* vector. **A.** Cloning strategy using homologous recombination in yeast for fusion of GFP to the C-terminus of the *PMA1* gene. **B.** Confirmation of PCR amplification of the *PMA1* ORF (3.5 kb) plus a 2 kb promoter sequence. **C.** Confirmation of positive *PMA1:GFP* clones in yeast by PCR using *PMA1*-specific primers.

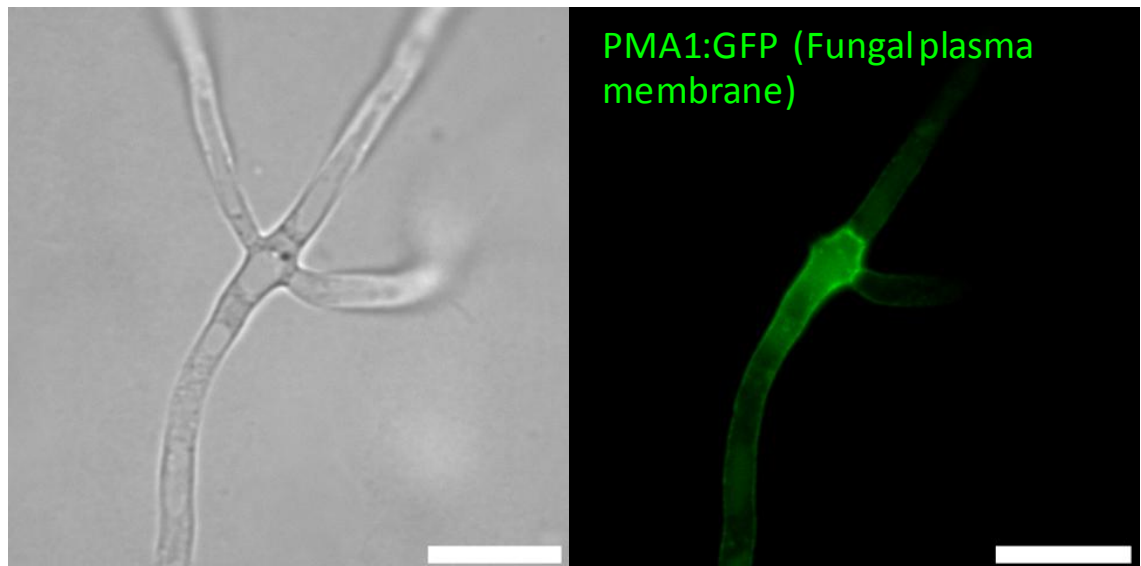


Figure 5.16 Visualisation and localisation of the Pma1:GFP marker during *in vitro* vegetative growth. A small mycelial plug of *PMA1:GFP* strain was inoculated onto liquid CM and grown for 24 hours. GFP signal could be observed around the tips of vegetatively growing hyphae, suggesting that the *PMA1:GFP* marker is a successful marker for labelling of the fungal plasma membrane. Scale bars represent 10 μm .

5.3.9.3 Visualising the fungal plasma membrane using the *PMA1:GFP* vector enables the structure of the fungal plasma membrane around the BIC to be determined

Having confirmed localisation of Pma1:GFP to the plasma membrane, the construct was deemed suitable to investigate the relationship between the fungal plasma membrane and the BIC. Conidia of the *PMA1:GFP PWL2:mRFP*-expressing *M. oryzae* strain were inoculated onto rice leaf sheath and incubated in a moist chamber at 24°C. After 24 hours post inoculation, rice blast infection sites were examined by epifluorescence microscopy of epidermal leaf tissue. Consistent with the role of Pma1 as an integral membrane-bound proton pump, GFP fluorescence was observed surrounding intracellularly growing hyphae, as shown in Figure 5.17A. When the BIC-localised effector *PWL2:mRFP* was simultaneously expressed, a lack of co-localisation between the reporter genes suggests that the fungal plasma membrane is spatially separated from the BIC. Further to this, the BIC structure was not surrounded by a fungal plasma membrane and appeared to reside outside the limits of the fungal plasma membrane (Figure 5.17). A number of infection sites were examined (n = 30) where the fungal plasma membrane and the BIC was clearly visible by epifluorescence microscopy. At none of these infection sites did the fungal plasma membrane co-localise with the BIC, nor did the fungal plasma membrane surround the BIC structure. With the exception of the accumulation of avirulence effectors, the presence of the BIC outside the host plasma membrane would strongly suggest that the BIC is almost exclusively a plant-derived structure.

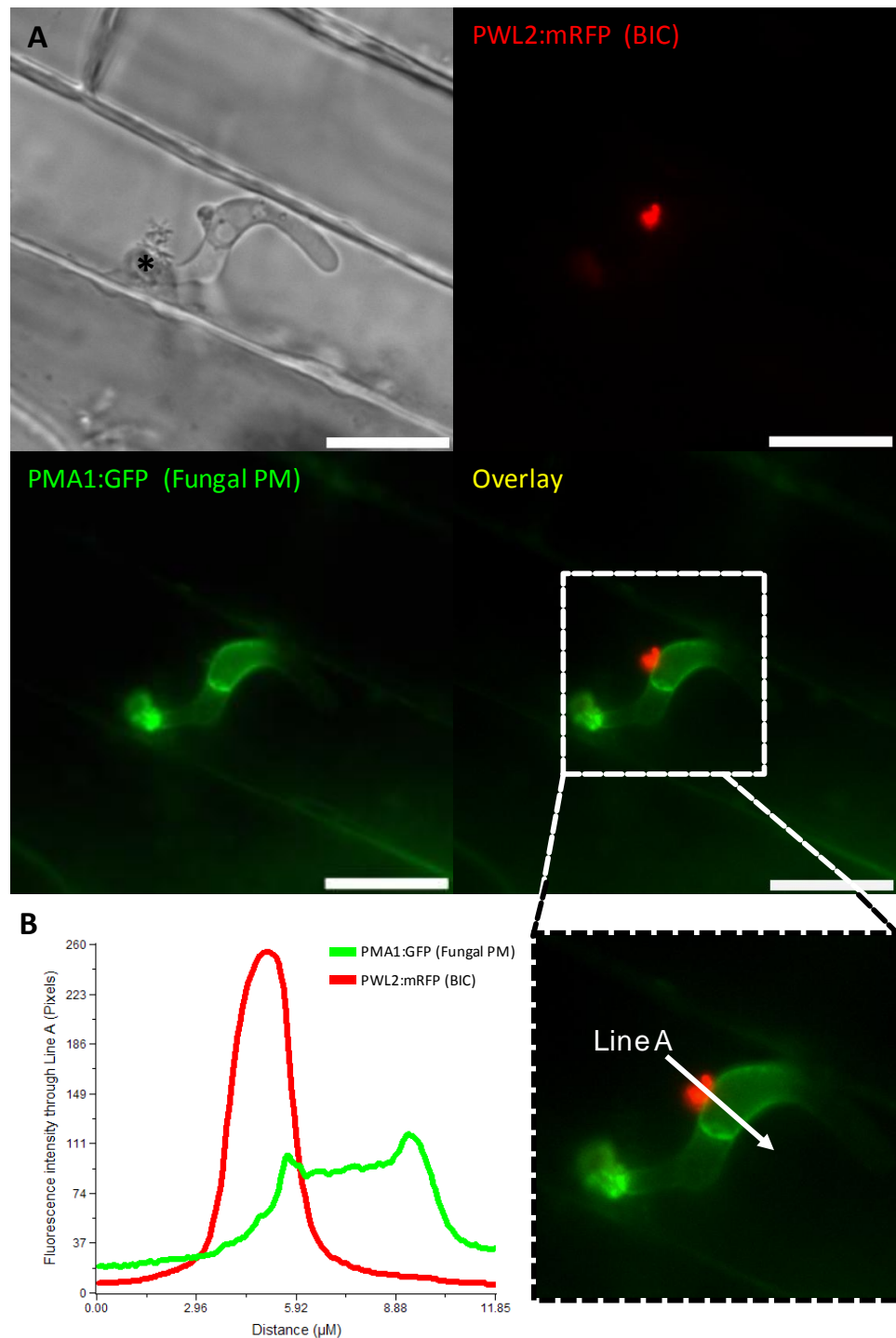
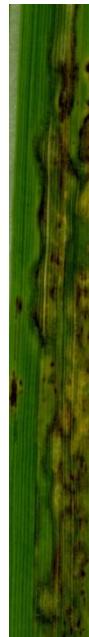


Figure 5.17 The BIC resides outside the fungal plasma membrane. **A.** The fungal plasma membrane marker *PMA1:GFP* (Green) co-expressed with the BIC marker *PWL2:mRFP* (Red). After 23 hours post inoculation on epidermal leaf tissue, GFP could be seen to localise to the fungal plasma membrane and completely outlined invasively growing hyphae. **B.** Lack of co-localisation demonstrated by a fluorescence intensity distribution through Line A which dissects fluorescence derived from the expression of *PWL2:mRFP* and *PMA1:GFP*. Lack of colocalisation demonstrates that the BIC structure is not comprised of material derived from the fungal plasma membrane. The BIC appears to reside outside the fungal plasma membrane, suggesting that the nature of the structure is plant-based. Co-localisation between the GFP and RFP fluorescent signals was not observed at any of the infection sites examined. Black asterisk in DIC image highlights the site of appressorium formation. Scale bars represent 10 μm

5.3.10.1 Using transgenic *Oryza sativa* cv. *sasanishiki* plants to study compatible and incompatible interactions

As stated, all plant expression vectors were transformed in to the rice cultivar *Oryza sativa* cv. *sasanishiki*, which harbours the rice resistance gene *Pia* (Yoshida *et al.*, 2009). Recently, two new *M. oryzae* isolates were identified, and referred to as TH68-126 and TH68-140 which express the avirulence effectors *AVR-Pii* and *AVR-Pia* respectively (Yoshida *et al.*, 2009). It is thought that the AVR effectors *AVR-Pii* and *AVR-Pia* interact either directly or indirectly with the rice cytoplasmic resistance genes (R genes) *Pii* and *Pia*, respectively, to mediate a hypersensitive resistance (HR) response. Consequently, expression of *AVR-Pia* by TH68-140 results in HR / incompatibility response by *Oryza sativa* cv. *sasanishiki* upon plant detection of a *Pia* / *AVR-Pia* interaction. In contrast, the TH68-126 isolate harbours the effector *AVR-Pii*, which does not interact with the rice *Pia* resistance gene expressed by the *Sasanishiki* cultivar. This consequently means that the *Sasanishiki* cultivar is susceptible to the *M. oryzae* isolate TH68-126, and disease ensues when this strain is inoculated onto *Sasanishiki* plants (Figure 5.18). Having successfully transformed and confirmed expression of the plant ER-retention marker (GFP:HDEL vector) in the *Sasanishiki* cultivar, changes in host ER during an HR response can therefore be examined by inoculation of TH68-126 and TH68-140 strains.

A



Oryza sativa cv.
sasanishiki leaves
Express the rice
resistance gene *Pia*

TH68-126
AVR-Pii

TH68-140
avr-pii

B

Strain	Avirulence Effector	Phenotype on Sasanishiki cultivar
TH68-126	AVR-Pii	Susceptible (Compatible Interaction)
TH68-140	AVR-Pia	Resistant (Incompatible Interaction)

Figure 5.18 Using the *Oryza sativa* cv. *sasanishiki* cultivar for studying compatible and incompatible interactions. **A.** Seedlings of the rice cultivar *Oryza sativa* cv. *sasanishiki* were inoculated with conidial suspensions of identical concentrations (5×10^4 spores ml^{-1}) of the *M. oryzae* isolates TH68-140 and TH68-126. The TH68-140 isolate is unable to cause disease, while the *sasanishiki* cultivar is susceptible to infection from TH68-126. **B.** The rice *Oryza sativa* cv. *sasanishiki* is resistant to the TH68-140 isolate due to expression of the rice resistance gene *Pia*, which is thought to bind to the avirulence fungal effector AVR-Pia mediating a hypersensitive response (HR) and thereby preventing disease.

5.3.10.2 Inoculation of *M. oryzae* isolate TH68-140 on transgenic *GFP:HDEL* plants reveals that the host nucleus is recruited to the site of appressorium formation

In order to understand the nature of incompatible HR responses, the *M. oryzae* isolate TH68-140 was inoculated onto *GFP:HDEL*-expressing transgenic plants. In addition to localising an intricate network of endoplasmic reticulum, expression of the *GFP:HDEL* vector in plants localises the host nucleus by localising perinuclear endoplasmic reticulum (Figure 5.9B). Upon inoculation of the *M. oryzae* TH68-140 strain on *GFP:HDEL* transgenic plants, the host nucleus appeared to migrate to the site of conidial attachment at an early stage of infection (4 hpi) (Figure 5.19). At later stages of infection the host nucleus appeared to accumulate under the site of early (8 hpi) and mature appressorium (24 hpi) formation (Figure 5.19B). This suggests that the host re-configures its host cellular organelles in response to fungal invasion during an HR response.

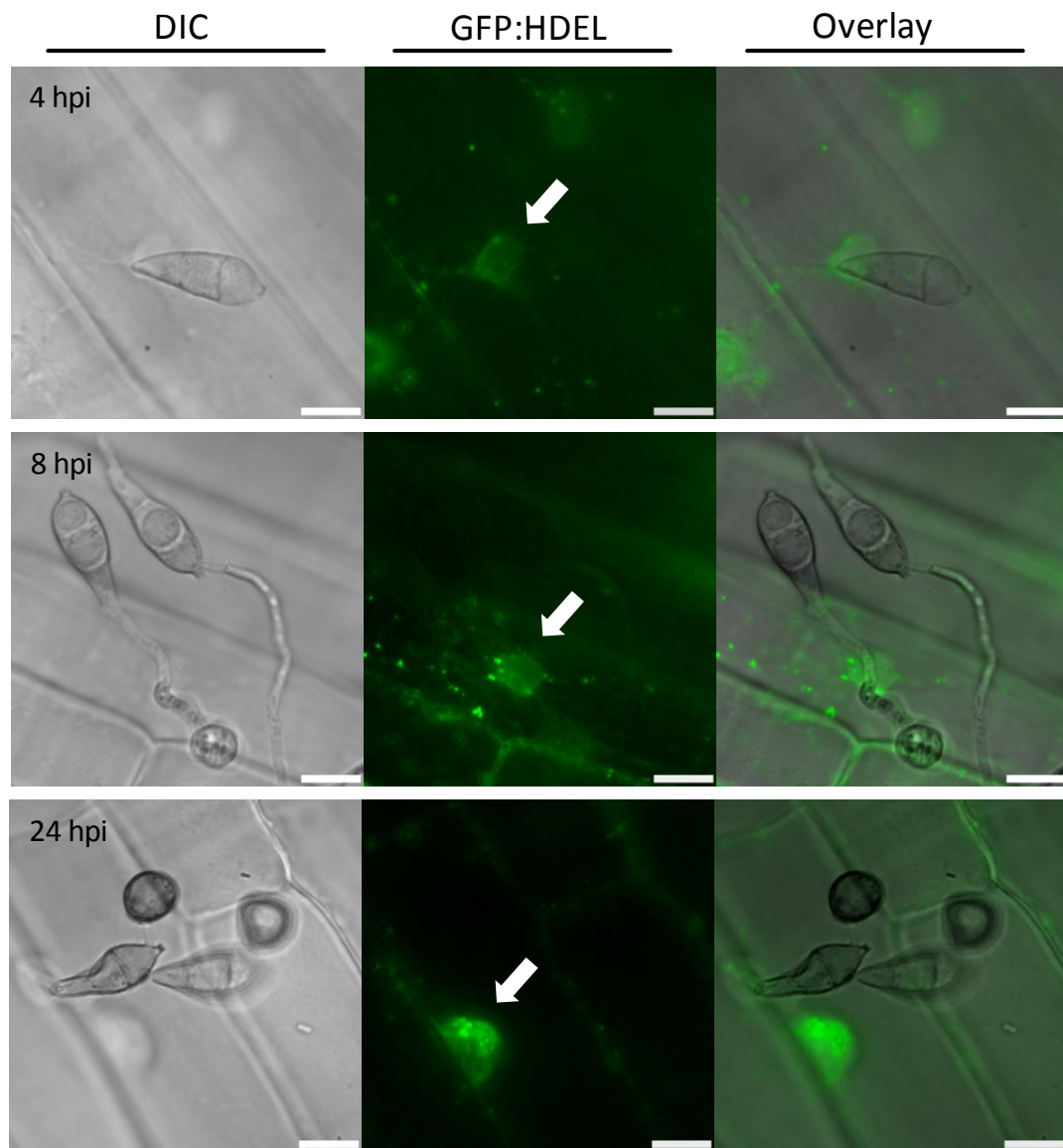


Figure 5.19 During an Incompatible HR, the host nucleus as demonstrated by perinuclear ER is recruited to the site of appressorium formation. Transgenic *Oryza sativa* cv. *sasanishiki* plants expressing the ER-retention marker *GFP:HDEL* were inoculated with the *M. oryzae* isolate TH68-140. During appressorium formation perinuclear ER could be seen to accumulate near the site of conidial attachment and germination (at 4 hpi). At later stages of infection (8 hpi and 24 hpi), perinuclear ER could also be observed accumulating under the site of appressorium formation. White arrows indicate accumulation of perinuclear ER as demonstrated by the *GFP:HDEL* marker. Scale bars represent 10 μm

5.4 Discussion

The Extra-Invasive Hyphal Membrane (EIHM) is the plant-derived membrane that surrounds and extends around a *M. oryzae* fungal hypha during biotrophic growth (Kankanala *et al.*, 2007). Although the EIHM has previously been visualised using electron microscopy of early rice blast infection on leaf tissue (Kankanala *et al.*, 2007), and at later stages of infection on root tissue (Marcel *et al.*, 2010), there was no evidence prior to this study that showed that the EIHM is continuous around an entire intracellular hypha (Kankanala *et al.*, 2007). Invagination of the EIHM during rice blast infection is likely to place tension on the EIHM, and membrane biogenesis is likely to be required to accommodate the growing fungal pathogen at this site of tension. Although septins are not present in plants (Hall *et al.*, 2008), this may involve a mechanism similar to the septin-mediated plasma membrane reshaping which is required during motility and blebbing of T-cells (Gilden *et al.*, 2012). Early reports in the literature provided contradictory hypotheses about the nature of the plant membrane structure around an intracellular *M. oryzae* hyphae. Heath *et al.*, (1992) suggested that *M. oryzae* invasive hyphae breach the host cell membrane and grow directly within the epidermal cytoplasm, which is in contrast to previous reports suggesting that invasive hyphae are separated from the host cytoplasm by an invaginated host cell membrane (Koga and Horino, 1984). Using stable transgenic rice lines expressing the plant plasma membrane marker LTi6B:GFP (Kurup *et al.*, 2005), we were able to test formally the hypothesis that the EIHM invaginates and extends completely around an intracellular hypha. Interestingly, invagination of the host cell membrane during biotrophic growth is a characteristic previously reported during infection by a number of other fungal plant pathogens. The intracellular corn smut pathogen, *Ustilago maydis*, for example, has previously been shown to become encased within a plant-derived plasma membrane, which was visualised by epifluorescence microscopy in the maize line ZmPIN1a-YFP that expresses a YFP-tagged version of the PIN1 protein and localises to the plant plasma membrane (Doehlemann *et al.*, 2009).

Although we were able to confirm and visualise the EIHM, it is not clear at this stage whether the structure of the EIHM differs in nature to that of non-infected plant plasma membrane.

Biotrophic oomycete plant pathogens such as the filamentous *Hyaloperonospora arabidopsis* (Hpa) and the late blight pathogen *Phytophthora infestans* form haustoria within host cells, which are specialised pathogenic hyphae required for suppression of host defence responses and the acquisition of nutrients (O’Connell and Panstruga, 2006). As oomycetes grow within host cells, haustoria become enveloped by a plant-derived plasma membrane known as the Extra-Haustorial Membrane (EHM) which represents an immediate interface between the pathogen and host. This EHM is tethered to the neck bands at the site of host cell entry, and the sealed compartment between the EHM and the oomycete referred to as the Extra Haustorial Matrix (EHMx) (Bushnell, 1972). The EHM was initially thought to be an extension of the plant plasma membrane formed by invagination (Koh *et al.*, 2005; O’Connell and Panstruga, 2006), although recent evidence has suggested that the EHM has a distinct membrane structure to that of the plant plasma membrane (Micali *et al.*, 2011; Lu *et al.*, 2012). During powdery mildew infection of *Arabidopsis thaliana* by the oomycete pathogen *Golovinomyces orontii*, the EHM could not be labelled by eight plasma membrane-specific antibodies. In contrast, the plant resistance protein RPW8.2 was specifically recruited to the EHMs of mature haustoria, suggesting that the EHM is a specialized membrane that is modified and distinct from the bulk plasma membrane (Micali *et al.*, 2011). Further to this, transient expression of fluorescently-labelled YFP-PIP1:4, a plant aquaporin, and ACA8-GFP, a calcium-driven ATPase, in *A. thaliana* demonstrate that these proteins are resident within the non-infected plant plasma membrane but are excluded from the EHM during Hpa infection. In contrast, transient expression of fluorescently labelled PEN1-GFP, a plant syntaxin, and FLS2-GFP, a membrane receptor kinase that recognises the bacterial PAMP Fls2, accumulates at the EHM and the plasma membrane (Lu *et al.*, 2012). These reports highlight that there are both differences and similarities in the nature of the plant proteins that are recruited to the EHM compared with the plant plasma membrane (Lu *et al.*, 2012). Further localisation of native rice plasma membrane proteins will be critical to establish if the nature of the EHM is distinct from the rice plasma membrane in a similar way that the EHM is different from the plasma membrane. This might

include the expression and localisation of fluorescently-labelled pathogenesis-related membrane proteins, such as the Chitin-Elicitor Binding Protein (CEBiP) receptor (Kaku *et al.*, 2006).

In addition to understanding how host cell structures become altered to accommodate biotrophic invasive hyphae, we were interested in characterising the membrane structure around the Biotrophic Interfacial Complex (BIC). First reports on the BIC were provided by Kankanala *et al.* (2007), in which the apical tips of primary invasive hyphae were observed to contain highly membranous caps when treated with the membrane tracker dye FM4-64. Using fluorescent markers, a number of Biotrophy Associated (Bas) proteins and avirulence effector proteins such as Avr-Pita were shown to accumulate at the tips of these filamentous primary hyphae (Mosquera *et al.*, 2009). At this stage, the polarised nature in which these effectors are secreted implicates the Spitzenkörper, polarisome and exocyst components for their delivery and subsequent translocation (Harris *et al.*, 2005; Virag and Harris, 2006; Steinberg, 2007; Shoji *et al.*, 2008; Brand and Gow, 2009). As invasive hyphae continue to grow within host cells, primary filamentous hyphae differentiate into secondary pseudohyphae that are more bulbous in morphology (Kankanala *et al.*, 2007). At this stage, fluorescently-labelled effector proteins continue to accumulate within the BIC, which now occupies a sub-apical position on the side of secondary pseudohyphae. Interestingly, Fluorescence Recovery After Photobleaching (FRAP) experiments have demonstrated that fluorescently-labelled effectors continue to accumulate at sub-apical BICs, raising speculation that the original ER-dependent secretory apparatus remains next to the BIC after primary hyphae have differentiated into secondary hyphae (Khang *et al.*, 2010). The correlation between the accumulation of BIC-localised effectors within host cytoplasm has raised the hypothesis that the BIC is the portal for delivery and entry of rice blast effectors into the host cytoplasm, although it is not currently known how these effector molecules are secreted into the BIC (Khang *et al.*, 2010; Valent and Khang, 2010).

Initial experiments using a *M. oryzae* strain expressing the BIC marker *PWL2:mRFP* (Khang *et al.*, 2010) demonstrated complete co-localisation between the plant cell membrane and endoplasmic reticulum with the BIC (Figure 5.11), confirming previous observations that the

BIC is a highly membranous structure (Kankanala *et al.*, 2007; Mosquera *et al.*, 2009). Following on from these observations, we reasoned that the BIC could be a plant-based rather than a fungal-based structure (Kankanala *et al.*, 2007). As fungal cytoplasm appeared incapable of diffusing into the BIC (Figure 5.13), we hypothesised that the BIC could be separate membrane-bound structure and we were prompted to define the limits of a fungal hypha in relation to the BIC. We generated the fungal plasma membrane marker *PMA1:GFP* which appropriately labelled the fungal plasma membrane both *in vitro* (Figure 5.15) and during biotrophic growth (Figure 5.16). As demonstrated by Figure 5.16, the BIC appeared to reside outside the limits of the fungal plasma membrane, providing evidence that the BIC is plant-based in nature rather than fungal. In light of these results, further fungal plasma membrane markers are needed to confirm this observation. One such marker might include the *M. oryzae* homologue of the *Ustilago maydis* protein Sso1, which has previously been shown to localise to the fungal plasma membrane (Schuster *et al.*, 2011). At this stage, we cannot rule out that a fungal-derived plasma membrane surrounds the BIC and the *M. oryzae* Pma1 protein is merely excluded from here due to the nature of its function and pattern of localisation.

The rice lines generated here will be a useful tool in the future to investigate differences in HR during *M. oryzae* infection mediated by a Pii / AVR-Pii interaction when transgenic plants are inoculated with the recently identified *M. oryzae* isolates TH68-140 and TH68-126 (Yoshida *et al.*, 2009). The transgenic rice lines will be key to investigate non-host resistance responses in rice (Li *et al.*, 2011), of which relatively little is known. The presence of autofluorescence emanating from the plant cell wall is a feature indicative of the hypersensitive response (Koga *et al.*, 1988; Zellerhoff *et al.*, 2006). During this HR response, a thickening of the plant cell wall was observed, consistent with an incompatible response (data not shown). Preliminary experiments reported here suggest that the host nucleus is recruited to the site of conidial attachment and appressorium formation during an HR response. Migration of host nuclei to the haustorial site of *Blumeria graminis* has previously been observed upon infection of *Arabidopsis thaliana* (Glawe, 2008).

Chapter 6. General Discussion

Although the genetic determinants of appressorium formation in *M. oryzae* have been well described (for reviews see Talbot, 2003; Caracuel-Rios and Talbot, 2007; Wilson and Talbot, 2009), relatively little is understood about the biotrophic growth phase of *M. oryzae*, or the function and secretion of effector proteins during this stage of the lifecycle (Jia *et al.*, 2000; Kankanala *et al.*, 2007; Mosquera *et al.*, 2009; Khang *et al.*, 2010). This study aimed to broaden our understanding of the biotrophic growth phase of the rice blast fungus and to understand how and why effector proteins are secreted by *M. oryzae* during intracellular biotrophic growth. Two main objectives were set out to achieve this. The first involved the functional characterisation and localisation of a secreted LysM effector protein, Slp1, whilst the second involved defining the nature of the plant-fungal interface during early host cell colonisation using a suite of genetically engineered transgenic rice lines.

Plants contain membrane-bound receptors known as pattern-recognition receptors (PRRs) and these receptors act as a first line of defence to enable pathogen detection (Collmer and Alfano, 2004; Jones and Dangl, 2005; Kaku *et al.*, 2006; de Jonge *et al.*, 2010; Kishimoto *et al.*, 2010; Zipfel and Robatzek, 2010; Thomma *et al.*, 2011). Binding of conserved pathogen-derived molecules, known as pathogen associated molecular patterns (PAMPs), to PRRs results in the initiation of plant immune signalling cascades (Torres *et al.*, 2006). One of the earliest manifestations of this response is the release of reactive oxygen species (ROS) such as superoxide radicals (O_2^-), and its dismutation product, hydrogen peroxide (Wojtaszek *et al.*, 1997; Mellersh *et al.*, 2002; Torres *et al.*, 2006). During *M. oryzae* infection, the release of ROS has been detected at the site of conidial attachment of *M. oryzae* to the leaf surface (Pasechnik *et al.*, 1998). Binding of PAMPs to PRRs initiates a plant immune response, referred to as PAMP-triggered immunity (PTI). To overcome PTI, plant pathogenic organisms secrete cytoplasmic effectors which suppress plant PTI, resulting in effector-triggered susceptibility (ETS). Effector-triggered immunity (ETI) occurs when the plant deploys cytoplasmic resistance (R) gene products which bind either directly or indirectly to plant pathogen cytoplasmic effectors (Jones and Dangl, 2006). One such PRR in rice is the membrane receptor CEBiP, a chitin-binding

LysM glycoprotein which, upon binding chitin oligosaccharides, acting as a PAMP, initiates a PTI in which ROS are released and defence-related genes are transcribed (Yamaguchi *et al.*, 2005; Kaku *et al.*, 2006). During *M. oryzae* infection, it is thought that release of chitin oligosaccharides from invasive hyphae can act as elicitors, causing the plant to mount a resistance response including the release of ROS (Kishimoto *et al.*, 2010). Recent evidence has suggested that an additional LysM glycoprotein receptor kinase OsCERK interacts co-operatively with CEBiP to initiate immune responses (Shimzu *et al.*, 2010). Although the precise relationship between CEBiP and OsCERK1 has yet to be determined, immunoprecipitation assays using a membrane preparation from rice cells have indicated that CEBiP and OsCERK1 form a receptor complex, which was confirmed using yeast two hybrid analysis that indicated that CEBiP and OsCERK1 can form hetero or homo-dimers (Shimizu *et al.*, 2010). In *Arabidopsis thaliana*, two LysM receptor proteins, LYM1 and LYM3 CERK1, have been shown to bind bacterial-derived peptidoglycans, and thereby mediate detection and immune responses to Gram positive and Gram negative bacteria (Willmann *et al.*, 2011). Chitin oligosaccharides released from *M. oryzae* hyphal tips can be detected by CEBiP (Kaku *et al.*, 2006; Kishimoto *et al.*, 2010), although it has yet to be confirmed whether CEBiP resides on the invaginated EIHM formed around *M. oryzae* hyphae during intracellular growth (Kankanala *et al.*, 2007). Confirmation of CEBiP at the EIHM could be achieved by stable expression of fluorescently labelled CEBiP in rice cells during infection by *M. oryzae*.

We wanted to investigate the way in which *M. oryzae* overcomes chitin-induced defence responses. Plant-derived ROS can have anti-microbial properties (Levine *et al.*, 1994), and we were therefore interested in examining the strategies deployed by *M. oryzae* to overcome such a potential barrier to infection. Initial interrogation of the *M. oryzae* genome (Dean *et al.*, 2005), enabled us to identify two putative secreted proteins containing LysM domains, which have previously been shown to have peptidoglycan and polysaccharide binding properties, including the ability to bind chitin (Buist *et al.*, 2008; Nakagawa *et al.*, 2011; Bensmihen *et al.*, 2011). The *M. oryzae* genome encodes seven proteins with predicted LysM domains (Dean *et al.*, 2005), although the function of only one of these, a putative CVNH-LysM lectin, has thus far

been examined (Koharudin *et al.*, 2011). I named these LysM proteins Slp1 and Slp2, for Secreted LysM Proteins 1 and 2, which both share significant peptide sequence homology to the *Cladosporium fulvum* effector protein Ecp6 (Bolton *et al.*, 2008; de Jonge *et al.*, 2010). We were able to generate recombinant Slp1 protein using heterologous expression in the *Pichia pastoris* system (Kombrink, 2012). Slp1 was found to have chitin-binding properties, but does not protect fungal hyphae from hydrolysis by exogenous chitinase enzymes, in contrast to the previously described *C. fulvum* effector Avr4 (Van den Burg *et al.*, 2006; van Esse *et al.*, 2007). Initial experiments on tomato cell suspensions demonstrated that Slp1 was capable of suppressing chitin-induced medium alkalinisation (Felix *et al.*, 1993; de Jonge *et al.*, 2010), which prompted us to test whether Slp1 was also capable of suppressing chitin-induced responses in its native host. We demonstrated that in rice cells, Slp1 suppressed the chitin-triggered oxidative burst and defence gene expression, including *PAL1* and *rBT*. Previous work on *C. fulvum*, suggested that the effector protein Ecp6 is also capable of suppressing the chitin-triggered oxidative burst and host defence gene expression (de Jonge *et al.*, 2010), suggesting that such effectors might share a common evolutionary ancestor. Targeted gene replacement of *SLP1* resulted in null mutants that were significantly reduced in virulence. In contrast to studies on the *C. fulvum* effector Ecp6 (de Jonge *et al.*, 2010), we were able to confirm that the reduced virulence phenotype of $\Delta slp1$ could be restored when inoculated onto CEBiP RNAi rice lines (Kaku *et al.*, 2006). This idea was consistent with our observation that Slp1 competes with CEBiP for chitin-binding. I propose here that the reduced virulence phenotype of the $\Delta slp1$ null mutant is therefore a direct consequence of competition with CEBiP for chitin scavenging. A model explaining the proposed relationship between Slp1 and CEBiP is presented in Figure 6.1.

Using a genetically engineered reporter strain of *M. oryzae* which expresses *SLP1::GFP*, we examined the sub-cellular localisation of Slp1, which was found to accumulate around the tips of biotrophically growing hyphae in the space between the EIHM and the fungal plasma membrane (Kankanala *et al.*, 2007; Mosquera *et al.*, 2009). Significantly, the release of chitin oligosaccharides is most likely to occur at the tips of biotrophic hyphae, and the inability to restore the virulence phenotype of the $\Delta slp1$ mutant by complementation with the *SLP1*²⁷⁻

¹⁶²:*GFP* construct supports a functional role for Slp1 at the plant-fungal interface where detection of chitin by the plant is most likely to occur. Interestingly, expression of *SLP1* could not be confirmed in axenic culture, a feature which is consistent with a role for Slp1 as a secreted *M. oryzae* effector protein (Mosquera *et al.*, 2009). Previous studies in which transcriptional profiling of *M. oryzae* during biotrophic growth was performed, demonstrated that *SLP1* is more highly expressed by biotrophic intracellular hyphae compared to mycelium grown *in vitro*, and results presented here are consistent with this observation (Mosquera *et al.*, 2009). Slp1:*GFP* was observed to outline intracellular growing hyphae, but did not localise with symplastic delivered effector proteins, including fluorescently labelled Pwl2:mRFP and Avr-Pia:¹⁻¹⁹mRFP at the Biotrophic Interfacial Complex (BIC) (Mosquera *et al.*, 2009; Yoshida *et al.*, 2009; Khang *et al.*, 2010). We were able to demonstrate, however, that Slp1:*GFP* co-localises with the putative apoplastic effector protein BAS4:mRFP, which accumulates uniformly around biotrophic hyphal tips (Mosquera *et al.*, 2009; Khang *et al.*, 2010). I therefore propose that Slp1 is an apoplastic effector protein (Mosquera *et al.*, 2009). Using surface plasmon resonance technology, we also showed that Slp1 has a high affinity for chitin oligosaccharides with similar binding affinities to that of the *C. fulvum* effector protein Ecp6 (Mentlak *et al.*, 2012a). We therefore cannot currently rule out the possibility that Slp1:*GFP* localises exclusively to the apoplast as Slp1 may become integrated into the extracellular cell wall matrix as it is secreted at hyphal tips. Immuno-localisation and ultra-structural localisation of Slp1 during biotrophic growth will help to establish the extent of assembly of Slp1 in the cell wall or extracellular matrix, or whether Slp1 is freely secreted into the external milieu of the apoplastic space. Further assays in which attachment of an NLS-coding region to *SLP1:GFP* will also help to confirm or refute the hypothesis of a host cytoplasmic target for Slp1.

Although we were able to confirm the localisation of Slp1 at the hyphal tips of biotrophic hyphae, further experiments are required to understand which molecular secretion signals dictate whether an effector is directed to the apoplastic space or to the BIC. In this study, we attempted to re-configure the molecular mechanisms of Slp1 secretion by genetic manipulation. Attempts to re-direct Slp1:*GFP* to the BIC by replacement of the Slp1 secretion peptide with the

BIC-localised Avr-Pia signal peptide were unsuccessful. Future experiments should focus on the contribution of promoter and upstream un-translated regions (5'UTR) of effector-encoding genes. Such experiments should focus on alternating the *SLP1* promoter with the promoter from a BIC-localised symplastic effector-encoding gene to determine if the promoter sequence contributes to preferential BIC-localisation.

Several independent lines of evidence presented here suggest that, in addition to chitin, Slp1 has the capacity to form homo-dimers. Co-precipitation assays with insoluble chitin initially demonstrated that Slp1 was able to bind chitin. Multiple bands were, however, present in these precipitation assays, and mass-spectrometry analysis was performed to confirm that these bands corresponded to recombinant Slp1 protein and were not indeed artefacts from the *Pichia pastoris* over-expression system (Kombrink, 2012). In order to test the idea of Slp1 dimerisation, an *SLP1* cDNA was cloned into the bait and prey vectors, and yeast-two hybrid analysis was performed. Yeast-two hybrid analysis confirmed a potential Slp1-Slp1 interaction under high-stringency conditions, suggesting that Slp1 had a high affinity for homo-dimerisation. Finally, we removed a nucleotide sequence from the coding region of *SLP1* encoding the initial 27 amino acids, and expressed this allele in *M. oryzae* as a translational fusion to GFP. Mis-localisation of the fluorescent signal within the fungal cytoplasm was manifested as large aggregates, and I propose that this corresponds to Slp1 aggregation within the fungal cytoplasm. Although not clear at this stage, Slp1 dimerisation might be important as an additional means of preventing chitin oligosaccharides from reaching CEBiP, which would otherwise result in the initiation of a plant immune response (Yamaguchi *et al.*, 2005; Kaku *et al.*, 2006). For instance, Slp1 polymerisation might shield the fungal cell wall more efficiently and in the apoplast, presenting a greater surface area for chitin oligomer binding. We are currently co-crystallising Slp1 with chitin oligosaccharides (GlcNAc)₈ to attempt to answer this question.

During the biotrophic growth phase of the rice blast fungus, the plant plasma membrane is not breached by *M. oryzae*, and is thought instead to become invaginated, establishing the Extra Invasive Hyphal Membrane (EIHM) which becomes tightly apposed (in close proximity)

against an intracellular fungal hypha (Kankanala *et al.*, 2007). The identification of the EIHM by ultrastructural analysis helped to dispel previous contradictory reports in the literature regarding host membrane dynamics during biotrophic colonisation of host cells (Koga and Horino, 1984; Heath *et al.*, 1992). Initial reports suggested that the invasive hyphae of *M. oryzae* are separated from the host cytoplasm by an invaginated host cell membrane (Koga and Horino, 1984), whereas Heath *et al.*, (1992) suggested that *M. oryzae* invasive hyphae breach the host cell membrane and grow directly within the host cytoplasm of epidermal cells. In this study, the EIHM was visualised directly by live-cell imaging using transgenic rice lines targeting the fluorescent marker protein GFP to the plant plasma membrane (Kurup *et al.*, 2005). We were able to confirm that the EIHM is continuous around an entire intracellular biotrophic hypha. It is not clear, however, if the nature and structure of the EIHM differs from that of the bulk non-infected plant plasma membrane. To this end, it remains unclear whether *M. oryzae* forms an analogous haustorial structure in a manner similar to that of biotrophic oomycete pathogens such as the late blight pathogen *Phytophthora infestans* or *Hyaloperonospora arabidopsis* (O'Connell and Panstruga, 2006; Micali *et al.*, 2011; Lu *et al.*, 2012). During biotrophic growth, *H. arabidopsis* and *P. infestans* form specialised pathogenic hyphae, known as haustoria, which are required for suppression of host defence responses and the acquisition of nutrients (O'Connell and Panstruga, 2006). As oomycetes grow within a host cell, haustoria become enveloped by a plant-derived plasma membrane known as the Extra-Haustorial Membrane (EHM), and recent evidence has suggested that the EHM has a distinct membrane structure to that of a non-infected plant plasma membrane (Micali *et al.*, 2011; Lu *et al.*, 2012). During powdery mildew infection of *Arabidopsis thaliana* by the oomycete pathogen *Golovinomyces orontii*, the EHM could not be labelled by eight plasma membrane-specific antibodies, including antibodies which recognise membrane resident proteins such as aquaporins. In contrast, the plant resistance protein RPW8.2 was specifically recruited to the EHM of haustoria, suggesting that the EHM is a specialized membrane that is modified and distinct from the bulk plasma membrane (Micali *et al.*, 2011). Further to this, transient expression of fluorescently labelled PEN1-GFP, a plant syntaxin, and FLS2-GFP, a membrane

receptor kinase that recognises the bacterial PAMP Flg22, accumulates at the EHM and the plasma membrane (Lu *et al.*, 2012).

We were able to confirm that the rice plasma membrane and endoplasmic reticulum accumulates at the Biotrophic Interfacial Complex (BIC), a membrane-rich sub-apical structure apposed to fungal invasive hyphae which accumulates fluorescently labelled effectors during biotrophic growth (Mosquera *et al.*, 2009; Khang *et al.*, 2010). It is not clear at this stage whether the BIC is a portal for effector delivery into the host cytoplasm, as suggested (Valent and Khang, 2010), and the structure of the BIC has yet to be confirmed (Khang *et al.*, 2010). Using a *M. oryzae* reporter strain which localises GFP to the fungal plasma membrane, I have shown here that the BIC resides outside the fungal plasma membrane and cell wall, suggesting that the BIC is made exclusively of plant cellular material. Localising other fungal plasma membrane proteins around the BIC will enable us to confirm this observation. The inability of fungal cytoplasmically expressed GFP to diffuse freely into the BIC provides further support to the hypothesis that the BIC is a plant-based structure. Transformation of the rice cultivars *Oryza sativa* cv. *sasanishiki* and *O. sativa* cv. *hitomebore* will, in future, help to understand how host cellular components change during compatible and incompatible interactions by inoculation of the recently identified *M. oryzae* strains TH68-126 and TH68-140 respectively (Yoshida *et al.*, 2009). The rice cultivar *O. sativa* cv. *sasanishiki* expresses the rice blast resistance gene *Pia*, whereas the rice cultivar *O. sativa* cv. *hitomebore* expresses the rice blast resistance gene *Pii* (Yoshida *et al.*, 2009). During infection, the *M. oryzae* isolate TH68-126 expresses the avirulence gene *AVR-Pii*, whilst the TH68-140 isolate expresses the avirulence gene *AVR-Pia* (Yoshida *et al.*, 2009). The availability of transgenic rice lines which target the fluorescent marker GFP to various cellular components will in future serve as a useful tool in which to study compatible and incompatible interactions, as well as non-host resistance responses, of which relatively little is known. An understanding of how the plant cytoskeleton changes during rice blast infection will also be facilitated by expression of the LifeAct:GFP and KMD:RFP constructs (Deeks *et al.*, 2010) in rice, which is currently underway. Indeed, further research is required to understand the nature of plant-fungal interface during rice blast infection. Future

research should focus on understanding the nature of endocytosis and uptake of symplastic effector proteins by the plant. This will be facilitated by expression of fluorescently labelled Ara6 and Ara7, two Rab GTPase which are involved in the endocytic pathways in *A. thaliana* (Euda *et al.*, 2001; Nielsen *et al.*, 2008). A greater understanding of how *M. oryzae* secretes effector proteins is required, particularly to understand how effector delivery and secretion occurs. Identification of the fungal Spitzenkörper, polarisome and exocyst components in relation to the BIC, will also help to understand the significance of the BIC in effector secretion and to understand how the delivery of apoplastic and symplastic effector proteins compares.

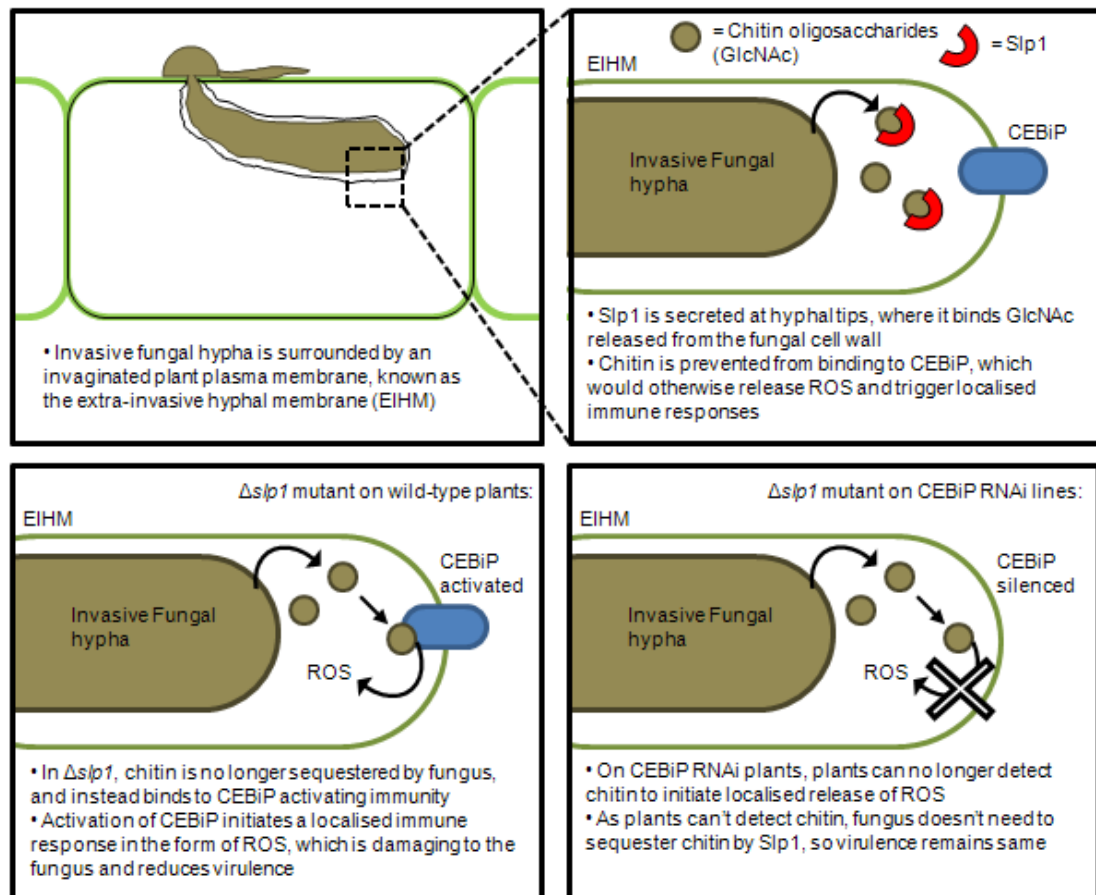


Figure 6.1 Hypothetical model describing the relationship between Slp1 and CEBiP

Chapter 7. Bibliography

- Adachi, K. and Hamer, J. E. (1998) Divergent cAMP signalling pathways regulate growth and pathogenesis in the rice blast fungus *Magnaporthe grisea*. *Plant Cell*, **10**: 1361-1373
- Agrios, G. N. (1997) *Plant Pathology*. San Diego: Academic Press
- Altschul, S. F., Gish, W., Miller, W., Myers, E. W. and Lipman, D. J. (1990) Basic Local alignment search tool. *Journal of Molecular Biology*, **215**: 403-410
- Alfano, J. R., and Collmer, A. (2004) Type III secretion system effector proteins: Double agents in bacterial disease and plant defense. *Annual Review of Phytopathology*, **42**: 385-414.
- Ballini, E., Morel, J. –B., Droc, G., Price, A., Courtois, B., Nottegham, J. –L. and Tharreau, D. (2008) A genome-wide meta-analysis of rice blast resistance genes and quantitative trait loci provides new insights into partial and complete resistance. *Molecular Plant Microbe Interactions*, **21**: 859-868
- Baluska, F., Simaj, J., Napier, R. and Volkmann, D. (1999) Maize calreticulum localizes preferentially to plasmodesmata in root apex. *The Plant Journal*, **19**: 481-488
- Barr, M. E. (1977) *Magnaporthe*, *Telimenella* and *Hyponectria* (Phycosporiaceae). *Mycologia*, **69**: 952-966
- Bateman, A. and Bycroft, M. (2000) The structure of the LysM domain from *E. coli* membrane-bound lytic murein transglycosylase D (MltD). *Journal of Molecular Biology* **299**: 1113-1119
- Batoko, H., Zheng, H-Q., Hawes, C. and Moore, I. (2000) A Rab1 GTPase is required for transport between the endoplasmic reticulum and Golgi apparatus and for normal Golgi movement in plants. *The Plant Cell*, **12**: 2201-2217
- Basu, S. K., Dutta, M., Goyal, A., Bhormik, P. K., Kumar, J., Nandy, S., Scagliusi, S. M. and Prasad, R. (2010) Is genetically modified the answer for the next green revolution? *GM crops*, **1**: 68-79
- Bensmihen, S., de Billy, F. and Gough, C. (2011) Contribution of NFP LysM domains to the recognition of Nod factors during *Medicago truncatula*/*Sinorhizobium meliloti* symbiosis. *PLoS One*, **6** PMID: 22087221
- Bernard, M. and Latgé, J. P. (2001) *Aspergillus fumigatus* cell wall: composition and biosynthesis. *Medical Mycology*, **39**: 9-17
- Birch, P. R. J., Armstrong, M., Bos, J., Boevink, P., Gilroy, E. M., Taylor, R. M., Wawra, S., Pritchard, L., Conti, L., Ewan, R., Whisson, S. C., van West, P., Sadanandom, A. and Kamoun, S. (2009) Towards understanding the virulence functions of RXLR effectors of the oomycete plant pathogen *Phytophthora infestans*. *Journal of Experimental Botany*, **60**: 1133-1140
- Bölker, M. (1998) Sex and crime: heterotrimeric G proteins in fungal mating and pathogenesis. *Fungal Genetics and Biology*, **25**: 143-156
- Boller, T. and Felix, G. (2009) A renaissance of elicitors: perception of microbe-associated molecular patterns and danger signals by pattern recognition receptors. *Annual Review of Plant Biology*, **60**: 379-406

- Bolton, M. D., van Esse, H. P., Vossen, J. H., de Jonge, R., Stergiouopoulos, I., Stulemeijer, I. J. E., van den Burg, G. C. M., Borrás-Hidalgo, O., Dekker, H. L., de Wit, P. J. G. M., Joosten, M. H. A. J. And Thomma, B. H. J. (2008) The novel *Cladosporium fulvum* lysine motif effector Ecp6 is a virulence factor with orthologues in other fungal species. *Molecular Microbiology*, **69**: 119-136
- Bourett, T. M. and Howard, R. J. (1990) *In vitro* development of penetration structures in the rice blast fungus *Magnaporthe grisea*. *Canadian Journal of Botany*, **68**: 329-342
- Boyd, C., Hughes, T., Pypaert, M., and Novick, P. J. (2004) Vesicles carry most exocyst subunits to exocytic sites marked by the remaining two subunits, Sec3p and Exo70p. *The Journal of Cell Biology*, **167**: 889-901
- Bradley, D. J., Kjellbom, P. and Lamb, C. J. (1992) Elicitor- and wound-induced oxidative cross-linking of a proline-rich plant cell wall protein: a novel, rapid defense response. *Cell*, **10**: 21-30
- Brand, A. & Gow, N. A. R. (2009) Mechanisms of hypha orientation of fungi. *Current Opinion in Microbiology*, **12**:350-357
- Brower, S. M., Honts, J. E. and Adams, A. E. M. (1995) Genetic analysis to the fimbrin-actin binding interaction in *Saccharomyces cerevisiae*. *Genetics*, **140**: 91-101
- Browning, H., Hackney, D. D. & Nurse, P. (2003) Targeted movement of cell end factors in fission yeast. *Nature Cell Biology*, **5**: 812-818
- Bruno, K. S., Tenjo, F., Li, L., Hamer, J. E. and Xu, J. R. (2004) Cellular localisation and role of kinase activity of *PMK1* in *Magnaporthe grisea*. *Eukaryotic Cell*, **3**: 1525-1532
- Buist, G., Steen, A., Kok, J. and Kuipers, O. P. (2008) LysM, a widely distributed protein motif for binding to (peptide)glycans. *Molecular Microbiology* **68**: 838-847
- Bushnell, W. R. (1972) The physiology of fungal haustoria. *Annual Review of Phytopathology*, **10**: 151-176
- Caracuel-Rios, Z. and Talbot, N. J. (2008) Silencing the crowd: high-throughput functional genomics in *Magnaporthe oryzae*. *Molecular Microbiology* **68**: 1341-1344.
- Chen, J., Zheng, W., Zheng, S., Zhang, D., Sang, W., Chen, X., Guangpu, L., Guodong, L. and Wang, Z. (2008) Rac1 is required for pathogenicity and Chm1-dependent conidiogenesis in rice fungal pathogen *Magnaporthe grisea*. *PLoS Pathogens*, **4** doi:10.1371/journal.ppat.1000202
- Chenna, R., Sugaware, H., Koike, T., Lopez, R., Gibson, T. J., Higgins, D. G. and Thompson, J. D. (2003) Multiple sequence alignment with the Clustal series of programs. *Nucleic Acids Research*, **31**: 3497-3500
- Choi, A. H. C., and O'Day, D. H. (1984) Calcofluor staining of cellulose during microcyst differentiation in wild-type and mutant stains of *Polysphondylium pallidum*. *Journal of Bacteriology*, **157**: 291-296
- Choi, W. and Dean, R. A. (1997) The adenylate cyclase *MAC1* of *Magnaporthe grisea* controls appressorium formation and other aspects of growth and development. *The Plant Cell*, **9**: 1973-1983

- Chilton, M.-D., Currier, T. C., Farrand, S. K., Bendich, A. J., Gordon, M. O. and Nester, E. W. (1974) *Agrobacterium tumefaciens* DNA and PS8 bacteriophage DNA not detected in crown gall tumors. *Proceedings of the National Academy of Science USA*, **71**: 3672-3676
- Christou, P., and Twyman, R. M. (2004) The potential of genetically enhanced plants to address food insecurity. *Nutritional Research Reviews*, **17**: 23-42
- Chumley, F. G. and Valent, B. (1990) Genetic analysis of melanin-deficient, non-pathogenic mutants of *Magnaporthe grisea*. *Molecular Plant-Microbe Interactions*, **3**: 135-143
- Cole, R. A. and Fowler, J. E. (2006) Polarizes growth: maintaining focus on the tip. *Current Opinion in Plant Biology*, **9**: 579-588
- Cutler, S. R., Ehrhardt, D. W., Griffiths, J. S. and Somerville, C. R. (2000) Random GFP:cDNA fusions enable visualization of sub-cellular structures in cells of *Arabidopsis* at a high frequency. *Proceedings of the National Academy of Science, USA*, **97**: 3718-3723
- De Datta, S. K., Tauro, A. C. and Balaoing, S. N. (1968) Effect of plant type and nitrogen level on the growth characteristics and grain yield of Indica rice in the tropics. *Agronomy Journal*, **60**: 643-647
- de Jong, J. D., McCormack, B. J., Smirnoff, N. and Talbot, N. J. (1997) Glycerol generates turgor in rice blast. *Nature*, **389**: 244-245
- de Jonge, R., van Esse, H. P., Kombrink, A., Shinya, T., Desaki, Y., Bours, R., van der Krol, S., Shibuya, N., Joosten, M. H. A. J. and Thomma, B. P. H. J. (2010) Conserved fungal LysM effector Ecp6 prevents chitin-triggered immunity in plants. *Science*, **329**: 953-955
- de Jonge, R. and Thomma, B. P. H. J. (2009) Fungal LysM effectors: Extinguishers of host immunity? *Trends in Microbiology*, **17**: 151-157
- de Wit, P. J., Mehrabi, R., Van den Burg, H. A., Stergiopoulos, I. (2009) Fungal effector proteins: past, present and future. *Molecular Plant Pathology* **10**: 735-747
- De Zwann, T. M., Carroll, A. M., Valent, B. and Sweigard, J. A. (1999) *Magnaporthe grisea* Pth11p is a novel plasma membrane protein that mediates appressorium differentiation in response to inductive substrate cues. *The Plant Cell*, **11**: 2013-2030
- Dean, R. A., Talbot, N. J., Ebbole, D. J., Farman, M. L., Mitchell, T. K., Orbach, M. J., Thon, M., Kulkarni, R., Xu, J. R., Pan, H., Read, N. D., Lee, Y.-H., Carbone, I., Brown, D., Oh, Y. Y., Donofrio, N., Jeong, J. S., Soanes, D. M., Djovonic, S., Kolomiets, E., Rehmeier, C., Li, W., Harding, M., Kim, S., Lebrun, M. H., Bohnert, H., Coughlan, S., Butler, J., Calvo, S., Ma, L. J., Nicol, R., Purcell, S., Nusbaum, C., Galagan, J. E. and Birren, B. W. (2005) The genome sequence of the rice blast fungus *Magnaporthe grisea*. *Nature*, **434**: 980-986
- Deeks, M. J., Fenrych, M., Smertenko, A., Bell, K. S., Oparka, K., Cvr Kova, F., Arsk, V. and Hussey, P. J. (2010) The plant formin AtFH4 interacts with both actin and microtubules, and contains a newly identified microtubule-binding domain. *Journal of Cell Science*, **123**: 1209-1215

- Denecke, J., De Rycke, R. and Botterman, J. (1992) Plant and mammalian sorting signals for protein retention in the endoplasmic reticulum contain a conserved epitope. *EMBO Journal*, **11**: 2345-2355
- Dereeper, A., Guignon, V., Blanc, G., Audic, S., Buffet, S., Chevent, F., Dufavard, J. F., Guindon, S., Lefort, V., Lescot, M., Claverie, J. M. and Gascuel, O. (2008) Phylogeny.fr: Robust phylogenetic analysis for the non-specialist. *Nucleic Acids Research*. **36** (Web server issue): W465-W469
- Desaki, Y., Miya, A., Venkatesh, B., Tsuyuma, S., Yamane, H., Kaku, H., Minami, E. and Shibuya, N. (2006) Bacterial lipopolysaccharides induce defence responses associated with programmed cell death in rice cells. *Plant Cellular Physiology*, **47**: 1530-1540
- Dixon, M. S., Jones, D. A., Keddie, J. S., Thomas, C. M., Harrison, K. and Jones, J. D. G. (1996) The tomato Cf-2 disease resistance locus comprises two functional genes encoding leucine-rich repeat proteins. *Cell*, **84**: 451-459
- Doehlemann, G., van der Linde, K., Asmann, D., Schwammbach, D., Hof, A., Mohanty, A., Jackson, D. and Kahmann, R. (2009) Pep1, a secreted effector protein of *Ustilago maydis*, is required for successful invasion of plant cells. *PLoS Pathogens*, **5**: doi:10.1371/journal.ppat.1000290
- Ebbole, D. J. (2007) *Magnaporthe* as a model for understanding host-pathogen interactions. *Annual Review of Phytopathology*, **45**: 437-456
- Egan, M. J., Wang, Z.-Y., Jones, M. A., Smirnov, N., Talbot, N. J. (2007) Generation of reactive oxygen species by fungal NADPH oxidases is required for rice blast disease. *Proceedings of the National Academy of Science, USA*, **104**: 11772-11777.
- Egan, M. J. and Talbot, N. J. (2008) Genomes, free radicals and plant cell invasion: recent developments in plant pathogenic fungi. *Current Opinion in Plant Biology* **11**: 367-372
- Ellis, J. G. and Dodds, P. N. (2011) Showdown at the RXLR motif: serious differences of opinion in how effector proteins from filamentous eukaryotic pathogens enter plant cells. *Proceedings of the National Academy of Science USA*, **108**: 14381-14382
- Food and Agricultural Organization (2009) How to feed the world in 2050
- Felix, G., Grosskopf, D. G., Regenass, M., Basse, C. W. and Boller, T. (1991) Elicitor-induced ethylene biosynthesis in tomato cells. *Plant Physiology*, **97**: 19-25
- Felix, G., Regenass, M. and Boller, T. (1993) Specific perception of sub-nanomolar concentration of chitin fragments by tomato cells: induction of extracellular alkalisation, changes in protein phosphorylation, and establishment of refractory state. *Plant Journal*, **4**: 307-316
- Felix, G., Duran, J. D., Volko, S. and Boller, T. (1999) Plants have a sensitive perception system for the most conserved domain of bacterial flagellin. *Plant Journal*, **18**: 265-276
- Felsenstein, J. (1981) Evolutionary trees from DNA sequences – A maximum likelihood approach. *Journal of Molecular Evolution*, **17**: 368-376
- Feinburg, A. P. and Vogelstein, B. (1983) A technique for radiolabelling DNA restriction endonuclease fragments to high specific activity. *Analytical Biochemistry*, **132**: 6-13

- France, Y. E., Boyd, C., Coleman, J., and Novick, P. J. (2006) The polarity-establishment component Bem1p interacts with the exocyst complex through the Sec15p subunit. *Journal of Cell Science*, **119**: 876-888
- Garvey, K. J., Saedi, M. S. and Ido, J. (1986) Nucleotide sequence of *Bacillus* phage phi 29 genes 14 and 15: homology of gene 15 with other phage lysozymes. *Nucleic Acids Research*, **14**: 10001-10008
- Gilbert, R. D., Johnson, A. M. and Dean, R. (1996) Chemical signals responsible for appressorium formation in the rice blast fungus *Magnaporthe grisea*. *Physiological and Molecular Plant Pathology*, **48**: 335-346
- Gilden, J. K., Peck, S., Chen, Y-C. M. and Krummel, M. F. (2012) The septin cytoskeleton facilitates membrane retraction during motility and blebbing. *Journal of Cell Biology*, **196**: 103-114
- Gietz, D., Stjean, A., Woods, R. A. and Sciestl, R. H. (1992) Improved method for high-efficiency transformation of intact yeast cells. *Nucleic Acids Research*, **20**: 1425-1425
- Gilbert, M.J., Thornton, C.R., Wakley, G.E., Talbot, N.J. (2006) A P-type ATPase required for rice blast disease and induction of host resistance. *Nature*, **440**: 535-539
- Glawe, D. A. (2008) The powdery mildews: a review of the World's most familiar (yet poorly known) plant pathogens. *Annual Review of Phytopathology*, **46**: 27-51
- Godfray, H. C. J., Beddington, J. R., Crute, I. R., Haddad, L., Lawrence, D., Muir, J. F., Pretty, J., Robinson, S., Thomas, S. M. and Toulmin, C. (2010) Food security: the challenge of feeding 9 billion people. *Science*, **327**: 812-818
- Goff, S. A. (1999) Rice as a model for cereal genomics. *Current Opinion in Plant Biology*, **2**: 86-89
- Guo, W., Roth, D., Walch-Solimena, C. and Novick, P. J. (1999) The exocyst is an effector for Sec4p, targeting secretory vesicles to sites of exocytosis. *The EMBO Journal*, **18**: 1071-1080
- Gurr, S. J., Unkles, S. E. and Kinghorn, J. R. (1987) The structure and organization of nuclear genes of filamentous fungi. In *Gene Structure in Eukaryotic Microbes*, pgs 93-139. Edited by J. R. Kinghorn. Oxford: IRL Press
- Hall, P. A., Hilary-Russell, S. E. and Pringle, J. R. (2008) *The septins*. John Wiley and Sons.
- Hamer, J. E., Howard, R. J., Chumley, F. G. and Valent, B. (1988) A mechanism for surface attachment in spores of a plant pathogenic fungus. *Science*, **239**: 288-290
- Harrington, B. J. and Hageage, G. J. (1991) Calcofluor white: tips for improving its use. *Clinical Microbiology Newsletters*, **13**: 3-5
- Harris, S. D., Read, N. D., Robertson, R. W., Shaw, B., Seiler, S., Plamann, M. and Momany, M. (2005) Polarisome meets Spitzenkörper: microscopy, genetics and genomics coverage. *Eukaryotic Cell*, **4**: 225-229
- He, B. & Guo, W. (2009) The exocyst complex in polarized exocytosis. *Current Opinion in Cell Biology*, **21**: 537-542

- Heath, M. C., Howard, R. J., Valent, B. and Chumley, F. G. (1992) Ultrastructural interactions of one strain of *Magnaporthe grisea* with goosegrass and weeping lovegrass. *Canadian Journal of Botany*, **70**: 779-787
- Heath, M. C., Valent, B., Howard, R. J. and Chumley, F. G. (1990) Interactions of two strains of *Magnaporthe grisea* with rice, goosegrass and weeping lovegrass. *Canadian Journal of Botany*, **68**: 1627-1637
- Hibberd, J. M., Sheehy, J. and Langdale, J. A. (2008) Using C4 photosynthesis to increase the yield of rice – rationality and feasibility. *Current Opinion in Plant Biology*, **11**: 228-231
- Hiei, Y., Ohta, S., Komari, T. and Kumashiro, T. (1994) Efficient transformation of rice (*Oryza sativa* L.) mediated by *Agrobacterium* and sequence analysis of the T-DNA. *Plant Journal*, **6**: 271-282
- Hiei, Y. and Komari, T. (2008) *Agrobacterium*-mediated transformation of rice using immature embryos or calli induced from mature seed. *Nature Protocols*, **3**: 824-834
- Hill, J., Donald, K. and Griffiths, D. E. (1991) DMSO-enhanced whole cell yeast transformation. *Nucleic Acids Research*, **19**: 5791-5791
- Hoefle, C. and Hückelhoven, R. (2008) Enemy at the gates: traffic at the plant cell pathogen interface. *Cellular Microbiology*, **10**: 2400-2407
- Hogenhout, S. A., Van der Hoorn, R. A. L., Terauchi, R. and Kamoun, S. (2009) Emerging concepts in effector biology of plant-associated organisms. *Molecular Plant-Microbe Interactions*, **22**: 115-122
- Howard, R. J., Ferrari, M. A., Roach, D. H., and Money, N. P. (1991) Penetration of hard substances by a fungus employing enormous turgor pressures. *Proceedings of the National Academy of Science USA*, **88**: 11281-11284
- Ito, H., Fukuda, Y., Murata, K. and Kimura, A. (1983) Transformation of intact yeast-cells treated with alkaline cations. *Journal of Bacteriology*, **153**: 163-168
- Jensen, R. E. and Johnson, A. E. (1999) Protein translocation: is Hsp70 pulling my chain? *Current Biology*, **21**: 779-782
- Jeon, J., Park, S.-Y., Chi, M.-H., Choi, J., Park, J., Rho, H.-S., Kim, S., Goh, J., Yoo, S., Choi, J., Park, J.-Y., Yi, M., Yang, S., Kwon, M.-J., Han, S.-S., Kim, B. R., Khang, C. H., Park, B., Lim, S.-E., Jung, K., Kong, S., Karunakaran, M., Oh, W.-B., Kang, S. and Lee, Y.-H. (2007) Genome-wide functional analysis of pathogenicity genes in the rice blast fungus. *Nature Genetics*, **39**: 561-565
- Jia, Y., McAdams, S. A., Bryan, G. T., Howard, H. P. and Valent, B. (2000) Direct interaction of resistance gene and avirulence gene products confers rice blast resistance. *EMBO Journal*, **19**: 4004-4014
- Jones, J. D. G. and Dangl, J. L. (2006) The plant immune system. *Nature*, **444**: 323-329
- Joosten, M. H. A. J., Bergmans, C. J. B., Meulenhoff, E. J. S., Cornelissen, B. J. C. and de Wit, P. J. G. M. (1990) Purification and serological characterization of three basic 15-kilodalton pathogenesis-related proteins from tomato. *Plant Physiology*, **94**: 585-591

- Joosten, M. H. A. J., Verbakel, H. M. Nettekoven, M. E., Van Leeuwen, J., van der Vossen, R. T. M. and de Wit, P. J. G. M. (1995) The phytopathogenic fungus *Cladosporium fulvum* is not sensitive to the chitinase and β -1,3-glucanase defence proteins of its host, tomato. *Physiological and Molecular Plant Pathology*, **46**: 45-59
- Kaku, H., Nishizawa, Y., Ishii-Minami, N., Akimoto-Tomiyama, C., Dohmae, N., Takio, K., Minami, E. and Shibuya, N. (2006) Plant cells recognize chitin fragments for defense signalling through a plasma membrane receptor. *Proceedings of the National Academy of Science, USA*, **103**: 11086-11091
- Kale, S. D., Gu, B., Capelluto, D. G. S., Dou, D., Feldman, E., Rumore, A., Arredondo, F. D., Hanlon, R., Fudal, I., Rouxel, T., Lawrence, C. B., Shan, W. and Tyler, B. (2010) External lipid PI3P mediates entry of eukaryotic pathogen effectors into plant and animal host cells. *Cell*, **142**: 284-295
- Kamoun, S. (2006) A catalogue of the effector secretome of plant pathogenic oomycetes. *Annual Review of Phytopathology*, **44**: 41-60
- Kankanala, P., Czymmek, K. & Valent, B. (2007) Roles for rice membrane dynamics and plasmodesmata during biotrophic invasion by the blast fungus. *The Plant Cell* **19**: 706-724
- Kang, S., Sweigard, J. A. and Valent, B. (1995) The *PWL* host specificity gene family in the rice blast fungus *Magnaporthe grisea*. *Molecular Plant-Microbe Interactions*, **8**: 939-948
- Kanneganti, T. D., Huitema, E., Cakir, C. and Kamoun, S. (2006) Synergistic interactions of the plant cell death pathways induced by *Phytophthora infestans* Nep1-like protein PiNPP1.1 and INF1 elicitor. *Molecular Plant-Microbe Interactions*, **19**: 854-863
- Kampinga, H. H. and Braig, E. A. (2010) The HSP70 chaperone machinery: proteins as drivers of functional specificity. *National Review of Molecular and Cellular Biology*, **11**: 579-592
- Kershaw, M.J., Wakley, G., Talbot, N.J. (1998) Complementation of the Δ *mpg1* mutant phenotype in *Magnaporthe grisea* reveals functional relationships between fungal hydrophobins. *EMBO Journal* **17**: 3838-3849
- Kershaw, M. J. and Talbot, N. J. (2009) Genome-wide functional analysis reveals that infection-associated fungal autophagy is necessary for rice blast disease. *Proceedings of the National Academy of Science, USA*, **106**: 15967-15972
- Ketelaar, T., Allwood, E. G., Anthony, R., Voigt, B., Menzel, D. and Hussey, P. J. (2004) The actin-interacting protein AIP1 is essential for actin organization and plant development. *Current Biology*, **14**: 145-149
- Khang, C. H., Park, S-Y., Lee, Y-H., Valent, B. and Kang, S. (2008) Genome organization and evolution of the *AVR-Pita* avirulence gene family in the *Magnaporthe grisea* species complex. *Molecular Plant-Microbe Interactions*, **21**: 658-670
- Khang, C. H., Berruyer, R., Giraldo, M. C., Kankanala, P., Park, S-Y., Czymmek, K., Kang, S. and Valent, B. (2010) Translocation of *Magnaporthe oryzae* effectors into rice cells and their subsequent cell-to-cell movement. *The Plant Cell* **23**: 1-16

- Kishimoto, K., Kouzai, Y., Kaku, H., Shibuya, N., Minami, E. and Nishizawa, Y. (2010) Perception of the chitin oligosaccharides contributes to disease resistance to blast fungus *Magnaporthe oryzae* in rice. *The Plant Journal*, **64**: 343-354
- Koga, H. and Horino, O. (1984) Electron microscopical observation of rice leaves infected with *Pyricularia oryzae* in compatible and incompatible combinations at the interface between invading hyphae and host cytoplasm in epidermal cells of leaf sheath. *Annual Phytopathological Society Japan*, **50**: 375-378
- Koga, H., Zeyen, R. J., Bushnell, W. R. and Ahlstrand, G. G. (1988) Hypersensitive cell death, autofluorescence and insoluble silicon accumulation in barley leaf epidermal cells under attack by *Erysiphe graminis* f.sp *hordei*. *Physiological and Molecular Plant Pathology*, **32**: 392-409
- Koh, S., André, A., Edwards, H., Ehrhardt, D., and Somerville, S. (2005) *Arabidopsis thaliana* subcellular responses to compatible *Erysiphe cichoracearum* infections. *Plant Journal*, **44**: 516-529
- Koharudin, L.M., Viscomi, A.R., Montanini, B., Kershaw, M.J., Talbot, N.J., Ottonello, S., Gronenborn, A.M. (2011) Structure-function analysis of a CVNH-LysM lectin expressed during plant infection by the rice blast fungus *Magnaporthe oryzae*. *Structure* **19**: 662-674
- Kombrink, A. (2012) Heterologous production of fungal effectors in *Pichia pastoris*. *Methods in Molecular Biology*, **835**: 209-217
- Konstrad, J. W. (1997) Virulence and cAMP in smuts, blasts and blights. *Trends in Plant Science*, **2**: 193-199
- Konzack, S., Rischitor, P. E., Enke, C., and Fischer, R. (2005) The role of the kinesin motor KipA in microtubule organization and polarized growth of *Aspergillus nidulans*. *Microbiology of the Cell*, **16**: 497-506
- Krappmann, S., Sasse, C. and Braus, G. H. (2006) Gene targeting in *Aspergillus fumigatus* by homologous recombination is facilitated in a non-homologous end-joining deficient genetic background. *Eukaryotic Cell*, **5**: 212-215
- Kruger, J., Thomas, C. M., Golstein, C., Dixon, M. S., Smoker, M., Tang, S., Mulder, L. and Jones, J. D. G. (2002) A tomato cysteine protease required for Cf-2-dependent disease resistance and suppression of autonecrosis. *Science*, **296**: 744-747
- Kulkarni, R. D., Thon, M. R., Pan, H. and Dean, R. A. (2005) Novel G-protein-coupled receptor-like proteins in the plant pathogenic fungus *Magnaporthe grisea*. *Genome Biology*, **6**: R24
- Kurup, S., Runions, J., Köhler, U., Laplaze, L., Hodge, S. and Haseloff, J. (2005) Marking cell lineages in living tissues. *The Plant Journal*, **42**: 444-453
- Langdale, J. A. (2011) C4 cycles: past, present and future research on C4 photosynthesis. *Plant Cell*, **23**: 3879-3892
- Lenne, J. M., Takan, J. P., Mgonja, M. A., Manyasa, E. O., Kaloki, P., Wanyera, N., Okwadi, J., Muthumeenakshi, S., Brown, A. E., Tamale, M. and Sreenivasaprasad, S. (2007) Finger millet blast disease management – A key entry point for fighting malnutrition and poverty in East Africa. *Outlook on Agriculture*, **36**: 101-108

- Levine, A., Tenhaken, R., Dixon, R. and Lamb, C. (1994) H₂O₂ from the oxidative burst orchestrates the plant hypersensitive disease resistance response. *Cell*, **79**: 583-593
- Leung, H., Lehtinen, U., Karjalainen, R., Skinner, D., Tooley, P., Leong, S. and Ellingboe, A. (1989) Transformation of the rice blast fungus *Magnaporthe grisea* to hygromycin B resistance. *Fungal Current Genetics*, **17**: 409-411
- Li, J., Jiang, D., Zhou, H., Li, F., Yang, J., Hong, L., Fu, X., Li, Z., Liu, Z., Li, J., Zhuang, C. (2011) Expression of RNA-interference/antisense transgenes by the cognate promoters of target genes is a better gene-silencing strategy to study gene functions in rice. *PLoS ONE*, **6**: e17444 doi:10.1371/journal.pone.0017444
- Li, H., Goodwin, P. H., Han, Q., Huang, L. and Kang, Z. (2011) Microscopy and proteomic analysis of the non-host resistance of *Oryza sativa* to the wheat leaf rust fungus, *Puccinia triticina* f. sp. *Tritici*. *Plant Cell Reports*, PMID: 22038417
- Lindeburg, M., Stavrinides, J., Chang, J. H., Alfano, J. R., Collmer, A., Dangl, J. L., Greenburg, J. T., Mansfield, J. W. and Guttman, D. S. (2005) Proposed guidelines for a unified nomenclature and phylogenetic analysis of Type III hop effector proteins in the plant pathogen *Pseudomonas syringae*. *Molecular Plant-Microbe Interactions*, **18**: 275-282
- Liu, Z.Y., Bos, J.I., Armstrong, M., Whisson, S.C., da Cunha, L., Torto-Alalibo, T., Win, J., Avrova, A. O., Wright, F., Birch, P. R. and Kamoun, S. (2005) Patterns of diversifying selection in the phytotoxin-like scr74 gene family of *Phytophthora infestans*. *Molecular Biology and Evolution*, **22**: 659-672
- Lu, Y-J., Schornack, S., Spallek, T., Geldner, N., Chory, J., Schellmann, S., Schumacher, K., Kamoun, S. and Robatzek, S. (2012) Patterns of plant subcellular responses to successful oomycete infections reveal differences in host cell reprogramming and endocytic trafficking. *Cellular Microbiology*, PMID: 22233428
- Luderer, R., Takken, F. L. W., de Wit, P. J. G. M., and Joosten, M. H. A. J. (2002) *Cladosporium fulvum* overcomes Cf-2 mediated resistance by producing truncated AVR2 elicitor proteins. *Molecular Microbiology*, **45**: 875-884
- Malz, S. and Sauter, M. (1999) Expression of two PIP genes in rapidly growing internodes of rice is not primarily controlled by meristem activity of cell expansion. *Plant Molecular Biology*, **40**: 985-995
- Marcel, S., Sawers, R., Oakeley, E., Angliker, H. and Paskowski, U. (2010) Tissue-adapted invasion strategies of the rice blast fungus *Magnaporthe oryzae*. *Plant Cell*, **22**: 3177-3187
- Mellersh, D. G., Foulds, I. V., Higgins, V. J. and Heath, M. C. (2002) H₂O₂ plays different roles in determining penetration failure in three diverse plant-fungal interactions. *Plant Journal*, **29**: 257-268
- Mentlak, T. A., Kombrink, A., Shinya, T., Ryder, L. S., Otomo, I., Saitoh, H., Terauchi, R., Nishizawa, Y., Shibuya, N., Thomma, B. P. H. J. and Talbot, N. J. (2012a) Effector-mediated suppression of chitin-triggered immunity by *Magnaporthe oryzae* is necessary for rice blast disease. *The Plant Cell*, **24**: 322-335

- Mentlak, T. A., Talbot, N. J. and Kroj, T. (2012b) Effector translocation and delivery by the rice blast fungus *Magnaporthe oryzae*. In “Effectors in plant-microbe interactions” Ed. Francis Martin and Sophien Kamoun. Wiley Blackwell Press.
- Micali, C. O., Neumann, U., Grunewald, D., Panstruga, R., and O'Connell, R. (2011) Biogenesis of a specialized plant-fungal interface during host cell internalization of *Golovinomyces orontii* haustoria. *Cellular Microbiology*, **13**: 210-226
- Michael, A. J. (2001) International and public health group symposium on “Nutritional challenges in the new millennium. The impact of climatic and other environmental changes on food production and population health in the coming decades. *Proceedings of the Nutrition Society*, **60**: 195-201
- Mitchell, T. K. and Dean, R. A. (1995) The cAMP-dependent protein kinase catalytic subunit is required for appressorium formation and pathogenesis by the rice blast fungus *Magnaporthe grisea*. *The Plant Cell*, **7**: 1869-1878
- Miya, A., Albert, P., Shinya, T., Desaki, Y., Ichimura, K., Shirasu, K., Narusaka, Y., Kawakami, N., Kaku, H. and Shibuya, N. (2007) CERK1, a LysM receptor kinase, is essential for chitin elicitor signaling in *Arabidopsis*. *Proceedings of the National Academy of Science*, **104**: 19613-19618
- Monheit, J. E., Cowan, D. F., and Moore, D. G. (1984) Rapid detection of fungi in tissues using calcofluor white and fluorescence microscopy. *Archives of Pathology and Laboratory Medicine*, **108**: 616-618
- Mosquera, G., Giraldo, M. C., Khang, C. H., Coughlan, S. and Valent, B. (2009) Interaction transcriptome analysis identifies *Magnaporthe oryzae* BAS1-4 as Biotrophy-Associated secreted proteins in rice blast disease. *The Plant Cell*, **21**: 1273-1290
- Munro, C. A. and Gow, N. A. (2001) Chitin synthesis in human pathogenic fungi. *Medical Mycology*, **39**: 41-53
- Murashige, T. and Skoog, F. (1962) A revised medium for rapid growth and bioassays with tobacco tissue cultures. *Physiological Plant*, **15**: 473-497
- Nakagawa, T., Kaku, H., Shimoda, Y., Sugiyama, A., Shimamura, M., Takanashi, K., Yazaki, K., Aoki, T., Shibuya, N. and Kouchi, H. (2011) From defense to symbiosis: limited alterations in the kinase domain of LysM receptor-like kinases are crucial for evolution of legume-*Rhizobium* symbiosis. *Plant Journal*, **65**: 169-180
- Nelson, J. W. (2003) Adaptation of core mechanisms to generate cell polarity. *Nature*, **422**: 766-774
- Nielsen, E., Cheung, A. Y. and Ueda, T. (2008) The regulatory RAB and ARF GTPases for vesicular trafficking. *Plant Physiology*, **147**: 1516-1526
- Nottogham, J. L. and Silue, D. (1992) Distribution of mating type alleles in *Magnaporthe grisea* populations pathogenic on rice blast. *Phytopathology*, **82**: 421-424
- O'Connell, R. J., and Panstruga, R. (2006) Tête à tête inside a plant cell: establishing compatibility between plants and biotrophic fungi and oomycetes. *New Phytologist*, **171**: 699-718

- Oh, Y., Donofrio, N., Pan, H., Coughlan, S., Brown, D. E., Meng, S., Mitchell, T. and Dean, R. A. (2008) Transcriptome analysis reveals new insight into appressorium formation and function in the rice blast fungus *Magnaporthe oryzae*. *Genome Biology*, **9**: PMID: 18492280
- Oldenburg, K. R., Vo, K. T., Michaelis, S. and Paddon, C. (1997) Recombination-mediated PCR-directed plasmid construction in vivo in yeast. *Nucleic Acids Research*, **25**: 451-452
- Oliva, R., Win, J., Raffaele, S., Boutemy, L., Bozkurt, T. O., Chapparo, A., Segretin, M. E., Stam, R., Schornack, S., Cano, L. M., van Damme, M., Huitema, E., Thines, M., Banfield, M. J. and Kamoun, S. (2010) Recent developments in effector biology of filamentous plant pathogens. *Cellular Microbiology*, **12**: 705-715
- Orbach, M. J., Farrall, L., Sweigard, J. A., Chumley, F. G. and Valent, B. (2000) A telomeric avirulence gene determines efficacy for the rice blast resistance gene Pi-ta. *The Plant Cell*, **12**: 2019-2032
- Pagny, S., Cabanes-Macheteau, M., Gillikin, J. W., Leborgne-Castel, N., Lerouge, P., Boston, R. S., Faye, L. and Gomord, V. (2000) Protein recycling from the Golgi apparatus to the endoplasmic reticulum in plants and its minor contribution to calreticulum retention. *The Plant Cell*, **12**: 739-756
- Park, G., Xue, C., Zhao, X., Kim, Y., Orbach, M. and Xu, J-R. (2006) Multiple upstream signals converge on the adaptor protein Mst50 in *Magnaporthe grisea*. *Plant Cell*, **18**: 2822-2835
- Pasechnik, T. D, Aver'yanov, A. A., Lapikova, V. P., Kovalenko, E. D. and Kolomietz, T. M. (1998) The involvement of activated oxygen in the expression of the vertical and horizontal resistance of rice to blast disease. *Russian Journal of Plant Physiology*, **45**: 371-378
- Rasconi, S., Jobard, M., Jouve, L. and Sime-Ngando, T. (2009) Use of calcofluor white for detection, identification and quantification of phytoplanktonic fungal parasites. *Applied and Environmental Microbiology*, **75**: 2545-2553
- Reese, T. A., Liang, H. E., Tager, A. M., Luster, A. D., Van Rooijen, N., Voehringer, D. and Locksley, R. M. (2007) Chitin induces accumulation in tissue of innate immune cells associated with allergy. *Nature*, **447**: 92-96
- Reiser, V., Ruis, H. and Ammerer, G. (1999) Kinase activity-dependent nuclear export opposes stress-induced nuclear accumulation and retention of Hog1 mitogen-activated protein kinase in the budding yeast *Saccharomyces cerevisiae*. *Molecular Biology of the Cell*, **10**: 1147-1161
- Royal Society, London (2009) Reaping the benefits: science and the sustainable intensification of Global Agriculture. Royal Society of London.
- Runions, J., Brach, T., Kuhner, S. and Hawes, C. (2006) Photoactivation of GFP reveals protein dynamics within the endoplasmic reticulum membrane. *Journal of Experimental Botany*, **57**: 43-50
- Sambrook, J., Fritsch, F. E., and Maniatis, T. (1989) Molecular Cloning: A laboratory manual. Cold Spring Harbor Laboratory Press

- Saunders, D.G., Aves, S.J., Talbot, N.J. (2010) Cell cycle-mediated regulation of plant infection by the rice blast fungus. *Plant Cell* **22**: 497-507.
- Saunders, D. G., Dagdas, Y. F. and Talbot, N. J. (2010) Spatial uncoupling of mitosis and cytokinesis during appressorium-mediated plant infection by the rice blast fungus *Magnaporthe oryzae*. *Plant Cell* **22**: 2417-2428.
- Schneider, D. R. S., Saraiva, A. M., Azzoni, A. R., Miranda, H. R., de Toledo, M. A., Pelloso, A. C. and Souza, A. P. (2010) Overexpression and purification of *PWL2D*, a mutant of the effector protein *PWL2* from *Magnaporthe grisea*. *Protein Expression and Purification*, **74**: 24-31
- Schiestl, R. H. and Gietz, R. D. (1989) High-efficiency transformation of intact yeast cells using single stranded nucleic acids as a carrier. *Current Genetics*, **16**: 339-346
- Schuster, M., Treitschke, S., Kilaru, S., Molloy, J., Harmer, N. J. and Steinberg, G. (2012) Myosin-5, kinesin-1 and myosin-17 cooperate in secretion of fungal chitin synthase. *EMBO Journal*, **31**: 214-227
- Sesma, A. and Osbourn, A. E. (2004) The rice leaf blast pathogen undergoes developmental processes typical of root-infecting fungi. *Nature*, **431**: 582-586
- Shibuya, N., Ebisu, N., Kamada, Y., Kaku, H., Conn, J. and Ito, Y. (1996) Localization and binding characteristics of a high-affinity binding site for N-acetylchitoooligosaccharide elicitor in the plasma membrane from suspension-cultured rice cells suggest a role as a receptor for the elicitor signal at the cell surface. *Plant Cellular Physiology* **37**: 894-898
- Shimzu, T., Nakano, T. Takamizawa, D., Desaki, Y., Ishii-Minami, N., Nishizawa, Y., Minami, E., Okada, K., Yamane, H., Kaku, H. and Shibuya, N. (2010) Two lysM receptor molecules CEBiP and OsCERK1, cooperatively regulate chitin elicitor signalling in rice. *Plant Journal*, **64**: 202-214
- Shinya, T., Osada, T., Desaki, Y., Hatamoto, M., Yamanaka, Y., Hirano, H., Takai, R., Che, F. S., Kaku, H. and Shibuya, N. (2010) Characterization of receptor proteins using affinity cross-linking with biotinylated ligands. *Plant Cellular Physiology*, **51**: 262-270
- Shoji, J. –Y., Arioka, M. and Kitamoto, K. (2008) Dissecting the cellular components of the secretory pathway in filamentous fungi: Insights into their application for protein production. *Biotechnology Letters*, **30**: 7-14
- Silva, C. P., Nomura, E., Freitas, E. G., Brugnaro, C. and Urashima, A. S. (2009) Efficiency of alternative treatments in the control of *Pyricularia grisea* in wheat seeds. *Tropical Plant Pathology*, **34**: 127-131
- Skamnioti, P. and Gurr, S. J. (2009) Against the grain: safeguarding rice from rice blast disease. *Trends in Biotechnology*, **27**: 141-150
- Soanes, D.M., Alam, I., Cornell, M.J., Wong, H.M., Hedeler, C., Paton, N.W., Rattray, M., Hubbard, S.J., Oliver, S.G. and Talbot, N.J. (2008) Comparative genome analysis of filamentous fungi reveals gene family expansions associated with fungal pathogenesis. *PLoS ONE* **3**: e2300.

- Southern, E. M. (1975) Detection of specific sequences among DNA fragments separated by gel electrophoresis. *Journal of Molecular Biology*, **98**: 503
- Spellig, T., Bottin, A. and Kahmann, R. (1996) Green Fluorescent Protein (GFP) as a new vital marker in the phytopathogenic fungus *Ustilago maydis*. *Molecular Genetics and Genomics*, **252**: 503-509
- Steinburg, G. (2007) Hyphal growth: a tale of motors, lipids and the Spitzenkörper, *Eukaryotic Cell*, **6**: 351-360
- Stergiopoulos, I. and de Wit, P. J. (2009) Fungal effector proteins. *Annual Review of Phytopathology*, **47**: 233-263
- Strange, R. N. and Scott, P. R. (2005) Plant disease: a threat to global food security. *Annual review of phytopathology*, **43**: 83-116
- Sweigard, J. A., Carroll, A. M., Kang, S., Farrall, L., Chumley, F. G. and Valent, B. (1995) Identification, cloning and characterization of *PWLP*, a gene for host species specificity in the rice blast fungus. *The Plant Cell*, **7**: 1221-1233
- Sweigard, J. A., Chumley, F. G., Carroll, A., Farrall, L. and Valent, B. (1997) A series of vectors for fungal transformation. *Fungal genetics Newsletter*, **44**: 52-53
- Talbot, N. J., Ebbole, D. J., Hamer, J. E. (1993) Identification and characterization of *MPGI*, a gene involved in pathogenicity from the rice blast fungus *Magnaporthe grisea*. *The Plant Cell*, **5**: 1575-1590
- Talbot, N. J. (1995) Having a blast: exploring the pathogenicity of *Magnaporthe grisea*. *Trends in Microbiology*, **3**: 9-16
- Talbot, N. J. (2003) On the trail of a cereal killer: exploring the biology of *Magnaporthe grisea*. *Annual Review of Microbiology*, **57**: 177-202
- Tanaka, S., Ichikawa, A., Yamada, K., Tsuji, G., Nishiuchi, T., Mori, M., Koga, H., Nishizawa, Y., O'Connell, R. and Kubo, Y. (2010) *HvCEBiP*, a gene homologous to rice chitin receptor *CEBiP*, contributes to basal resistance of barley to *Magnaporthe oryzae*. *BMC BMC Plant Biology* 2010, **10**:288 doi:10.1186/1471-2229-10-288
- The International Rice Genome Sequencing Project (2005) The Map-based sequence of the rice genome. *Nature*, **436**: 793-800
- Tian, M., Benedetti, B. and Kamoun, S. (2005) A second Kazal-like protease inhibitor from *Phytophthora infestans* inhibits and interacts with the apoplastic pathogenesis-related protease P69B of tomato. *Plant Physiology*, **138**: 1785-1793
- Thinlay, X., Finckh, M. R., Bordeos, A. C. and Zeigler, R. S. (2000) Effects and possible causes of an unprecedented rice blast epidemic on the traditional farming system of Bhutan. *Agriculture, Ecosystems and Environment*, **78**: 237-248
- Thomma, B. P. H. J., Nürnberger, T. and Joosten, M. H. A. J. (2011) Of PAMPs and Effectors: the blurred PTI-ETI dichotomy. *The Plant Cell*, **23**: 4-15

- Thompson, J. D., Higgins, D. G. and Gibson, T. J. (1994) ClustalW: Improving the sensitivity of progressive multiple sequence alignment through sequence weighting, position-specific gap penalties and weight matrix choice. *Nucleic Acids Research*, **22**: 4673-4680
- Toriyama, K. and Hinata, K. (1985) Cell suspension and protoplast culture in rice. *Plant Science*, **41**: 179-182
- Torres, M. A., Jones, J. D. G. and Dangl, J. L. (2006) Reactive oxygen species signaling in response to pathogens. *Plant Physiology*, **141**: 373-378
- Tsukada, K., Ishizaka, M., Fukisawa, W., Iwasaki, Y., Yamaguchi, T., Minami, E. and Shibuya, N. (2002) Rice receptor for chitin oligosaccharides elicitor does not couple to heterotrimeric G-protein: elicitor responses of suspension cultured rice cells from *Daikoku* dwarf (d1) mutants lacking a functional G-protein α -subunit. *Physiological Plant*, **116**: 373-382
- Ueda, T., Yamaguchhi, M., Uchimiya, H. and Nakano, A. (2001) Ara6, a plant-unique novel type Rab GTPase, functions in the endocytic pathways of *Arabidopsis thaliana*. *EMBO Journal*, **20**: 4730-4741
- Urashima, A. S. and Kato, H. (1994) Varietal resistance and chemical control of wheat blast fungus. *Summa Phytopathologica*, **20**: 107-112
- Urashima, A. S., Lavorent, N. A., Goulart, A. C. P. and Mehta, Y. R. (2004) Resistance spectra of wheat cultivars and virulence diversity of *Magnaporthe grisea* isolates in Brazil. *Fitopatologia Brasileira*, **29**: 511-518
- Valent, B., Farrall, L. and Chumley, F. G. (1991) *Magnaporthe grisea* genes for pathogenicity and virulence identified through a series of backcrosses. *Genetics*, **127**: 87-101
- Valent, B. and Khang, C. H. (2010) Recent advances in rice blast effector research. *Current Opinion in Plant Biology*, **13**: 434-441
- Van Damme, M., Cano, L. M., Oliva, R., Schornack, S., Segretin, M.E., Kamoun, S. and Raffaele, S. (2012) Evolutionary and functional dynamics of oomycete effector genes, In “*Effectors in Plant-Microbe Interactions*”. Wiley Blackwell Press
- Van Den Burg, H. A., Harrison, S. J., Joosten, M. H. A. J., Vervoot, J. and de Wit, P. J. G. M. (2006) *Cladosporium fulvum* Avr4 protects fungal cell walls against hydrolysis by plant chitinases accumulating during infection. *Molecular Plant-Microbe Interactions*, **19**: 1420-1430
- van Esse, H. P., Bolton, M. D., Stergiopoulos, I., de Wit, P. J. G. M. and Thomma, B. P. H. J. (2007) The chitin-binding *Cladosporium fulvum* effector protein Avr4 is a virulence factor. *Molecular Plant Microbe Interactions*, **20**: 1092-1101
- Vega, K. and Kalkum, M. (2011) Chitin, chitinase responses, and invasive fungal infections. *International Journal of Microbiology*, MID: 22187561 [PubMed - in process] PMCID: PMC3236456
- Veneault-Fourrey, C., Barooah, M., Egan, M., Wakley, G., Talbot, N.J. (2006) Autophagic fungal cell death is necessary for infection by the rice blast fungus. *Science* **312**: 580-583.
- Veneault-Fourrey, Talbot, N.J. (2007) Autophagic cell death and its importance for fungal developmental biology and pathogenesis. *Autophagy* **3**: 126-12

- Virag, A. & Harris, S. D. (2006) The Spitzenkörper: a molecular perspective. *Mycological Research*, **110**: 4-13
- Voigt, B., Timmers, A. C. J., Samaj, J., Müller, J., Baluska, F. and Menzel, D. (2004) GFP-fABD2 fusion construct allows in vivo visualization of the dynamic actin cytoskeleton in all cells of *Arabidopsis* seedlings. *European Journal of Cell Biology*, **84**: 595-608
- Wang, G., Fiers, M., Ellendorf, U., Wang, Z., de Wit, P. J. G. M., Angenent, G. C. and Thomma, B. P. H. J. (2010) The diverse roles of extracellular leucine-rich repeat-containing receptor-like proteins in plants. *Critical Review in Plant Science*, **29**: 285-299
- Whisson, S. C., Boevink, P. C., Moleleki, L., Avrova, A. O., Morales, J. G., Gilroy, E. M., Armstrong, M. R., Grouffaud, S., van West, P., Chapman, S., Hein, I., Toth, I. K., Pritchard, L. and Birch, P. R. J. (2007) A translocation signal for delivery of oomycete proteins into host plant cells. *Nature*, **450**: 115-118
- Wilson, R.A., Talbot, N.J. (2009) Under pressure: investigating the biology of plant infection by *Magnaporthe oryzae*. *Nature Reviews Microbiology* **7**: 185-19
- Willmann, R., Lajunen, H. M., Erbs, G., Newman, M-A., Kolb, D., Tsuda, K., Katagiri, F., Fliegmann, J., Bono, J-J., Cullimore, J. V., Jehle, A. K., Gotz, F., Kulik, A., Molinaro, A., Lipka, V., Gust, A. A. and Nurnberger, T. (2011) *Arabidopsis* lysine-motif proteins LYM1 and LYM3CERK1 mediate bacterial peptidoglycan sensing and immunity to bacterial infection. *Proceedings of the National Academy of Science USA*, **108**: 19824-19829
- Win, J., Morgan, W., Bos, J., Ksenia, K. V. Cano, L. M., Chapparó-Garcia, A., Ammar, R., Staskawicz, B. J. and Kamoun, S. (2007) Adaptive evolution has targeted the C-terminal domain of the RXLR effectors of plant pathogenic oomycetes. *Plant Cell*, **19**: 2349-2369
- Wojtaszek, P. (1997) Oxidative burst an early plant response to pathogen infection. *The biochemical Journal*, **15**: 681-692
- Wu, H., Rossi, G. & Brennwald, P. (2008) The ghost in the machine: small GTPases as spatial regulators of exocytosis. *Trends in Cell Biology*, **18**: 397-404
- Zhao, X. and Xu, J. R. (2007) A highly conserved MAPK-docking site in Mst7 is essential for Pmk1 activation in *Magnaporthe grisea*. *Molecular Microbiology*, **63**: 881-894
- Xu, J. R. and Hamer, J. E. (1996) MAP kinase and cAMP signalling regulate infection structure formation and pathogenic growth in the rice blast fungus *Magnaporthe grisea*. *Genes and Development*, **10**: 2696-2706
- Xu, J. R. (2000) Map kinases in fungal pathogens. *Fungal Genetics Biology*, **31**: 137-152
- Yaeno, T., Li, H., Chaparro-Garcia, A., Schornack, S., Koshiba, S., Watanabe, S., Kigawa, T., Kamoun, S. and Shirasu, K. (2011) Phosphatidylinositol monophosphate-binding interface in the oomycete RXLR effector AVR3a is required its stability in host cells to modulate plant immunity. *Proceedings of the National Academy of Science USA*, **108**: 14682-14687
- Yamaguchi, T., Minami, E., Ueki, J. and Shibuya, N. (2005) Elicitor induced activation of phospholipases plays an important role for the induction of defense responses in suspension-cultured rice cells. *Plant Cellular Physiology*, **46**: 579-587

- Yi, M., Chi, M-H., Khang, C. H., Park, S-Y., Kang, S., Valent, B. and Lee, Y-H. (2009) The ER chaperone *LHS1* is involved in asexual development and rice infection by the blast fungus *Magnaporthe oryzae*. *The Plant Cell*, **21**: 681-695
- Yoshida, K., Saitoh, H., Fujisawa, S., Kanzaki, H., Matsumura, H., Yoshida, K., Tosa, Y., Chuma, I., Takano, Y., Win, J., Kamoun, S. and Terauchi, R. (2009) Association genetics reveals three novel avirulence genes from the rice blast fungal pathogen *Magnaporthe oryzae*. *The Plant Cell*, **21**: 1573-1591
- Yu, J., Hamari, Z., Han, K., Seo, J., Reyes-Dominguez, Y. and Scazzocchio, C. (2004) Double-joint PCR: a PCR-based molecular tool for gene manipulations in filamentous fungi. *Fungal Genetics Biology*, **41**: 973-981
- Zheng, W., Chen, J., Liu, W., Zheng, S., Zhou, J., Lu, G. and Zonghua, W. (2007) A Rho3 homolog is essential for appressorium development and pathogenicity of *Magnaporthe grisea*. *Eukaryotic Cell*, **6**: 2240-2250
- Zheng, W., Zhao, Z., Chen, J., Liu, W., Ke, H., Zhou, J., Lu, G., Darvill, A. G., Albersheim, P., Wu, S. and Wang, Z. (2009) A Cdc42 ortholog is required for penetration and virulence of *Magnaporthe grisea*. *Fungal Genetics and Biology*, **46**: 450-460
- Zhao, X., Kim, Y., Park, G. and Xu, J. R. (2005) A mitogen-activated protein kinase cascade regulating infection-related morphogenesis in *Magnaporthe grisea*. *Plant Cell*, **17**: 1317-1329
- Zellerhoff, N., Jarosch, B., Groenewald, J. Z., Crous, P. W. and Schaffrath, U. (2006) Nonhost resistance of barley is successfully manifested against *Magnaporthe grisea* and a closely related *Pennistemon*-infecting lineage but is overcome by *Magnaporthe oryzae*. *Molecular Plant-Microbe Interactions*, **19**: 1014-1022
- Zeigler, R. S., Leong, S. A. and Peng, P. S. (1994) Rice blast disease. In: *Rice Blast Disease*. Cab International, Wallingford, CT
- Zipfel, C. and Robatzek, S. (2010) PAMP-triggered immunity: veni, vidi,...? *Plant Physiology*, **154**: 551-554

Appendix 1

Mentlak, T. A., Kombrink, A., Shinya, T., Ryder, L. S., Otomo, I., Saitoh, H., Terauchi, R., Nishizawa, Y., Shibuya, N., Thomma, B. P. H. J. and Talbot, N. J. (2012) Effector mediated suppression of chitin-triggered immunity by *Magnaporthe oryzae* is necessary for rice blast disease. *The Plant Cell*, **24**: 322-335

Effector-Mediated Suppression of Chitin-Triggered Immunity by *Magnaporthe oryzae* Is Necessary for Rice Blast Disease

Thomas A. Mentlak,^a Anja Kombrink,^b Tomonori Shinya,^c Lauren S. Ryder,^a Ippei Otomo,^c Hiromasa Saitoh,^d Ryohei Terauchi,^d Yoko Nishizawa,^e Naoto Shibuya,^c Bart P.H.J. Thomma,^b and Nicholas J. Talbot^{a,1}

^aSchool of Biosciences, University of Exeter, Geoffrey Pope Building, Exeter EX4 4QD, United Kingdom

^bLaboratory of Phytopathology, Wageningen University, 6708 PB Wageningen, The Netherlands

^cDepartment of Life Sciences, Faculty of Agriculture, Meiji University, Kawasaki, Kanagawa 214-8571, Japan

^dIwate Rice Biotechnology Center, Kitakami, Iwate 024-0003, Japan

^eDivision of Plant Sciences, National Institute of Agrobiological Sciences, Tsukuba, Ibaraki 305-8634, Japan

Plants use pattern recognition receptors to defend themselves from microbial pathogens. These receptors recognize pathogen-associated molecular patterns (PAMPs) and activate signaling pathways that lead to immunity. In rice (*Oryza sativa*), the chitin elicitor binding protein (CEBiP) recognizes chitin oligosaccharides released from the cell walls of fungal pathogens. Here, we show that the rice blast fungus *Magnaporthe oryzae* overcomes this first line of plant defense by secreting an effector protein, Secreted LysM Protein1 (Slp1), during invasion of new rice cells. We demonstrate that Slp1 accumulates at the interface between the fungal cell wall and the rice plasma membrane, can bind to chitin, and is able to suppress chitin-induced plant immune responses, including generation of reactive oxygen species and plant defense gene expression. Furthermore, we show that Slp1 competes with CEBiP for binding of chitin oligosaccharides. Slp1 is required by *M. oryzae* for full virulence and exerts a significant effect on tissue invasion and disease lesion expansion. By contrast, gene silencing of *CEBiP* in rice allows *M. oryzae* to cause rice blast disease in the absence of Slp1. We propose that Slp1 sequesters chitin oligosaccharides to prevent PAMP-triggered immunity in rice, thereby facilitating rapid spread of the fungus within host tissue.

INTRODUCTION

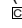
The filamentous fungus *Magnaporthe oryzae* is one of the most devastating plant pathogens, causing blast disease in a significant number of agronomically important crops, including rice (*Oryza sativa*), barley (*Hordeum vulgare*), and finger millet (*Eleusine coracana*) (Wilson and Talbot, 2009). To cause disease, infection structures called appressoria are required for penetration of the host plant (Talbot, 2003; Wilson and Talbot 2009). After penetration of the host surface, the fungal penetration peg differentiates to form a thin filamentous primary hypha and the fungus grows without causing disease symptoms. At this time, an intimate relationship between the host and pathogen is established, in which the host plasma membrane is not breached, but instead appears to become invaginated, thereby sealing the invading fungus in a host-derived plasma membrane, known as the extrainvasive hyphal membrane (EIHM) (Kankanala et al.,

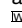
2007). Filamentous hyphae grow briefly within host cells before differentiating into bulbous secondary pseudohyphae, which propagate rapidly within the host cell (Kankanala et al., 2007). The fungus then moves into neighboring plant cells at pit field sites, potentially using plasmodesmata to traverse between rice cells (Kankanala et al., 2007). Rice blast disease symptoms only become visible following a prolonged biotrophic phase in which the fungus spreads extensively within rice tissue, suggesting that *M. oryzae* can evade host recognition and proliferate in living plant cells by active suppression of plant immunity.

During the early stages of infection, *M. oryzae* is believed to secrete effector proteins to suppress host defenses (Mosquera et al., 2009; Khang et al., 2010), although the precise function of rice blast effectors has not yet been determined. The best characterized *M. oryzae* effector, Avr-Pita, was first identified because it is recognized in rice cultivars carrying the *Pi-ta* resistance gene. The intracellular *Pi-ta* resistance gene product and Avr-Pita have been shown to interact directly (Jia et al., 2000), suggesting that Avr-Pita is secreted by the fungus and delivered across the host plasma membrane into rice cells. Avr-Pita is predicted to encode a metalloprotease, but its role in fungal virulence and the targets of its putative proteolytic activity have not yet been determined (Jia et al., 2000). Recent studies have confirmed that Avr-Pita is delivered into the cytoplasm of rice cells and have also led to the discovery of an infection structure, known as the biotrophic interfacial complex (BIC),

¹ Address correspondence to n.j.talbot@exeter.ac.uk.

The author responsible for distribution of materials integral to the findings presented in this article in accordance with the policy described in the Instructions for Authors (www.plantcell.org) is: Nicholas J. Talbot (n.j.talbot@exeter.ac.uk).

 Some figures in this article are displayed in color online but in black and white in the print edition.

 Online version contains Web-only data.
www.plantcell.org/cgi/doi/10.1105/tpc.111.092957

which forms as a subapical bulbous structure at the periphery of invasive pseudohyphal cells (Mosquera et al., 2009; Khang et al., 2010). During biotrophic intracellular growth, this structure accumulates effector proteins by an unknown mechanism, and it has been proposed that BICs may be used to mediate the delivery of rice blast effectors into the host cytoplasm (Khang et al., 2010).

In this study, we set out to identify novel effectors secreted by the rice blast fungus. We were particularly interested in determining whether *M. oryzae* deploys effectors in the apoplast, the space between the fungal cell wall and the host plasma membrane. Secretion of apoplastic effectors is a common strategy of many extracellular fungal pathogens, but it is not clear whether intracellular colonizing fungi, such as *M. oryzae*, require extracellular effectors during tissue invasion (Mosquera et al., 2009; Jia et al., 2000).

The intercellular fungal pathogen *Cladosporium fulvum*, which causes leaf-mold disease of tomato (*Solanum lycopersicum*), colonizes the spaces between tomato spongy mesophyll cells and secretes several apoplastic effectors during colonization of tomato leaves (Thomma et al., 2005; van Esse et al., 2008). Many of these effectors also have Avr functions and are perceived by cognate Cf receptor gene products residing in the host plasma membrane (Wang et al., 2010). Effectors of *C. fulvum* are thought to be entirely apoplastic, which reflects the nature of pathogenic colonization. Interestingly, an effector known as Ecp6 was recently identified from *C. fulvum* that is secreted during infection (Bolton et al., 2008). Ecp6 contains LysM domains that have previously been implicated in carbohydrate binding and has been shown to bind chitin (de Jonge et al., 2010). Ecp6 may therefore suppress host recognition of chitin and pathogen-associated molecular pattern (PAMP)-triggered immunity through the scavenging of PAMP molecules (de Jonge et al., 2010). Although experiments have suggested a virulence function for this effector (Bolton et al., 2008), the cognate chitin elicitor receptor in tomato with which Ecp6 competes has yet to be identified.

In this report, we show that *M. oryzae* secretes a novel effector, which we have named Slp1, for Secreted LysM Protein 1. Intriguingly, although *M. oryzae* colonizes rice intracellularly, Slp1 shows strong similarity to *C. fulvum* Ecp6 and contains two LysM domains. Using live-cell imaging of rice tissue, we show that Slp1 specifically accumulates at the plant-fungal interface during the early stages of rice blast infections and that its delivery to this interface is vital for its biological function. We also demonstrate that Slp1 specifically binds chitin and is able to suppress chitin-triggered immunity in rice suspension cells, including the generation of reactive oxygen species (ROS). Slp1 competes for chitin binding with the rice pattern recognition receptor (PRR) chitin elicitor binding protein (CEBiP), which is required for chitin-triggered immunity in rice, acting in cooperation with the LysM receptor-like kinase Os-CERK1 (Shimizu et al., 2010). Finally, we show that Slp1 is important for rice blast disease and necessary for disease lesion expansion. When considered together, our results provide evidence that although the rice blast fungus invades and occupies plant cells, it must deploy an apoplastic effector to suppress PAMP-triggered immunity to facilitate its growth within rice tissue.

RESULTS

Slp1 Accumulates at the Plant-Fungal Interface during Biotrophic Growth

In this study, we set out to identify novel rice blast effector proteins secreted by invasive hyphae during plant infection. To visualize the host-pathogen interface directly, we first generated transgenic rice plants in which an LTi6B:green fluorescent protein (GFP) gene fusion (Kurup et al., 2005) was expressed, resulting in GFP becoming targeted to the rice plant plasma membrane. We found that the rice plasma membrane does invaginate around invasive hyphae within rice epidermal cells and becomes tightly apposed to the fungal cell wall, as shown in Figure 1A. It is clear, therefore, that there is a close association between *M. oryzae* hyphal cell walls and the rice plasma membrane during plant infection. To identify potential effector-encoding genes involved in modulating the host-pathogen interaction, we identified genes encoding putatively secreted gene products that were upregulated during biotrophic growth compared with growth in axenic culture (Mosquera et al., 2009). One putative effector identified using these criteria was found to contain two putative LysM domains, which have previously been shown to bind carbohydrates in a number of proteins (Buist et al., 2008). We named this LysM domain-containing protein Slp1. Proteins containing LysM domains are ubiquitous in nature, and Slp1 shares significant homology with other predicted fungal LysM proteins (de Jonge and Thomma, 2009), including most notably the *C. fulvum* effector Ecp6, as shown in Supplemental Figures 1 and 2 online. Interestingly, the *M. oryzae* genome contains seven other LysM domain-containing proteins. One of these LysM proteins (gene ID MGG_03468), which we have called Slp2, was also found to show strong similarity to the *C. fulvum* Ecp6 protein, as shown in Supplemental Figure 2 online. However, we did not detect expression of *SLP2* during plant infection (data not shown) and have not yet been able to find a clear phenotype for $\Delta slp2$ mutants. We have therefore focused our research effort on determining the biological role of Slp1 during biotrophic growth of *M. oryzae*.

We hypothesized that Slp1 might act as an effector protein and decided to examine its localization during host tissue colonization (Mosquera et al., 2009; Khang et al., 2010). Putative apoplastic effectors secreted by intercellular fungal pathogens, such as *C. fulvum*, are invariably Cys rich (de Jonge et al., 2010), and as Slp1 contains six Cys residues, we further hypothesized that Slp1 might be secreted into the space between the fungal cell wall and the rice plasma membrane (see Supplemental Figure 2 online). To investigate the localization of Slp1, we engineered a strain of *M. oryzae* expressing a *SLP1:GFP* gene fusion under control of a native 2-kb promoter fragment. Live-cell imaging of infected rice leaf epidermis was performed to examine the cellular localization of Slp1 during fungal growth within rice cells. After the fungus penetrated the host cell, at ~24 to 28 h after inoculation (HAI), fluorescence could be observed to accumulate at the plant-fungal interface and was specifically observed to outline pseudohyphal fungal cells, as shown in Figure 1B. As the fungus moved into neighboring cells (at ~32 to 36 HAI), fluorescence was observed accumulating at the tips of

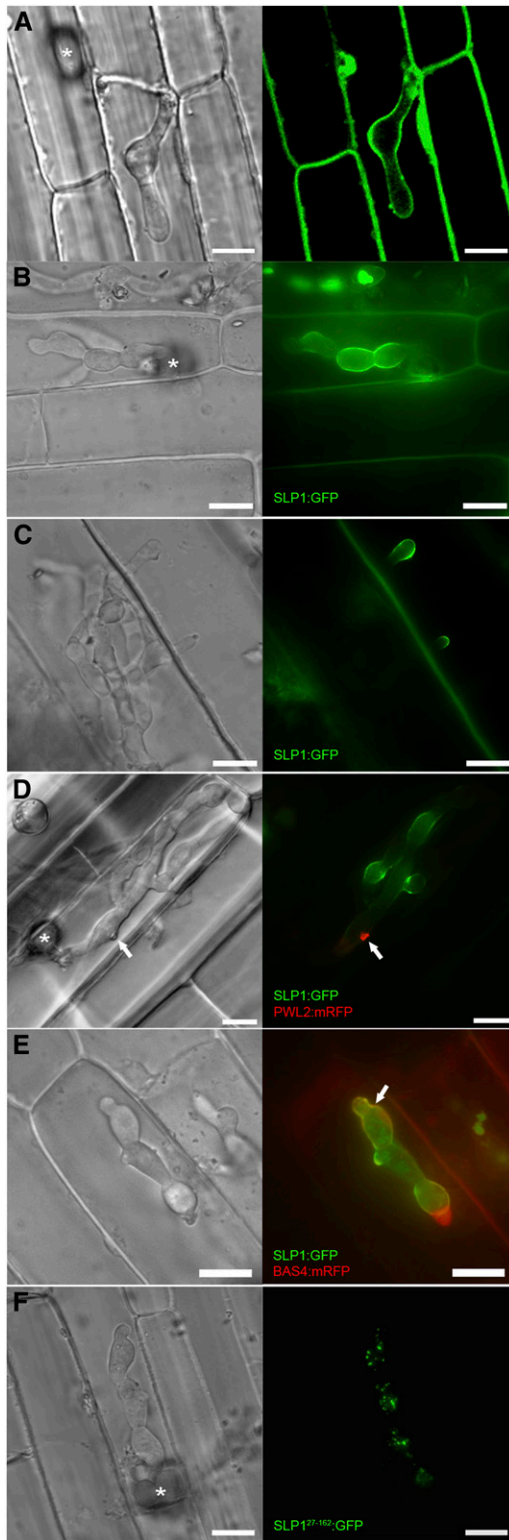


Figure 1. Slp1 Accumulates at the Plant-Fungal Interface during Biotrophic Growth.

(A) Laser confocal micrograph of *M. oryzae* invasive hyphae-colonizing epidermal leaf cells of a transgenic line of rice expressing LTI6B:GFP.

invasive hyphae that were invading new host cells. At this time, fluorescence ceased to accumulate at the host-pathogen interface within the initially infected host cell (Figure 1C). At no stage was fluorescence observed within host cells nor could fluorescence be observed in other fungal structures, including conidia, germ tubes, or appressoria, as shown in Supplemental Figure 3 online. From these observations, we conclude that Slp1 is specifically expressed when the fungus is growing intracellularly within its host, a feature associated with putative rice blast effector proteins (Mosquera et al., 2009; Khang et al., 2010). Next, we wanted to examine whether the localization pattern of Slp1 differs from that of previously described rice blast effectors, which accumulate at BIC structures (Mosquera et al., 2009; Khang et al., 2010). We therefore engineered a strain of *M. oryzae* that simultaneously expressed a *SLP1:GFP* gene fusion and a *Pathogenicity on Weeping Lovegrass2 (PWL2):monomeric red fluorescent protein (mRFP)* gene fusion. PwL2 is a previously characterized BIC-localized effector, known to be delivered into the cytoplasm of rice cells during plant infection by *M. oryzae* (Khang et al., 2010). We undertook live-cell imaging of infected rice epidermis, as shown in Figure 1D and Supplemental Movie 1 online. Interestingly, at >80% of infection sites observed between 24 and 32 HAI, colocalization between *SLP1:GFP* and *PWL2:mRFP* could not be observed ($n > 100$). Taken together, we conclude that Slp1 accumulates between the invaginated host plasma membrane and the fungal cell wall during initial invasion of rice cells and is therefore distinct from previously identified BIC-localized effectors.

Having established that Slp1 was not a BIC-localized effector protein, we were interested in trying to colocalize Slp1 with other rice blast effectors that appear to accumulate in the apoplast. One potential effector, presumed to be apoplastic in localization, is Bas4 (Mosquera et al., 2009; Khang et al., 2010). We therefore engineered an *M. oryzae* strain that simultaneously expresses

The rice cell plasma membrane becomes invaginated around the growing fungal hyphae.

(B) Cellular localization of Slp1:GFP in *M. oryzae* during biotrophic growth on epidermal rice cells at 24 HAI. Fluorescence was initially observed accumulating at the tips of invasive hyphae at the plant-fungal interface and was later found to surround invasive hyphae.

(C) At 36 HAI, Slp1:GFP fluorescence could be observed accumulating at the tips of filamentous hyphae-invading adjacent cells. At this time, fluorescence was no longer observed in initially infected host cells.

(D) Lack of colocalization between *SLP1:GFP* and *PWL2:mRFP*. A Guy11 *M. oryzae* transformant expressing both the *SLP1:GFP* and *PWL2:mRFP* constructs was used to visualize the cellular localization of Slp1 and the BIC-localized effector PwL2 in planta. At 24 HAI, the Slp1-Gfp signal surrounded invasive hyphae, whereas PwL2 accumulates at the BIC (white arrow).

(E) Partial colocalization of *M. oryzae* Slp1:GFP and Bas4:mRFP fusion proteins in the apoplastic space surrounding fungal invasive hyphae. White arrow indicates site of colocalization.

(F) Cellular localization of Slp1²⁷⁻¹⁶²:GFP at 24 HAI on leaf sheath tissue. Slp1²⁷⁻¹⁶²:GFP aggregates can be seen localizing within the cytoplasm of fungal invasive hyphae. White asterisk indicates the site of appressorium formation at the leaf surface.

Bars = 10 μ m.

SLP1:GFP and *BAS4:mRFP*. At 24 HAI, there did appear to be some colocalization between Slp1 and Bas4, as shown in Figure 1E. Although the two proteins appeared to colocalize, there were, however, significant areas where Slp1:GFP accumulated, but Bas4:mRFP did not. In view of our observation that Slp1 accumulates at the fungal-plant interface, we next investigated how the protein is delivered to the apoplast during biotrophic growth. *SLP1* encodes a small secreted protein of 162 amino acids, with a predicted N-terminal signal peptide of 27 amino acids in length (based on SignalP 3.0 analysis). To test the significance of this secretion sequence, we engineered an *M. oryzae* strain in which the coding region of the first 27 amino acids of *SLP1* was removed. A new start codon was introduced and the resulting coding region fused to *GFP*. Expression of the *SLP1*²⁷⁻¹⁶²:*GFP* construct was driven by the native 2.0-kb *SLP1* promoter fragment. Removal of the signal peptide prevented Slp1:GFP from reaching the tips of invasively growing hyphae, and Slp1 was no longer observed accumulating in the apoplastic space (Figure 1F). The resultant intracellular Slp1²⁷⁻¹⁶²:GFP instead appeared to accumulate as aggregates in the fungal cytoplasm. Cellular mislocalization of SLP1²⁷⁻¹⁶²:GFP is consistent with the hypothesis that Slp1 is an apoplastic effector, the secretion of which is dependent on a peptide sequence within the initial 27 amino acids.

Slp1 Is a Virulence Determinant in *M. oryzae*

To test the contribution of Slp1 to rice blast disease, a targeted gene deletion of *SLP1* was performed in *M. oryzae* (see Supplemental Figure 4 online). Fungal spores of the resulting Δ *slp1* mutant and the isogenic wild-type Guy11 strain were harvested, adjusted to uniform concentrations, and applied to 21-d-old seedlings of the blast-susceptible rice cultivar CO-39 (Figure 2). Deletion of *SLP1* significantly reduced the ability of *M. oryzae* to cause disease, and the symptoms of plants inoculated with Δ *slp1* spores were highly reduced when compared with plants infected with the wild-type Guy11 strain (Figure 2A). To quantify the reduction in virulence, both lesion density and lesion size were analyzed using image analysis software (ImageJ). The mean lesion size generated by the Δ *slp1* mutant was found to be significantly smaller than that of the Guy11 wild type (*t* test, $P < 0.01$) (Figure 2B). The mean lesion size for Guy11 was calculated to be 1.15 mm² (\pm SE 0.049, $n > 100$ lesions), while the mean lesion size of the Δ *slp1* mutant was calculated to be 0.31 mm² (\pm SE 0.025, $n > 100$). Additionally, the mean lesion density per unit area of the Δ *slp1* mutant (11.1 ± 5.7 , $n = 49$) was found to be significantly lower than that of the wild type (40.7 ± 10.8 , $n = 28$; *t* test, $P < 0.01$) (Figure 2C). Complementation analysis using the *SLP1:GFP* construct was performed, and reintroduction of the *SLP1* gene was found to restore virulence to *M. oryzae* (see Supplemental Figure 5 online). Deletion of the Slp1 signal peptide prevented complementation of the Δ *slp1* mutant phenotype (see Supplemental Figure 6 online).

We also evaluated whether Δ *slp1* mutants were impaired in their ability to form functional infection structures or whether the virulence phenotype was simply a consequence of a reduction in fitness. We harvested spores of the Δ *slp1* mutant and wild-type strains and compared their ability to form appressoria on an

inductive glass surface (Figure 2D). After 24 h, Δ *slp1* mutants were capable of forming mature appressoria in a manner identical to that of the wild-type *M. oryzae* strain. Vegetative growth rates and behavior in axenic culture were also identical to Guy11. From these observations, we conclude that the virulence phenotype of the Δ *slp1* mutant is associated with a reduced ability of the Δ *slp1* mutant to proliferate within host tissues, rather than a reduced capacity to make successful penetration structures. To test this idea, we examined and compared host tissues infected with a Δ *slp1* mutant compared with the isogenic Guy11. We initially counted the number of cells occupied by the fungus at 48 HAI and found that the number of host cells occupied by a Δ *slp1* mutant was significantly lower than the wild-type Guy11 strain ($n = 15$, two-tailed *t* test, $P = 0.014$) (Figure 2E). At 48 HAI, the mean number of host cells occupied by Δ *slp1* was found to be 4.29 cells (SD \pm 2.5), while the mean number of cells occupied by Guy11 was 7.33 (SD \pm 3.6). At 48 HAI, the Δ *slp1* mutant had only just started to colonize neighboring cells, while Guy11 had become well established at 48 HAI, with bulbous hyphae fully ramified in host tissues (Figure 2F). We conclude that Slp1 is necessary for efficient rice tissue invasion by *M. oryzae* to bring about rice blast disease.

M. oryzae Slp1 Is a Chitin Binding Protein

To define the biological function of Slp1, we cloned and overexpressed a *SLP1* cDNA in *Pichia pastoris* (de Jonge et al., 2010). Recombinant Slp1 protein was isolated and purified. As Slp1 contains two putative LysM domains, we were initially interested to see whether the protein was capable of binding to specific polysaccharides. After incubating purified Slp1 protein with insoluble cell wall polysaccharides, we observed that Slp1 specifically coprecipitated with insoluble crab shell chitin and chitin beads and was detected in the insoluble pellet fraction following affinity precipitation (Figure 3). Slp1 did not, however, precipitate with any other tested cell wall polysaccharides, including chitosan (deacetylated chitin) and the plant cell wall polysaccharides cellulose and xylan, as evidenced by Slp1 remaining in the supernatant fraction after affinity precipitation (Figure 3A). Interestingly, not only did Slp1 appear to bind specifically to chitin and not to other polysaccharides, several bands were evident in both the pellet and supernatant fractions, suggesting that Slp1 is likely to be glycosylated or potentially forms oligomers. To ensure that these higher molecular weight protein bands were not contaminants from the protein overexpression system, mass spectrometry was performed on the gel fragments after in-gel trypsin digestion. Slp1 was detected in all of these experiments, confirming that the higher molecular weight protein bands were not due to expression artifacts and suggesting that Slp1 is likely to show abnormal electrophoretic mobility due to being a glycoprotein as reported for other LysM proteins (Kaku et al., 2006) or potentially to form multimers. We were interested in determining whether Slp1 had the capacity to form multimers based on a protein-protein interaction. We therefore performed high-stringency yeast two-hybrid analysis in which an *SLP1* cDNA was simultaneously cloned into bait and prey vectors of the Matchmaker GAL4 two-hybrid system (Clontech). Using this system, we were able to detect a strong

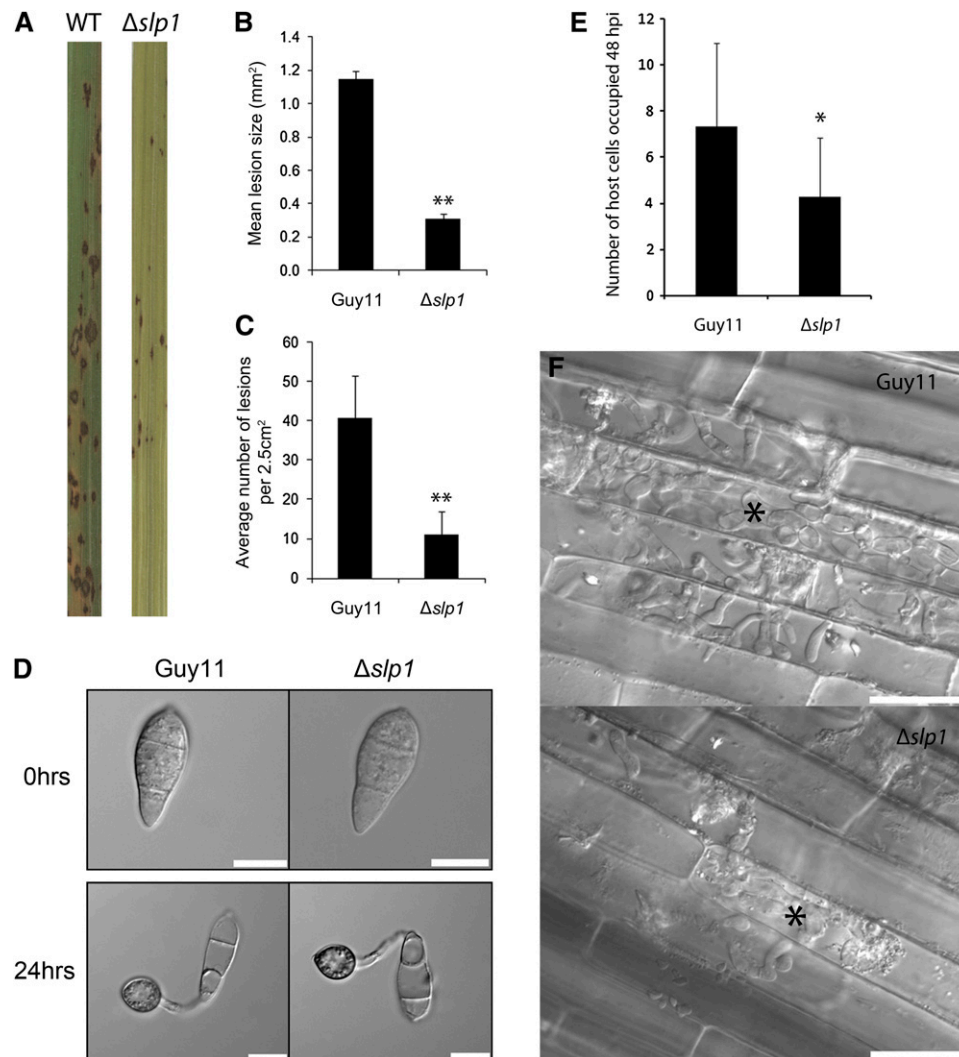


Figure 2. *SLP1* Is a Virulence Determinant in *M. oryzae* Required for Rice Tissue Invasion.

(A) Conidial suspensions of equal concentration (5×10^{-4} spores mL^{-1}) from *M. oryzae* Guy11 (wild type [WT]) or $\Delta slp1$ mutants were used to inoculate 21-d-old seedlings of the blast susceptible rice cultivar CO-39. Disease symptoms were reduced on plants inoculated with $\Delta slp1$ mutants.

(B) Bar chart of mean lesion size of plants inoculated with Guy11 and the $\Delta slp1$ mutant. Mean lesion size was significantly reduced in plants inoculated with the $\Delta slp1$ mutant compared with the isogenic wild type (t test, $P < 0.01$). Error bars denote ± 1 SE.

(C) Bar chart of mean lesion density of seedlings infected with Guy11 strain and the $\Delta slp1$ mutant per unit area. Mean lesion density was significantly reduced in $\Delta slp1$ mutant infections (t test, $P < 0.01$). Error bars denote 1 SD. Double asterisks in **(B)** and **(C)** denote $P < 0.01$ from two-tailed t test.

(D) Null $\Delta slp1$ mutants produce normal conidia and form appressoria in a time-dependent manner comparable to that of the wild-type Guy11 strain. Conidia of both Guy11 and $\Delta slp1$ mutant strains were harvested and set to a concentration of 5×10^{-4} spores mL^{-1} . Spores were inoculated onto hydrophobic glass cover slips and incubated in a moist chamber at 26°C and examined by light microscopy. The morphology of conidia and appressoria was not altered in $\Delta slp1$ mutants. Bars = $10\text{ }\mu\text{m}$.

(E) Bar chart showing the number of rice host cells occupied after 48 HAI with the $\Delta slp1$ mutant compared with Guy11. After 48 h, the number of host cells occupied by the fungus was recorded ($n = 15$ infection sites). At this time point, the number of host cells occupied by the $\Delta slp1$ mutant was found to be significantly lower than that of the wild-type Guy11 strain (two-tailed t test, $P = 0.014$). Asterisk denotes $P < 0.05$.

(F) Typical infection sites of rice leaf sheath inoculated with $\Delta slp1$ and Guy11, showing greater fungal proliferation and tissue invasion by the wild-type strain. Images were recorded 48 HAI. Asterisk marks the first infected host cell. Bar = $30\text{ }\mu\text{m}$.

[See online article for color version of this figure.]

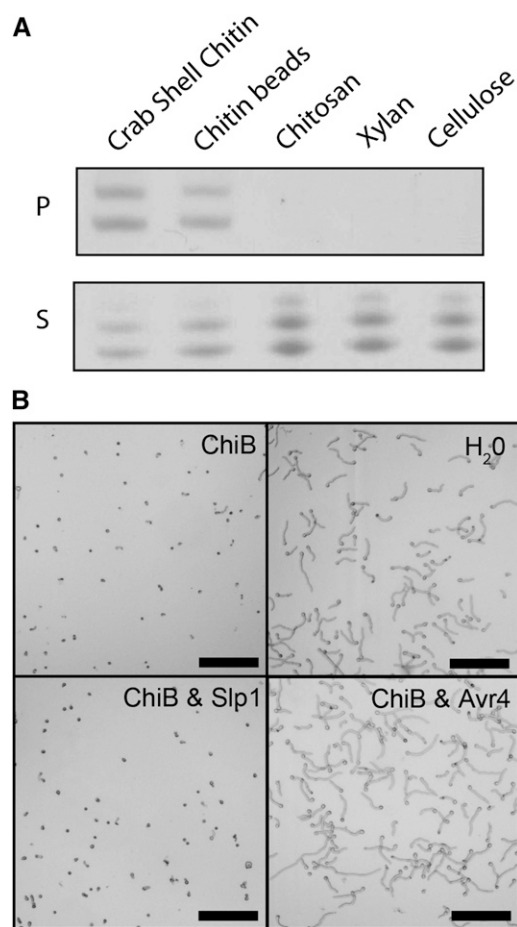


Figure 3. Slp1 Binds Specifically to Chitin Oligosaccharides.

(A) Affinity precipitation experiments showing that Slp1 coprecipitates with insoluble crab shell chitin and chitin beads and was detected in the insoluble pellet fraction (P) following SDS-PAGE and Coomassie blue staining. Slp1 did not precipitate with other insoluble polysaccharides, including chitosan (deacetylated chitin) or the plant cell wall polysaccharides xylan and cellulose. Instead, Slp1 remained in the nonprecipitated supernatant fraction (S) after incubation with these polysaccharides.

(B) Slp1 does not provide protection from hyphal tip hydrolysis by chitinase enzymes. Micrographs of *T. viride* spores taken 24 h after addition of either water or crude extract of tomato leaves containing intracellular basic chitinases (ChiB). Pretreatment with 10 μ M Avr4 prevented hydrolysis of *T. viride* hyphal tips by basic chitinase (Avr4 and ChiB), whereas pretreatment with 10 μ M Slp1 (Slp1 and ChiB) did not. Bars = 10 μ m.

potential interaction between Slp1 monomers (see Supplemental Figure 7 online). This preliminary observation is consistent with the Slp1 effector having the capacity to form protein aggregates.

As Slp1 appeared to be capable of binding chitin, we reasoned that Slp1 might bind to chitin in the fungal cell walls of invasive hyphae, thereby shielding hyphal tips from hydrolysis by plant-derived chitinases. Initial experiments demonstrated that when *M. oryzae* was grown in culture, it was not susceptible to disruption by crude extract of chitinase (data not shown). In many fungi, cell wall-incorporated proteins within a glucan

matrix can reduce the accessibility of chitinase enzymes (Joosten et al., 1995; van den Burg et al., 2006). To address this, we used *Trichoderma viride* as a model species, which has been used widely to test this hypothesis (van den Burg et al., 2006; van Esse et al., 2007; de Jonge et al., 2010). We incubated *T. viride* spores with a crude extract of tomato leaves containing intracellular basic chitinases, in the presence or absence of the purified Slp1 protein, as shown in Figure 3B. Unlike the *C. fulvum* effector Avr4, which has previously been shown to protect hyphae from the hydrolysis of chitinases (van den Burg et al., 2006; van Esse et al., 2007), Slp1 was unable to protect *T. viride* spores from hydrolysis by chitinase enzymes. Previously, concentrations as low as 10 μ M of Avr4 have been shown to provide hyphal tip protection from chitinase enzymes (Kaku et al., 2006; de Jonge and Thomma, 2009). In our experiments, even at concentrations of up to 100 μ M of Slp1, protection from chitinases was not observed. Slp1 therefore shares characteristics with Ecp6, which also fails to protect fungal hyphae against hydrolysis by chitinases (de Jonge et al., 2010). Consequently, Slp1 is not likely to be involved in the protection of fungal hyphae from chitinases.

Slp1 Is a Competitive Inhibitor of the PRR Protein CEBiP and Suppresses Chitin-Induced Immune Responses in Rice Cells

During plant infection, the release of chitin oligosaccharides from hyphal tips can help to facilitate pathogen recognition by host plant cells (Kaku et al., 2006; van den Burg et al., 2006). Given the ability of Slp1 to bind chitin (Figure 3) and accumulate at the plant-fungal interface (Figure 1), we hypothesized that Slp1 might be involved in disrupting chitin-induced perception of the fungus in rice plants. To investigate whether Slp1 was capable of suppressing chitin-triggered immunity in rice cells, we tested whether Slp1 could suppress the chitin-induced oxidative burst (Yamaguchi et al., 2005). In the presence of nanomolar concentrations of an oligomer of *N*-acetyl glucosamine [(GlcNAc)₈], rice suspension cells release ROS, which can be measured using luminol-dependent chemiluminescence. Upon incubating rice suspension cells with 1 nM (GlcNAc)₈, chemiluminescence was detected after 20 min, as shown in Figure 4A. However, this oxidative burst was suppressed in the presence of a 10-fold molar excess of Slp1 (10 nM). Furthermore, we noticed that after 120 min, suppression of the oxidative burst was still observed in the presence of 10 nM Slp1, although suppression was much greater in the presence of a 100-fold molar excess of Slp1 (Figure 4A). This latter concentration of Slp1 was capable of suppressing the chitin-induced oxidative burst across all time points examined.

To determine whether the ability of Slp1 to suppress chitin-triggered immunity was of wider significance, we also measured immunity responses in tomato suspension cells. In the presence of nanomolar concentrations of chitin oligosaccharides [(GlcNAc)₈], plant cell suspensions have previously been shown to react by medium alkalization (Felix et al., 1993). To test whether Slp1 might play a role in suppressing chitin-based responses in other plant species, we tested whether Slp1 could suppress a

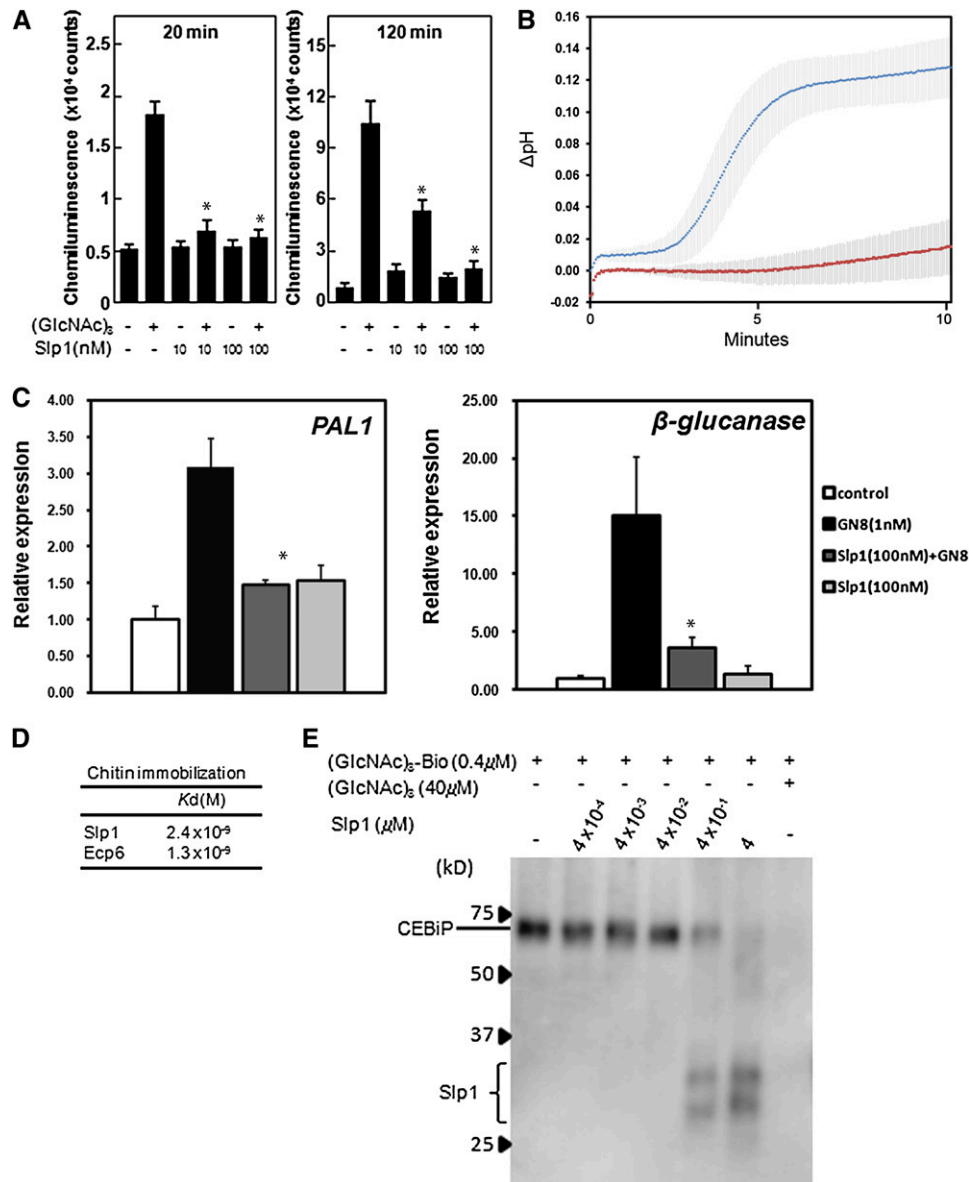


Figure 4. SIp1 Is a Competitive Inhibitor of the PRR Protein CEBiP and Suppresses Chitin-Induced Immune Responses in Rice Cells.

(A) SIp1 inhibits the chitin-induced oxidative burst in rice suspension cells. Production of ROS 20 or 120 min after induction with 1 nM (GlcNAc)₆ was determined in the absence or presence of SIp1 (10 and 100 nM). The experiment was performed twice with similar results. Mean with SE of three replicate experiments is shown, and asterisks indicate significant differences ($P < 0.01$) when compared with the 1 nM (GlcNAc)₆ treatment.

(B) Medium alkalization of tomato cell suspensions is suppressed in the presence of SIp1. After treatment with 1 nM chitin oligosaccharides [(GlcNAc)₆] (top line), the pH of the tomato cell suspensions increases after ~2 min. Upon incubation with 1 nM (GlcNAc)₆ and a 10-fold molar excess of SIp1 (10 nM) (bottom line), medium alkalization was inhibited. Error bars represent ± 1 SD of three independent replicate experiments.

(C) Expression of rice defense genes *PAL1* and β -glucanase induced by GlcNAc is suppressed in the presence of SIp1. The bars display the relative transcript level of the chitin-responsive genes normalized to the constitutively expressed ubiquitin gene. The mean with SE of two replicate experiments is shown, and asterisks indicate significant differences ($P < 0.05$) when compared with the 1 mM (GlcNAc)₆ treatment.

(D) Affinities of fungal LysM effectors for (GlcNAc)₆ determined by SPR analysis. Affinities between Ecp6 and SIp1 for (GlcNAc)₆ were measured using the (GlcNAc)₆-immobilized mode.

(E) Protein gel blot analysis using an anti-biotin antibody showing affinity labeling of a microsomal membrane preparation (rice MF) from suspension-cultured rice cells containing the PRR CEBiP, with biotinylated (GlcNAc)₆ [(GlcNAc)₆-Bio], in the presence or absence of SIp1 and nonbiotinylated (GlcNAc)₆. The experiment was performed twice with similar results.

[See online article for color version of this figure.]

chitin-induced pH shift in tomato cell suspensions. We observed that in the presence of a 10-fold molar excess of Slp1 (10 nM), medium alkalization of tomato suspensions cells was inhibited (Figure 4B). We therefore conclude that Slp1 is capable of suppressing chitin-induced immune responses in plant cells.

Chitin-triggered immunity is known to result in induction of pathogenesis-related genes, and we therefore sought to determine the effect of the Slp1 effector on induction of rice defense gene expression. We therefore performed quantitative RT-PCR (qRT-PCR) and examined changes in expression of the rice Phenylalanine lyase gene, *PAL1*, and the β -glucanase-encoding gene, *rBG*. In the presence of 1 nM (GlcNAc)₈, expression of both *PAL1* and *β -glucanase* increased significantly (Figure 4C). However, the increase in gene expression was suppressed when a 100-fold molar excess of Slp1 was also included, consistent with the role of Slp1 in preventing chitin-triggered immunity responses in rice.

In rice, the pattern recognition receptor LysM protein CEBiP resides at the rice plasma membrane and is able to bind to chitin oligosaccharides (Shibuya et al., 1996; Kaku et al., 2006). We hypothesized that Slp1 might therefore function to compete with the CEBiP recognition receptor residing at the invaginated rice cell membrane. CEBiP is a LysM domain-containing protein and interacts with the LysM receptor-like kinase protein CERK1 to bring about plant defense responses (Shimizu et al., 2010). CEBiP has been shown to contribute to rice blast disease resistance (Kishimoto et al., 2010). We therefore performed a competition assay in which a microsomal membrane preparation containing the receptor protein CEBiP was isolated from rice suspension cells. When this membrane fraction was incubated with 0.4 μ M biotinylated *N*-acetylchito-octaose (GlcNAc)₈, labeling of CEBiP occurred (Figure 4E). When an equimolar amount of Slp1 (0.4 μ M) was added, a significant portion of biotinylated (GlcNAc)₈ bound to the effector, suggesting that Slp1 is capable of competing with CEBiP for chitin binding in this assay. When a 10-fold molar excess of Slp1 (4 μ M) was added, binding of biotinylated (GlcNAc)₈ to the membrane fraction containing CEBiP was almost entirely blocked and resulted in the almost exclusive labeling of Slp1 (Figure 4E).

We also determined the affinity kinetics of Slp1 for chitin oligosaccharides using surface plasmon resonance (SPR) technology. Using SPR, we tested for binding of Slp1 and Ecp6 to the ligand (chitin oligosaccharides [(GlcNAc)₈]). Using the ligand-immobilized method, in which chitin oligosaccharides are immobilized to the sensor chip, we were able to calculate dissociation constants (K_d values) for both Slp1 and Ecp6 (Figure 4D). We estimated that the affinity for chitin oligosaccharides was similar for both Slp1 and Ecp6, with K_d values of 2.4×10^{-9} M and 1.3×10^{-9} M, respectively. Previously, the K_d value of CEBiP for chitin oligosaccharides was calculated as 2.9×10^{-8} M (Shibuya et al., 1996). Full rate constant values, including the K_d and K_{on} values, for the association of Slp1 for chitin oligosaccharides can be found in Supplemental Table 1 online. These results suggest that Slp1 and Ecp6 both show a high affinity for chitin oligosaccharides, which is consistent with the ability of Slp1 to act as competitive inhibitor of CEBiP. When all of these results are considered together, we conclude that the *M. oryzae* Slp1 protein competes directly with chitin

receptor proteins in rice and is able to suppress chitin-induced immunity.

Targeted Gene Silencing of CEBiP in Rice Restores the Ability of Δ slp1 Mutants of *M. oryzae* to Cause Rice Blast Disease

We were interested in establishing whether the ability of the Slp1 effector to act as a competitive inhibitor of CEBiP, thereby suppressing PAMP-triggered immunity, was the reason why *M. oryzae* Δ slp1 mutants showed a significant reduction in their ability to cause rice blast disease. We therefore obtained transgenic rice lines of cultivar Nipponbare, in which the CEBiP-encoding gene had been silenced using RNA interference (RNAi; Kishimoto et al., 2010). These rice lines have previously been shown to lack chitin-triggered immune responses and to exhibit increased susceptibility to rice blast disease (Kishimoto et al., 2010). We inoculated the CEBiP RNAi plants, and corresponding wild-type Nipponbare rice lines, with the *M. oryzae* Δ slp1 mutant and Guy11 strain. Strikingly, we observed that the Δ slp1 mutant was as virulent as Guy11 when inoculated onto CEBiP RNAi plants (Figure 5). On CEBiP RNAi plants, the mean number of host cells occupied by the fungus at 48 HAI by the Guy11 and Δ slp1 strain was 9.4 ($SD \pm 3.21$) and 10.2 ($SD \pm 2.83$), respectively. Furthermore, on CEBiP RNAi plants, no significant difference in host tissue colonization was observed between Guy11 and the Δ slp1 mutant (two-tailed *t* test, $n = 34$ infection sites, $P = 0.322$). By contrast, when nonsilenced Nipponbare rice lines were inoculated, the mean number of host cells occupied by Guy11 and the Δ slp1 mutant was 8.1 ($SD \pm 2.63$) and 3.7 ($SD \pm 1.78$), respectively. The mean number of host cells colonized by the Δ slp1 mutant was significantly lower than the wild-type Guy11 (two-tailed *t* test, $P < 0.01$) (Figure 5). We also found that spray inoculation of CEBiP-RNAi seedlings with the Δ slp1 mutant led to restoration of the number of disease lesions (data not shown). We conclude that it is the ability of Slp1 to act as a competitive inhibitor of CEBiP that is its principal function during rice blast disease and that this role is highly significant in determining the outcome of the host-pathogen interaction.

DISCUSSION

In this study, we set out to investigate the mechanisms used by the rice blast fungus to colonize living rice tissue. We focused on whether effector proteins secreted by *M. oryzae* during biotrophic growth could be involved in perturbing the way that rice plants initially detect the invading fungus by means of PAMP molecules, such as chitin oligosaccharides. Our results provide evidence that *M. oryzae* deploys an effector, Slp1, to suppress chitin-induced host defense responses in rice tissue and that this is significant in the development of rice blast disease. By contrast with previously described rice blast effectors (Jia et al., 2000; Khang et al., 2010), Slp1 accumulates in the apoplastic space at the plant-fungal interface and, in particular, is associated with colonization of new rice cells by the fungus during invasive growth. At this stage, however, we cannot exclude that Slp1 is secreted and subsequently becomes incorporated into the

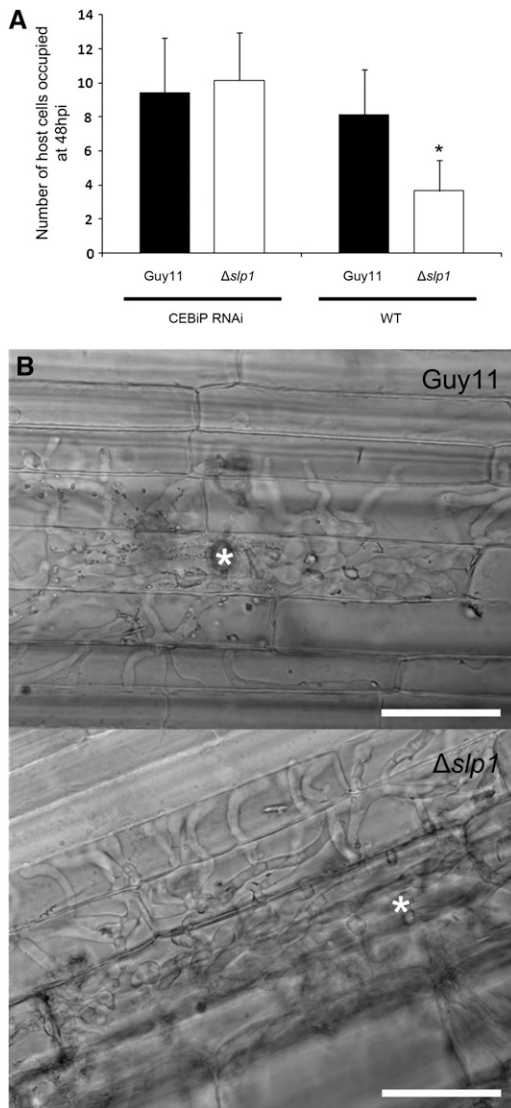


Figure 5. The Ability of a $\Delta slp1$ Mutant to Cause Rice Blast Disease Is Restored When Inoculated onto a Rice Cultivar in Which CEBiP Has Been Silenced by RNAi.

(A) At 48 HAI, host cell colonization of the $\Delta slp1$ mutant was similar to that of Guy11 on a CEBiP RNAi line of cultivar Nipponbare (two-tailed t test, $P = 0.323$). On wild-type nontransformed Nipponbare, the $\Delta slp1$ mutant was significantly reduced in its ability to colonize host tissue (two-tailed t test, $P < 0.01$). Error bars represent 1 SD.

(B) Micrographs of typical infection sites of Guy11 and $\Delta slp1$ on leaf sheath tissue from the CEBiP RNAi line. White asterisks mark the initial site of host cell entry. Bars = 35 μ m.

fungal cell wall matrix. Immunolocalization of Slp1 will help us to establish the precise localization of Slp1 at the plant-fungal interface. Having demonstrated a chitin binding role of Slp1, it is highly likely that Slp1 binds chitin oligosaccharides in the cell wall matrix in addition to free chitin oligosaccharides in the apoplastic space. We showed, by infecting a transgenic rice cultivar expressing a plant plasma membrane-targeted Lti6b-GFP, that

M. oryzae invasive hyphae are encased by the invaginated plant cell membrane (or EIHM), suggesting an intimate interaction between the fungus and host, consistent with studies that have used the lipophilic styryl dye FM4-64 to investigate the nature of plant cell colonization by the rice blast fungus (Kankanala et al., 2007; Mosquera et al., 2009). Furthermore, the pattern of localization of Slp1 is strikingly different than that of BIC-localized (Khang et al., 2010) effector proteins that are subsequently delivered across the EIHM to the host cytoplasm (Khang et al., 2010). The pattern of localization of Slp1-GFP is similar to that of the putative rice blast effector protein BAS4 (Mosquera et al., 2009). Fusions of BAS4 to the fluorescent protein enhanced GFP have previously been shown to outline completely invasively growing biotrophic hyphae (Mosquera et al., 2009; Khang et al., 2010), although no function has yet been assigned to BAS4, and the significance of its apoplastic localization in rice blast disease has yet to be determined. The partial colocalization of Slp1-GFP and Bas4-mRFP reported here are consistent with Slp1 being apoplastically localized but highlight its secretion from actively growing invasive hyphal tips as they colonize new rice cells, which contrasts with the pattern of Bas4 secretion. These localization results support a distinct function for Slp1 compared with those of host cell-delivered effectors, which are likely to bind to intracellular targets within host plant cells (Jia et al., 2000). The molecular basis of effector translocation into host cells by fungal pathogens is not yet known, although a conserved mechanism involving phospholipid binding at the host cell membrane has been proposed in eukaryotic pathogens, such as oomycetes and fungi (Kale et al., 2010).

As a consequence of its ability to bind chitin, we set out to determine whether Slp1 was capable of altering the chitin-triggered immune response of rice, the native host of *M. oryzae*. An increasing body of evidence has implicated the chitin elicitor receptor CEBiP in rice immunity (Kaku et al., 2006; Shimizu et al., 2010; Kishimoto et al., 2010). CEBiP is a plasma membrane glycoprotein that contains two LysM domains and shows high affinity for chito-oligosaccharides (Kaku et al., 2006). A reduction in CEBiP expression in cultured rice cells leads to a decrease in chitin elicitor-triggered defense responses, including ROS generation and expression of plant defense-associated genes (Kaku et al., 2006). CEBiP interacts with the chitin elicitor receptor kinase CERK1, which is also necessary for chitin-triggered immunity responses (Shimizu et al., 2010). In *Arabidopsis thaliana*, a similar LysM receptor-like kinase is implicated in chitin-triggered immunity and fungal resistance (Miya et al., 2007; Wan et al., 2008). CEBiP and CERK1 appear to form a plasma membrane heterooligomeric receptor complex in response to chitin oligosaccharides (Shimizu et al., 2010). Significantly, CEBiP is also directly implicated in resistance to rice blast disease; silencing of the *CEBiP* gene in rice allowed enhanced proliferation of *M. oryzae* in rice tissue, while expression of a novel CEBiP/Xa21 chimeric receptor led to more pronounced rice blast resistance (Kishimoto et al., 2010).

Evidence reported here indicates that Slp1 is capable of competing with the CEBiP receptor for chitin oligosaccharides [either (GlcNAc)₆ or (GlcNAc)₈] and suppressing chitin-triggered defense responses, such as ROS generation and induction of plant defense genes. We also showed that Slp1 is capable of

suppressing chitin-triggered immune responses more generally because it is able to suppress medium alkalinization of tomato cell suspensions. SPR analysis also provided evidence that Slp1 has a similar affinity for chitin oligosaccharides as the *C. fulvum* effector Ecp6 (de Jonge et al., 2010) and predicted a higher affinity than previously reported for CEBiP (Shibuya et al., 1996). However, it is also worth noting that affinity measurements of chitin elicitor receptors vary significantly depending on the method used, with isothermal calorimetry and SPR (in either effector or ligand-immobilized modes) all showing significant variation (Shibuya et al., 1996; de Jonge et al., 2010). The K_d value of Ecp6 obtained by SPR using the effector-immobilized mode was, for instance, 3.8×10^{-7} M, while the value obtained previously by isothermal titration calorimetry was only 3.7×10^{-6} M (de Jonge et al., 2010). Generally the K_d values obtained by SPR have a tendency to give smaller values compared with other methods, probably because of the faster binding of the ligand to the immobilized protein on the sensor tip (Jecklin et al., 2009). Limitation of the accessible K_d range in the case of isothermal titration calorimetry may also contribute to the difficulty in comparing these values directly. At this stage, we cannot make any confident conclusions regarding the differential affinity of CEBiP and Slp1. It will be necessary in the future to measure the relative concentration of Slp1 and CEBiP directly at the rice–*M. oryzae* interface, although this is currently an extremely difficult technical challenge. However, we predict that Slp1 is likely to accumulate to a higher molar concentration at the host plasma membrane interface than the membrane-bound CEBiP receptor because the *SLP1* gene is highly expressed during initial invasive growth of *M. oryzae* and live-cell imaging suggests that a significant amount of the effector is present at the host-pathogen interface (Figure 1). The significant reduction in virulence associated with the *M. oryzae* $\Delta slp1$ mutant and the reduced proliferation of the fungus in plant tissue were all consistent with a role for Slp1 in competitive inhibition of the CEBiP receptor, but we were keen to test this hypothesis directly. We therefore inoculated transgenic rice in which the CEBiP receptor gene had been silenced by RNAi (Kishimoto et al., 2010) with the $\Delta slp1$ mutant. The fact that the $\Delta slp1$ mutant caused rice blast normally in this CEBiP RNAi line provides strong evidence that in the absence of a chitin-triggered immune response to suppress, Slp1 does not serve any additional function during plant infection. Rather, the clear virulence phenotype associated with the $\Delta slp1$ mutant on normal wild-type rice cultivars must be associated with its ability to bind chitin and suppress CEBiP-mediated chitin-triggered immunity, consistent with the reduced ability of the mutant to colonize rice cells and the restoration of virulence by reintroduction and expression of *SLP1*. When considered together with the previously reported role of CEBiP in rice blast resistance (Kishimoto et al., 2010), it seems very likely that the interplay between Slp1 and CEBiP is pivotal in determining the progression of rice blast disease.

In addition to binding chitin, we suggest that Slp1 has the capacity to bind to itself, putatively forming homodimers. Recently, yeast two-hybrid analysis was used to demonstrate a positive interaction between the extracellular LysM receptor domains of CEBiP and CERK1 (Shimizu et al., 2010), although fungal LysM effector proteins that have recently been investi-

gated have not appeared to share this property (de Jonge et al., 2010; Marshall et al., 2011). Although a biological reason for the multimerization of Slp1 in *M. oryzae* has not yet been demonstrated and our observations must be considered preliminary, it is possible that Slp1 forms multimers to provide an additional means of shielding bound chitin oligosaccharides or as a means of increasing its space-filling potential in the narrow apoplastic space around invasive hyphae, thereby enhancing its competitive inhibition of the host receptor CEBiP. Determining a crystal structure of Slp1 and studying its ability to form homodimers and multimeric complexes, in addition to its precise chitin oligomer binding characteristics, will enable a rigorous means of testing this hypothesis.

Previous identification of Ecp6 in the extracellular pathogen *C. fulvum* provided the first evidence that suppression of chitin-triggered immunity might be a means by which biotrophic fungal pathogens with this mode of tissue colonization overcome host defenses (de Jonge and Thomma, 2009; de Jonge et al., 2010). Although this and other studies have suggested a function for LysM effectors in suppressing chitin-based immune responses, there has not, until now, been evidence to link the presumed function of these proteins as suppressors of PAMP-triggered immunity to a role in plant disease. Our study has tested this idea and found evidence that the Slp1 effector of *M. oryzae* plays a role in rice blast disease due solely to its function in suppression of chitin-triggered defense responses. A large number of putatively secreted LysM domain-containing fungal proteins have been identified in fungi (de Jonge and Thomma, 2009), suggesting that overcoming this initial line of host defense may be fundamental to the successful infection of plants by pathogenic fungi.

METHODS

Fungal Strains, Growth Conditions, and DNA Analysis

Strains were grown on complete medium as described previously (Talbot et al., 1993). To carry out plant infection assays, spores were harvested from 10- to 14-d-old plate cultures in sterile distilled water and washed twice. Spores were counted using a hemocytometer (Corning) and confirmed using three independent cell counts. Rice plant infections were performed by spraying 21-d-old seedling of the rice blast susceptible rice cultivar CO-39 with spore suspensions at a concentration of 5×10^4 spores mL⁻¹ in 0.2% gelatin, unless stated otherwise, and as described previously (Talbot et al., 1993). Disease symptoms were allowed to develop for 7 d, unless stated otherwise. Infected leaves were imaged using an Epson Workforce scanner at a resolution of 1200 dpi. Lesion size was determined using ImageJ, a freely available image analysis software package from the National Institutes of Health.

Generation and Infection of Transgenic Rice Cultivars

The LTi6B:GFP gene fusion targets GFP to the plant plasma membrane (Kurup et al., 2005) and was obtained from John Runions and Chris Hawes (Oxford Brookes University). The construct was transformed into rice callus into *Oryza sativa* cv Sasanishiki (Yoshida et al., 2009) using standard plant transformation protocols. Rice transformants were grown on 100 μ g mL⁻¹ hygromycin, confirmed by DNA gel blot, and expression checked by qRT-PCR, immunoblotting, and epifluorescence microscopy. T1 transformants

were grown and backcrossed to generate stable T2 plants. For infection experiments, *Magnaporthe oryzae* conidia were harvested and inoculated onto rice leaf sheath at a concentration of 10^5 spores mL^{-1} . Leaf tissue was incubated at 26°C in a moist chamber and fluorescence examined after 24 HAI by epifluorescence microscopy. Transgenic rice lines of cultivar Nipponbare, in which CEBiP had been silenced by RNAi, were as described previously (Kishimoto et al., 2010). CEBiP RNAi seeds were dehusked, surface sterilized using standard procedures, and grown on Murashige and Skoog media containing 25 mg L^{-1} hygromycin for 7 d before being transplanted to soil. For the inoculation of CEBiP RNAi plants, the Δslp1 mutant and Guy11 strains were inoculated at a density of 10^3 spores mL^{-1} onto 4-week-old leaf sheath tissue, as described previously (Mosquera et al., 2009). Leaf tissue was examined at 48 HAI, and the number of host cells occupied by biotrophically growing fungal hyphae in the upper epidermal leaf layer was counted. Experiments were repeated three times.

Phylogenetic Analysis

Phylogenetic tree construction used the phylogenetic analysis program PhyML (Dereeper et al., 2008). Phylogenies were constructed using the sequences shown in Supplemental Data Set 1 online, which were acquired based on a support value of 1 e^{-10} with Slp1. Sequence alignments were then generated using ClustalW (Chenna et al., 2003) and manually adjusted to optimize alignments.

Targeted Gene Replacement of *SLP1*

Targeted gene replacement of the *M. oryzae SLP1* gene was performed using the split marker strategy as modified by Kershaw and Talbot (2009). Gene replacement was performed by replacing the 600-bp *SLP1* locus with a hygromycin resistance selectable marker *HPH*, encoding a 1.4-kb hygromycin phosphotransferase resistance cassette. The two overlapping parts of the *hph* templates were PCR amplified using primers M13F with HY and M13R with YG (see Supplemental Table 2 online) as described previously (Kershaw and Talbot, 2009). A 1-kb DNA fragment upstream and downstream of the *SLP1* open reading frame was additionally generated using the primers LF5'*SLP1* and LF3'*SLP1* and RF5'*SLP1* and RF3'*SLP1* amplified from genomic DNA of the Guy11 strain. A second-round PCR reaction was performed to fuse the overlapping split *hph* marker templates with the left and right flanking regions of the *SLP1* locus. The wild-type *M. oryzae* Guy11 strain was then transformed with these deletion cassettes ($2 \text{ }\mu\text{g}$ of each flank). Putative transformants were selected in the presence of hygromycin B ($200 \text{ }\mu\text{g mL}^{-1}$) and checked by DNA gel blot analysis according to standard molecular techniques (Sambrook et al., 1989). Gene sequences and regions either side of *SLP1* were retrieved from the *M. oryzae* genome database at the Broad Institute (<http://www.broadinstitute.org/annotation/fungi/magnaporthe/>). All primer sequences used in this study can be found in Supplemental Table 2 online.

Generation of *SLP1:GFP* and *SLP1²⁷⁻¹⁶²:GFP* Gene Fusions

To generate an *SLP1:GFP* gene fusion, the *SLP1* gene was amplified to include a 2-kb region upstream of the *SLP1* start codon to additionally include the native promoter region using primers 5'*SLP1:GFP* with 3'*SLP1:GFP* (see Supplemental Table 2 online) amplified from genomic DNA. To generate an *SLP1²⁷⁻¹⁶²:GFP* gene fusion, a 2-kb region upstream of the *SLP1* start codon was amplified using the primers 5'*SLP1:GFP* and 3'*SLP-Prom*, and a 468-bp fragment was amplified using the primers 5'*SLP1-nosp* and 3'*SLP1:GFP* from genomic DNA (see Supplemental Table 2 online). These PCR fragments were then transformed with *HindIII*-digested pYSGFP-1 (Saunders et al., 2010) into *Saccharomyces cerevisiae*. In-frame gene fusions were created by gap-repair cloning based on homologous recombination in yeast (Oldenburg et al., 1997).

Constructs were confirmed by sequencing through the gene fusion (MWG Operon) and then transformed into the *M. oryzae* Guy11 strain. At least three independent *SLP1:GFP* transformants were confirmed prior to experimental observations.

Light and Epifluorescence Microscopy

Epifluorescence microscopy was used to visualize GFP and RFP samples using a Zeiss Axioskop 2 microscope with differential interference contrast to image bright-field images. To visualize *SLP1:GFP* and *PWL2:mRFP* on leaf epidermis, conidia were harvested and inoculated onto rice leaf sheath tissue at a concentration of 10^5 spores mL^{-1} as described previously (Kankanala et al., 2007). Infected tissue was then excised and mounted onto a glass slide and observed using an IX81 inverted microscope (Olympus) and a UPlanSApo $\times 100/1.40$ oil objective. Images were analyzed using the software package MetaMorph (Molecular Devices).

Production of Recombinant Slp1 Protein

RNA was extracted from infected leaf tissue 144 HAI. cDNA synthesis was performed on 500 ng of DNAase I (Invitrogen) treated RNA using the Affinityscript qPCR synthesis kit (Stratagene) according to the manufacturer's guidelines. cDNA of *SLP1* was cloned using the primers 5'ATG-*SLP1* and 3'TAG-*SLP1* and cloned into the vector pGEM-T (Promega) according to the manufacturer's instructions. Affinity-tagged Slp1 was generated in the yeast *Pichia pastoris* by amplifying the *SLP1* cDNA using primers 5'Slp-pic9 and 3'Slp1-pic9 to include a 5' in-frame His₆-FLAG-tag and subsequently cloned into vector pPIC9 (Invitrogen). Fermentation to produce recombinant Slp1 was performed as described in (Joosten et al., 1995; de Jonge et al., 2010). His₆-FLAG-tagged Slp1 was purified using a Ni²⁺-NTA Superflow column (Qiagen) according to the manufacturer's instructions.

Affinity Precipitation of Slp1 with Polysaccharides

The affinity of Slp1 for various polysaccharides was investigated by incubating $50 \text{ }\mu\text{g/mL}$ of Slp1 with 5 mg of chitin beads (New England Biolabs), crab shell chitin, chitosan, xylan, or cellulose (Sigma-Aldrich) as described previously (de Jonge et al., 2010). Protein and the polysaccharide of interest were incubated at 4°C on a rocking platform in a final volume of 1 mL of water. After 16 h, the insoluble pellet fraction was centrifuged (5 min, $13,000\text{g}$), and the supernatant was collected. The insoluble fraction was pelleted and rinsed a further three times in distilled sterile water to remove unbound protein. Both the supernatant and the pelleted fractions were then boiled in $200 \text{ }\mu\text{L}$ of 1% SDS solution before being examined by SDS-PAGE and Coomassie Brilliant Blue staining.

Cell Protection Assays Using Crude Extract of Chitinase from Tomato Leaves

Intracellular basis chitinases were extracted as described previously (Joosten et al., 1990, 1995). A $50\text{-}\mu\text{L}$ aliquot of *Trichoderma viride* spores was incubated overnight at room temperature at a concentration of $100 \text{ conidia mL}^{-1}$. Recombinant Slp1 or Avr4 was then added to a final concentration of 10 or $100 \text{ }\mu\text{M}$ (Joosten et al., 1995; de Jonge et al., 2010). After 2 h of incubation, $5 \text{ }\mu\text{L}$ crude chitinase extract was added and spores were visualized microscopically after ~ 2 to 4 h.

Medium Alkalinization of Tomato Cell Suspensions

Suspension-cultured tomato (*Solanum lycopersicum*) cell line Msk8 was maintained as described previously (Felix et al., 1991). To examine medium alkalinization, 2.5 mL aliquots of Msk8 suspension cultured cells were placed into 12-well plates. This was placed on a rotary shaker at

200 rpm and left for 2 h to settle. On addition of either 1 nM (GlcNAc)₆ or 1 nM (GlcNAc)₆ and 10 nM Slp1, the pH of the cells, while shaking, was monitored continuously for 10 min using a glass electrode and recorded, as described by de Jonge et al. (2010). Prior to addition of the experimental to the cell medium, chitin oligosaccharides and recombinant protein were incubated at room temperature to equilibrate.

SPR Analysis

Affinities of LysM effectors to chitin oligosaccharides were analyzed by SPR measurements using a Biaore X100 instrument (GE Healthcare). In the effector-immobilized assay system, effectors were covalently immobilized by amine coupling to Sensor Chip CM5 according to the manufacturer's protocol (GE Healthcare). Binding kinetics was measured by multicycle kinetics mode using Biacore X100 control software. In the (GlcNAc)₆-immobilized assay system, biotinylated (GlcNAc)₈ (Kaku et al., 2006) was coupled to a streptavidin preimmobilized sensor chip (Sensor Chip SA; GE Healthcare). Binding kinetics were measured by single-cycle kinetics mode using Biacore X100 control software. Either (GlcNAc)₈ or effector solution was introduced onto the surface at a flow rate of 30 μ L/min with HBS-EP+ buffer. The interaction was monitored at 25°C as the change in the SPR response. After monitoring for 2 min, the HBS-EP+ buffer was introduced onto the sensor chip to initiate dissociation.

Affinity Labeling of Rice Membranes with Biotinylated (GlcNAc)₈

Affinity labeling with biotinylated (GlcNAc)₈ was performed as described previously (Shinya et al., 2010). Suspension-cultured rice cells of *O. sativa* cv Nipponbare were maintained in a modified N-6 medium as described previously (Tsukada et al., 2002). A microsomal membrane preparation from suspension-cultured rice cells was mixed with biotinylated (GlcNAc)₈ in the presence or absence of Slp1 and adjusted to 30 μ L with binding buffer. After incubation for 1 h on ice, 3 μ L of 3% ethylene glycol bis[succinimidylsuccinate] solution (Pierce) was added to the mixture and kept for 30 min. The reaction was stopped by the addition of 1 M Tris-HCl, mixed with SDS-PAGE sample buffer, boiled for 5 min, and used for SDS-PAGE. Immunoblotting was performed on an Immun-Blot polyvinylidene fluoride membrane (Bio-Rad Laboratories). Detection of biotinylated proteins was performed using a rabbit antibody against biotin (Bethyl Laboratories) as a primary antibody and horseradish peroxidase-conjugated goat anti-rabbit IgG (Chemicon International) as a secondary antibody. Biotinylated proteins were detected by the chemiluminescence with Immobilon Western Detection reagents (Millipore).

Measurement of ROS Generation and Gene Expression Analysis

ROS generation induced by elicitor treatment was analyzed by chemiluminescence due to the ferricyanide-catalyzed oxidation of luminol (5-amino-2,3-dihydro-1,4-phthalazinedione) (Desaki et al., 2006). Briefly, 40 mg of cultured cells was transferred into the 1 mL of fresh medium in a 2-mL centrifuge tube and preincubated for 30 min on a thermomixer shaker at 750 rpm. After the preincubation, (GlcNAc)₈ was separately added to the culture medium in the absence or presence of Slp1. For gene expression studies using qRT-PCR, total RNA was prepared from each rice cultivar (40 mg) using an RNeasy plant mini kit (Qiagen) and subjected to cDNA synthesis using a QuantiTect reverse transcription kit (Qiagen). qRT-PCR was performed using TaqMan gene expression assay reagent using a model 7500 Fast Real-Time PCR system (Applied Biosystems). The 18S rRNA was used as an internal control to normalize the amount of mRNA. All primers used are shown in Supplemental Table 2 online.

Yeast Two-Hybrid Analysis

SLP1 cDNA was cloned into pGEMT using the primers 5'SLP1-BamHI and 3'SLP1-EcoRI. *SLP1* cDNA was then digested and cloned as a *Bam*HI-

*Eco*RI fragment into the bait vectors pGBKT7 and pGADT7 (Clontech). Sequencing of both constructs was performed using T7 primer to ensure the constructs were in frame. Yeast two-hybrid analysis was then performed using the Matchmaker GAL4 Two-Hybrid System 3 (Clontech) according to the manufacturer's instructions, as described previously (Wilson et al., 2010).

Accession Number

Sequence data from this article can be found in the GenBank/EMBL databases under accession number MGG10097.

Supplemental Data

The following materials are available in the online version of this article.

Supplemental Figure 1. Phylogeny of Fungal LysM Proteins with a Bootstrap Support Value of 100.

Supplemental Figure 2. Multiple Sequence Alignment of the LysM Domains from a Number of Fungal Species.

Supplemental Figure 3. SLP1 Is Not Expressed in Conidia, Germ Tubes, or Incipient or Mature Appressoria.

Supplemental Figure 4. Targeted Gene Replacement of *SLP1* and Confirmation by DNA Gel Blotting.

Supplemental Figure 5. Complementation Analysis of Δ *slp1* Mutants.

Supplemental Figure 6. *SLP1*^{27-162::GFP} Fails to Complement the Virulence Phenotype of the Δ *slp1* Mutant.

Supplemental Figure 7. High Stringency Yeast Two-Hybrid Analysis of a Putative Slp1-Slp1 Protein Interaction.

Supplemental Table 1. Rate Constants for Association and Dissociation of Slp1 with Chitin Oligomers Derived by Surface Plasmon Resonance Analysis.

Supplemental Table 2. Primers Used in This Work.

Supplemental Movie 1. Laser Confocal Micrograph of Invasive Hyphae of *M. oryzae* Showing Three-Dimensional Projection.

Supplemental Data Set 1. Text File of the Alignment of Fungal LysM Proteins Used for the Phylogenetic Analysis in Supplemental Figure 1.

ACKNOWLEDGMENTS

T.A.M. was supported by a Sainsbury Studentship awarded to N.J.T. by the Gatsby Charitable Foundation. B.P.H.J.T. is supported by a Vidi grant of the Research Council for Earth and Life Sciences (ALW) of the Netherlands Organization for Scientific Research. N.S. is funded from the Program for Promotion of Basic Research Activities for Innovative Bioscience (PROBRAIN). We thank Barbara Valent (Kansas State University) for kindly donating the *PWL2:mRFP* construct.

AUTHOR CONTRIBUTIONS

T.A.M. and N.J.T. designed the project. T.A.M., A.K., T.S., L.S.R., I.O., H.S., R.T., Y.N., N.S., and B.P.H.J.T. performed experiments, and all authors contributed to analysis and interpretation of the results. T.A.M. and N.J.T. wrote the article with contributions, revisions, and edits from N.S. and B.P.H.J.T.

Received October 21, 2011; revised December 15, 2011; accepted January 3, 2012; published January 20, 2012.

REFERENCES

- Bolton, M.D., et al. (2008). The novel *Cladosporium fulvum* lysin motif effector Ecp6 is a virulence factor with orthologues in other fungal species. *Mol. Microbiol.* **69**: 119–136.
- Buist, G., Steen, A., Kok, J., and Kuipers, O.P. (2008). LysM, a widely distributed protein motif for binding to (peptido)glycans. *Mol. Microbiol.* **68**: 838–847.
- Chenna, R., Sugawara, H., Koike, T., Lopez, R., Gibson, T.J., Higgins, D.G., and Thompson, J.D. (2003). Multiple sequence alignment with the Clustal series of programs. *Nucleic Acids Res.* **31**: 3497–3500.
- de Jonge, R., and Thomma, B.P.H.J. (2009). Fungal LysM effectors: Extinguishers of host immunity? *Trends Microbiol.* **17**: 151–157.
- de Jonge, R., van Esse, H.P., Kombrink, A., Shinya, T., Desaki, Y., Bours, R., van der Krol, S., Shibuya, N., Joosten, M.H., and Thomma, B.P. (2010). Conserved fungal LysM effector Ecp6 prevents chitin-triggered immunity in plants. *Science* **329**: 953–955.
- Dereeper, A., Guignon, V., Blanc, G., Audic, S., Buffet, S., Chevenet, F., Dufayard, J.F., Guindon, S., Lefort, V., Lescot, M., Claverie, J.M., and Gascuel, O. (2008). Phylogeny.fr: Robust phylogenetic analysis for the non-specialist. *Nucleic Acids Res.* **36**(Web Server issue): W465–W469.
- Desaki, Y., Miya, A., Venkatesh, B., Tsuyumu, S., Yamane, H., Kaku, H., Minami, E., and Shibuya, N. (2006). Bacterial lipopolysaccharides induce defense responses associated with programmed cell death in rice cells. *Plant Cell Physiol.* **47**: 1530–1540.
- Felix, G., Grosskopf, D.G., Regenass, M., Basse, C.W., and Boller, T. (1991). Elicitor-induced ethylene biosynthesis in tomato cells: characterization and use as a bioassay for elicitor action. *Plant Physiol.* **97**: 19–25.
- Felix, G., Regenass, M., and Boller, T. (1993). Specific perception of subnanomolar concentrations of chitin fragments by tomato cells: induction of extracellular alkalisation, changes in protein phosphorylation, and establishment of a refractory state. *Plant J.* **4**: 307–316.
- Jecklin, M.C., Schauer, S., Dumelin, C.E., and Zenobi, R. (2009). Label-free determination of protein-ligand binding constants using mass spectrometry and validation using surface plasmon resonance and isothermal titration calorimetry. *J. Mol. Recognit.* **22**: 319–329.
- Jia, Y., McAdams, S.A., Bryan, G.T., Hershey, H.P., and Valent, B. (2000). Direct interaction of resistance gene and avirulence gene products confers rice blast resistance. *EMBO J.* **19**: 4004–4014.
- Joosten, M.H.A.J., Bergmans, C.J.B., Meulenhoff, E.J.S., Cornelissen, B.J.C., and De Wit, P.J.G.M. (1990). Purification and serological characterization of three basic 15-kilodalton pathogenesis-related proteins from tomato. *Plant Physiol.* **94**: 585–591.
- Joosten, M.H.A.J., Verbakel, H.M., Nettekoven, M.E., Van Leeuwen, J., van der Vossen, R.T.M., and de Wit, P.J.G.M. (1995). The phytopathogenic fungus *Cladosporium fulvum* is not sensitive to the chitinase and β -1,3-glucanase defense proteins of its host, tomato. *Physiol. Mol. Plant Pathol.* **46**: 45–59.
- Kaku, H., Nishizawa, Y., Ishii-Minami, N., Akimoto-Tomiyama, C., Dohmae, N., Takio, K., Minami, E., and Shibuya, N. (2006). Plant cells recognize chitin fragments for defense signaling through a plasma membrane receptor. *Proc. Natl. Acad. Sci. USA* **103**: 11086–11091.
- Kale, S.D., et al. (2010). External lipid PI3P mediates entry of eukaryotic pathogen effectors into plant and animal host cells. *Cell* **142**: 284–295.
- Kankanala, P., Czymbek, K., and Valent, B. (2007). Roles for rice membrane dynamics and plasmodesmata during biotrophic invasion by the blast fungus. *Plant Cell* **19**: 706–724.
- Kershaw, M.J., and Talbot, N.J. (2009). Genome-wide functional analysis reveals that infection-associated fungal autophagy is necessary for rice blast disease. *Proc. Natl. Acad. Sci. USA* **106**: 15967–15972.
- Khang, C.H., Berruyer, R., Giraldo, M.C., Kankanala, P., Park, S.Y., Czymbek, K., Kang, S., and Valent, B. (2010). Translocation of *Magnaporthe oryzae* effectors into rice cells and their subsequent cell-to-cell movement. *Plant Cell* **22**: 1388–1403.
- Kishimoto, K., Kouzai, Y., Kaku, H., Shibuya, N., Minami, E., and Nishizawa, Y. (2010). Perception of the chitin oligosaccharides contributes to disease resistance to blast fungus *Magnaporthe oryzae* in rice. *Plant J.* **64**: 343–354.
- Kurup, S., Runions, J., Köhler, U., Laplaze, L., Hodge, S., and Haseloff, J. (2005). Marking cell lineages in living tissues. *Plant J.* **42**: 444–453.
- Marshall, R., Kombrink, A., Motteram, J., Loza-Reyes, E., Lucas, J., Hammond-Kosack, K.E., Thomma, B.P.H.J., and Rudd, J.J. (2011). Functional analysis of in planta expressed LysM effector homologues from the non-biotrophic fungus *Mycosphaerella graminicola* reveals varying contributions to virulence. *Plant Physiol.* **156**: 756–769.
- Miya, A., Albert, P., Shinya, T., Desaki, Y., Ichimura, K., Shirasu, K., Narusaka, Y., Kawakami, N., Kaku, H., and Shibuya, N. (2007). CERK1, a LysM receptor kinase, is essential for chitin elicitor signaling in Arabidopsis. *Proc. Natl. Acad. Sci. USA* **104**: 19613–19618.
- Mosquera, G., Giraldo, M.C., Khang, C.H., Coughlan, S., and Valent, B. (2009). Interaction transcriptome analysis identifies *Magnaporthe oryzae* BAS1-4 as biotrophy-associated secreted proteins in rice blast disease. *Plant Cell* **21**: 1273–1290.
- Oldenburg, K.R., Vo, K.T., Michaelis, S., and Paddon, C. (1997). Recombination-mediated PCR-directed plasmid construction *in vivo* in yeast. *Nucleic Acids Res.* **25**: 451–452.
- Sambrook, J., Fritsch, E.F., and Maniatis, T. (1989). *Molecular Cloning: A Laboratory Manual*. (Cold Spring Harbor, NY: Cold Spring Harbor Laboratory Press).
- Saunders, D.G., Dagdas, Y.F., and Talbot, N.J. (2010). Spatial uncoupling of mitosis and cytokinesis during appressorium-mediated plant infection by the rice blast fungus *Magnaporthe oryzae*. *Plant Cell* **22**: 2417–2428.
- Shibuya, N., Ebisu, N., Kamada, Y., Kaku, H., Cohn, J., and Ito, N. (1996). Localization and binding characteristics of a high-affinity binding site for N-acetylchitooligosaccharide elicitor in the plasma membrane from suspension-cultured rice cells suggest a role as a receptor for the elicitor signal at the cell surface. *Plant Cell Physiol.* **37**: 894–898.
- Shimizu, T., Nakano, T., Takamizawa, D., Desaki, Y., Ishii-Minami, N., Nishizawa, Y., Minami, E., Okada, K., Yamane, H., Kaku, H., and Shibuya, N. (2010). Two LysM receptor molecules, CEBiP and OsCERK1, cooperatively regulate chitin elicitor signaling in rice. *Plant J.* **64**: 204–214.
- Shinya, T., Osada, T., Desaki, Y., Hatamoto, M., Yamanaka, Y., Hirano, H., Takai, R., Che, F.S., Kaku, H., and Shibuya, N. (2010). Characterization of receptor proteins using affinity cross-linking with biotinylated ligands. *Plant Cell Physiol.* **51**: 262–270.
- Talbot, N.J. (2003). On the trail of a cereal killer: Exploring the biology of *Magnaporthe grisea*. *Annu. Rev. Microbiol.* **57**: 177–202.
- Talbot, N.J., Ebbole, D.J., and Hamer, J.E. (1993). Identification and characterization of *MPG1*, a gene involved in pathogenicity from the rice blast fungus *Magnaporthe grisea*. *Plant Cell* **5**: 1575–1590.
- Thomma, B.P.H.J., VAN Esse, H.P., Crous, P.W., and DE Wit, P.J.G.M. (2005). *Cladosporium fulvum* (syn. *Passalora fulva*), a highly specialized plant pathogen as a model for functional studies on plant pathogenic *Mycosphaerellaceae*. *Mol. Plant Pathol.* **6**: 379–393.
- Tsukada, K., Ishizaka, M., Fujisawa, Y., Iwasaki, Y., Yamaguchi, T., Minami, E., and Shibuya, N. (2002). Rice receptor for chitin oligosaccharides elicitor does not couple to heterotrimeric G-protein:

- elicitor responses of suspension cultured rice cells from Daikoku dwarf (*d1*) mutants lacking a functional G-protein α -subunit. *Physiol. Plant.* **116**: 373–382.
- van den Burg, H.A., Harrison, S.J., Joosten, M.H.A.J., Vervoort, J., and de Wit, P.J.G.M. (2006). *Cladosporium fulvum* Avr4 protects fungal cell walls against hydrolysis by plant chitinases accumulating during infection. *Mol. Plant Microbe Interact.* **19**: 1420–1430.
- van Esse, H.P., Bolton, M.D., Stergiopoulos, I., de Wit, P.J.G.M., and Thomma, B.P.H.J. (2007). The chitin-binding *Cladosporium fulvum* effector protein Avr4 is a virulence factor. *Mol. Plant Microbe Interact.* **20**: 1092–1101.
- van Esse, H.P., Van't Klooster, J.W., Bolton, M.D., Yadeta, K.A., van Baaren, P., Boeren, S., Vervoort, J., de Wit, P.J.G.M., and Thomma, B.P.H.J. (2008). The *Cladosporium fulvum* virulence protein Avr2 inhibits host proteases required for basal defense. *Plant Cell* **20**: 1948–1963.
- Wan, J., Zhang, X.-C., Neece, D., Ramonell, K.M., Clough, S., Kim, S. Y., Stacey, M.G., and Stacey, G. (2008). A LysM receptor-like kinase plays a critical role in chitin signaling and fungal resistance in *Arabidopsis*. *Plant Cell* **20**: 471–481.
- Wang, G., Fiers, M., Ellendorff, U., Wang, Z., de Wit, P.J.G.M., Angenent, G.C., and Thomma, B.P.H.J. (2010). The diverse roles of extracellular leucine-rich repeat-containing receptor-like proteins in plants. *Crit. Rev. Plant Sci.* **29**: 285–299.
- Wilson, R.A., Gibson, R.P., Quispe, C.F., Littlechild, J.A., and Talbot, N.J. (2010). An NADPH-dependent genetic switch regulates plant infection by the rice blast fungus. *Proc. Natl. Acad. Sci. USA* **107**: 21902–21907.
- Wilson, R.A., and Talbot, N.J. (2009). Under pressure: Investigating the biology of plant infection by *Magnaporthe oryzae*. *Nat. Rev. Microbiol.* **7**: 185–195.
- Yamaguchi, T., Minami, E., Ueki, J., and Shibuya, N. (2005). Elicitor-induced activation of phospholipases plays an important role for the induction of defense responses in suspension-cultured rice cells. *Plant Cell Physiol.* **46**: 579–587.
- Yoshida, K., Saitoh, H., Fujisawa, S., Kanzaki, H., Matsumura, H., Yoshida, K., Tosa, Y., Chuma, I., Takano, Y., Win, J., Kamoun, S., and Terauchi, R. (2009). Association genetics reveals three novel avirulence genes from the rice blast fungal pathogen *Magnaporthe oryzae*. *Plant Cell* **21**: 1573–1591.

Effector-Mediated Suppression of Chitin-Triggered Immunity by *Magnaporthe oryzae* Is Necessary for Rice Blast Disease

Thomas A. Mentlak, Anja Kombrink, Tomonori Shinya, Lauren S. Ryder, Ippei Otomo, Hiromasa Saitoh, Ryohei Terauchi, Yoko Nishizawa, Naoto Shibuya, Bart P.H.J. Thomma and Nicholas J. Talbot
Plant Cell; originally published online January 20, 2012;
DOI 10.1105/tpc.111.092957

This information is current as of January 30, 2012

Supplemental Data	http://www.plantcell.org/content/suppl/2012/01/13/tpc.111.092957.DC1.html
Permissions	https://www.copyright.com/ccc/openurl.do?sid=pd_hw1532298X&issn=1532298X&WT.mc_id=pd_hw1532298X
eTOCs	Sign up for eTOCs at: http://www.plantcell.org/cgi/alerts/ctmain
CiteTrack Alerts	Sign up for CiteTrack Alerts at: http://www.plantcell.org/cgi/alerts/ctmain
Subscription Information	Subscription Information for <i>The Plant Cell</i> and <i>Plant Physiology</i> is available at: http://www.aspb.org/publications/subscriptions.cfm

Appendix 2

Mentlak, T. A., Talbot, N. J. and Kroj, T. (2012) Effector translocation and delivery by the rice blast fungus *Magnaporthe oryzae*. In “Effectors in Plant-Microbe Interactions”, Edited by Francis Martin and Sophien Kamoun. Wiley-Blackwell Press.

Section 4

Effector Trafficking: Processing/Uptake by Plants and Secretion/Delivery by Microbes

9 Effector Translocation and Delivery by the Rice Blast Fungus *Magnaporthe oryzae*

Thomas Mentlak, Nicholas J. Talbot, and Thomas Kroj

9.1 Introduction

Rice blast is the most serious disease of cultivated rice and leads to very significant harvest losses each year. Current research is aimed at understanding the biology of plant infection and, in particular, determining how the fungus is able to proliferate within living rice cells, suppressing host defenses, gaining nutrition, and growing rapidly to bring about disease symptoms and yield losses. In this chapter, we explore recent evidence regarding the identity and biological function of effector proteins that are produced by the fungus during rice infection. We critically evaluate the experimental evidence that suggests that rice blast effector proteins are delivered into plant cells, and attempt to shed light on the likely mechanisms involved in exocytosis of effectors and host cell delivery. Finally, we take a forward look at the experimental strategies that will be necessary to determine the biological functions of effectors and how they are delivered.

Au: Please check the hierarchical level of all section headings for correctness.

9.2 The Fungus *Magnaporthe oryzae*

The rice blast fungus *Magnaporthe oryzae* is a filamentous, heterothallic ascomycete, that causes disease in more than 50 grass species, including several economically important crops such as rice (*Oryza sativa*), barley (*Hordeum vulgare*), wheat (*Triticum aestivum*), and millet (*Eleusine coracana*). It has been estimated that between 10% and 30% of the annual rice harvest is lost due to rice blast disease (Zeigler et al., 1994), making *M. oryzae* one of the most significant disease-causing microbes and a continued threat to global food security. Rice blast research has tended to focus predominantly on the prepenetration stage of plant infection and investigating how the fungus breaches the host cuticle (for a review see Wilson and Talbot, 2009). By contrast, the biotrophic growth phase of *M. oryzae* within living rice cells is poorly understood. Identifying potential fungal effector proteins and the means by which

they are delivered into plant cells is therefore a major goal of rice blast research because it offers fundamental new insight into the manner in which fungi can modulate and perturb host cell physiology and signaling in favor of the invading pathogen.

9.2.1 *The Infection Cycle of Magnaporthe oryzae*

The rice blast fungus is capable of infecting all of the aerial parts of a rice plant, including the leaf, stem, nodes, neck, and panicle (Wilson and Talbot, 2009). Foliar infection by *M. oryzae* commences when a three-celled asexual spore lands on the leaf surface and attaches to the leaf at its apex. The fungus perceives a range of signals, such as the absence of exogenous nutrients, the presence of a hard hydrophobic surface and the presence of plant-derived cutin monomers. These signals stimulate *M. oryzae* conidia to form short polarized germ tubes that rapidly differentiate into dome-shaped, melanin pigmented cells called appressoria, which form within 6 hours of spore germination. Enormous turgor develops within the appressorium, enabling a narrow penetration peg to develop at the base of the infection cell, which ruptures the tough plant cuticle. Research on rice blast disease has focused largely on characterizing the genetic determinants of appressorium formation and understanding their developmental biology (Wilson and Talbot, 2009). Indeed, a number of the developmental regulators involved in appressorium morphogenesis have now been functionally characterized (for reviews, see Talbot, 2003; Wilson and Talbot, 2009).

After initial rupture of the plant cuticle, foliar infection continues and the penetration peg differentiates first into a primary invasive hypha, which then develops into thicker, bulbous, secondary invasive hyphae that proliferate within rice cells. When the first invaded rice epidermal cell is filled with branched, bulbous invasive hyphae, neighboring cells are invaded. Live-cell imaging suggests that secondary invasive hyphae reaching the plant cell wall grow along the inside of the cell wall before swelling slightly and projecting highly constricted hyphae across the host cell wall to colonize new rice cells (Kankanala et al., 2007). Microscopic analysis, and the extreme constriction of hyphae during cell wall crossing, suggests that *M. oryzae* may use plasmodesmata at pit field sites to pass into neighboring cells (Kankanala et al., 2007). Consistent with this idea, *M. oryzae* does not colonize stomatal guard cells that lack plasmodesmata (Kankanala et al., 2007). Host cells remain intact during these early biotrophic infection stages, as demonstrated by plasmolysis experiments in which infected cells were exposed to hyperosmotic sucrose solutions resulting in shrinking of the rice protoplast and retraction of the host plasma membrane around fungal invasive hypha. This result is consistent with the hypothesis that the host plasma membrane remains intact during the

biotrophic growth phase, and that rice cells remain viable during *M. oryzae* infection (Kankanala et al., 2007). After 3–4 days, the fungus alters its growth habit and adopts a necrotrophic lifestyle, in which cell wall degrading enzymes are secreted and host cells killed. Only at this stage do typical disease symptoms become visible, characterized by large necrotic lesions along the leaf (Wilson and Talbot, 2009).

After the fungus has penetrated the host cuticle, the host plasma membrane invaginates and develops into the extrainvasive hyphal membrane (EIHM), which develops around the invasive fungal hyphae (Kankanala et al., 2007). This host-derived plasma membrane surrounds the pathogen as it grows and differentiates within the rice cells. The inability of the membrane tracker dye FM4-64 to reach the fungal plasma membrane during this stage of biotrophic invasion suggests that the plant–fungus interface is sealed from the plant apoplast and is a separate compartment (Kankanala et al., 2007). However, almost nothing is known regarding the way in which plant cellular components are altered in response to invasion by the blast fungus.

During the early biotrophic growth phase when the fungus is sealed by the EIHM, rice blast effectors are believed to be secreted at the plant–fungus interface. These proteins are then thought to be delivered into the host cytoplasm to modulate plant innate immunity and promote further growth and disease, by manipulating host metabolism and physiology (Kankanala et al., 2007). The biological functions of *M. oryzae* effectors are so far largely unknown. The mechanism of effector translocation in plant pathogenic fungi is also not yet understood. However, significant efforts have been made in recent years to identify the rice blast effector catalog and to understand the molecular basis of effector delivery (Mosquera et al., 2009; Khang et al., 2010; Valent and Khang, 2010). In order to understand how the rice blast fungus secretes effector proteins during biotrophic growth, it is first necessary, however, to review how fungi carry out polarized exocytosis of proteins during normal growth and development. In this way, a formal evaluation of the conservation or divergence of the component processes can be undertaken.

9.3 Hyphal Tip Secretion in Filamentous Fungi

To cause disease *M. oryzae* has evolved a mechanism to deliver effector proteins from the fungus into the cytoplasm of host rice cells. In contrast to plant pathogenic bacteria, where the delivery of effectors using the type III secretion system has been well characterized, no dedicated structure for the secretion and delivery of effectors is known in plant pathogenic fungi, including the rice blast fungus. However, the first step in this process is clearly the secretion of the protein from invasive hyphae. In vegetative hyphae, the process of protein secretion starts when translated proteins are directed into the lumen of the

endoplasmic reticulum (ER) for protein folding and glycosylation, based on the presence of a signal peptide at the *N*-terminus of the protein. Here, peptides are packaged into vesicles and subsequently directed toward the Golgi apparatus for further protein modification. Mature proteins are then trafficked in vesicles from the Golgi along cytoskeletal components to the plasma membrane for exocytosis.

The *M. oryzae* genome contains homologs of the heat shock protein (Hsp70) family of yeast, which are known to act as ER chaperones to direct unfolded proteins into the ER lumen. In *Saccharomyces cerevisiae*, the ER luminal proteins Lhs1 and Kar2p mediate delivery of proteins into the ER lumen for protein modification. Mutation of the *M. oryzae* *LHS1* homolog, results in mutants unable to secrete extracellular enzymes such as xylosides, arabinosidases, glucanases, and laccases. Interestingly, they are also unable to localize fluorescently labeled effector proteins to the biotrophic interfacial complex (BIC, see below) in invasive hyphae (Yi et al., 2009). Δ *lhs1* mutants are unable to induce a hypersensitive response (HR) in an *AVR-Pita/Pi-ta* incompatible interaction. When considered together, this suggests that delivery of effector proteins into the ER lumen by chaperone proteins is critical not only for functional protein modification, but also for subsequent stages of exocytosis, and the successful secretion of effector proteins into the host.

In a separate study a novel gene *MgAPT2*, which encodes a P-type ATPase, was identified as serving a role in effector secretion by *M. oryzae* (Gilbert et al., 2006). *MgApt2* encodes an aminophospholipid translocase involved in maintaining the asymmetrical distribution of aminophospholipids in cellular membranes. *Mgapt2* deletion mutants form morphologically normal appressoria, but are unable to cause disease symptoms and are inhibited in their ability to secrete extracellular enzymes. Significantly, Δ *mgapt2* mutant strains are also unable to elicit HR on the resistant rice cultivar IR-68. This suggests that successful delivery of effectors requires a functional Apt2 protein. Further characterization of the Δ *mgapt2* mutant may enable a deeper understanding of the initial stages of effector secretion (Wilson and Talbot, 2009).

Although little is currently known about how proteins are specifically secreted in *M. oryzae*, particularly during biotrophic intracellular growth, many of the likely components can be identified based on studies in model organisms such as the budding yeast, *S. cerevisiae*. Because the molecular components and mechanisms involved in hyphal tip secretion are often highly conserved (Wu et al., 2008; He and Guo, 2009), understanding hyphal tip secretion in yeast and filamentous fungi serves as a useful framework within which to understand how effector proteins may be secreted during biotrophic growth of *M. oryzae*.

Like other filamentous fungi, *M. oryzae* carries out apical growth to a distinct region of a growing cell, a process known as polarized growth, which is a fundamental feature of the growth habit of filamentous fungi (Steinberg,

2007). In *M. oryzae*, polarized growth can be observed during the prepenetration stages of infection, when an axis of polarity is set up in the germ tube that emerges from the apex of the fungal spore. Polarized growth is essential in many fungal pathogens for successful invasion of host tissues and formation of mature mating structures (Brand and Gow, 2009). The asymmetrical distribution of proteins and cellular functions can, however, also be observed in a wide range of eukaryotic organisms, ranging from the polarized growth of pollen tubes and root hairs in plants (reviewed in Cole and Fowler, 2006) to the release of neurotransmitters at mammalian nerve synapses (Nelson, 2003; Virag and Harris, 2006b). Under suitable conditions, *M. oryzae* and other filamentous fungi can undergo continuous and indefinite polarized growth. During polarized growth of filamentous fungi, protein secretion occurs largely through the same mechanisms as eukaryotic protein secretion. Mature and properly folded proteins are packaged into secretory vesicles having been directed through the secretory pathway with the ER and Golgi, and delivered to the plasma membrane at the hyphal tip for exocytosis (Conesa et al., 2001; Steinberg, 2007; Shoji et al., 2008). Protein secretion in filamentous fungi requires three fundamental cellular components: the Spitzenkörper, the polarisome, and the exocyst.

9.3.1 The Role of the Spitzenkörper in Hyphal Growth and Development

In filamentous fungi, secretory vesicles are transported from the Golgi to the cell periphery via the activity of kinesin motor proteins (Steinberg, 2007). They are delivered to a “vesicle organization center” known as the Spitzenkörper, which is found within the cell apex of polarized hyphae (see Fig. 9.1). The Spitzenkörper is visible by microscopy as a refractile body at the center point of the hyphal apex (Harris et al., 2005; Virag and Harris, 2006a). As well as proteins destined for the cell surface, secretory vesicles also contain cell wall components required for hyphal cell growth and extension, such as chitin and glucans. The Spitzenkörper is only present in filamentous fungal hyphae (such as *Aspergillus nidulans*, *Neurospora crassa*, and *M. oryzae*) but is not present in yeasts (*S. cerevisiae*, *Schizosaccharomyces pombe*), which either do not form true hyphae or instead undergo pseudohyphal growth during their life cycle (Virag and Harris, 2006a). The Spitzenkörper operates to maintain the unidirectional movement of vesicles to the hyphal tip apex (see Fig. 9.1). A high concentration of vesicles at the hyphal tip is a characteristic of the Spitzenkörper, but the size and shape of the structure differs spatiotemporally in hyphae and also between species (Steinberg, 2007). Variation in the size and shape of secretory vesicles can also be observed at the Spitzenkörper and whether the contents of such “micro” and “macro” vesicles differ in their respective cargos remains a matter of debate (Virag and Harris, 2006a; Steinberg,

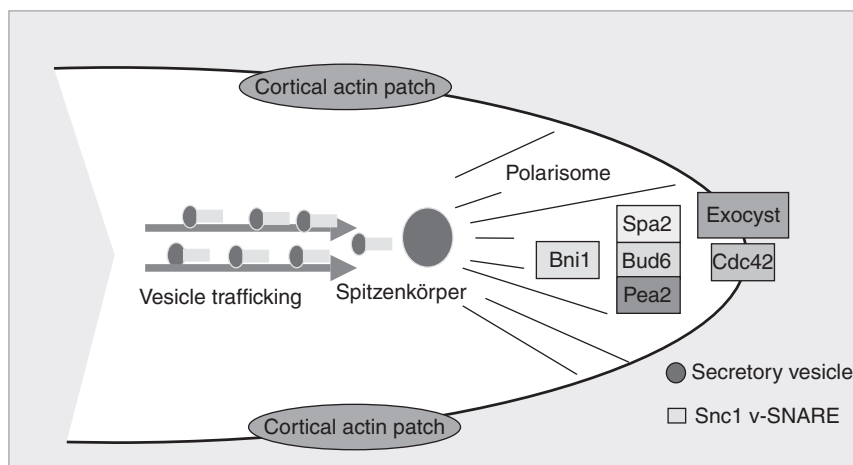


Fig. 9.1 Polarized growth regulation and secretion in filamentous fungi. Fungal hyphae are organized such that secretory vesicles, which carry the enzymes and structural components for cell wall biogenesis, as well as secreted proteins, are transported via microtubules to the hyphal apex. There, a structure known as the Spitzenkörper acts as a vesicle organizing center and transports vesicles to the hyphal tip. The hyphal tip is organized via a complex of proteins collectively termed the polarisome. This organizes the actin cytoskeleton and is essential for polarized growth. The octameric exocyst complex spatially regulates polarized exocytosis and final delivery of secretory vesicles to the hyphal tip.

2007). A number of other cell components accumulate at the Spitzenkörper, including ribosomes, microtubules and microfilaments. Although relatively little is known about how vesicles are organized at the Spitzenkörper, the structure does seem to be involved in polarized growth, because the Spitzenkörper can only be observed in the actively growing regions of highly polarized hyphal tips (Steinberg, 2007). The temporal and dynamic nature of the Spitzenkörper within a single hypha has led some to argue that the Spitzenkörper is merely a visible manifestation of the accumulation of vesicles and cellular movements at the hyphal tip, rather than being a discrete cellular component (Virag and Harris, 2006). The disappearance of the Spitzenkörper when polarized growth ceases lends further support to this idea. Little is known about the components of the Spitzenkörper, its role in infection-related development and pathogenesis in fungal pathogens, or how the Spitzenkörper is regulated and assembled (Harris et al., 2005). Although genetic determinants affecting the size and shape of the Spitzenkörper have been described in filamentous fungi (Browning et al., 2003; Konzack et al., 2005), how the Spitzenkörper is regulated remains to be elucidated. It is also not yet clear whether invasive hyphae produced by pathogenic fungi such as *M. oryzae* have a discrete, visible Spitzenkörper during periods of polarized growth.

9.3.2 *The Polarisome Complex and its Role in Secretion in Fungi*

In yeast, a cap-shaped multiprotein complex called the polarisome is found beneath the apical plasma membrane in polarized cells. The polarisome is thought to organize cytoskeletal and cellular components and direct them toward the tip apex to enable functional polarized cell extension, during yeast mating, for instance (Casamayor and Snyder, 2002). The yeast polarisome is made up of four proteins: Bni1, Spa2, Bud6, and Pea2. Arguably, the most central protein in this complex is the formin, Bni1, which binds to actin and mediates, directed filament assembly at the hyphal tip (Harris et al., 2005). The other components of the polarisome are thought to regulate the activity of Bni1 by ensuring the appropriate timing and location of its activity. Together, this protein complex is responsible for interactions with Rho-GTPases, such as the signaling protein Cdc42, and mediates the formation of unbranched linear actin filaments. These actin cables are used for the transport of exocytic vesicles from the Spitzenkörper to the hyphal membrane for exocytosis.

The release of publicly available genome data of filamentous fungi has enabled the identification of homologs of the yeast polarisome complex in filamentous fungi. Although several polarisome protein homologs have been identified, it is not known whether these fungal homologs function in the same way as in yeast species (Virag and Harris, 2006a). Although filamentous fungi possess homologs of Bni1, Spa2, and Bud6, no homologs of Pea2 have been identified (Harris and Momany, 2004). A homolog of Bni1 in *Aspergillus nidulans*, known as SepA, was characterized and shown to localize to an area slightly subapical from the hyphal tip, suggesting localization to the Spitzenkörper rather than the polarisome (Sharpless and Harris, 2002). Further to this, SpaA and BudA, homologs of the yeast scaffold protein Spa2 and Bud6, have been identified and characterized in the filamentous fungus *A. nidulans* (Virag and Harris, 2006b). SpaA was shown to localize to the hyphal tip apex as predicted for a polarisome complex protein, whereas BudA was found to function mainly in formation of septa, providing evidence that the polarisome components function differently between filamentous and nonfilamentous fungi (Virag and Harris, 2006b). The ability to establish multiple axes of polarity is distinct to filamentous fungi and cannot be explained by a direct extrapolation of what is known in yeast (Harris and Momany, 2004). Further characterization of polarisome components, including gene functional and localization studies are needed in order to understand how the polarisome functions in filamentous fungi. Some clues may be derived from studies in *Candida albicans*, an opportunistic human pathogen that is capable of true hyphal, pseudohyphal, and budding growth morphologies at different stages of the life cycle. The polarisome in *C. albicans* mediates cell-cycle dependent growth (for review, see Berman, 2006), but is not present in pseudohyphal cells, suggesting that polarisome components are spatially and temporally

dynamic at different developmental stages and in morphologically distinct cell types. During the biotrophic invasion of rice cells by *M. oryzae*, bulbous pseudohyphal like cells proliferate within host cells (Kankanala et al., 2007). The polarisome of the rice blast fungus and its role in biotrophic growth has not been investigated but it will be interesting to investigate whether polarisome components are present in invasive hyphae, and if they play an important function in effector secretion and its spatial regulation.

9.3.3 The Exocyst Complex and its Role in Polarized Exocytosis in Fungi

Secretory vesicles are delivered to the Spitzenkörper along microtubules, which are subsequently moved on actin cables to the exocyst complex, an octomeric protein complex, which mediates the fusion of secretory vesicles to the plasma membrane in polarized hyphae. In yeast, these eight proteins are Sec3, Sec5, Sec6, Sec8, Sec10, Sec15, Exo70, and Exo84 (He and Guo, 2008). The protein components of the exocyst are structurally conserved between organisms, and often characterized by a series of helical bundles containing linked α -helices, suggesting a common evolutionary origin (He and Guo, 2009). Fusion of exocytic vesicles to the plasma membrane is mediated by the exocyst, with the assistance of a number of soluble *N*-ethylmaleimide-sensitive factor attachment protein receptors (SNAREs), such as Snc1 and Snc2, as well as Rho, Rab, and Ral GTPases, including Cdc42, Rho1, and Rho3 (Fig. 9.1) (for reviews see Wu et al., 2008; He and Guo, 2009). Initial tethering of the secretory vesicle is mediated by Sec4, a Rab GTPase, which has been described as the master regulator of post-Golgi trafficking (France et al., 2006). Sec4, when in a GTP-bound state, binds directly to Sec15 and together they mediate assembly and regulation of the exocyst complex (Guo et al., 1999). Anchoring of the exocyst complex to the plasma membrane involves Sec3 and Exo70, which have been shown to bind directly to phosphatidylinositol 4,5-bisphosphate (PI(4,5)P₂). Positively charged residues on Sec3 and Exo70 are required for binding to the negatively charged PI(4,5)P₂ residing in the phospholipid bilayer of the plasma membrane (Cole and Fowler, 2006). Sec3 interacts with Rho1 and Cdc42, and is thought to self-assemble at polarized sites of exocytosis independently of actin cables (Yamashita et al., 2010). Exo70, in contrast to Sec3, interacts with Rho3 at the plasma membrane and its delivery to polarized sites of tip growth appears to be dependent on actin cables (Boyd et al., 2004). Similarly, the delivery of the other exocyst components to the plasma membrane is also thought to depend on actin cables.

The significance of the exocyst to effector delivery in *M. oryzae* is unknown. The *M. oryzae* homolog of Rho3, the Rab GTPase that interacts with Exo70 in yeast, is however, necessary for pathogenicity during rice blast disease, indicating that Rho3 is a key determinant of appressorium development (Zheng

et al., 2007). Although $\Delta mgrho3$ null mutants form abnormal appressoria and are unable to initiate disease, they are also unable to cause disease on abraded leaf surface, consistent with a role for Rho3 during invasive growth. A Cdc42 homolog has also been identified and described in *M. oryzae* and is necessary for plant disease. Cdc42 null mutants form abnormal appressoria, but the precise function of this homolog in exocytosis or its interaction with the exocyst is not currently known (Zheng et al., 2009). It will be particularly illuminating to determine the precise function of the exocyst in *M. oryzae* and its spatial organization during plant infection.

9.4 Identification of *Magnaporthe oryzae* Effectors

The first rice blast effectors were identified in studies that set out to clone cultivar- or species-specific avirulence genes. Positional cloning was used to identify the *Avr* genes *AVR-Pi-ta* and *AVR-Piz-t*, which trigger resistance responses on rice varieties carrying the corresponding *R* genes. The *PWL* gene family was identified on the basis of their ability to trigger nonhost resistance in weeping lovegrass (*Eragrostis curvula*) (Sweigard et al. 1995, Khang et al., 2005). The function of these small secreted proteins in disease development is not understood. It is thought that they target host proteins or processes to promote infection and have become recognized as *Avr* proteins in weeping lovegrass.

Large-scale genome sequencing has allowed the prediction of the entire secreted proteome of *M. oryzae* and this has served as a useful basis for identifying putative effector-encoding genes. Depending on the signal peptide prediction software utilized and filters for elimination of false positives, the proportion of putatively secreted proteins in the total *M. oryzae* proteome varies from 7% to 22%. Using 11,109 predicted *M. oryzae* proteins from strain 70-15, a combination of the programs SignalP 2.1 and ProtComp identified 739 (~7%) secreted proteins (Dean et al., 2005), while SignalP 3.0 and TargetP, combined with filters for mitochondrial and transmembrane proteins identified 1306 (12%) secreted proteins using the same dataset (Yoshida et al., 2009). SignalP 3.0 and WoLFPSORT predicted 1546 (12%) secreted proteins, on the basis of 12,841 predicted *Magnaporthe* proteins from 70-15 (Soanes et al., 2008) and a pipeline integrating six prediction programs for secreted proteins (SignalP, SigPred, SigCleave, RPSP, PSortII, and TargetP) and four rules to filter for false positives (presence of more than one transmembrane domain, ER retention signal, nuclear localization, or mitochondria-targeting signal) identified 2470 secreted proteins among 11,069 *M. oryzae* proteins, representing some 22% of the total proteome (Choi et al., 2010). In these studies, a high proportion of the secreted proteins were small peptides of unknown function. A precise classification of the whole effector complement of *M. oryzae* is,

Au: You have cited reference "Khang et al., 2005" in sentence "The *PWL* gene family was identified . . . (*Eragrostis curvula*)." but you have not given this reference in the reference list. Could you please provide the details of the reference to be included in the reference list?

however, far from being complete, because a substantial proportion of false positives and false negatives is likely with purely bioinformatic predictions. A significant number of gene models furthermore suffer from incorrect annotation of the translational start site, preventing, for example, the detection of some putative signal peptides. In particular, genes with plant-specific expression patterns seem to be frequently misannotated because the predicted gene models are not corrected by EST data due to the low number of *in planta* cDNA sequencing studies in *M. oryzae* (Kim et al., 2010). Moreover, many putative effector genes are likely to be missed by automatic gene finding software and are therefore not present in the analyzed proteomes. This is because the generally used size cut-off for valid gene models is 100 amino acids (aa), and therefore, small peptides are often omitted (Dean et al., 2005). Some of the validated *Magnaporthe* effectors, such as AVR-Pii and AVR-Pia, for instance, are proteins smaller than 100 aa and when a size cut-off of 50 aa was used in a study where a *Magnaporthe* field isolate was resequenced, a much higher number of potential effector genes were detected (Yoshida et al., 2009).

As effectors act on plant cellular or biochemical functions, an important criterion for their detection is infection-specific expression, or at least preferential expression during plant infection. At present, our knowledge of the *in planta* transcriptome is rather limited. This is due to the low biomass of the fungus compared to that of the host during early stages of infection. Sequencing studies of cDNA from early infection have only identified relatively small numbers of fungal ESTs. For example, one study found that fungal ESTs from early stage infection represented less than 0.1% of the total ESTs (Jantasuriyarat et al., 2005). In contrast, at later infection stages, fungal cDNAs make up 25% of the total cDNAs (Kim et al., 2001, 2010), but at this point the fungus is colonizing the leaf in a necrotrophic manner, and growing intercellularly. The *M. oryzae* transcriptome during the early stages of plant infection has been analyzed using oligonucleotide micro arrays and a combination of high inoculum applied to the very sensitive leaf sheath tissue (Mosquera et al., 2009). A total of 1120 fungal genes expressed during the biotrophic invasion of the first epidermal plant cell were identified. Among these genes, approximately 140 encoded secreted proteins. Ninety of them were of unknown function and specifically or preferentially expressed during biotrophic invasive growth and named biotrophy-associated secreted (BAS) proteins. In the case of four of the BAS genes (*BAS1–4*), infection specific expression was confirmed. However, loss of function mutants corresponding to three of these genes were not altered in virulence, suggesting that considerable redundancy in virulence-associated effector function exists in *M. oryzae*. Interestingly, the four BAS proteins showed different *in planta* localization patterns. A BAS1:GFP fusion accumulated inside biotrophically invaded host cells (Mosquera et al., 2009; Khang et al., 2010). The GFP fusion of BAS3, a cysteine-rich protein of 113 aa, strongly accumulated at the appressorium

penetration site and uniformly outlined invasive hyphae. At later infection stages, fluorescence accumulated where individual hyphae had crossed the plant cell wall. Green fluorescent protein (GFP) fusions of BAS4, a cysteine-rich protein of 102aa, uniformly outlined invasive hyphae. As a consequence, BAS4 was suggested to be an extracellular interfacial matrix protein.

Genes encoding putative effector proteins were enriched among genes that were highly expressed during biotrophic growth (Mosquera et al., 2009). These genes had not been detected in previous gene expression studies, which have used various growth media or appressoria-inducing substrates and may therefore be completely infection-specific (Ebbole et al., 2004).

Interestingly, *M. oryzae* Avr proteins and candidate effectors seem, in general, to have low natural nucleotide polymorphism, but do show a relatively high level of presence/absence polymorphism. For example, when 1032 loci-encoding secreted proteins were analyzed in 21 Japanese rice-infecting isolates of *M. oryzae* for presence/absence polymorphisms, 394 genes were identified in the genome of the reference strain 70-15 that were absent from a number of the other field strains (Yoshida et al., 2009). Analysis of the same 1032 loci for nucleotide polymorphism in a worldwide collection of 46 strains, however, identified only 227 polymorphic loci. Even higher levels of presence/absence polymorphism were identified among 316 genes identified in the genome of a Japanese field isolate of *M. oryzae*, Ina168, but not present in the genome sequence of the reference 70-15 strain (Yoshida et al., 2009). These results suggest that *M. oryzae* effectors show less sequence polymorphism than effectors identified in other pathogens, such as the oomycetes, which show highly polymorphic sets of effector-encoding genes with evidence of diversifying selection (Kamoun, 2006). However, the presence/absence polymorphism of effectors in different strains of the fungus suggests that the repertoire of effectors may be very large, but with considerable redundancy and variability between strains of *M. oryzae*. Population genetics approaches may allow identification of effectors under strong selection, while association genetics studies may predict further sets of putative effectors based on their presence or absence in cultivar-specific races of the fungus. The power of association genetics in *M. oryzae* was demonstrated by Yoshida et al. (2009), who were able to clone three effector-encoding genes with avirulence activity, *AVR-Pia*, *AVR-Pii*, and *AVR-Pik*, in a single experiment by association genetics.

Au: As per style, we need to define an acronym/abbreviation on its first occurrence in the text. Hence, through our search we have defined "GFP" as "Green fluorescent protein". Could you please confirm that it is OK?

9.4.1 *M. oryzae* Effectors that Cause Effector-Triggered Immunity (ETI)

More than 40 *M. oryzae* AVR genes have been identified by race profiling. To date, eight of them have been cloned. With the exception of the unusual AVR gene *ACE1*, which encodes an enzyme of secondary metabolism [a hybrid

polyketide synthase, nonribosomal peptide synthetase (Bohnert et al., 2004)], all the cloned *M. oryzae* Avr genes encode small secreted proteins.

PWL proteins (for pathogenicity toward weeping lovegrass) confer avirulence on weeping lovegrass (*E. curvula*) and constitute a small gene family with a varying number of members in *M. oryzae* strains with different species specificities (Kang et al., 1995; Sweigard, 1995). PWL proteins are secreted, glycine-rich proteins of 110–140 aa in size (Schneider et al., 2010). PWL2 is expressed and secreted specifically during invasive biotrophic growth and appears to be translocated into host cells (Khang et al., 2010). The role of PWL proteins during infection and their contribution to virulence is not known.

The AVR-Pita encoded effector triggers resistance on rice varieties possessing the resistance gene, *Pi-ta*, and has been cloned by map-based cloning. AVR-Pita encodes a secreted protein of 223 aa with similarity to class 35, deuterolysin neutral zinc proteases (Orbach et al., 2000). In addition to the signal peptide, it possesses a putative propeptide that may be cleaved for activation of AVR-Pita. Cleavage would liberate a mature 176 aa derivative of AVR-Pita named AVR-Pita₁₇₆. AVR-Pita₁₇₆ has been shown to interact directly in yeast two hybrid assays and far western analysis with its cognate R protein, Pi-ta, which is a CC-NBS-LRR class resistance gene product (Jia et al., 2000). AVR-Pita is specifically expressed and secreted during infection and an AVR-Pita:GFP gene fusion leads to the accumulation of fluorescently labeled AVR-Pita during invasive biotrophic growth (Khang et al., 2010). AVR-Pita is probably translocated into host cells because Pi-ta is predicted to be cytoplasmic and also because transient expression of AVR-Pita₁₇₆ inside rice cells carrying *Pi-ta* triggers HR (Jia et al., 2000). Interestingly, expression of full length AVR-Pita including the signal peptide and the propeptide in rice cells does not trigger HR, suggesting that specific maturation of AVR-Pita is necessary (i.e., cleavage of the propeptide) or that AVR-Pita is not able to re-enter plant cells upon secretion without additional factors of the pathogen. The contribution of AVR-Pita to fungal virulence and its molecular function are not known. In particular, it remains an open question as to whether AVR-Pita encodes an active protease. Physical interaction with Pi-ta and elicitation of HR are abolished by point mutations in the putative catalytic center of AVR-Pita, but protease activity has not been directly demonstrated, while the AVR-Pita propeptide also differs in composition and length from those of the classical class 35 metalloproteases in *M. oryzae* and other fungi (Monod et al., 2002). AVR-Pita shows elevated nucleotide polymorphism (Yoshida et al., 2009) and the locus is particularly unstable under laboratory and field conditions. This may be due to its subtelomeric localization (Khang et al., 2008).

The AVR-CO39 locus has been restricted to a 1.06-kb fragment of a weeping lovegrass-infecting *M. oryzae* strain by chromosome walking (Farman and Leong, 1998). It contains several potential open reading frames (ORFs). ORF3, which encode a secreted protein of 89 aa, has been suggested to correspond

to *AVR-CO39* (Farman and Leong, 1998; Peyyala and Farman, 2006). *AVR-CO39* is widely distributed in *M. oryzae* strains infecting cereals and grasses, but absent, or inactivated by a transposon insertion, in rice-infecting *M. oryzae* isolates (Farman et al., 2002; Tosa et al., 2004). It is recognized in rice in a cultivar-specific manner by the *Pi-CO39* resistance gene (Chauhan et al., 2002).

AVR-Piz-t confers avirulence on rice varieties carrying the resistance gene *Piz-t* and was isolated by map-based cloning (Li et al., 2009). It encodes a secreted protein of 108 aa with unknown function and without homology to other proteins in databases. Interestingly, *AVR-Piz-t* inhibits Bax-triggered cell death in a *Nicotiana benthamiana* transient assay, suggesting that it might act as a cell death inhibitor during infection. *AVR-Piz-t* is inactivated in certain isolates by insertion of a *Pot3* transposon in the promoter or by a single nucleotide polymorphisms changing valine at position 41 into alanine (Li et al., 2009).

AVR-Pia, *AVR-Pii*, and *AVR-Pik* confer avirulence on rice varieties carrying the cognate resistance genes, *Pi-a*, *Pi-i*, and *Pi-k*, respectively. They have been cloned using association genetics (Yoshida et al., 2009), and *AVR-Pia* has been cloned independently by map-based cloning (Miki et al., 2009). All three effectors carry potential secretion signals and are small in size (85 aa, 70 aa, and 133 aa, respectively) and are of unknown function. Only *AVR-Pii* possess homologs in the *M. oryzae* genome with which it shares two conserved motifs: m-1, which has the consensus LxAR, which is also present in *AVR-Piz-t* and other *Magnaporthe* effectors and m-2 with the cysteine-histidine consensus Cx₂Cx₁₂H, similar to the C2H2 zinc finger motif involved in protein-protein interactions. All three effectors seem to be translocated into host cells because expression of alleles without secretion signal sequences inside resistant rice protoplasts triggered HR (Yoshida et al., 2009). This is consistent with the putatively cytoplasmic localization of the two NBS-LRR class proteins required for *Pik-m* specific resistance (Ashikawa et al., 2008). All three effectors show extensive presence/absence polymorphism in rice-infecting *M. oryzae* strains (Yoshida et al., 2009). *AVR-Pik* also shows allelic variability, with five allelic variants of *Avr-Pik* identified. The D variant was recognized in varieties with *Pik*, *Pik-m*, and *Pik-p*, while the E variant was only recognized in varieties with *Pik*. The C variant was not recognized (Yoshida et al., 2009).

9.5 To BIC or Not to BIC—That Is the Question

To investigate the localization of effectors, genetically engineered *M. oryzae* strains have been developed that express translational fusions between effectors and fluorescent marker proteins (effector:FPs), such as GFP and RFP.

These marker strains have revealed a characteristic localization pattern for translocated effectors such as AVR-Pita, PWL1, PWL2, and BAS1, in which effector:FPs accumulate preferentially in a membrane-rich punctate structure at the biotrophic fungus–plant interface, which has been named the biotrophic interfacial complex (BIC) (Khang et al., 2010). Other secreted *Magnaporthe* proteins such as BAS4 or cutinase, which are not thought to be translocated, show only weak accumulation in BICs, but instead show strong and uniform fluorescence outlining invasive hyphae. Another putative nontranslocated effector, BAS3:FP, shows strong accumulation under appressorium-penetration sites and at cell wall crossing points, but only weak BIC localization. The particular enrichment of translocated effectors at BICs provides evidence for a potential role of the BIC in the translocation of effectors into the host cytoplasm. However, this has to be strengthened by further characterization and functional analysis of the BIC structure.

Interestingly, the localization of the BIC shows a two-stage development during the infection process. During the early stages of cell invasion, immediately after either cuticle penetration or after crossing the plant cell wall, the BIC is localized at the tip of primary filamentous invasive hyphae (Khang et al., 2010). As the secondary, bulbous invasive hyphae develops the BIC, however, becomes localized at a subapical position (see Fig. 9.2). The BIC remains at this now subapical position as secondary pseudohyphae proliferate elsewhere in the cell. When the invaded cell is almost completely filled with branched bulbous secondary hyphae, and neighboring cells start to be invaded, the initial BIC disappears. New BICs then form at the tips of filamentous hyphae that are invading new cells because effector:FPs accumulate at the tips of these invading hyphae.

Currently, it is not known whether effector:FPs are directly secreted into BICs by targeted exocytosis, or whether effectors are secreted at multiple sites of invasive hyphae and ultimately accumulate into BICs by an unknown molecular mechanism. Primary invasive hyphae exhibit typical filamentous tip growth and it can reasonably be assumed that effector:FPs are delivered directly into BICs at this stage by standard hyphal tip secretion mechanisms involving the Spitzenkörper, polarisome, and exocyst components. At later stages of infection, when the BIC is present subapically, effector:FP secretion into the BIC continues as demonstrated by FRAP experiments (Khang et al., 2010). After bleaching of fluorescence of PWL2:GFP in apical BICs by intense laser light, fluorescence reaccumulated at subapical BICs within 2.5 hours. The continual movement of effector:FPs into the BIC at this stage of infection could be due to the maintenance of the original apical secretory apparatus using conventional ER-related secretory components after cellular differentiation from a filamentous to a pseudohyphal morphology. In order to understand how effectors accumulate into BICs, simultaneous visualization of the secretory apparatus, including the Spitzenkörper and exocyst components,

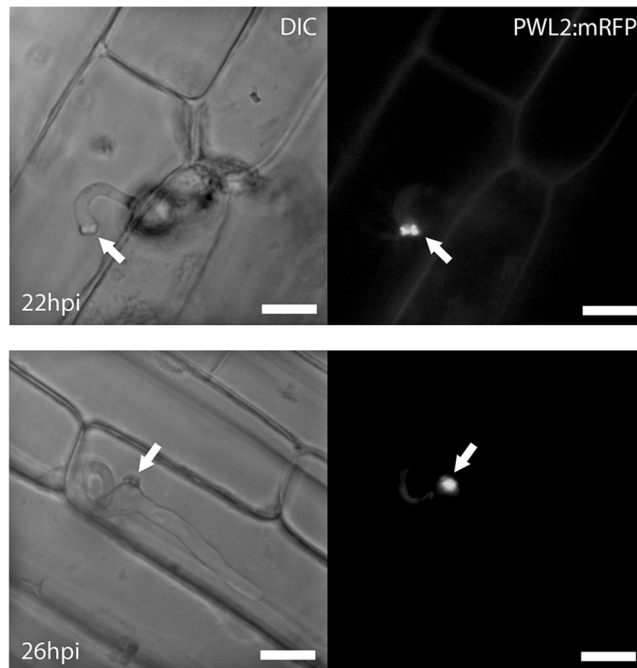


Fig. 9.2 *Magnaporthe oryzae* strains expressing *PWL2:mRFP*, which localizes to BICs as indicated by arrows. After 22 hours postinoculation (hpi), the *PWL2:mRFP* fusion protein localizes to the apical tip region of primary filamentous hyphae (top). After 26 hpi, the fungus has differentiated to form bulbous secondary hyphae. At this time, *PWL2:mRFP* protein continues to localize to the BIC, which is now at a subapical position located on the side of bulbous pseudohyphae (bottom). Scale bar represents 10 μ m.

as well as preferential effector:FP accumulation at BICs is required. Additionally, mutants that lack individual components of the secretory apparatus are also needed to understand the significance of the BIC as an active site for exocytosis and to determine the role of this structure in effector translocation.

Surprisingly, preferential BIC localization is not dependent on the sequence of the mature effector protein, but is instead dependent on the signal peptide directing the effector into the secretory pathway (Mosquera et al., 2009). Fungal strains expressing fusions between the *PWL2* or *AVR-Pita* secretion signal peptide and GFP show preferential BIC labeling, while strains expressing fusions between GFP and the *BAS4* or the cutinase secretion signal peptide show weak BIC labeling and more uniform outlining of invasive hyphae (Khang et al., 2010). To what extent the promoter and the 5' UTR (Untranslated Region) may eventually also contribute to preferential BIC localization, remains to be determined. The specific motifs required for BIC localization and

how these motifs function to direct proteins toward the BIC requires further investigation.

9.6 Effector Translocation into Host Rice Cells by *M. oryzae*

Although the role of the BIC in effector translocation is still unclear, there is now clear experimental evidence that effectors are translocated by *M. oryzae* into the host cytoplasm. Initial in vitro studies using the yeast two hybrid system demonstrated that the AVR-Pi-ta effector interacts directly with the intracellular R protein Pi-ta, consistent with uptake of fungal proteins by host rice cells during infection (Jia et al., 2000), providing the first line of evidence that Avr effectors of the rice blast fungus might be delivered into host cytoplasm. Currently, there are two other lines of evidence that lend support to the notion of effector translocation into the host cytoplasm. Transient expression of alleles of the Avr effectors AVR-Pia, AVR-Pii, and AVR-Pik, deleted for their signal peptide, elicit an HR in rice protoplasts indicating that these *M. oryzae* effectors act inside host cells (Yoshida et al., 2009). Interestingly, alleles including signal peptides also trigger HR. A transient assay based on leaf bombardment has shown that Avr-Pita can be translocated into soybean leaves independently of pathogens (Kale et al., 2010). This suggests, that upon secretion, effectors can enter host cells autonomously, i.e., independently of pathogens and pathogen-derived structures. The internalization of the effectors AvrL567 and AvrM from the flax rust pathogen *Melanospora lini* into the host cytoplasm was demonstrated using transient assays in the absence of the pathogen (Rafiqi et al., 2010). Whether or not effectors enter autonomously into plant cells, by some currently unknown receptor-mediated endocytosis, or whether effector translocation relies on pathogen-derived structures or mechanisms, such as the BIC, remains a central question. In order for the results from transient expression assays to be conclusive, additional controls have to be performed to preclude the possibility that the activity of Avr effector alleles containing signal peptides is not artifactual and not simply due to the detection of nonsecreted Avr effectors by R proteins. Independent experimental approaches like in vitro translocation assays and structure-function analysis of Avr effectors will help to address this question.

The second line of evidence that lends support to the internalization of rice blast effector proteins into the host cytoplasm is based on live-cell imaging, in which effector:FPs have been detected within the host cytoplasm. Using a translational fusion of the fluorescent marker monomeric red fluorescent protein (mRFP) to PWL2. Khang et al. (2010) demonstrated that PWL2 accumulates in rice host cytoplasm during infection. This was achieved with the assistance of two novel assays that were required to concentrate the fluorescent signal, either by plasmolysis of host cells, concentrating the fluorescent signal

in the shrinking rice protoplast, or by attaching a nuclear localization signal (NLS) to the fluorescent signal, which concentrates the fluorescently labeled effector protein in the host nucleus. Surprisingly, fluorescently labeled PWL2 was also detected in neighboring host cells distal to the current site of infection, suggesting that translocated rice blast effectors are capable of cell-to-cell movement, potentially via plasmodesmata (Khang et al., 2010). Cell-to-cell movement of effectors could be a strategy that has evolved in order to prime neighboring cells for imminent fungal invasion, thereby facilitating fungal colonization of its host.

Further tracking of fluorescently labeled PWL2 suggests that effector movement into neighboring cells is dependent on host-cell type. A reduced systemic movement of PWL2 was observed originating from “vein-associated” infection sites compared with movement of PWL2 from “regular” epidermal leaf cells where a greater level of systemic effector movement was observed. The reduced movement of PWL2 from “vein-associated” cells into other cells may be because PWL2 binds to cell-type-specific targets decreasing the levels of leakage into adjacent cells. Secondly, differences in PWL2 movement might be explained by physiological differences in the size of the plasmodesmal aperture between the two host cell-types. The dilation of plasmodesmata is dependent on the physiological and developmental state of the plant cell. Systemic movement of PWL2:mRFP could therefore be explained by variation in the level of plasmodesmal dilation between vein-associated and nonvein-associated cells. Thirdly, PWL2 could be more lowly expressed in vein-associated cells compared to regular epidermal cells. This hypothesis relies on the ability of the fungus to sense its current environment and adjust the expression of certain effectors accordingly. Understanding how these effectors move into neighboring cells should remain a high priority, which will be facilitated by a comparison of transcriptional profiling of infection between varying cell types.

Finally, systemic movement of effector proteins into neighboring cells was shown to be dependent on the molecular weight of the effector. Using variants of fluorescent proteins that vary in molecular weight, Khang et al. (2010) demonstrated that effectors that have a greater molecular weight showed a reduced level of systemic movement. This reduced systemic movement of larger proteins is consistent with the movement of effectors through plasmodesmata. Further research is required in order to understand which effectors are capable of systemic movement, and to demonstrate that these effectors do move through plasmodesmata, or through some as yet unknown mechanism.

9.7 Concluding Remarks

In recent years, it has become increasingly evident that the rice blast fungus produces a wide range of effector molecules that perturb and subvert

host cell signaling and plant defence mechanisms. How these effectors are delivered into host cells is not clear, but it seems likely that the fungus deploys a somewhat variant form of polarized exocytosis. This may involve a specialized membrane-rich structure, such as the BIC. It will be particularly interesting to study the localization and organization of the polarisome and exocyst components in invasive hyphae, in order to determine how secretory processes occur in intracellular invasive hyphae, when compared with polarized vegetative hyphae. This may provide insight into the manner in which effector proteins are initially secreted into the apoplast, prior to take-up by plant cells. The translocation of effectors into host cells clearly takes place, given that they can be physically detected in living rice cells and their biological activity assayed following transient expression in rice protoplasts. How *M. oryzae* effectors enter host cells, and whether there are specific uptake signals, as identified in oomycete effectors, is unclear. Further structure-function studies of rice blast effectors will be needed to clarify this issue and, in particular, if effector uptake has a basically conserved biochemical basis in fungi and oomycetes, as suggested recently (Kale et al., 2010). The ability to carry out live-cell imaging, coupled with the excellent genetics and genomics resources available in *M. oryzae*, means that rapid progress should now be possible in identifying the underlying principles that govern effector uptake, as well as defining the molecular targets and varied biological functions of effectors.

References

- Ashikawa, I., Hayashi, N., Yamane, H., et al. (2008) Two adjacent nucleotide-binding site-Leucine-rich repeat class genes are required to confer *Pikm*-specific rice blast resistance. *Genetics* **180**, 2267–2276.
- Berman, J. (2006) Morphogenesis and cell cycle progression in *Candida albicans*. *Current Opinion in Microbiology* **9**, 595–601.
- Bohnert, H.U., Fudal, I., Dioh, W., Tharreau, D., Notteghem, J.L., & Lebrun, M.H. (2004). A putative polyketide synthase/peptide synthetase from *Magnaporthe grisea* signals pathogen attack to resistant rice. *Plant Cell* **16**, 2499–2513.
- Boyd, C., Hughes, T., Pypaert, M., et al. (2004) Vesicles carry most exocyst subunits to exocytic sites marked by the remaining two subunits, Sec3p and Exo70p. *The Journal of Cell Biology* **167**, 889–901.
- Brand, A. & Gow, N.A.R. (2009) Mechanisms of hypha orientation of fungi. *Current Opinion in Microbiology* **12**, 350–357.
- Browning, H., Hackney, D.D., & Nurse, P. (2003) Targeted movement of cell end factors in fission yeast. *Nature Cell Biology* **5**, 812–818.
- Casamayor, A. & Snyder, M. (2002) Bud-site selection and cell polarity in budding yeast. *Current Opinion Microbiology* **5**, 179–186.
- Chauhan, S., Farman, M.L., Zhang, H.B., et al. (2002) Genetic and physical mapping of a rice blast resistance locus, *PiCO39(t)*, that corresponds to the avirulence gene *AVR-CO39* of *Magnaporthe grisea*. *Molecular Genetics and Genomics* **267**, 603–612.

- Choi, J., Park, J., Kim, D., et al. (2010) Fungal secretome database: integrated platform for annotation of fungal secretomes. *BMC Genomics* **11**, 105–120.
- Conesa, A., Punt, P.J., van Luijk, N., et al. (2001) The secretion pathway in filamentous fungi: a biotechnological view. *Fungal Genetics and Biology* **33**, 155–171.
- Cole, R.A. & Fowler, J.E. (2006) Polarizes growth: maintaining focus on the tip. *Current Opinion in Plant Biology* **9**, 579–588.
- Dean, R.A., Talbot, N.J., Ebbole, D.J., et al. (2005) The genome sequence of the rice blast fungus *Magnaporthe grisea*. *Nature* **434**, 980–986.
- Ebbole, D.J., Jin, Y., Thon, M., et al. (2004). Gene discovery and gene expression in the rice blast fungus, *Magnaporthe grisea*: analysis of expressed sequence tags. *Molecular Plant-Microbe Interactions* **17**, 1337–1347.
- Farman, M.L. & Leong, S.A. (1998) Chromosome walking to the *AVR1-CO39* avirulence gene of *Magnaporthe grisea*: discrepancy between the physical and genetic maps. *Genetics* **150**, 1049–1058.
- Farman, M.L., Eto, Y., Nakao, T., et al. (2002) Analysis of the structure of the *AVR1-CO39* avirulence locus in virulent rice-infecting isolates of *Magnaporthe grisea*. *Molecular Plant-Microbe Interactions* **15**, 6–16.
- France, Y.E., Boyd, C., Coleman, J., et al. (2006) The polarity-establishment component Bem1p interacts with the exocyst complex through the Sec15p subunit. *Journal of Cell Science* **119**, 876–888.
- Gilbert, M.J., Thornton, C.R., Wakley, G.E., et al. (2006) A P-type ATPase required for rice blast disease and induction of host resistance. *Nature*, **440**: 980–986
- Guo, W., Roth, D., Walch-Solimena, C., et al. (1999) The exocyst is an effector for Sec4p, targeting secretory vesicles to sites of exocytosis. *The EMBO Journal* **18**, 1071–1080.
- Harris, S.D. & Momany, M. (2004) Polarity in filamentous fungi: moving beyond the yeast paradigm. *Fungal Genetics and Biology* **41**, 391–400.
- Harris, S.D., Read, N.D., Robertson, R.W., et al. (2005) Polarisome meets Spitzenkörper: microscopy, genetics and genomics coverage. *Eukaryotic Cell* **4**, 225–229.
- He, B. & Guo, W. (2009) The exocyst complex in polarizes exocytosis. *Current Opinion in Cell Biology* **21**, 537–542.
- Jantasuriyarat, C., Gowda, M., Haller, K., et al. (2005) Large-scale identification of expressed sequence tags involved in rice and rice blast fungus interaction. *Plant Physiology* **138**, 105–115.
- Jia, Y., McAdams, S.A., Bryan, G.T., et al. (2000) Direct interaction of resistance gene and avirulence gene products confers rice blast resistance. *The EMBO Journal* **19**, 4004–4014.
- Jones, J.D.G. & Dangl, J.L (2006) The Plant Immune System. *Nature* **444**, 323–329.
- Kale, S.D., Gu, B., Capelluto, D.G.S., et al. (2010) External lipid PI3P mediates entry of Eukaryotic pathogen effectors into plant and animal host cells. *Cell* **142**, 284–295.
- Kamoun, S. (2006) A catalog of the effector secretome of plant pathogenic oomycetes. *Annual Review of Phytopathology* **44**, 41–60.
- Kang, S., Sweigard, J.A., & Valent, B. (1995) The PWL host specificity gene family in the blast fungus *Magnaporthe grisea*. *Molecular Plant-Microbe Interactions* **8**, 939–948.
- Kankanala, P., Czymmek, K., & Valent, B. (2007) Roles for rice membrane dynamics and plasmodesmata during biotrophic invasion by the blast fungus. *The Plant Cell* **19**, 706–724.
- Khang, C.H., Park, S-Y., Lee, Y-H., et al. (2008) Genome organization and evolution of the *AVR-Pita* avirulence gene family in the *Magnaporthe grisea* species complex. *Molecular Plant-Microbe Interactions* **21**, 658–670.
- Khang, C.H., Berruyer, R., Giraldo, M.C., et al. (2010) Translocation of *Magnaporthe oryzae* effectors into rice cells and their subsequent cell-to-cell movement. *The Plant Cell* **23**, 1–16.
- Kim, S., Park, J., Park, S-Y., et al. (2010) Identification and analysis of *in planta* expressed genes of *Magnaporthe oryzae*. *BMC Genomics* **11**, 104–118.
- Kim, S., Ahn, I-P., & Lee, Y-H. (2001) Analysis of genes expressed during rice-Magnaporthe grisea interactions. *Molecular Plant-Microbe Interactions* **14**, 1340–1346.

Au: Reference
“Jones and
Dangl, 2006” is
not cited in the
text. To confirm
to the house
style, every
reference
mentioned in the
list must be cited
in the text.
Could you please
cite the
reference in the
text, or should it
be removed
from the
reference list?
Please confirm.

- Konzack, S., Rischitor, P.E., Enke, C., et al. (2005) The role of the kinesin motor KipA in microtubule organization and polarized growth of *Aspergillus nidulans*. *Microbiology of the Cell* **16**, 497–506.
- Li, W., Wang, B., Wu, J., et al. (2009) The *Magnaporthe oryzae* avirulence gene *AvrPiz-t* encodes a predicted secreted protein that triggers the immunity in rice mediated by the blast resistance gene *Piz-t*. *Molecular Plant-Microbe Interactions* **22**, 411–420.
- Miki, S., Matsui, K., Kito, H., et al. (2009) Molecular characterization of the *AVR-Pia* locus from a Japanese field isolate of *Magnaporthe oryzae*. *Molecular Plant Pathology* **10**, 361–374.
- Monod, M., Capoccia, S., L  chenne, B., Zaugg, C., Holdom, M., & Jousson, O., 2002. Secreted proteases from pathogenic fungi. *International Journal of Medical Microbiology* **292**, 405–419.
- Mosquera, G., Giraldo, M.C., Khang, C.H., et al. (2009) Interaction transcriptome analysis identifies *Magnaporthe oryzae* BAS1–4 as Biotrophy-associated secreted proteins in rice blast disease. *The Plant Cell* **21**, 1273–1290.
- Nelson, J.W. (2003) Adaptation of core mechanisms to generate cell polarity. *Nature* **422**, 766–774.
- Orbatt, M.J., Farrall, L., Sweigard, J.A., et al. (2000) A telomeric avirulence gene determines efficacy for the rice blast resistance gene *Pi-ta*. *The Plant Cell* **12**, 2019–2032.
- Peyyala, R. & Farman, M.L. (2006) *Magnaporthe oryzae* isolates causing gray leaf spot of perennial ryegrass possess a functional copy of the *AVR1-CO39* avirulence gene. *Molecular Plant Pathology* **7**, 157–165.
- Rafiqi, M., Gan, P.H.P., Ravensdale, M., et al. (2010) Internalization of flax rust avirulence proteins into flax and tobacco cells can occur in the absence of the pathogen. *The Plant Cell* **22**, 2017–2032.
- Schneider, D.R.S., Saraiva, A.M., Azzoni, A.R., et al. (2010). Overexpression and purification of PWL2D, a mutant of the effector protein PWL2 from *Magnaporthe grisea*. *Protein Expression and Purification* **74**, 24–31.
- Sharpless, K.E. & Harris, S.D. (2002) Functional characterization and localization of the *Aspergillus nidulans* forming sepA. *Molecular Biology of the Cell* **13**: 469–479
- Soanes, D.M., Alam, I., Cornell, M., et al. (2008) Comparative genome analysis of filamentous fungi reveals gene family expansions associated with fungal pathogenesis. *PLoS One* **3**, 1–15.
- Steinberg, G. (2007) Hyphal growth: a tale of motors, lipids and the Spitzenk  rper. *Eukaryotic Cell* **6**, 351–360.
- Sweigard, J.A., Carroll, A.M., Kang, S., et al. (1995) Identification, cloning and characterization of *PWL2*, a gene for host species specificity in the rice blast fungus. *The Plant Cell* **7**, 1221–1233.
- Talbot, N.J. (2003) On the trail of a cereal killer. *Annual Reviews Microbiology* **57**, 177–202.
- Tosa, Y., Hirata, K., Tamba, H., et al. (2004) Genetic constitution and pathogenicity of *Lolium* isolates of *Magnaporthe oryzae* in comparison with host-species specific pathotypes of the blast fungus. *Phytopathology* **94**, 454–462.
- Virag, A. & Harris, S.D. (2006a) The Spitzenk  rper: a molecular perspective. *Mycological Research* **110**, 4–13.
- Virag, A. & Harris, S.D. (2006b) Functional characterization of *Aspergillus nidulans* homologs of *Saccharomyces cerevisiae* Spa2 and Bud6. *Eukaryotic Cell* **5**, 881–895.
- Wilson, R. & Talbot, N.J. (2009) Under pressure: investigating the biology of plant infection by *Magnaporthe oryzae*. *Nature Reviews Microbiology* **7**, 185–195.
- Wu, H., Rossi, G., & Brennwald, P. (2008) The ghost in the machine: small GTPases as spatial regulators of exocytosis. *Trends in Cell Biology*, **18**, 397–404.
- Yamashita, M., Kurokawa, K., Sato, Y., et al. (2010) Structural basis for the Rho- and phosphoinositide-dependent localization of the exocyst subunit Sec3. *Nature Structural and Molecular Biology* **17**, 180–186.
- Yi, M., Chi, M.-H., Hyun, C.H., et al. (2009) The ER chaperone *LHS1* is involved in asexual development and rice infection by the blast fungus *Magnaporthe oryzae*. *The Plant Cell* **21**, 681–695.
- Yoshida, K., Saitoh, H., Fujisawa, S., et al. (2009) Association genetics reveals three novel avirulence genes from the rice blast fungal pathogen *Magnaporthe oryzae*. *The Plant Cell* **21**, 1573–1591.

EFFECTOR TRANSLOCATION AND DELIVERY

243

- Zheng, W., Chen, J., Liu, W., et al. (2007) A Rho3 homolog is essential for appressorium development and pathogenicity of *Magnaporthe grisea*. *Eukaryotic Cell* **6**, 2240–2250.
- Zheng, W., Zhao, Z., Chen, J., et al. (2009) A Cdc42 ortholog is required for penetration and virulence of *Magnaporthe grisea*. *Fungal Genetics and Biology* **46**, 450–460.
- Zeigler, R.S., Leong, S.A., & Peng, P.S. (1994) Rice blast disease. In: *Rice Blast Disease*. Cab International, Wallingford, CT.

